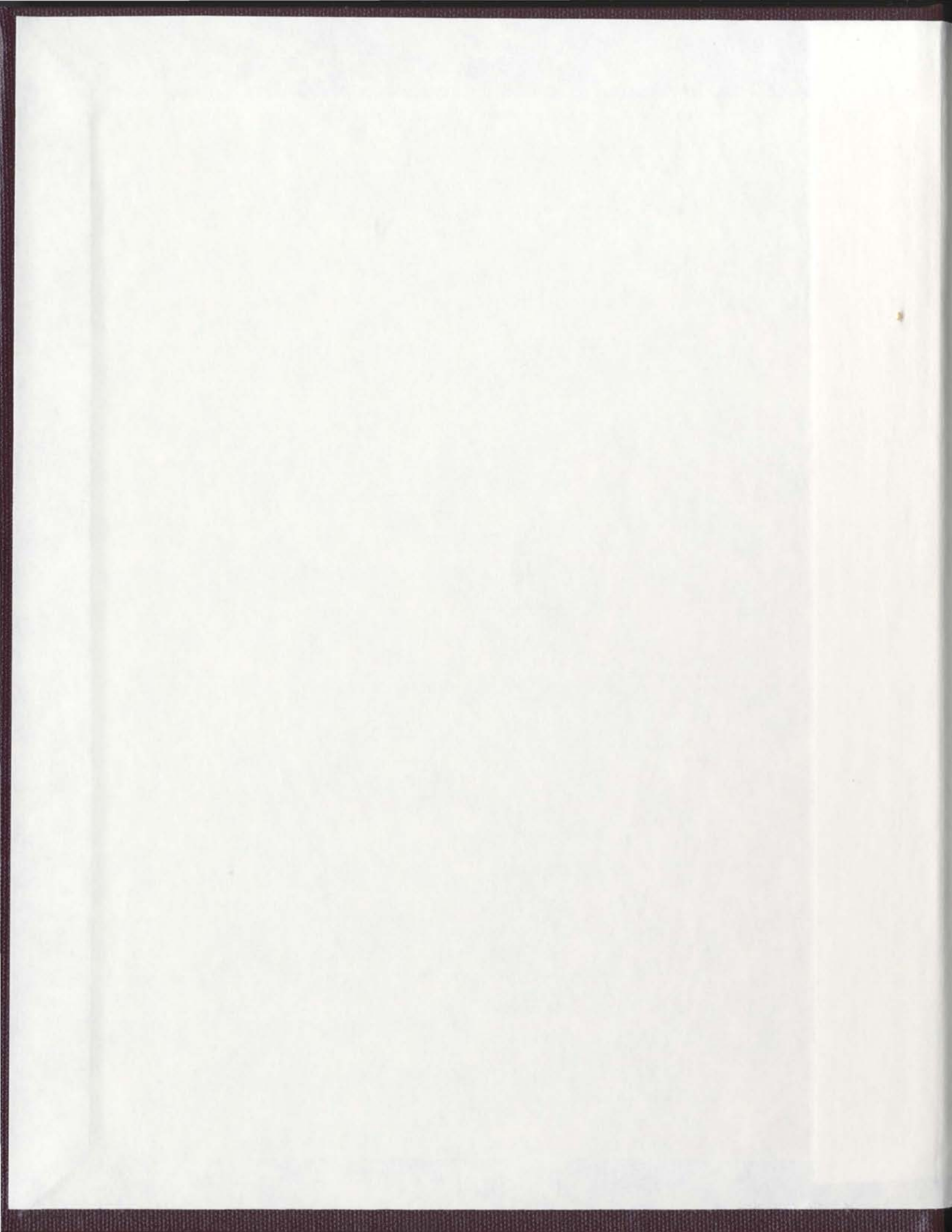


CHARACTERISING DISSOLVED NITRATE IN
PRECIPITATION USING STABLE NITROGEN AND
OXYGEN ISOTOPES

VANESSA EILEEN LEE



CHARACTERISING DISSOLVED NITRATE IN PRECIPITATION
USING STABLE NITROGEN AND OXYGEN ISOTOPES

by

Vanessa Eileen Lee, B.Sc. (Hons.)

A thesis submitted to the School of Graduate
Studies in partial fulfilment of the
requirements for the degree of Master of
Science

Department of Earth Sciences
Memorial University of Newfoundland

May 2005



St. John's

Newfoundland



Library and
Archives Canada

Published Heritage
Branch

395 Wellington Street
Ottawa ON K1A 0N4
Canada

Bibliothèque et
Archives Canada

Direction du
Patrimoine de l'édition

395, rue Wellington
Ottawa ON K1A 0N4
Canada

0-494-06645-8

Your file *Votre référence*

ISBN:

Our file *Notre référence*

ISBN:

NOTICE:

The author has granted a non-exclusive license allowing Library and Archives Canada to reproduce, publish, archive, preserve, conserve, communicate to the public by telecommunication or on the Internet, loan, distribute and sell theses worldwide, for commercial or non-commercial purposes, in microform, paper, electronic and/or any other formats.

The author retains copyright ownership and moral rights in this thesis. Neither the thesis nor substantial extracts from it may be printed or otherwise reproduced without the author's permission.

In compliance with the Canadian Privacy Act some supporting forms may have been removed from this thesis.

While these forms may be included in the document page count, their removal does not represent any loss of content from the thesis.

AVIS:

L'auteur a accordé une licence non exclusive permettant à la Bibliothèque et Archives Canada de reproduire, publier, archiver, sauvegarder, conserver, transmettre au public par télécommunication ou par l'Internet, prêter, distribuer et vendre des thèses partout dans le monde, à des fins commerciales ou autres, sur support microforme, papier, électronique et/ou autres formats.

L'auteur conserve la propriété du droit d'auteur et des droits moraux qui protègent cette thèse. Ni la thèse ni des extraits substantiels de celle-ci ne doivent être imprimés ou autrement reproduits sans son autorisation.

Conformément à la loi canadienne sur la protection de la vie privée, quelques formulaires secondaires ont été enlevés de cette thèse.

Bien que ces formulaires aient inclus dans la pagination, il n'y aura aucun contenu manquant.


Canada

ABSTRACT

Single event precipitation samples were collected at two sites in Newfoundland for stable isotopic analysis of nitrogen and oxygen of dissolved nitrate. Nitrate, the second largest acidifying component of rain, is formed during the oxidation of NO and NO₂, collectively known as NO_x, as well as other nitrogen species. Both natural and anthropogenic sources exist, however fossil fuel combustion in power plants and vehicles are the main contributors of NO_x to the atmosphere. Nitrogen isotopes of nitrate may give insight into the source of the atmospheric oxinitrogen species, while oxygen isotopes may provide information about the type of oxidation the NO_x emissions have undergone. The isotopic signatures, in combination with chemical and meteorological data, were used to characterise the main controls of the nitrate in the precipitation.

The two sites chosen for this study represent different types of environments: St. John's is a marine/urban location, while McIvers is a marine/rural site with no major point sources in the area. St. John's precipitation samples generally displayed characteristics of oil combustion emissions from stationary sources (high V, Ni) with smaller inputs from the ocean. Samples collected at McIvers were not as strongly affected by inputs from fossil fuel combustion, and generally had stronger marine signatures along with wood combustion and vehicle emissions. However, several samples collected at this location did display characteristics of oil combustion as well as smelting processes, confirming that the site is affected by long range transport of pollutants from North America.

Nitrogen isotopes appear to be controlled by the source of the nitrogen emissions.

Fossil fuel combustion in stationary sources results in $\delta^{15}\text{N}$ values close to 0‰, vehicle NO_x emissions range from -2 to -13‰, while natural sources such as soil and oceanic emissions can result in NO_x with values as low as -20‰. A seasonality in $\delta^{15}\text{N}$ was observed at both sites, whereby samples collected during the warmer season (Apr.-Sept.) exhibited more positive $\delta^{15}\text{N}$ values than those collected during the cold season (Oct.-Mar.). Chemical data revealed that both sites were affected more strongly by anthropogenic emissions during the warm months, while the influence of the ocean was dominant during the cold periods.

The oxygen isotopic composition of nitrate in this study appears to be controlled by atmospheric transformations of the oxinitrogen species, which are related to temperature. Summer samples, mainly oxidised by ozone, had more positive ^{18}O signatures than their winter counterparts. There is no evidence that the $\delta^{18}\text{O}$ of the nitrate in this study is controlled by the sources of the nitrate.

This study has provided valuable isotopic measurements of atmospheric nitrate. To the author's knowledge, the method used in this study for isolating and processing dissolved nitrate in precipitation for stable isotopic analysis had not been previously applied to single rain events, making this study unique. As well, it has shown through the combination of isotopic and chemical data how nitrogen isotopes of precipitation nitrate are controlled by sources, while the oxygen isotopes of these compounds are controlled by atmospheric oxidation processes.

ACKNOWLEDGEMENTS

Firstly, I would like to thank my supervisor, Dr. Moire Wadleigh, for all of her support and encouragement over the duration of this project. Working with her was a very enjoyable learning experience, and her knowledge and advice was greatly appreciated. This thesis is dedicated to her memory.

Special thanks to Dr. Robyn Jamieson, who did not hesitate to help me with this project when I really needed her. Your friendly guidance will not be forgotten.

I would like to extend my warmest thanks to Carson and Sheila Burrige who willingly “adopted” a rain collector in their backyard for a year. Their dedication and care in the operation of the collector was invaluable to the success of this project. Many thanks to their daughter, Carolyn, for getting her parents interested in this study.

Many people in the Earth Sciences Department have helped me out in some way or another, especially Alison Pye and Pam King. Thanks to both of you for your continued willingness to help me with all of my questions, lab-related or otherwise.

Thank you to all of my friends who supported me during this work. A big thanks goes to Susan, who listened to me when I was trying to figure things out. You always tried to help in any way possible, and for that I’m extremely grateful.

Finally, I would like to thank my parents, my sister and Mark for always believing that I could do this no matter what. They never doubted my abilities, and they have been a constant source of encouragement and support throughout my education, and for that I am the most grateful.

TABLE OF CONTENTS

ABSTRACT	ii
ACKNOWLEDGEMENTS	iv
TABLE OF CONTENTS	v
LIST OF TABLES	viii
LIST OF FIGURES	x

CHAPTER 1

INTRODUCTION

1.1 Introduction	1
1.2 Background	5
1.2.1 Rain Formation and Acid Rain	5
1.2.2 Atmospheric Nitrogen Cycle	9
1.2.2.1 Sources and Sinks	9
1.2.2.1.1 Natural Sources	11
1.2.2.1.2 Anthropogenic Sources	12
1.2.2.2 Atmospheric Transformations	13
1.2.3 Stable Isotopes	18
1.2.3.1 Fractionation Mechanisms	18
1.2.3.2 Nitrogen Isotopes	21
1.2.3.3 Oxygen Isotopes (Nitrate)	25
1.2.3.4 Oxygen Isotopes (Water)	32
1.3 Chemical Composition of Precipitation	34

CHAPTER 2

METHOD

2.1 Sample Sites	45
2.1.1 St. John's	45
2.1.2 McIvers	47

2.2	Sample Collection	48
2.3	Chemical Analysis	50
2.3.1	pH and Conductivity	50
2.3.2	Ion Chromatography	50
2.3.3	Inductively Coupled Plasma - Mass Spectrometry	51
2.4	Stable Isotopes	54
2.4.1	Nitrate Extraction	54
2.4.2	Nitrogen Isotopes	57
2.4.3	Oxygen Isotopes (Nitrate)	58
2.4.4	Oxygen Isotopes (Water)	60
2.5	Statistical Analysis	60
2.6	Meteorological Analysis	61

CHAPTER 3

RESULTS

3.1	Chemical Composition	63
3.1.1	pH and Conductivity	63
3.1.2	Major Ions	64
3.1.3	Trace Elements	69
3.2	Isotopic Composition	74
3.2.1	Nitrogen Isotopes	74
3.2.2	Oxygen Isotopes (Nitrate)	76
3.2.3	Oxygen Isotopes (Water)	76
3.3	Air Mass Back Trajectories	77

CHAPTER 4

INTERPRETATION

4.1	Basic Inferential Statistics	80
4.2	Principal Component Analysis	82

4.3 Air Mass Back Trajectories	88
4.4 St. John's	91
4.5 McIvers	116
4.6 Events Captured at Both Sites	127

CHAPTER 5

CONCLUSIONS

5.1 Overview	132
5.2 Further Work	136

REFERENCES	138
------------------	-----

APPENDIX I	148
------------------	-----

APPENDIX II	152
-------------------	-----

APPENDIX III	179
--------------------	-----

APPENDIX IV	204
-------------------	-----

LIST OF TABLES

Table 1.1	$\delta^{18}\text{O}$ of some common atmospheric oxidants	31
Table 1.2	Typical ion concentrations of marine and continental rain	35
Table 1.3	Summary of planetary emissions from trace metals from natural sources	38
Table 1.4	Trace metal concentrations in precipitation for urban, rural and remote areas	41
Table 1.5	Relative influence of anthropogenic activities on atmospheric trace metal concentrations	44
Table 2.1	Range of detection limits for elements of interest acquired by ICP-MS	53
Table 2.2	Precision values for elements of interest	53
Table 3.1	Numerical and volume-weighted averages and seasonal differences of $\delta^{15}\text{N}$ for both sites	75
Table 4.1	Statistically significant results of comparison of VWMs of species between locations	81
Table 4.2	Principal component analysis coefficients	83
Table 4.3	Precipitation nitrate concentration data from other studies in Newfoundland and Atlantic Canada	92
Table 4.4	Isotopic composition of St. John's samples with seaspray controls	97
Table 4.5	Nitrogen isotopic composition of St. John's samples with oil combustion controls	99
Table II.1	Descriptions of St. John's samples	153
Table II.2	Descriptions of McIvers samples	154
Table II.3	pH and conductivity for St. John's samples	155

Table II.4	pH and conductivity for McIvers samples	156
Table II.5	Anion concentrations for St. John's samples	157
Table II.6	Anion concentrations for McIvers samples	158
Table II.7	Cation concentrations for St. John's samples	159
Table II.8	Cation concentrations for McIvers samples	160
Table II.9	VWM ion concentrations for St. John's and McIvers	161
Table II.10	Statistical results of comparisons of VWM concentrations of ions for both locations	162
Table II.11	Seasonal VWM ion concentrations for St. John's and McIvers	163
Table II.12	Percent seaspray sulphate for St. John's samples	164
Table II.13	Percent seaspray sulphate for McIvers samples	165
Table II.14	ICP-MS data for St. John's samples	166
Table II.15	ICP-MS data for McIvers samples	170
Table II.16	VWM trace element concentrations for St. John's and McIvers	172
Table II.17	Statistical results of comparisons of VWM concentrations of trace elements for both locations	173
Table II.18	Seasonal VWM trace element concentrations for St. John's and McIvers	174
Table II.19	Isotope data for St. John's samples	175
Table II.20	Isotope data for McIvers samples	176
Table II.21	Statistical results of comparisons of VWMs of stable isotopes for both locations	177
Table II.22	Correlation matrix used to produce the PCA	178

LIST OF FIGURES

Figure 1.1	Global sulphur and nitrogen emissions	7
Figure 1.2	Canadian and US SO ₂ emissions	8
Figure 1.3	Canadian and US NO ₂ emissions	8
Figure 1.4	Atmospheric nitrogen cycle	10
Figure 1.5	$\delta^{15}\text{N}$ of some common nitrogen species	24
Figure 1.6	Atmospheric nitrogen cycle with $\delta^{15}\text{N}$ values of NO _x emissions	26
Figure 1.7	$\delta^{15}\text{N}$ nitrate values from other precipitation studies	27
Figure 1.8	$\delta^{18}\text{O}$ nitrate values from other precipitation studies	29
Figure 1.9	Rayleigh fractionation of $\delta^{18}\text{O}$ in meteoric waters	33
Figure 2.1	Map of Newfoundland showing the two sampling locations	46
Figure 2.2	Rain collector used in this study	49
Figure 2.3	Preconcentration apparatus used in this study	55
Figure 3.1	VWM ion concentrations for St. John's and McIvers	65
Figure 3.2	Seasonal VWM ion concentrations for St. John's	67
Figure 3.3	Seasonal VWM ion concentrations for McIvers	67
Figure 3.4	Winter VWM ion concentrations for St. John's and McIvers	68
Figure 3.5	Summer VWM ion concentrations for St. John's and McIvers	68
Figure 3.6	VWM trace element concentrations for St. John's and McIvers	70
Figure 3.7	Seasonal VWM trace element concentrations for St. John's	72
Figure 3.8	Seasonal VWM trace element concentrations for McIvers	72

Figure 3.9	Winter VWM trace element concentrations for St. John's and McIvers	73
Figure 3.10	Summer VWM trace element concentrations for St. John's and McIvers	73
Figure 3.11	Air mass back trajectory map for both locations	78
Figure 4.1	PC1 plotted against PC2	85
Figure 4.2	PC2 plotted against PC3	85
Figure 4.3	Scores of PC1 plotted against scores of PC2 with user defined source labels	87
Figure 4.4	Scores of PC2 plotted against scores of PC3 with user defined source labels	87
Figure 4.5	Scores of PC1 plotted against scores of PC2 using location labels	89
Figure 4.6	Scores of PC2 plotted against scores of PC3 using location labels	89
Figure 4.7	$\delta^{15}\text{N}$ variations with season and temperature for St. John's samples ..	102
Figure 4.8	NO_3^- (mg) variations for St. John's samples	104
Figure 4.9	$\delta^{18}\text{O}_{\text{NO}_3}$ variations with season and temperature for St. John's samples	108
Figure 4.10	$\delta^{18}\text{O}_{\text{H}_2\text{O}}$ variations with temperature for St. John's samples	113
Figure 4.11	$\delta^{18}\text{O}_{\text{NO}_3}$ versus $\delta^{18}\text{O}_{\text{H}_2\text{O}}$	115
Figure 4.12	NO_3^- (mg) variations for McIvers samples	120
Figure 4.13	$\delta^{15}\text{N}$ variations with season and temperature for McIvers samples ...	123
Figure 4.14	$\delta^{18}\text{O}_{\text{NO}_3}$ variations with season and temperature for McIvers samples .	125
Figure 4.15	$\delta^{18}\text{O}_{\text{H}_2\text{O}}$ variations with temperature for McIvers samples	128

Figure III.1	Air mass back trajectory calculated for sample SJS02-0123	180
Figure III.2	Air mass back trajectory calculated for sample SJ02-0314	181
Figure III.3	Air mass back trajectory calculated for sample SJ02-0322	182
Figure III.4	Air mass back trajectory calculated for sample SJ02-0328	183
Figure III.5	Air mass back trajectory calculated for sample SJ02-0429	184
Figure III.6	Air mass back trajectory calculated for sample SJ02-0510	185
Figure III.7	Air mass back trajectory calculated for sample SJ02-0531	186
Figure III.8	Air mass back trajectory calculated for sample SJ02-0606	187
Figure III.9	Air mass back trajectory calculated for sample SJ02-0624	188
Figure III.10	Air mass back trajectory calculated for sample SJ02-0709	189
Figure III.11	Air mass back trajectory calculated for sample SJ02-0710	190
Figure III.12	Air mass back trajectory calculated for sample SJ02-0807	191
Figure III.13	Air mass back trajectory calculated for sample SJ02-0820	192
Figure III.14	Air mass back trajectory calculated for sample SJ02-0825	193
Figure III.15	Air mass back trajectory calculated for sample SJ02-0906	194
Figure III.16	Air mass back trajectory calculated for sample SJ02-0910	195
Figure III.17	Air mass back trajectory calculated for sample SJ02-0917	196
Figure III.18	Air mass back trajectory calculated for sample SJ02-0928	197
Figure III.19	Air mass back trajectory calculated for sample SJ02-1001	198
Figure III.20	Air mass back trajectory calculated for sample SJ02-1020	199
Figure III.21	Air mass back trajectory calculated for sample SJ02-1114	200

Figure III.22	Air mass back trajectory calculated for sample SJ03-0131	201
Figure III.23	Air mass back trajectory calculated for sample SJ03-0201	202
Figure III.24	Air mass back trajectory calculated for sample SJ03-0202	203
Figure IV.1	Air mass back trajectory calculated for sample MCS02-0205	205
Figure IV.2	Air mass back trajectory calculated for sample MC02-0401	206
Figure IV.3	Air mass back trajectory calculated for sample MC02-0413	207
Figure IV.4	Air mass back trajectory calculated for sample MC02-0606	208
Figure IV.5	Air mass back trajectory calculated for sample MC02-0624	209
Figure IV.6	Air mass back trajectory calculated for sample MC02-0719	210
Figure IV.7	Air mass back trajectory calculated for sample MC02-0806	211
Figure IV.8	Air mass back trajectory calculated for sample MC02-0911	212
Figure IV.9	Air mass back trajectory calculated for sample MC02-0924	213
Figure IV.10	Air mass back trajectory calculated for sample MC02-1124	214
Figure IV.11	Air mass back trajectory calculated for sample MCS03-0126	215

CHAPTER 1

INTRODUCTION

1.1 Introduction

Nitrates and sulphates are the principal acidifying components of rain. Sulphur emissions have received more attention than nitrogen emissions in the past, mainly because sulphur dioxide has been the main contributor to acid rain in North America. In the past decade, federal control programs implemented in both Canada and the United States have led to a decrease in sulphur emissions, but neither country has significantly reduced nitrogen oxide emissions (Environment Canada, 1998). It is becoming increasingly clear that nitrogen compounds are having a large negative impact on the atmosphere and ecosystems in both countries. Human activities are severely altering the natural nitrogen cycle with inputs from oil- and coal-fired power plants and motor vehicles. According to an assessment performed by Environment Canada in 1997, only 3% of nitrogen oxide emissions in eastern North America are emitted from natural sources (Environment Canada, 1998). On a larger scale, global inputs continue to increase as industrialization spreads throughout more areas of the world. The ability to identify the different types of inputs of nitrogen compounds to the atmosphere may prove to be a valuable tool in future efforts to reduce the acidity of the atmosphere. Areas with little local industrial emissions are being impacted by distant sources due to long range transport of the pollutants. More detailed studies of the sources of these acidifying compounds as well as their locations may

lead to an increase in knowledge of the effects of NO_x emissions, and may force lawmakers to introduce stricter legislation forcing a reduction in NO_x emissions in the future.

The nitrogen cycle (N) is very complex, involving interactions and transformations of nitrogen in the atmosphere, earth and oceans. Due to the complexity of the nitrogen cycle as well as the difficulty in measuring and analyzing low concentrations of nitrate in precipitation, nitrogen studies have not received the same scientific attention as those related to sulphur. However, atmospheric nitrogen compounds have been studied to varying degrees for many years, especially since the 1950's when scientists such as Ångström and Högberg (1952) and Hoering (1957) began attempting to determine the sources of these compounds. Although Hoering (1957) did perform stable isotopic studies of nitrogen in the 1950's, it wasn't until recently that researchers such as Moore (1974), Freyer (1978, 1991) and Heaton (1986, 1987, 1990) began using stable isotopes of nitrogen as a tool for tracing nitrogen sources to the atmosphere. The isotopic signature of a particular atmospheric species such as nitrate appears to be controlled by the signature of the source or sources from which it originates. The isotope ratio in a particular compound may be altered by various physical and chemical processes as it moves through the atmosphere (Moore, 1977). Due to the fact that there is little transformation of nitrates as they travel through the atmosphere, their isotopic signature should be similar to that of the source of the compounds, providing a means of determining the relative importance of various sources to the atmosphere.

Nitrogen isotopes may give insight into the type of source from which the

compounds were emitted, however oxygen isotopes of nitrogen compounds may provide different information. Oxygen isotopes are fractionated during atmospheric transformation processes of the nitrogen compounds, resulting in nitrates with a distinct oxygen isotopic signature. These signatures can then be used to evaluate the oxidation processes that the nitrogen compounds have undergone, and may help determine whether the nitrate formation was local or distant, or what chemical reactions have affected the compounds. Oxygen isotopes of nitrate in precipitation have not been extensively studied in the past. Only three recent studies have evaluated both the nitrogen and oxygen isotopic composition of nitrate: Durka et al. (1994), Kendall et al. (1995b), and Hastings et al. (2003). These studies indicate the potential utility of $\delta^{18}\text{O}_{\text{NO}_3}$ to trace sources and/or atmospheric transformations of nitrate.

The objective of this study is to isotopically characterize dissolved nitrate in single event precipitation samples collected from two sites within the province of Newfoundland. This will be done by extracting nitrate from precipitation samples for stable nitrogen and oxygen isotope analyses using a recently developed method which has not been applied to single event precipitation samples before, making this study unique. Variations in the stable isotopic values will be used to identify and quantify sources of atmospheric nitrates at the two sites.

Two coastal sites within Newfoundland were selected for this year-long study. St. John's is located on the east coast of the province and is an urban area, while McIvers is located on the west coast of the province and represents a rural environment. It was

expected that each site may be affected differently by long range transport of pollutants due to their location within the province as well as the type of environment of each location. The rain collector for the St. John's site was located next to an oil-fired power station which was expected to influence the samples, thus representing an anthropogenically influenced environment. The McIvers collector was placed in an area with no immediate point sources, and would thus represent a more naturally influenced environment. Both sites had reliable and dedicated persons available to operate the rain collector at each location, which is crucial in this type of study. As well, both locations are coastal, so a marine influence may be observable.

The atmospheric nitrates collected from the two sites will be characterized using the stable isotopes of nitrogen and oxygen. Major ion and trace metal analyses of the rain in which the nitrates were found will be used to aid in source delineation of the nitrate in the samples. Isotopic and chemical data will also be used to show variations within the sites themselves as well as the processes that affect nitrogen in these two different environments, such as effects due to seasonality. Meteorological data will be used to further distinguish possible sources of nitrogen compounds to the atmosphere. This study will provide valuable stable nitrogen and oxygen isotopic measurements of precipitation nitrate.

1.2 Background

1.2.1 Rain Formation and Acid Rain

Clouds form when atmospheric water vapour condenses upon particles $>0.1 \mu\text{m}$ in diameter (Schlesinger, 1997). These hygroscopic particles, or condensation nuclei, are atmospheric aerosols such as soil dust particles, combustion products (H_2SO_4 and HNO_3) and sea salt (NaCl). Atmospheric gases, both natural and anthropogenic, become dissolved in the water droplets due to the large surface areas available for gas exchange between the droplets and gases (Berner and Berner, 1996). Precipitation occurs when the water droplets coalesce. Incorporation of atmospheric gases during condensation processes is considered to be the rainout component of precipitation, while gases incorporated into the raindrops as they fall through the atmosphere are termed washout constituents (Berner and Berner, 1996; Schlesinger, 1997).

Pure water containing no dissolved substances has a pH of 7. Natural rainwater is not "pure" water. It contains dissolved atmospheric gases (Berner and Berner, 1996). In its natural, unpolluted form, rainwater will have a pH of 5.6 due to the reaction of atmospheric CO_2 with H_2O (Galloway et al., 1976). The carbonic acid (H_2CO_3) created partly dissociates to produce bicarbonate and hydrogen ions, decreasing the pH from 7 to 5.6. Acid rain is therefore considered to be rain with a $\text{pH} < 5.6$. Overall, most natural rain will have a $\text{pH} > 5.0$ (Berner and Berner, 1996).

The first documentation of acid rain occurred in Europe in 1955, where the pH of rain in southern Sweden had values of 4 to 5 (Berner and Berner, 1996). The Industrial

Revolution, which began in the 19th century, as well as the creation of the internal combustion engine, resulted in more fossil fuel combustion, leading to an increase in acidifying emissions globally, especially over more industrialized regions such as North America. By the 1900's, increased industrial activities along with an increase in the number of automobiles have led to an increase in atmospheric pollution worldwide, especially over the past 50 years (Figure 1.1). The burning of fossil fuels such as coal, oil and gas results in the production of SO₂ and NO_x (NO and NO₂) gases. These compounds subsequently react with water and are oxidized in the atmosphere to form H₂SO₄ and HNO₃ (Galloway and Likens, 1981). These strong acids dissociate in rainwater to form free H⁺ ions, thus lowering the pH. Acid rain also occurs naturally in unpolluted areas due to the presence of natural acid compounds such as H₂SO₄ produced from the oxidation of biogenic, reduced-sulphur gases released primarily over the oceans.

Over the past 20 years, stricter emission control laws have led to a decrease in sulphur dioxide emissions in both Canada and the United States, while NO_x emissions have failed to decrease (Figures 1.2 and 1.3). Galloway and Likens (1981) found that nitric acid was becoming increasingly important relative to sulfuric acid in their bulk precipitation study. Heaton (1987) noted that nitrate is often considered to be the second most important acidifying agent in acid rain. As long as nitrogen oxides are entering the atmosphere, acid rain will continue to be a problem.

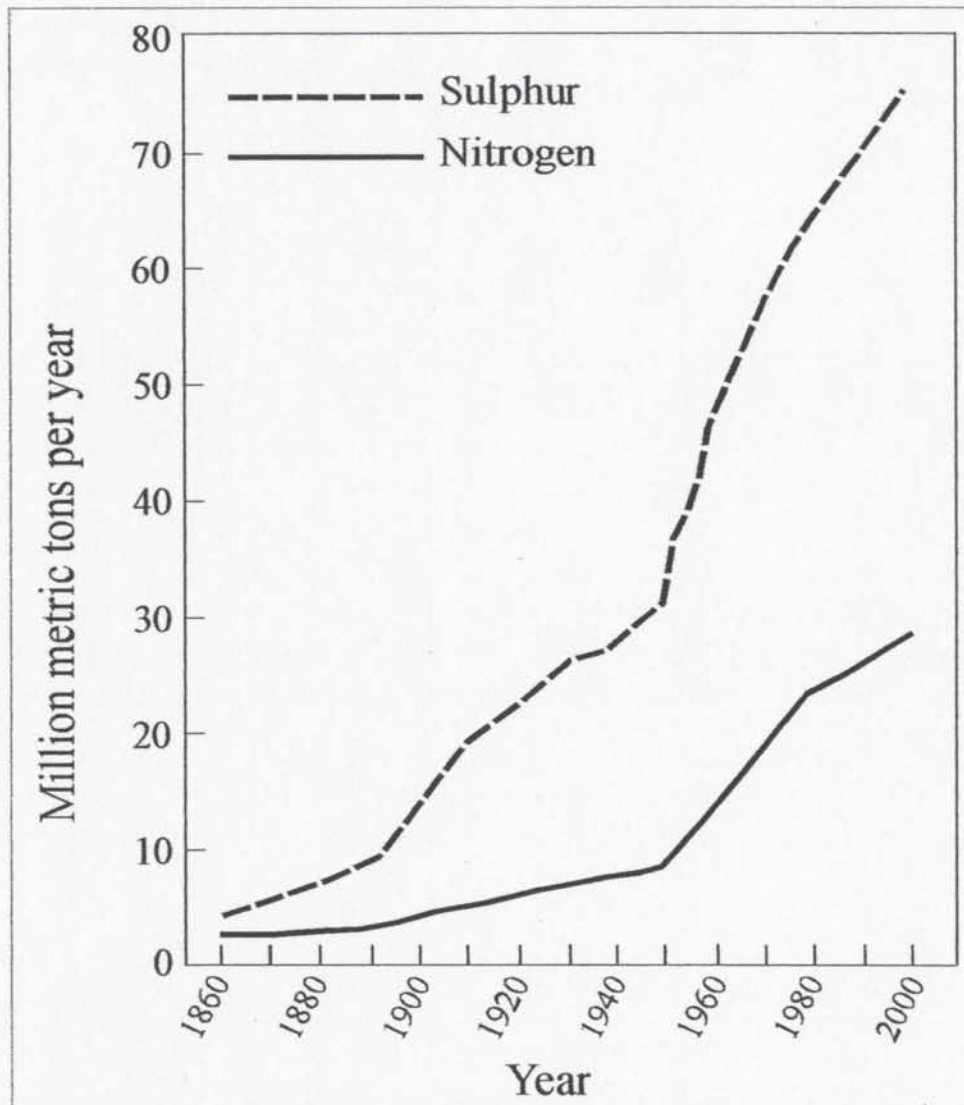


Figure 1.1 Global sulphur and nitrogen emissions (Mackenzie and Mackenzie, 1995).

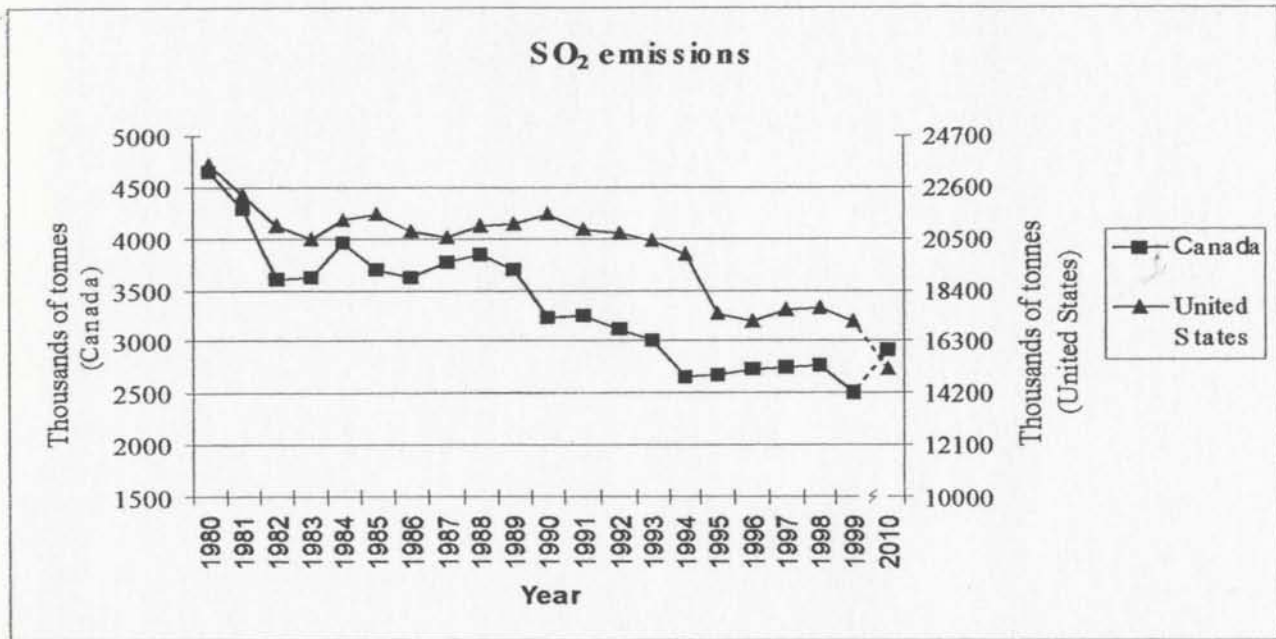


Figure 1.2 Canadian and U.S. SO₂ emissions estimated to 2010. Data from Vestreng (2003).

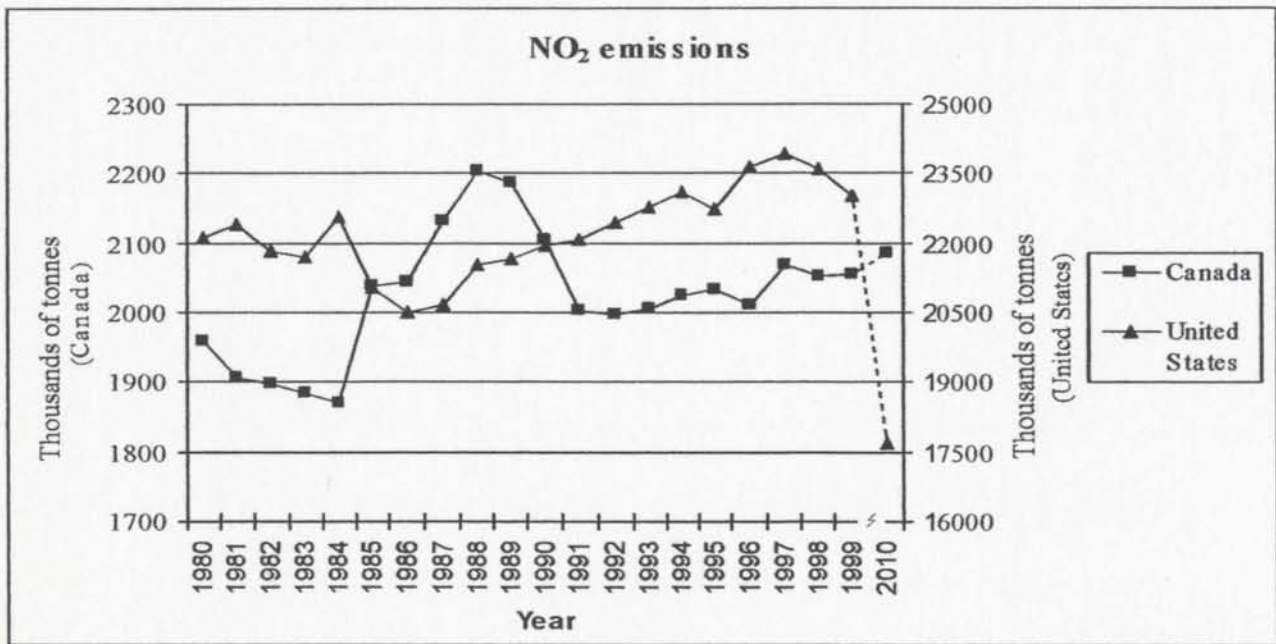


Figure 1.3 Canadian and U.S. NO₂ emissions estimated to 2010. Data from Vestreng (2003).

1.2.2 Atmospheric Nitrogen Cycle

Molecular nitrogen comprises 78% of the atmosphere by concentration and is relatively unreactive due to the strong covalent bonds between the nitrogen atoms. In general, nitrogen compounds containing an even number of nitrogen atoms (such as N_2 and N_2O) are less reactive than molecules containing an odd number of N atoms, known as fixed nitrogen. Conversion of N_2 does occur via nitrogen fixation, resulting in various forms of atmospheric nitrogen compounds including N_2O , NO , NO_2 , NO_3^- , NO_2^- , NH_3 and NH_4^+ . These compounds have nitrogen in valence states ranging from -3 (in NH_3) to +5 (in NO_3^-) (Schlesinger, 1997, Berner and Berner, 1996, Hoefs, 1997).

Figure 1.4, an illustration of the nitrogen cycle, shows the various fluxes of nitrogen through the atmosphere, land and oceans. In order for nitrogen, an essential nutrient of life, to be used by most biota it must be in a fixed form. Most of the fluxes in the cycle deal with fixed nitrogen, with denitrification processes returning the nitrogen in its molecular form to the atmosphere.

1.2.2.1 Sources and Sinks

There are two main sources of environmental nitrogen: natural and anthropogenic. Both of these sources play an important role in the nitrogen cycle, with anthropogenic sources becoming increasingly important as industries and automobile use continue to expand worldwide.

The largest sink for nitrogen is the atmosphere (Létolle, 1980), with some nitrogen

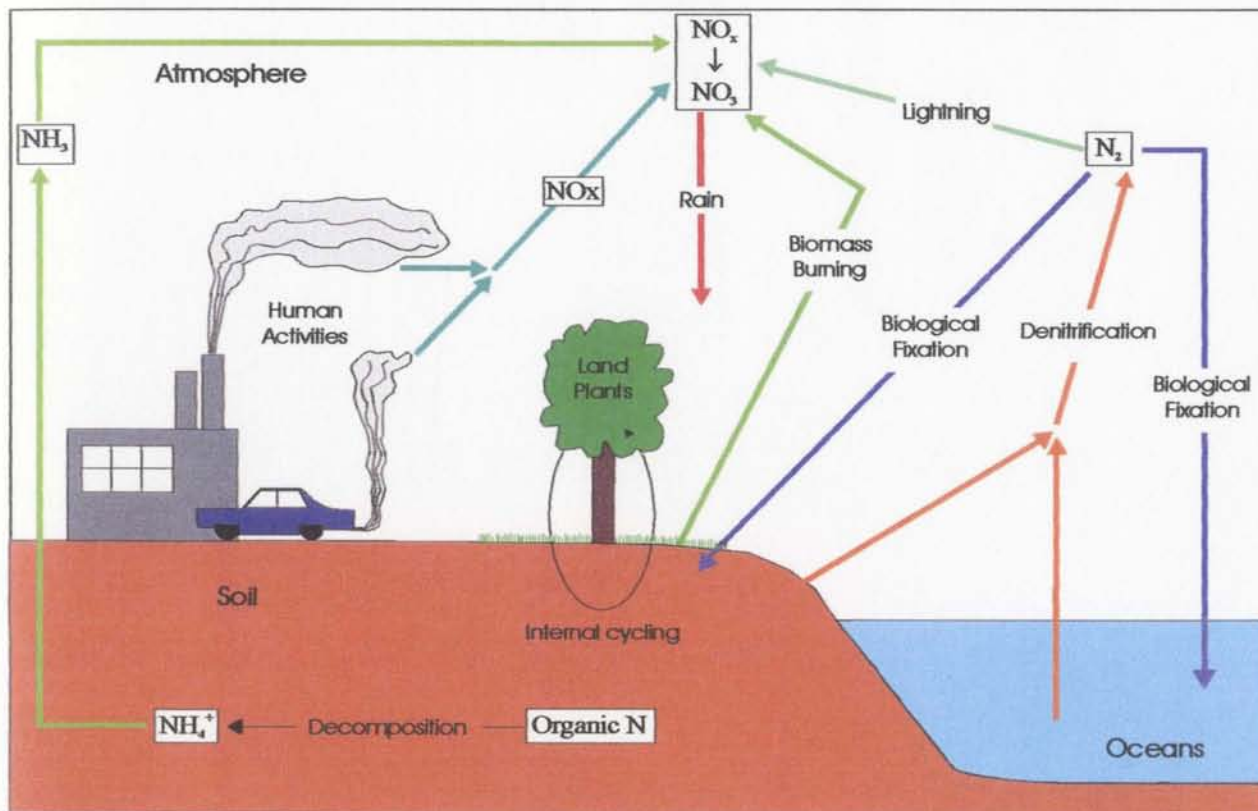


Figure 1.4 Atmospheric nitrogen cycle (after Schlesinger, 1997 and Berner and Berner, 1996).

being found in terrestrial biomass, soil organic matter and groundwater (Schlesinger, 1997).

1.2.2.1.1 Natural Sources

Naturally occurring processes in the environment result in the formation, reaction and scavenging of large quantities of nitrogen compounds (Robinson and Robbins, 1970). These processes, which include fixation by lightning, soil microbial activity and biomass burning, are responsible for only 35% of the input of NO_x to the atmosphere (Berner and Berner, 1996).

Ångström and Högberg (1952) and Hoering (1957) proposed nitrogen fixation via lightning discharges as a source of atmospheric fixed nitrogen. Lightning provides a momentary condition of high pressure and temperature which allows N_2 and O_2 to combine to form NO_x , introducing a small amount of fixed nitrogen to the cycle (Schlesinger, 1997).

Biological fixation, or the fixation of nitrogen by living organisms, provides a flux to both the terrestrial and marine environments. Nitrogen-fixing organisms such as blue-green algae and terrestrial bacteria, legumes and certain lichens convert unreactive N_2 to a usable form (Berner and Berner, 1996). Land plants fix some of the atmospheric nitrogen for their own use as well as using inorganic nitrogen from the soil, which is cycled back into the soil when the organism dies. Nitrogen may also be released into the atmosphere as NH_3 , NO_x and N_2 as biomass is volatilized naturally or during forest fires (Schlesinger,

1997). Ammonia, which is released from soils, biomass burning and the decomposition of excrement is the only natural alkaline gas found in the atmosphere. It plays an important role in the neutralization of anthropogenic acidity by reacting with sulphuric acid to produce ammonium sulphate aerosols (Brasseur et al., 1999).

1.2.2.1.2 Anthropogenic Sources

Humans have had a direct impact on the global nitrogen cycle. By planting nitrogen-fixing crops such as legumes, more N_2 is removed from the atmosphere than would normally occur in some areas. As well, biomass burning for land clearing results in ammonia, nitric oxides and elemental nitrogen being released to the atmosphere (Schlesinger, 1997). Although important, these impacts to the nitrogen cycle are minor when compared with the effects that industry and transportation has had on the cycle.

A specific industry which directly impacts the global nitrogen cycle is the production of nitrogen fertilizers through the Haber process. During this process, natural gas is burned to produce H_2 which is then combined with N_2 under high pressure and temperature, resulting in the formation of NH_3 (Schlesinger, 1997). This reduced form of nitrogen is then deposited on farm land and transferred to rivers where it eventually ends up in the oceans. Volatilization of NH_3 and denitrification can produce NO_x which is released to the atmosphere (Galloway and Likens, 1981). As well, fertilized agricultural systems are probably the largest anthropogenic source of nitrous oxide emissions to the atmosphere. Oceans are also considered to be a source of N_2O to the atmosphere as the

water is usually supersaturated with nitrous oxide (Brasseur et al., 1999). The N_2O is unreactive in the troposphere but is destroyed by photolysis or by reaction with excited oxygen atoms in the stratosphere. This can lead to the destruction of stratospheric ozone (Vitousek et al., 1997).

Ångström and Högberg (1952), Robinson and Robbins (1970), Heaton (1986) and Russell et al. (1998) all credited industrial contamination as a source of fixed atmospheric nitrogen. The burning of fossil fuels in power stations and manufacturing industries results in the oxidation of N_2 and fuel nitrogen to reactive NO_x gases which are released to the atmosphere, a process which occurs at high temperatures. This high temperature combustion process occurs in petrol-engined vehicles as well, resulting in atmospheric molecular nitrogen being oxidised and released as NO_x emissions to the atmosphere (Heaton, 1986, 1987 and 1990). Nitric oxide is the primary surface emission, but due to rapid interconversion between NO and NO_2 (Ridley and Atlas, 1999) combustion source NO_x is predominantly found as nitrogen dioxide in both urban and rural environments (Harrison et al., 2000).

1.2.2.2 Atmospheric Transformations

The majority of the nitrogen in the atmosphere is molecular nitrogen. In order for the N_2 to react with other compounds, high temperature conditions must exist, as is the case with lightning bolts. During lightning strikes, the N_2 is oxidised by O_2 in the following reaction:

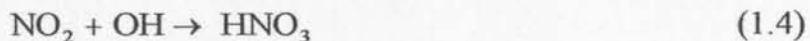


The two molecules of nitric oxide produced are very reactive and readily combine with ozone or peroxides in the atmosphere to produce nitrogen dioxide:



The HO_2 used in reaction 1.3 may be produced from atmospheric reactions involving OH or O_2 .

The nitrogen dioxide then reacts with atmospheric OH to form nitric acid:



The nitric acid, a strong acid, is removed by rain and completely dissociates in the raindrops to form hydrogen and nitrate ions:



The contribution of nitric acid from lightning bolt conversions of N_2 is quite small ($<3 \times 10^{12}$ g N/yr) compared to other sources of NO_x (Berner and Berner, 1996; Schlesinger, 1997).

Another relatively inert gas present in the atmosphere is nitrous oxide (N_2O). This gas, which is released during denitrification at the Earth's surface, is often not destroyed or removed in the troposphere; it is often transported upward into the stratosphere where it

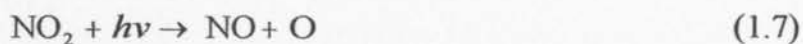
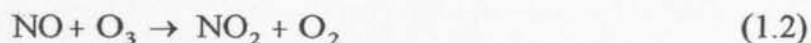
reacts with oxygen, providing a source of nitrogen oxides:



The excited oxygen atom (O^*) used in the above reaction is produced during the photolysis of O_3 in the stratosphere (Brasseur and Schimel, 1999). The NO in turn reacts with O_3 to form NO_2 (Reaction 1.2), which is then converted to nitric acid in the troposphere. The contribution of NO_x from the breakdown of N_2O is not a major one; this process has more of an impact in the destruction of stratospheric ozone. All of the above reactions, prior to the dissociation of nitric acid, involve the reaction of gaseous compounds with other gases, making them homogeneous reactions (Berner and Berner, 1996).

A large portion of the nitric acid found in the atmosphere is anthropogenic in origin. When NO and NO_2 are released to the atmosphere as combustion by-products from industry and vehicles, they undergo a series of reactions with other atmospheric constituents. These reactions occur fairly rapidly, with NO_x being completely converted to nitric acid in about one day (Berner and Berner, 1996; Schlesinger, 1997).

Daytime concentrations of atmospheric NO and NO_2 are mainly controlled through the oxidation of NO with O_3 , along with the photolytic reaction of NO_2 back to NO:



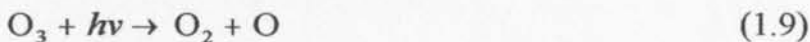
This catalytic cycle involves interconversion between the two oxides with no net change in the amount of NO_x present (Ridley and Atlas, 1999). Because this interaction is very fast,

the establishment of a photochemical stationary state of NO_x occurs within a few minutes (Freyer et al., 1993). The NO_2 produced may undergo photolysis (Reaction 1.7) resulting in the production of tropospheric ozone:



where M is a third body which carries away excess energy (Tyndall and Orlando, 1999).

NO_x also plays a role in the stratospheric ozone balance, but due to different reactions than above. The ozone produced may then be used in a variety of other reactions in the troposphere, such as the following which produces hydroxyl radicals:



The NO_2 in the atmosphere may also be removed during the day by its oxidation with OH radicals (Schlesinger, 1997), producing HNO_3 :



During the night, some of the NO_2 may be oxidized by O_3 to NO_3 :



The molecule of NO_3 produced may then react with NO_2 to form N_2O_5 , which may thermally decompose back to its original constituents or react heterogeneously with water surfaces to form nitrate:



The daytime removal reaction involving the oxidation of NO_2 with OH (Reaction 1.4) occurs preferentially during the summer months when increased solar radiation leads to higher OH concentrations. The cooler temperatures during winter months favour the nighttime reactions involving the formation and storage of N_2O_5 (Reactions 1.12 and 1.13). Because N_2O_5 is both thermally and photolytically unstable, cooler temperatures and longer nights allow for significant concentrations of this species to be reached (Freyer et al., 1993; Freyer, 1991, Hastings et al., 2003).

Ammonia can be released to the atmosphere from the soil N cycle, biomass burning, the production and application of fertilizers and a variety of industrial activities (Brasseur et al., 1999). This reduced nitrogen species can undergo chemical oxidation in the atmosphere, producing NO_x which will follow the same reaction pathways as above. Ammonia may also be involved in a heterogeneous reaction with atmospheric water to form ammonium and hydroxide ions:



Ammonia remains in the atmosphere for about 6 days before this reaction occurs, and the ammonium produced has an atmospheric residence time of about 5 days before it is removed by rain (Berner and Berner, 1996).

1.2.3 Stable Isotopes

1.2.3.1 Fractionation Mechanisms

Isotopes of an element are atoms which have a nucleus containing the same number of protons but a different number of neutrons, resulting in the isotopes having different masses from one another. The chemical and physical properties of the isotopes of an element are slightly different from one another due to these mass differences, which are more pronounced in elements with low atomic numbers. These mass differences are often large enough to allow isotopic fractionation to occur. Isotope fractionations are a result of chemical, physical and biological reactions which cause a change in the relative abundances of the stable isotopes of an element (Kendall et al., 1995a). In general, molecules containing heavy isotopes have higher dissociation energies and are therefore more stable than molecules containing light isotopes (Kendall and Caldwell, 1998). As a result, heavier isotopes tend to react less readily than the lighter isotopes. The fractionation between isotopes is represented by the symbol alpha (α) and is written as:

$$\alpha_{A-B} = \frac{R_A}{R_B}$$

where R_A and R_B represent the ratios of isotopes (e.g. $^{15}\text{N}/^{14}\text{N}$) in substances A and B respectively. The two ways in which fractionations can occur are through equilibrium isotope effects or kinetic isotope effects.

Equilibrium isotope effects pertain to situations in systems at chemical equilibrium in which the isotopic distribution changes between phases, substances or molecules with

no net reaction. For example, the exchange between two different nitrogen oxides, NO and NO₂, can be written:



Equilibrium constants can be expressed for isotope exchange reactions as:

$$K = \frac{(^{15}\text{N}/^{14}\text{N})_{\text{NO}_2}}{(^{15}\text{N}/^{14}\text{N})_{\text{NO}}}$$

When isotope exchange reactions involve the transfer of only one atom, the equilibrium constant, K, is identical to the fractionation factor $\alpha_{\text{NO}_2\text{-NO}}$. In general,

$$\alpha = K^{1/n}$$

where n represents the number of atoms exchanged. Typical α values for the above reaction at 25°C are 1.021, 1.039 and 1.040. Discrepancies exist between different authors, thus it is common to have more than one α value for a reaction (Létolle, 1980 and sources therein).

During equilibrium reactions, the heavier isotope preferentially accumulates in the species or compound with the higher oxidation state, causing that compound to become enriched in that particular isotope. Condensation of water vapour is an example of an equilibrium process during which the liquid phase becomes enriched in the heavier isotopes of oxygen and hydrogen, while the lighter isotopes remain in the vapour phase (Kendall et al., 1995a).

Kinetic isotope effects are associated with fast, incomplete or unidirectional

processes. Because lighter isotopes tend to react more quickly than heavy isotopes, these reactions provide products which are enriched in the lighter isotopes (Hoefs, 1997).

Fractionation factors for kinetic reactions can be calculated from the ratio of the rate constants for the isotopic substances. An example is the hydrolysis of nitric oxide to nitric acid which can be represented by two reactions:



where k_1 and k_2 are rate constants, and $k_1 \neq k_2$. The fractionation factor will be equal to k_1/k_2 , the ratio of the rate constants.

Kinetic fractionations occur during many biological processes which are generally unidirectional reactions. Bonds between heavier isotopes are generally stronger than those between lighter isotopes. As a result, organisms tend to use the lighter isotopic species due to the lower energy needed to break the weaker bonds associated with them, causing significant fractionations between the substrate (which retains the heavy isotopes) and the product created through the biological reaction (which contains the lighter isotopes). Slower reaction steps generally result in greater isotope fractionation as the organism has more time to select the lighter isotope, creating larger fractionations (Kendall et al., 1995a).

Several factors affect isotope fractionation, including chemical composition, availability of reactants, whether the system is open or closed, and temperature. Of these, temperature is the most important. As temperature increases the amount of fractionation

decreases due to a decrease in the difference of reactivity between the isotopes. This decrease in reactivity is caused by a decrease in the vibrational energy of the molecules. The amount of fractionation in a system can also vary depending on the number of steps in a reaction as well as the amount of intermediate species produced, both of which may involve equilibrium and kinetic isotope effects, making it difficult to calculate the expected fractionation within a system.

The standard method used to express isotopic values is the delta notation:

$$\delta^{15}\text{N} = \left(\frac{R_{\text{sample}}}{R_{\text{standard}}} - 1 \right) \times 10^3$$

expressed in units of parts per thousand or permil (‰), where R represents the ratio of the heavy to the light isotope (i.e. $^{15}\text{N}/^{14}\text{N}$) in both the sample and the standard. This notation represents the deviation of the ^{15}N in the sample from that of atmospheric N_2 , the standard nitrogen isotopic reference material which has a δ value of 0‰ (Russell et al., 1998). As with nitrogen, oxygen isotope values are reported in the standard delta notation, which measures the ratio of $^{18}\text{O}/^{16}\text{O}$ of the sample. The $\delta^{18}\text{O}$ value of the sample is reported with respect to Vienna Standard Mean Ocean Water (VSMOW). As with nitrate oxygen, the $^{18}\text{O}/^{16}\text{O}$ of precipitation is measured relative to VSMOW and is reported in ‰.

1.2.3.2 Nitrogen Isotopes

Nitrogen is an essential nutrient for all life, and is often a limiting factor in many ecosystems. It is one of the most abundant elements on earth, existing in the atmosphere,

lithosphere, hydrosphere and biosphere. Because nitrogen is found in valence states ranging from -3 (in NH_3) to +5 (in NO_3^-), a large number of biochemical transformations of this element are possible (Schlesinger, 1997). It is found in a wide range of environments and takes part in many processes within these environments. The two stable isotopes of nitrogen, ^{14}N and ^{15}N , have natural atmospheric abundances of 99.64% and 0.36%, respectively (Hoefs, 1987).

Nitrogen compounds may undergo many different transformations within the nitrogen cycle, resulting in the fractionation or segregation of the heavy and light isotopes of this element. This results in different nitrogen compounds having different isotopic signatures, allowing them to be used in isotopic tracer studies.

The most commonly measured nitrogen compound in precipitation studies is nitrate. NO_x , both natural and anthropogenic, is the most common precursor for NO_3^- . The NO_x undergoes a series of oxidation steps with the final product being HNO_3 . Nitric acid, a strong acid, then dissociates in atmospheric water resulting in dissolved nitrate in precipitation.

Nitrogen occurs in a range of valence states and in gaseous, dissolved and solid forms in the natural world. Biological processes have the largest fractionation effects on nitrogen isotopes. Myiake and Wada (1971) noted that NO_3^- produced during the oxidation of ammonia by marine bacteria had $\delta^{15}\text{N}$ values of -5 to -21‰. Inorganic processes also lead to fractionation. Natural gas formed from organic matter in the earth can have a range of $\delta^{15}\text{N}$ values from -20 to +45‰ (Létolle, 1980). As the gas migrates

through porous media, diffusion occurs resulting in a greater fractionation and therefore an increase in $\delta^{15}\text{N}$ in the gas. The original ^{15}N content of the source organic material, the length of time the gas forms from the material and the migration of the gas may result in a wide range of values. Fractionation mechanisms have been discussed in detail in a number of sources including Hoefs (1997), Faure (1998) and Létolle (1980).

Figure 1.5 shows the $\delta^{15}\text{N}$ of some important nitrogen species. The most influential anthropogenic sources of NO_x are fossil fuel combustion and vehicle emissions. Gasoline used in automobiles contains only a small amount of nitrogen, therefore NO_x gases emitted from automobiles are believed to come from "thermal NO" produced when atmospheric nitrogen ($\delta^{15}\text{N} = 0\text{‰}$) and oxygen combine at temperatures greater than 2000°C (Heaton, 1986). Measurements of exhaust NO_x from automobiles under varying loads resulted in a range of $\delta^{15}\text{N}$ values from -13 to -2‰. These more depleted signatures may be a result of kinetic fractionation due to the high energy required to break the triple bonds of the N_2 molecule during the formation of the NO. Idling vehicles were found to have the more depleted signature, while cars running under load had values of -2‰. It is possible that the combustion temperature in the engine of idling vehicles is not high enough for equilibrium conditions to exist, resulting in kinetic fractionation and therefore more depleted values. Cars running under increased load, however, may have a greater probability of reaching equilibrium due to higher peak combustion temperatures and longer reaction time, resulting in isotopic values closer to 0‰ (Heaton, 1990).

The burning of crude oil in power plants and other stationary sources occurs at

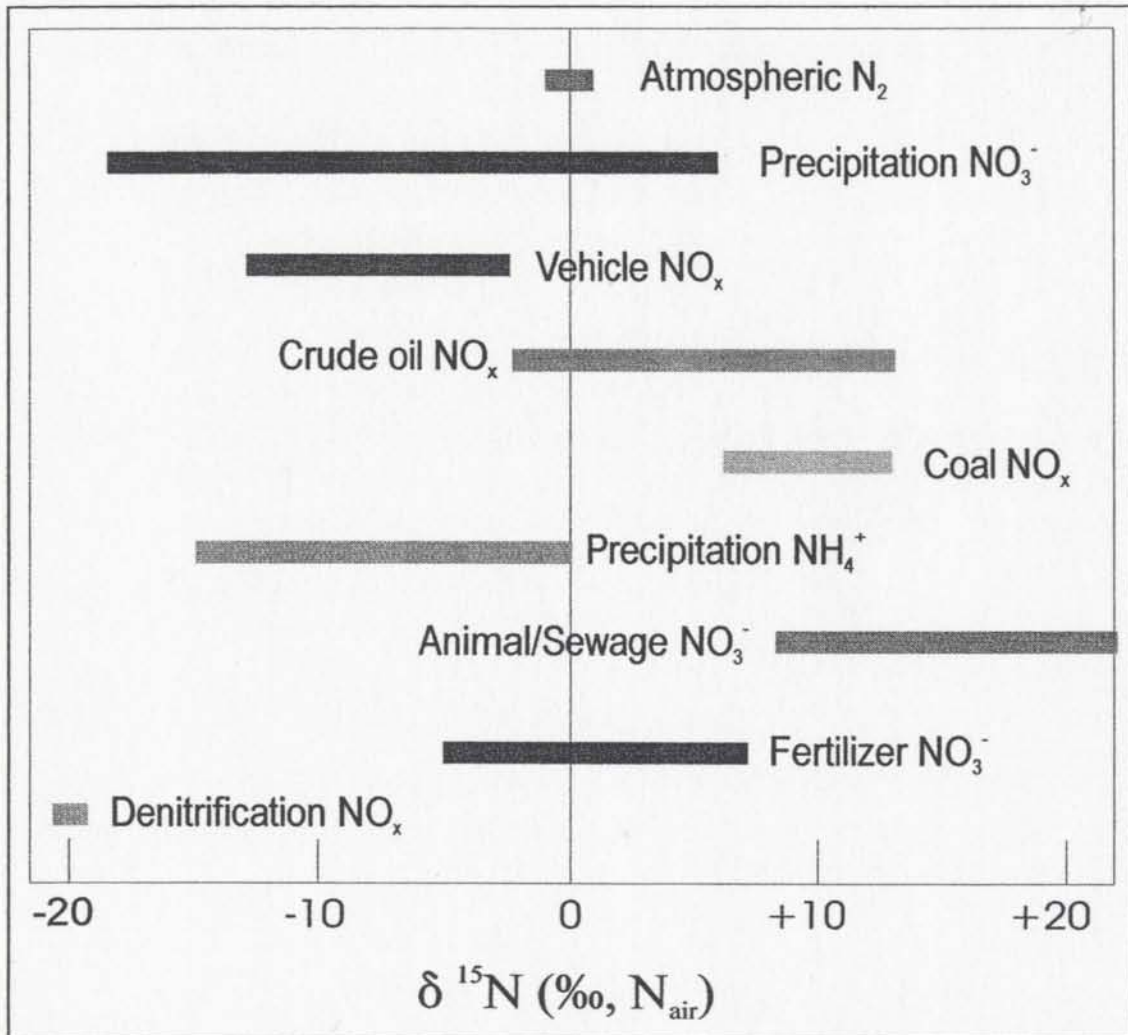


Figure 1.5 $\delta^{15}\text{N}$ of various important nitrogen species (from Heaton, 1986, 1987, 1990; Freyer 1991).

high temperatures, and involves the oxidation of fuel nitrogen, which has a $\delta^{15}\text{N}$ of -2‰ to $+13\text{‰}$, along with atmospheric nitrogen (Freyer, 1991). Because little fractionation occurs during this process, the pollutant NO_x emitted may have values similar to that found in the oil (Heaton, 1987). Heaton (1990) measured NO_x emitted during coal combustion and found values of $+6$ to $+13\text{‰}$, while the coal itself had a $\delta^{15}\text{N}$ of -2 to $+3\text{‰}$. He observed that little thermal NO was produced due to the fact that the combustion temperatures in coal-fired power plants were too low for this process to occur. All of the NO_x produced was therefore derived from the fuel nitrogen. He speculated that at post-combustion temperatures, ^{14}NO was destroyed more rapidly than ^{15}NO , causing the remaining NO to become progressively enriched in the heavier isotope. Figure 1.6 depicts the atmospheric nitrogen cycle with the $\delta^{15}\text{N}$ values of the various sources of NO_x emissions.

Several researchers have measured the nitrogen isotopic signatures of atmospheric nitrate in the past. The ^{15}N values of precipitation nitrate from various studies range from -18‰ to $+6\text{‰}$ (Figure 1.7).

1.2.3.3 Oxygen Isotopes (Nitrate)

Oxygen isotopes of atmospheric nitrate can provide information about transformations that have occurred to the compound. The oxygen isotopic composition of nitrate may be determined by the source of NO_x to the atmosphere. Another possible control of the $\delta^{18}\text{O}$ of nitrate is the oxidation processes which the compound has

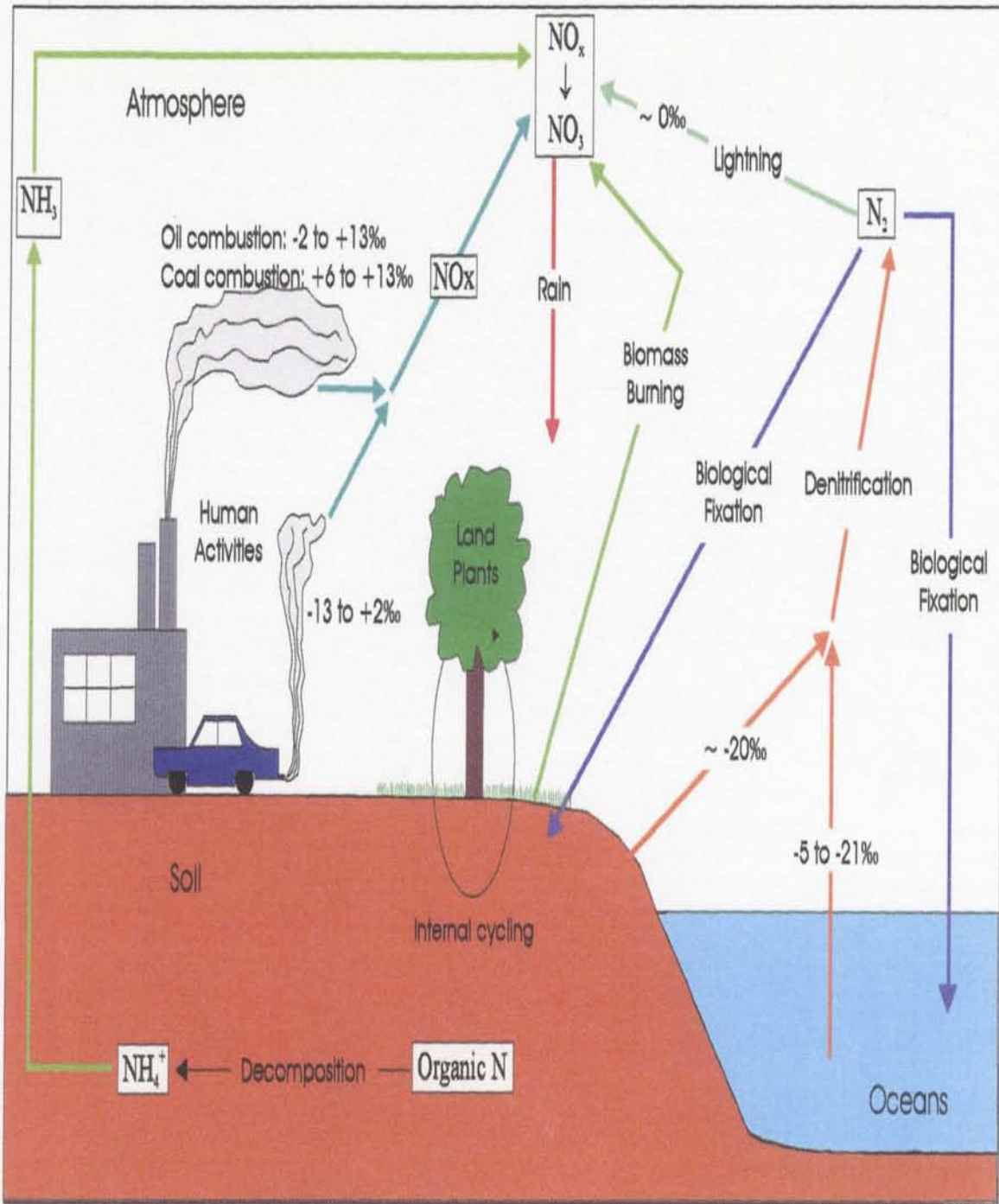


Figure 1.6 Atmospheric nitrogen cycle with nitrogen isotopic values for NO_x emissions (Values from Hoering (1957), Heaton (1990), Myiake and Wada (1971) and Freyer et al. (1993)).

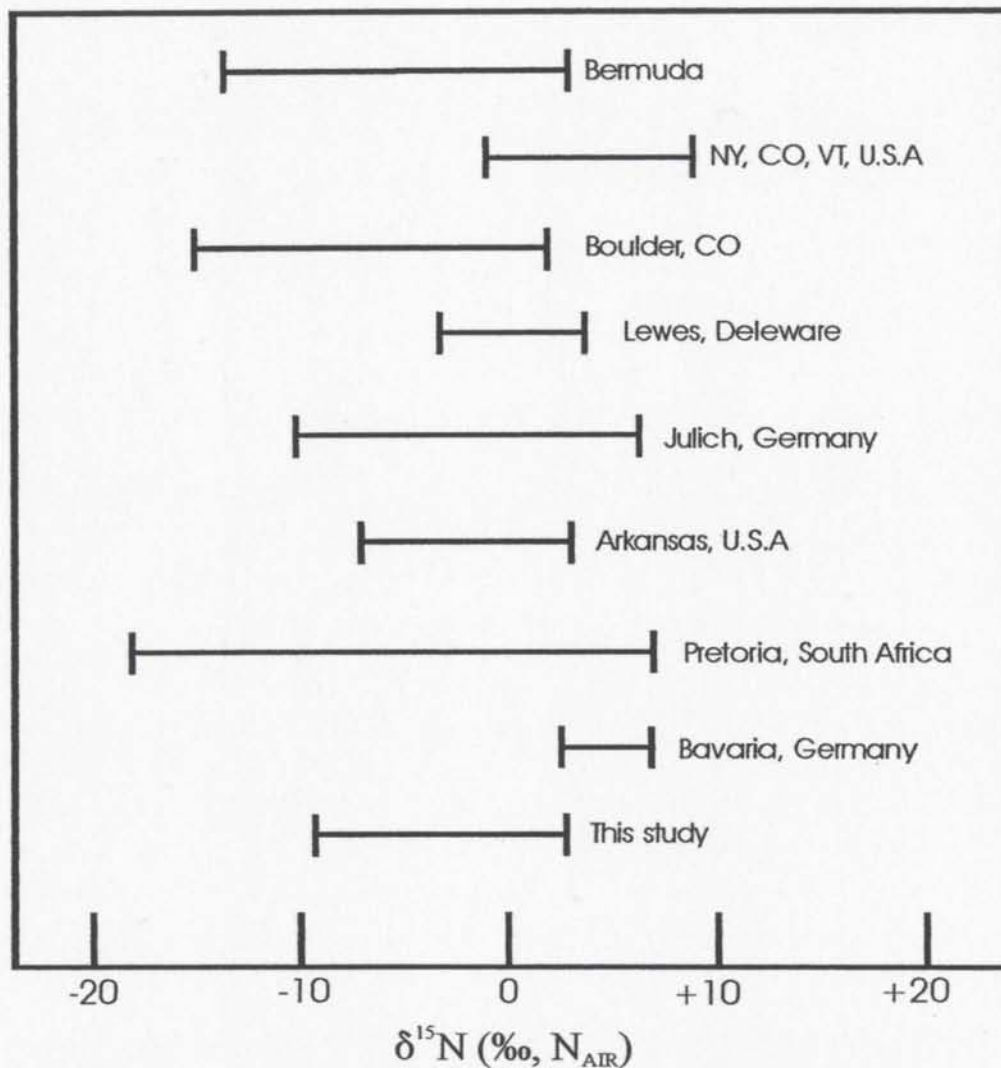


Figure 1.7 $\delta^{15}\text{N}$ nitrate values from various precipitation studies. Data from: Moore (1974, 1977) Colorado, Hoering (1957) Arkansas (bulk collection), Freyer (1978) Julich (bulk collection), Heaton (1987) South Africa (single events), Durka et al. (1994) Bavaria, Kendall et al. (1995b) NY, CO, VT (snow), Russell et al. (1998) Delaware (daily basis), and Hastings et al. (2003) Bermuda (daily basis).

undergone. Therefore $\delta^{18}\text{O}$ may reflect the source of the oxygen or the oxidation processes involved in the creation of the nitrate.

The three stable isotopes of oxygen, ^{16}O , ^{17}O and ^{18}O , have natural abundances of 99.763%, 0.0375% and 0.1995% respectively. In isotopic studies, the $^{18}\text{O}/^{16}\text{O}$ ratio is normally determined due to the higher abundance of these two isotopes and the greater mass difference between them (Hoefs, 1987).

Few $\delta^{17}\text{O}$ measurements have been made in nitrate due to the fact that fractionation processes were expected to affect the ^{17}O and ^{18}O in a predictable manner based on the relative difference in mass between the two isotopes. In recent years, however, mass-independent $\Delta^{17}\text{O}$ ($\Delta^{17}\text{O} = \delta^{17}\text{O} - 0.52 \times \delta^{18}\text{O}$) anomalies have been measured in rainwater nitrate. Because $\Delta^{17}\text{O}$ is not affected by fractionations associated with post-depositional nitrate transformation as is the case with $\delta^{18}\text{O}$, it may become a more sensitive and reliable tracer for environmental nitrate studies (Michalski et al., 2002). This new development currently has more applications in ground water studies, but may prove to be useful in atmospheric studies in the future.

The oxygen atoms in nitrate are thought to be derived from both atmospheric O_2 (+23.5‰) and environmental H_2O (normal range of -30 to +5‰). However, a much larger range of +18 to +86.5‰ has been found in studies from Germany, Bermuda and the United States (Figure 1.8). This larger range of oxygen isotopic values from nitrate indicates that fractionation of the oxygen isotopes from their source compositions may occur during atmospheric processes (Kendall, 1998 and sources therein).

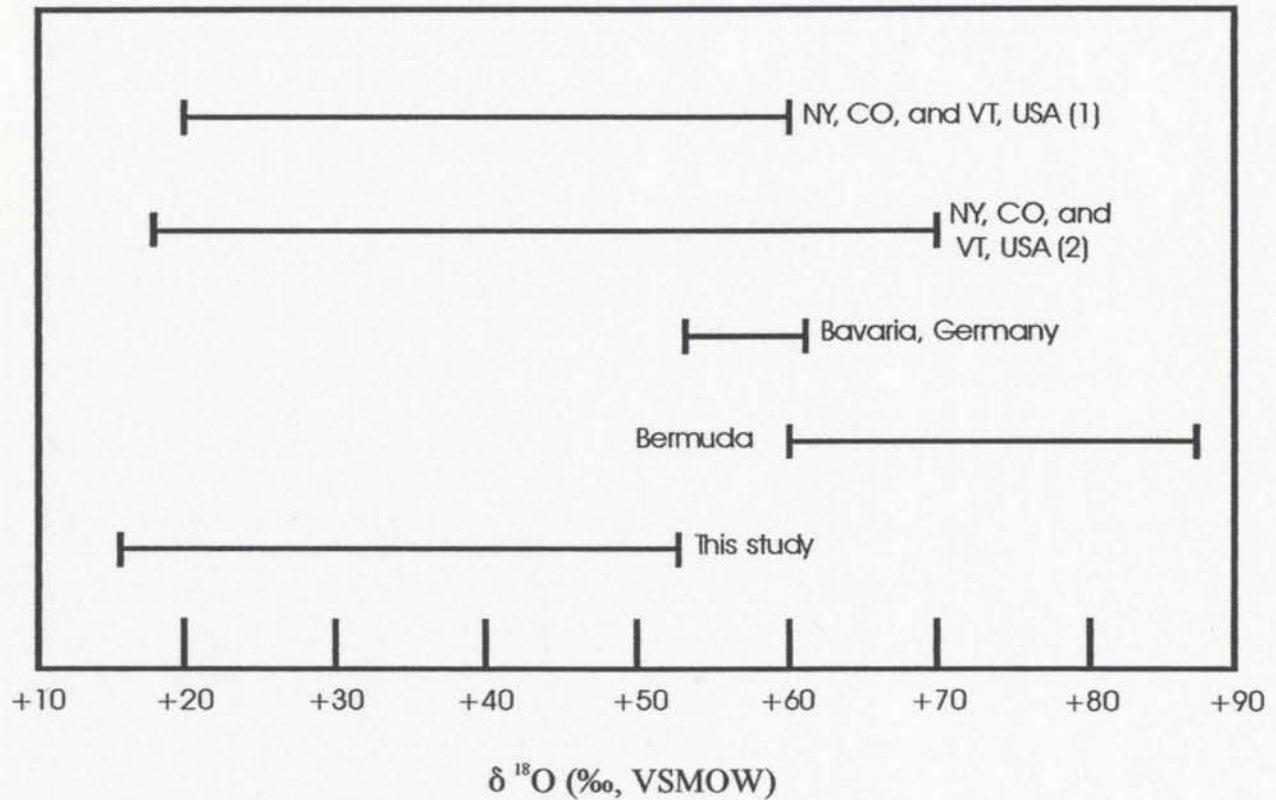


Figure 1.8 $\delta^{18}\text{O}$ nitrate values from various precipitation studies. Data from: Durka et al. (1994) Bavaria, Kendall et al. (1995b) NY, CO, VT (1) (snow), Kendall (1998) NY, CO, VT (2), and Hastings et al. (2003) Bermuda (daily basis).

Other possible explanations for the large range in $\delta^{18}\text{O}$ values are fractionation processes during the formation of nitrate in thunderstorms, incomplete fossil fuel combustion in both vehicle exhaust and power plants, as well as photochemical reactions in the atmosphere. The various oxidants in the atmosphere have different oxygen isotopic compositions (Table 1.1). Tropospheric O_3 has a $\delta^{18}\text{O}$ of $\sim+90$ to $+122\text{‰}$ (Krankowsky et al. (1995); Johnston and Thiemens, 1997). If ozone is the dominant oxidiser of NO_x prior to nitrate deposition (Reaction 1.2), the $\delta^{18}\text{O}$ value of the nitrate will reflect the isotopic composition of the ozone. Another species involved in the oxidation of atmospheric NO_x is the hydroxyl radical (Reaction 1.4). The majority of atmospheric OH is formed through the photolysis of ozone (Reactions 1.9 and 1.10) and may initially reflect the isotopic composition of ozone. However, Röckmann et al. (1998) believed that a fast isotopic exchange between the hydroxyl radical and tropospheric water vapour ($\delta^{18}\text{O}$ typically -30 to $+5\text{‰}$) may occur, resulting in the OH isotopic composition reflecting that of the H_2O . Reactions involving NO_x and OH would therefore result in nitrate with much lower $\delta^{18}\text{O}$ values than reactions involving O_3 . A third atmospheric constituent which may be involved in the formation of NO_3^- is the peroxy radical (Reaction 1.3), which might compete with ozone in the oxidation of NO to NO_2 . The oxygen atoms of the HO_2 molecule are believed to come from atmospheric O_2 ($+23.5\text{‰}$) and would therefore reflect this isotopic composition (Hastings et al., 2003, and sources therein). The varying isotopic compositions of atmospheric oxidants involved in the formation of nitrate may lead to the large range of $\delta^{18}\text{O}$ values of precipitation nitrate measured from

Table 1.1 $\delta^{18}\text{O}$ of some common atmospheric oxygen species.

Oxygen species	$\delta^{18}\text{O}$ (‰, VSMOW)	Reference
O_2	+23.5‰	Kendall (1998)
H_2O	-30 to +5‰	Kendall (1998)
O_3	~+90 to +122‰	Krankowsky et al. (1995); Johnston and Thiemens (1997)

various studies.

1.2.3.4 Oxygen Isotopes (Water)

The stable isotopic composition of the two oxygen atoms of a water molecule can be measured. The main controls on the $\delta^{18}\text{O}$ value of precipitation in an air mass at a given location are the temperature of condensation of the water, as well as the degree of rain-out which has occurred in the air mass (Kendall et al., 1995a). The condensation temperature of the water controls the fractionation factor associated with the formation of the precipitation; as the temperature decreases, the fractionation factor increases resulting in a more depleted ^{18}O value for the precipitation (Dansgaard, 1964). As a result, summer rain is isotopically more enriched in ^{18}O than winter rain.

Water droplets formed from condensing atmospheric water vapour do not remain in equilibrium with the vapour. The amount of precipitation which has condensed and been removed from an air mass also affects the ^{18}O composition of the rainwater or snow. The heavier oxygen isotope preferentially condenses in the precipitation. This fractionation and continuous removal of the heavier isotopes in the liquid phase, known as a Rayleigh fractionation, results in a characteristic trend in isotopic composition. As the precipitation continues to condense out of the air mass and is removed, the remaining water vapour becomes progressively more depleted in ^{18}O , resulting in isotopically lighter rainfall over the duration of the event (Kendall et al., 1995a). Figure 1.9 is an illustration of the trends in precipitation $\delta^{18}\text{O}$ in North America due to the combined effects of

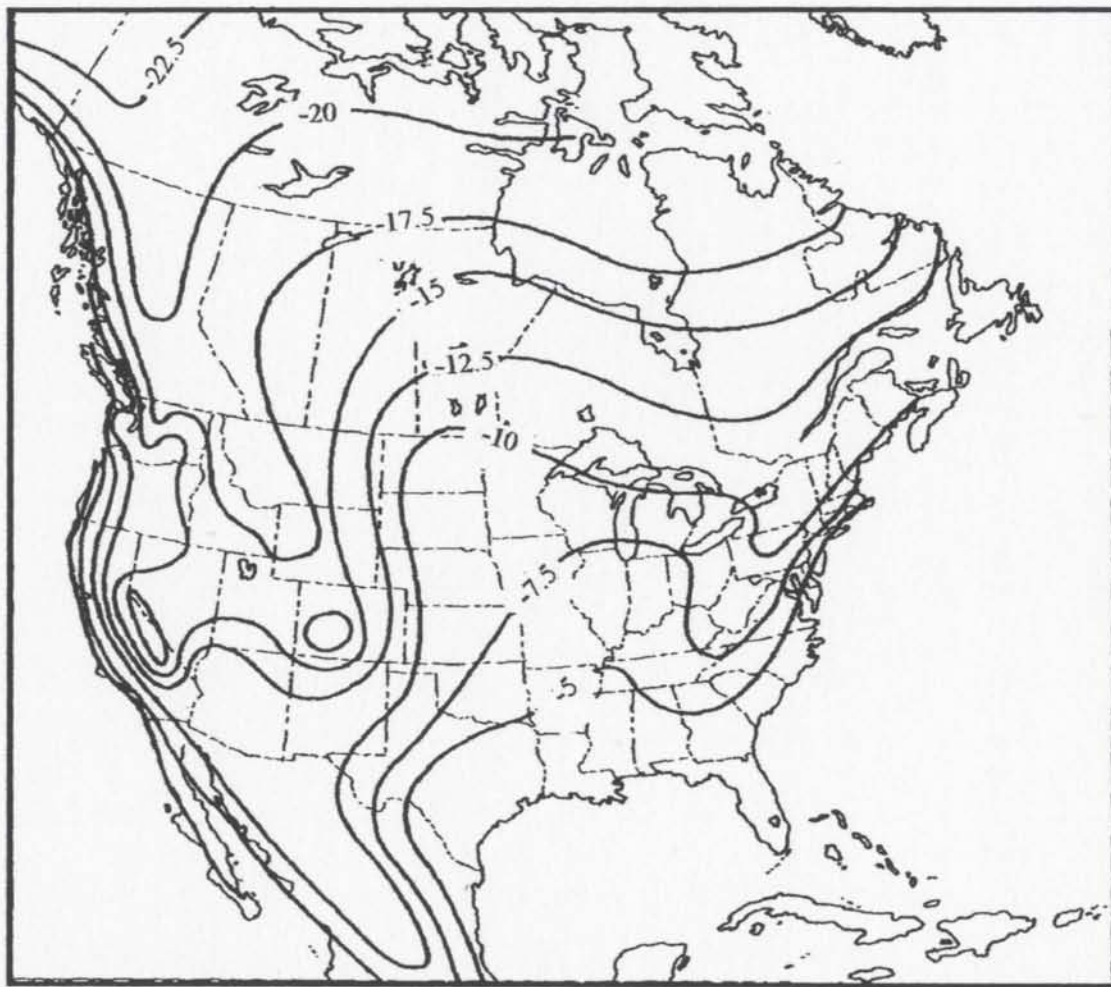


Figure 1.9 Distribution of $\delta^{18}\text{O}$ in North American meteoric waters (‰, VSMOW) (from Drever, 1982).

Rayleigh fractionation and temperature. The rain generally becomes progressively depleted in ^{18}O from the coast inland, from the equator towards the poles and from lower to higher elevations. The normal range of environmental water reported by Kendall (1998) is -30 to +5‰.

The oxygen isotopic composition of precipitation may be compared with the oxygen signature of the nitrate collected from the rain. If a relationship between the two measurements is found, it may indicate that the water vapour in the air mass was an oxidant involved in the formation of the nitrate.

1.3 Chemical Composition of Precipitation

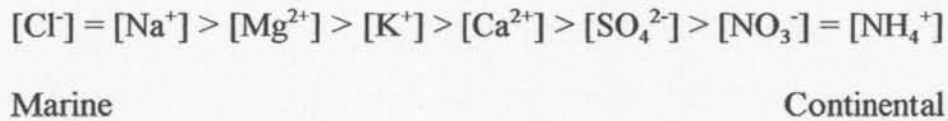
Stable isotopes are a useful tool in precipitation tracer studies. The chemical composition of the rainwater used in conjunction with stable isotopic values increases a researcher's ability to delineate sources for a particular rain event. In the past, the chemical composition of rain has been used to differentiate between marine and continental sources or natural and anthropogenic sources.

Rainwater is a dilute solution of elements. The dilution effect is a result of how the rain forms naturally in the atmosphere, a process which Berner and Berner (1996) view as purifying the water via natural distillation. Rainwater is commonly composed of major ions such as Na^+ , Cl^- , Mg^{2+} , Ca^{2+} . These ions can be classified as being typically marine or continental in nature. Table 1.2 contains typical ion concentrations of marine and continental rain. Marine rain is commonly dominated by Na^+ and Cl^- , while terrestrial rain

Table 1.2 Typical ionic concentrations in marine and continental rain (in mg/l) (from Berner and Berner, 1996).

Ion	Marine/Coastal Rain	Continental Rain
Na ⁺	1-5	0.2-1
K ⁺	0.2-0.6	0.1-0.3
NH ₄ ⁺	0.01-0.05	0.1-0.5
Mg ²⁺	0.4-1.5	0.05-0.5
Ca ²⁺	0.2-1.5	0.1-3.0
H ⁺	pH = 5-6	pH = 4-6
Cl ⁻	1-10	0.2-2
NO ₃ ⁻	0.1-0.5	0.4-1.3

contains more soil derived species such as Ca^{2+} and K^+ (Berg et al., 1995; Berner and Berner, 1996; Garty et al., 2001). Marine species are more important near the coast, where their concentrations are greatest. As the distance from the coast increases, the marine ion concentrations level off and terrestrial-sourced ions become more important. Typical concentrations when moving from a marine to a terrestrial environment are as follows:



Not all of these elements come from natural sources. Anthropogenic inputs such as biomass burning and fossil fuel combustion (NO_3^- , SO_4^{2-}) and industrial processes (e.g. industrial HCl) can contribute to the mixture of continental sources (Berner and Berner, 1996).

Major ion ratios in rainfall can be compared with those of sea water to determine how much of a species is derived from seaspray. This percent seaspray (PSS) calculation is performed by comparing the ratio of the species of interest (for example, sulphate) to a reference species as follows:

$$\text{PSS} = \left[\frac{(\text{SO}_4/\text{X})_{\text{seawater}}}{(\text{SO}_4/\text{X})_{\text{rain}}} \right] \times 100$$

where X is the concentration of the reference species (Jamieson and Wadleigh, 1999). The

reference species, usually Cl^- or Na^+ , is assumed to be conservative. That is, all of the Cl^- or Na^+ found in the precipitation is assumed to have come from seaspray. Cl^- may be introduced to the atmosphere through anthropogenic activities, so Na^+ is often used in PSS calculations. The seawater ratio of SO_4^{2-} to Na^+ is 0.252 (Savoie and Prospero, 1989). If $(\text{SO}_4/\text{X})_{\text{rain}} > 0.252$ then the SO_4 in the rain must come from additional sources, such as other natural or anthropogenic inputs. This calculation can be performed for other elements to determine importance of seaspray to their concentrations.

Other important constituents of precipitation are trace metals, which can be natural or anthropogenic in origin. Anthropogenic sources tend to be dominant for most metals in the atmosphere. However, natural emissions are thought to control the atmospheric concentrations of Se, As, Hg and Cd. There is a lack of data available about the quantity of such emissions, therefore estimates of emission rates or fluxes are not confirmed by measurements (Pacyna, 1986a).

There are several natural sources of trace metals to the atmosphere, the most common of which are wind erosion, volcanoes, forest fires, vegetation and seaspray (Pacyna et al., 1984; Pacyna, 1986a). Table 1.3 is a summary of planetary emissions of trace metals from natural sources. The dominant natural sources are windblown dust and volcanic particles. Extensive studies on both of these sources have been performed, however it is very difficult to measure the natural emissions. Migon and Caccia (1990) noted that rocks and soils have a greater natural abundance of heavy metals such as Pb, Cu, Zn and Cd than marine sources, resulting in continental areas exhibiting higher

Table 1.3 Planetary emissions of trace metals from natural sources (from Pacyna, 1986b)

	Windblown dust	Volcanic particles	Forest wild-fires	Vegetation	Seasalt	Total
Global production ($\times 10^9$)(kg/y)	6-1100	6.5-150	2-200	75-1000	300-2000	
As	0.24	7	0.16	0.26	0.14	7.8
Cd	0.25	0.50	0.01	0.2	0.002	0.96
Co	4	1.4				5.4
Cu	12	4	0.3	2.5	0.1	18.9
Cr	50	3.9				8.9
Mn	425	82		5	4	516
Ni	20	3.8	0.6	1.6	0.04	26
Pb	10	6.4	0.5	1.6	0.1	18.6
Se	0.3	0.1				0.4
V	50	6.9		0.2	9	66.1
Zn	25	10	0.5	10	0.02	4
Hg	0.03	0.03	0.1		0.003	0.16

All units in 10^6 kg except where indicated

concentrations of these elements in comparison to marine sites. Volcanic emission rates from individual volcanoes can vary greatly, making detailed calculations difficult.

Vegetation plays a somewhat important role in the emissions of Cu, Pb and Zn, while forest wildfires do not contribute a significant amount of metals to the atmosphere relative to other sources. Seaspray may introduce a minor amount of metals to the atmosphere through bubble bursting and gas exchange (Pacyna, 1986b).

Anthropogenic sources of metals to the atmosphere are much larger than their natural counterparts. The majority can be attributed to fossil fuel combustion (both stationary and mobile), metal processing and smelting and various industrial processes. The burning of fossil fuels is having a large impact on atmospheric chemistry. The element concentrations in crude oils vary depending on their source regions. In general, heavier oils contain higher amounts of trace metals (Pacyna, 1986a). Fossil fuel combustion results in the release of V, Ni, Co, Cu, Mo, Pb and Zn to the atmosphere (Pacyna et al., 1984; Pacyna, 1986a; Sloof, 1995; Nygård and Harju, 1983). Petroleum contains fairly high concentrations of vanadium while the metal occurs only sparsely in the natural environment. Because of this, V is used as a tracer of oil combustion processes (Nygård and Harju, 1983; Sloof, 1995; Garty et al., 2001). Ganor et al. (1988) believe that Ni behaves similarly to V.

Automobile exhaust is an important contributor to several atmospheric elements, especially Mn (Loranger and Zayed, 1994). Prior to 1990, Pb was added to gasoline as an antiknock agent. During the 1970's and 1980's, Pb was often used as a tracer for

automobile input to the atmosphere. An organic derivative of manganese was introduced to replace Pb as a gasoline additive in Canada in 1976, and completely replaced Pb as an antiknock agent by 1991 (Loranger and Zayed, 1994). Mn may now be used as a tracer of automobile pollution to the atmosphere, although Pb is still present in unleaded automobile exhaust (Que Hee, 1994). Vehicular traffic can also contribute Zn, which is added as a metal compound to lubricants (Pacyna, 1986a) and has been found in tire and brake lining abrasion (Huhn et al., 1995).

Metal processing and smelting can release trace elements to the air. Zn, Cd, As, Cu, Pb, Cr and Mn are emitted during mining, smelting processes and metal manufacturing (Pacyna et al., 1984; Pacyna, 1986b; Sloof, 1995). Incineration of large amounts of solid waste may lead to an increase in atmospheric Cd, Co, Cs and Sc, along with the volatile elements As, Sb and Se (Sloof, 1995). Several factors affect trace metal emissions from refuse incineration, including the design of the incinerator chamber, the chemical composition of the waste material, the amount of combustible and noncombustible material and the presence and efficiency of any control devices (Pacyna, 1986a). Residential wood burning may have an environmental impact, especially in more rural areas. The burning of wood in stoves and fireplaces can release significant amounts of Zn, Cu, Pb and Ni into the atmosphere (Pacyna, 1986a). Galloway et al. (1982) compiled a list of toxic element concentrations in wet deposition for urban, rural and remote areas from numerous studies, which can be seen in Table 1.4. The large ranges of values may indicate different natural and/or anthropogenic sources present in the study

Table 1.4 Median values and ranges of trace metals in precipitation (ppb) (from Galloway et al., 1982)

	Urban		Rural		Remote	
	Median	Range	Median	Range	Median	Range
As	5.8	5.8	0.286	0.005-4	0.019	0.019
Cd	0.7	0.48-2.3	0.5	0.08-46	0.008	0.004-0.639
Cr	3.2	0.51-15	0.88	< 0.1-30		
Co	1.8	1.8	0.75	0.01-1.5		
Cu	41	6.8-120	5.4	0.4-150	0.060	0.035-0.85
Pb	44	5.4-147	12	0.59-64	0.09	0.02-0.41
Mn	23	1.9-80	5.7	0.2-84	0.194	0.018-0.32
Hg	0.745	0.002-3.8	0.09	0.005-2.2	0.079	0.011-0.428
Mo	0.20	0.20				
Ni	12	2.4-114	2.4	0.6-48		
Ag	3.2	3.2	0.54	0.01-0.48	0.007	0.006-0.008
V	42	16-68	9	0.13-23	0.163	0.016-0.32
Zn	34	18-280	36	<1-311	0.22	0.007-1.1

Note: Mn had not replaced Pb as a gasoline additive at the time of this study

areas, or it may indicate long range transport of some metals from distant sources. Many metals, such as Zn, can be emitted by a number of sources. By looking at combinations of certain metals, a pattern may emerge indicating specific sources for the metals.

It is obvious that anthropogenic activities impact the trace metal composition of the atmosphere. While some of the trace metals do occur naturally, most increases are due to human activities. Historical evidence from ice cores, soils and lake sediments all show an increase in trace metals in the environment (Galloway et al., 1982). The study of enrichment factors and mobilization factors are other methods used, along with historical evidence, to examine the impact humans have had on trace metal concentrations in the atmosphere.

Enrichment factors are used to compare atmospheric trace metal concentrations to concentrations found in the crust. The enrichment factor (EF) for a particular element is calculated using the formula:

$$EF = \frac{(X/R)_{air}}{(X/R)_{crust}}$$

where X is the species of interest and R is a reference species (Galloway et al., 1982). The most commonly used reference material is Al, a prevalent crustal element. If an enrichment factor greater than one is calculated, it indicates that the atmosphere is enriched in the metal relative to the crust, implying that the metal has a different and/or

additional source other than the crust. If the $EF = 1$, the metal is not enriched in the atmosphere relative to the crust, indicating that the metal came from the crust. Crustal compositions vary in different study areas, introducing some uncertainty into this type of calculation. If improper reference material values are used, the calculated EF may be misleading.

Mobilization factors (MF) are used to compare the emission rates of natural and anthropogenic sources on a global scale. The MF is calculated by dividing the emission rate from human sources by the emission rate from natural sources, both of which are global emission rates. The calculation can also be performed on a more regional scale (Galloway et al., 1982).

The relative influence of anthropogenic activities on atmospheric trace metal concentrations can be seen in Table 1.5. The relative impacts of the elements were determined using enrichment factors and mobilization factors along with historical techniques which examine atmospheric deposition preserved in glaciers, peat bogs, soils and lake sediments (Galloway et al., 1982). Elements such as Cd, Pb, Cu and Zn are expected to have large enrichments, while V and Cr are in the moderate enrichment category. Ni, Co and Mn are expected to be impacted on a lower level. The expected enrichments are not surprising as anthropogenic activities are increasing worldwide. It is worth noting that these values were obtained prior to 1991 when Pb was replaced by Mn as an antiknock agent in gasoline. If an MF and EF were calculated using present day concentrations, one could imagine that Mn may be in the moderate to high category.

Table 1.5 Influence of anthropogenic emissions on atmospheric trace metal concentrations estimated through three techniques (Galloway et al., 1982)

Technique	Expected enrichment			
	Low	Moderate	Large	No data
Enrichment Factor	Co, Mn, Ni	Cr, V	Cd, Cu, Pb, Sb, Se, Zn	Ag, As, Be, Hg, Mo, Sn, Te, Tl
Mobilization Factor	Co, Mn, Hg	As, Cr, Ni, Se, V	Ag, Cd, Cu, Mo, Pb, Sb, Se, Sn Zn	Be, Te, Tl
Historical Factor	Co, Mn, Ni, Be	Cr, V, Cu, Ag, Zn, Se	As, Cd, Pb, Sb	Mo, Sn, Te, Tl, Hg

Note: Low \leq 2x enrichment, moderate = 2 to 4x and large \geq 4x

CHAPTER 2

METHODS

2.1 Sample Sites

Two sample sites located in Newfoundland were chosen for this study: St. John's (47°N, 52°W) and McIvers (49°N, 58°W) (Figure 2.1). Both represent coastal sites, with St. John's being a more urban and McIvers a more rural location.

2.1.1 St. John's

St. John's is located on the east coast of the province of Newfoundland and Labrador, and is the capital city of the province. The city has a population of about 173 000, with no heavy industrial activities. Because St. John's is a coastal city, a strong marine influence was expected. This site represents a marine/urban location. There are no major point sources of pollution in the city, however the Come by Chance oil refinery is located approximately 100 km from St. John's, while the Holyrood Generating Station is about 33 km away (Figure 2.1).

A collector was set up on the campus of Memorial University of Newfoundland. It was located in a weather station compound on the west side of the campus near a small oil-fired power plant. This plant, which burns approximately 7.5 million litres of Bunker C oil each year, provides heat and emergency power year round to the campus and nearby hospital. The oil burned at this facility contains approximately 300 ppm vanadium and

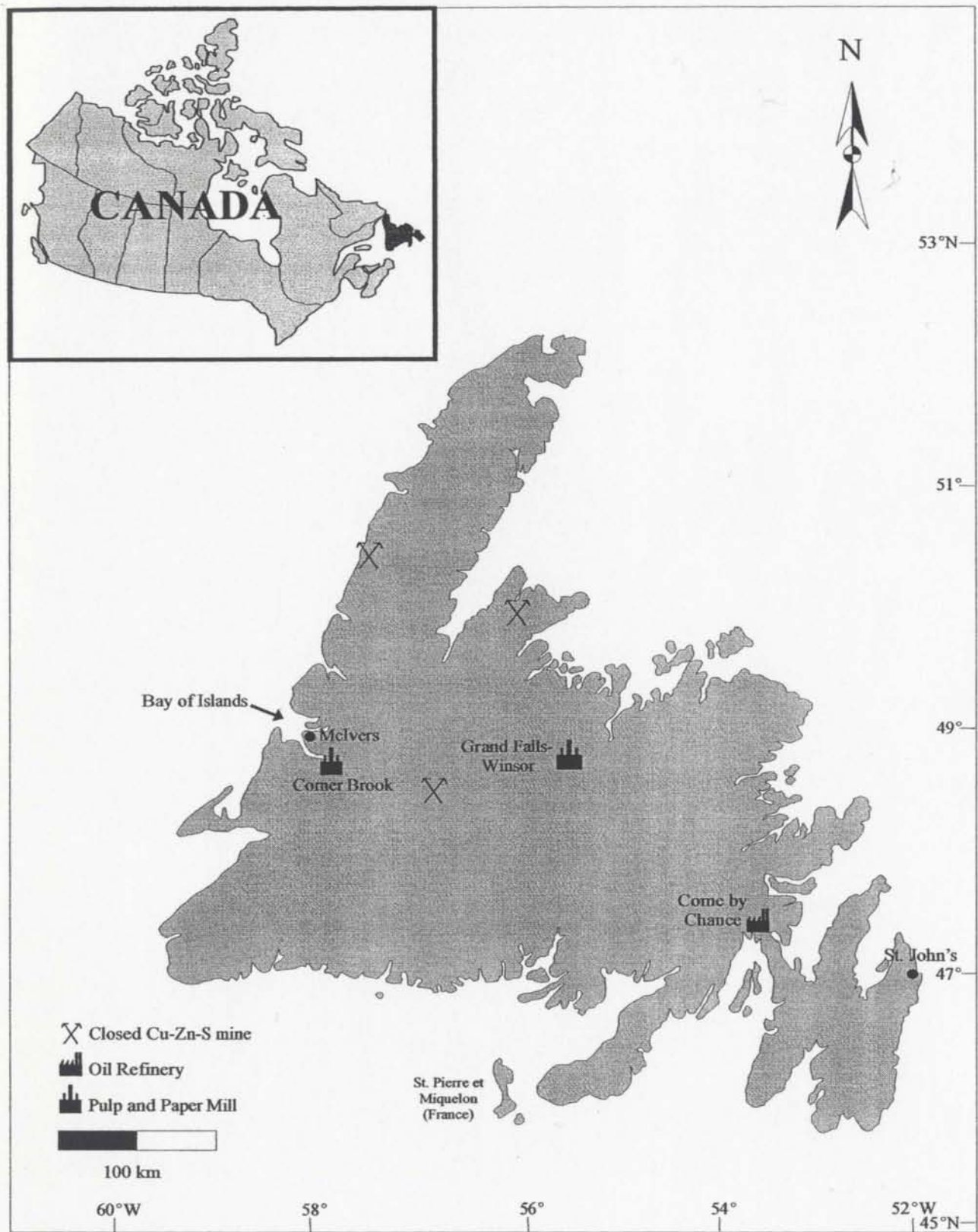


Figure 2.1 Map of Newfoundland showing sampling locations and major anthropogenic sources.

2.98 wt.% sulphur (John Dunne, pers. comm. 2003). The power plant emits less than 1000 tonnes of SO₂ annually (Jamieson and Wadleigh, 1999). There is an increase in oil combustion during the colder months of the year. Because the collector is located close to a major roadway, some automobile pollution is also expected. A wooded area extends for about 3 or 4 kilometres behind the collection site as part of C.A. Pippy Park. The Outer Ring Road, a major highway, was recently constructed within the park and is approximately 1.5 km away from the collection site.

Snow samples were collected about 1 km from the MUN sample site. This site, located in Pippy Park, was in front of the Pippy Park Administration Building, an area of little vehicular traffic.

2.1.2 McIvers

The town of McIvers is located in the Bay of Islands along the province's west coast (Figure 2.1). This small town, with a population of about 1000 people, is one of many located along the coastline throughout the Bay of Islands. There are no major pollution sources in the community itself, however a large pulp and paper mill operates in the city of Corner Brook, approximately 30 km to the southeast of McIvers. This mill, which burns Bunker C fuel (Norcliffe and Bates, 1997) operates year round and represents a potential anthropogenic pollution source to the area. Being located along the coast, the McIvers site is expected to have a strong marine influence, however it may be heavily influenced by the anthropogenic urban pollution from Corner Brook or long range

transport pollution from the rest of Canada and the United States. The only other sources of pollution in the town would be from motor vehicles and the burning of oil and wood for home heating. A collector was located in an open field near some houses within the town. Because this site is not located on a main road, there is little vehicular traffic. Snow samples were collected near the collector within the same field.

2.2 Sample Collection

Single event samples were collected for this study using rain collectors constructed out of wood and completely lined with 6 mil polyethylene sheeting to prevent contamination of the samples. As can be seen in the picture (Figure 2.2), the collector was built with one end lower than the other to ensure all sample would run down the collector and into a polyethylene cubitainer. A funnel, also lined with 6 mil polyethylene sheeting, was placed at the bottom of the collector. In order to ensure that enough rain was collected from each event, the collectors were designed with a 1 m² collection area, which collects 1 L of sample for every millimetre of rainfall. A lid, also lined with polyethylene plastic, is placed over the collector between sample periods to eliminate dry deposition to the collection surface. Upon the approach of a rainfall, the lid is removed from the collector and the collection surface is rinsed thoroughly with deionised and distilled water. The rain then flows down the collector, through the funnel and into a clean 20 L polyethylene cubitainer.



Figure 2.2 Rain collector used in this study.

2.3 Chemical Analysis

Every sample had a 500 ml aliquot removed for chemical analysis, as well as a 25ml aliquot for oxygen isotope analysis of water. The aliquots were taken as soon as the sample was collected from the St. John's site, and removed from McIvers samples upon their arrival at the laboratory.

2.3.1 pH and Conductivity

The pH of each sample was measured in the lab using an Orion model 290A pH Meter with Ross pH Combination Electrodes. The meter was calibrated for each use with two buffering solutions of pH 4 and 7. Conductivity was measured in the lab with an Orion model 122 Conductivity Meter, which has an accuracy of $\pm 0.5\%$ of the measured reading (Model 122 and 123 Conductivity/Temperature Meter Hand-held Set Instruction Manual, Orion). The probes of both instruments were thoroughly rinsed with distilled and deionised water between samples.

2.3.2 Ion Chromatography

Samples were analysed for anions using a Dionex DX-100 Ion Chromatograph. The concentrations of Cl^- , NO_3^- and SO_4^{2-} were measured using an IonPac AS4A-SC analytical column with an IonPac AG4A-SC Guard column and a Dionex ASRS-Ultra 4 mm suppressor. These analyses were performed using suppressed conductivity detection, with an eluent made of 1.8 mM Na_2CO_3 /1.7 mM NaHCO_3 solution. Details of the

instrumentation and procedure can be found in DX-100 Ion Chromatograph Operator's Manual (1991).

Cations concentrations were determined using the same instrument fitted with an IonPac CS12A Analytical column, IonPac CG12A Guard column and a Dionex CSRS-Ultra 4 mm suppressor. The analyses of Na^+ , NH_4^+ , K^+ , Mg^{2+} and Ca^{2+} were performed using a 20 mM H_2SO_4 eluent.

Calibration standards were prepared for both methods using NIST prepared standard solutions. Five standards with concentrations ranging from 0.1 ppm to 2 ppm were used to calibrate the instrument for anion analysis, while four calibration standards were used for the cation method, and ranged from 10 ppm to 1 ppm. The r^2 values calculated for each calibration set ensured that the calibrations were linear over the range of interest. The overall accuracy of the instrument, checked using QCPlus⁺ Rainwater Standard, was better than 8% for all ions. The overall precision for the instrument ranged from 1 to 12% for the eight ions measured.

2.3.3 Inductively Coupled Plasma - Mass Spectrometry

Measurement of 39 elements was performed using a HP 4500 ICP-MS located at Memorial University of Newfoundland Earth Sciences Department. The elements measured included Li, Be, B, Mg, Al, Si, P, S, Cl, Ca, Ti, V, Cr, Mn, Fe, Co, Ni, Cu, Zn, As, Se, Br, Rb, Sr, Mo, Ag, Cd, Sn, Sb, I, Cs, Ba, La, Ce, Hg, Tl, Pb, Bi and U. 10 ml of sample was filtered through a 0.45 μm filter and acidified with 100 μL of distilled 8 N

HNO₃. A 1 ml aliquot is then removed and diluted 10 fold with nitric acid. The sample is then placed in a 10 ml test tube and introduced into the ICP-MS via a CETEC autosampler. A description of this method can be found in Yun et al. (2003).

Data is acquired in cycles of 14 samples, with five different calibration standards analysed in each cycle. Each calibration standard is made up of a suite of elements which will not cause interelemental spectroscopic interferences. One blank is also run in each cycle to allow for background correction. Background noise, used to calculate the limits of detection for a run, may vary between runs. As a result, the limits of detection for different runs may vary. Samples for this study were run on seven different days. The ranges of detection limits acquired for elements of interest are shown in Table 2.1. The precision and accuracy of this analytical technique are examined by analysing reference materials of known composition, such as USGS waters T137 and T143. The precision for this method, calculated as the relative standard deviation (RSD), ranged between 0.2 and 24% (Table 2.2).

There are several elements which have more than one isotope measured by the ICP-MS. The concentration for that particular element is calculated based on which isotope has a better limit of detection and whether or not there are interferences associated with that particular isotope. The four elements with multiple isotopes measured are Li, Ca, Cr and Fe. Calcium (as well as magnesium) is measured by ion chromatography, so the ICP-MS results will not be used for these ions.

Table 2.1 Ranges of ICP-MS detection limits for elements of interest.

Element	Det Limit Range (ppb)	Element	Det Limit Range (ppb)
Al	0.35 - 1.59	As	0.02 - 0.40
V	0.20 - 0.89	Sr	0.01 - 0.04
Cr	0.09	Mo	0.01 - 0.07
Mn	0.05 - 0.34	Ag	0.004 - 0.14
Co	0.01 - 0.09	Cd	0.01 - 0.06
Ni	0.25	Ba	0.08 - 0.78
Cu	0.11 - 1.29	Pb	0.02 - 0.27
Zn	0.87		

Table 2.2 Relative standard deviation of ICP-MS technique for elements of interest.

Element	RSD	Element	RSD
Al	0.04 - 0.22	As	0.04 - 0.24
V	0.02 - 0.11	Sr	0.02 - 0.10
Cr	0.005 - 0.009	Mo	0.02 - 0.09
Mn	0.01 - 0.10	Ag	0.02 - 0.12
Co	0.08 - 0.11	Cd	0.02 - 0.09
Ni	0.002 - 0.03	Ba	0.02 - 0.21
Cu	0.01 - 0.11	Pb	0.01 - 0.07
Zn	0.02		

2.4 Stable Isotopes

2.4.1 Nitrate Extraction

Several methods have been developed to extract nitrate from large volume water samples. In general, it is easier to work with smaller sample volumes, so ion exchange techniques are often employed to concentrate the nitrate into a smaller sample size. In the past, nitrate extraction from waters with low nitrate concentrations was a difficult and lengthy process. Chang et al. (1999) created a more efficient and easier method for extraction of nitrate from rain, snow and surface waters with low nitrate concentrations. The method used to extract nitrates from each sample for this study was based on the method developed by Chang et al. (1999), which involves preconcentrating the nitrate and converting it to silver nitrate.

Initially, no pre-filtration of samples was performed as rain and snow water generally contains little dissolved organic compounds which would be of any concern. However, partway through the study period it was decided that pre-filtration was a necessary step to avoid overloading the ion exchange columns after several samples were lost. Samples collected on and after April 29th, 2002 were filtered prior to processing using a stainless steel high volume filtration unit fitted with 0.45 μm membrane nylon filters and pressurized with argon gas.

Preconcentration of nitrate was accomplished by gravity dripping each sample through a filter, a 5 ml column containing cation resin (hydrogen form) and a 5 ml column containing anion resin (chloride form) (Figure 2.3). Once the entire sample was passed

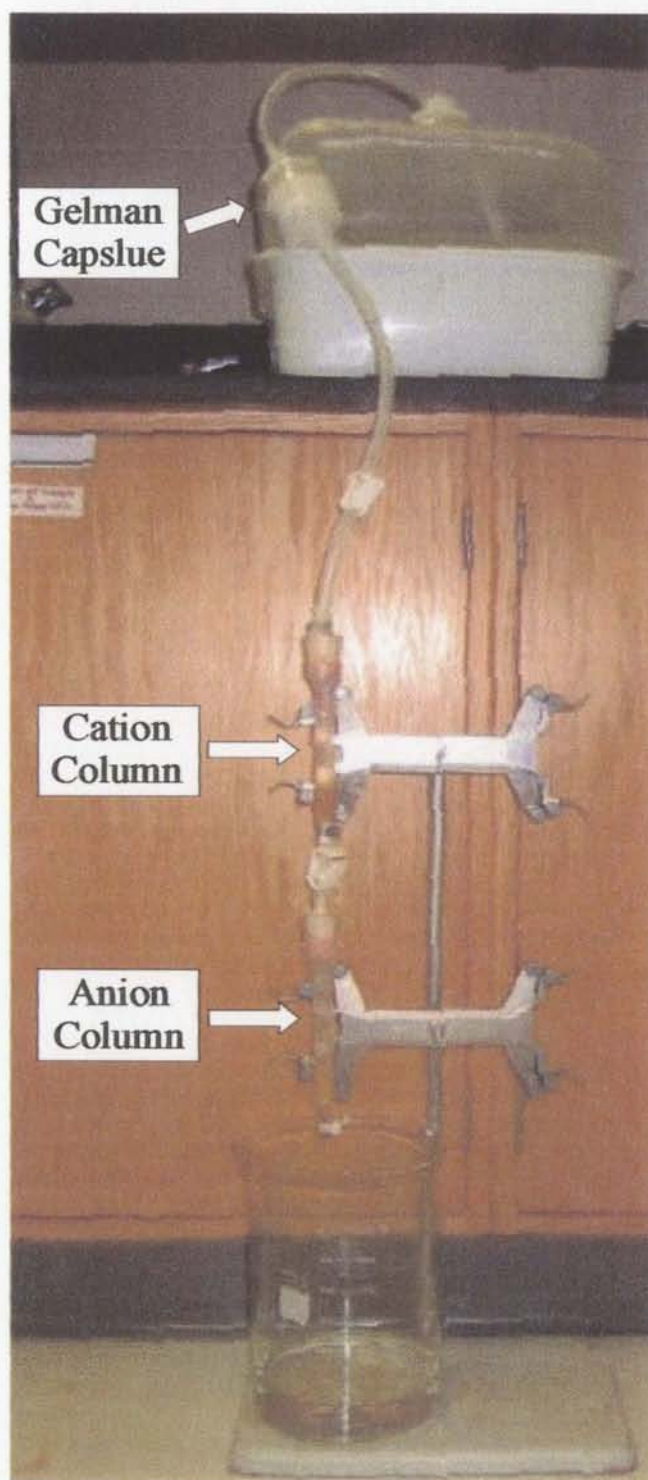


Figure 2.3 Preconcentration apparatus used in this study.

through the columns, the anion column was removed for further processing. All of the anions present in the sample were eluted from the anion exchange resin through the addition of 30 ml of 3 N HCl. Sixteen grams of silver oxide were added to neutralize the sample, resulting in the formation of AgCl precipitate. The pH was measured using pH paper, and was adjusted to between 5 and 6 by making small additions of Ag₂O. The sample was filtered to remove all AgCl, then BaCl₂ was added to precipitate any sulphates or phosphates present. The solution was filtered to remove any precipitate, then gravity drained through a 9 ml cation exchange resin column to remove excess Ba²⁺ ions from the sample. A small amount of Ag₂O was added to the eluent to precipitate excess Cl⁻ ions as AgCl. The pH was checked using pH paper, and if it was found to be 5 to 6, the sample was filtered into a pre-weighed 50 ml polyethylene centrifuge tube and placed in the refrigerator for storage. Appendix I contains a detailed outline of this method. At this point, the sample should consist entirely of silver nitrate in solution.

Overall, the extraction technique resulted in nitrate yields of 38 - 45%. These lower yields are due to the large number of steps involved in processing the nitrate as well as incomplete transfer of sample during filtering and freeze-drying. Chang et al. (1999) stated that low yields do not result in isotope fractionation. However, incomplete elution of the sample nitrate from the exchange resin would result in fractionations as the isotopically enriched nitrate is eluted from the column first (Silva et al., 2000).

2.4.2 Nitrogen Isotopes

A portion of AgNO_3 was removed to analyse for nitrogen isotopes. The amount taken depends on how much nitrate was initially present in the sample. Between 6 and 7 μmol of nitrate was needed in each silver capsule submitted for analysis, and at least two capsules per sample were needed to ensure reproducibility of the instrument. The sample aliquot underwent a series of freeze drying steps to solidify the sample. Prior to the final freeze drying step, the sample was split and pipetted into 2 to 4 silver capsules in which the solution was dried. Two to five milligrams of sucrose was added to the capsules containing the solid AgNO_3 , and each capsule was crimped shut and submitted for analysis. More details about this procedure can be found in Appendix I.

Samples were analysed by continuous flow isotope ratio mass spectrometry (CF-IRMS). There are several different steps involved in the processing of samples by this method. First, the sample was placed in the Carlo-Erba NA1500 Elemental Analyser (EA), which consists of an autosampler, oxidation/reduction furnace, water trap, carbon dioxide trap, gas chromatographic column (GC) and thermal conductivity detector (TCD). The entire EA system was flushed continuously with a carrier gas of Helium at a rate of 90 ml/min. The sample, which was enclosed in a silver capsule, was loaded into the autosampler, which then dropped the sample into the oxidation chamber (1050°C) just as a pulse of oxygen, flushed by He, arrived. The oxygen reacted with the AgNO_3 sample within the silver capsule producing N_2 gas, CO_2 gas and H_2O , the later two resulting from the sucrose added to the sample. The carbon dioxide gas was removed by a Carbosorb

CO₂ trap, while water was removed via a Mg(ClO₄)₂ water trap. The N₂ gas then passed through the GC column.

The He then carried the gas to the ConFloII interface, a split tube which is open to the atmosphere. This allowed for a portion of the He and combustion gas to enter directly into the ion source of the mass spectrometer (MS) via a fused glass capillary. The mass spectrometer used in the Department of Earth Sciences at Memorial University of Newfoundland is the Finnigan™ MAT 252. Helium carrier gas from the EA continuously flowed into the MS during operation. All of the combustion gas exiting the EA entered the ion source where signals for the gas of interest, as defined by the software and instrument configuration, were recorded. Two ammonium sulphate standards, USGS-25 and USGS-26 with accepted values of $-30.40 \pm 0.5\text{‰}$ and $53.50 \pm 0.5\text{‰}$ respectively (NIST, 1993), were used for calibration and quality control. IAEA-N1 ammonium sulphate, with an accepted $\delta^{15}\text{N}$ value of $0.43 \pm 0.07\text{‰}$, was used to ensure the accuracy of the measurements. Ten analyses of the standard yielded an average value of $0.35 \pm 0.14\text{‰}$. Both USGS-25 and USGS-26 were analysed thirty-five times to yield average values of $-30.23 \pm 0.29\text{‰}$ and $53.60 \pm 0.54\text{‰}$, respectively.

2.4.3 Oxygen Isotopes (Nitrate)

AgNO_{3(n)} samples were sent to the University of Calgary for oxygen isotope analyses. Each sample was freeze dried in customized wide mouth Nalgene bottles and the solid AgNO₃ was then analysed for ¹⁵N to test its purity. If the precipitate contained

greater than 5% N it was analysed for oxygen. A 100 to 300 μg aliquot of pure, homogenized AgNO_3 precipitate was weighed into a 4 mm x 3.2 mm high purity silver capsule and submitted for mass spectrometry.

As with the nitrogen isotope analyses, samples were analysed for ^{18}O using CF-IRMS. The sample was loaded into a FinniganTM MAT TC/EA Elemental Analyser, which was continuously flushed with helium gas at a rate of 90 ml/min, via an A200S autosampler. The silver capsule containing the sample was dropped into the High Temperature Conversion/Elemental Analyser (TC/EA) reactor (1450°C) where it was quantitatively converted to CO, along with H_2 and N_2 . The He gas then carried the gaseous TC products through a GC column where the CO was separated from the other gases.

The carbon monoxide gas produced was carried by the He to the ConFlo II open split/interface and into the ion source of the mass spectrometer. The instrument used in the Isotope Science Laboratory in the Department of Physics and Astronomy at the University of Calgary is a FinniganTM Mat Delta⁺ XL mass spectrometer. IAEA NO-3, a potassium nitrate with an accepted $\delta^{18}\text{O}$ value of 23.05‰, was used to calibrate the instrument while internal lab standards were run with each set of five samples to ensure quality control. Twenty seven analyses of the IAEA NO-3 standard yielded an average value of $23.18 \pm 1.56\text{‰}$.

2.4.4 Oxygen Isotopes (Water)

A 20 ml aliquot of each precipitation sample was taken at the time of its collection. The water was stored in a glass vial sealed with Parafilm™ and placed in a refrigerator until the time of analysis. Samples were sent to the University of Waterloo for analysis.

A 3 ml aliquot of sample was equilibrated with CO₂ for a minimum of 3 hours at a constant temperature of 25°C while shaking. After the CO₂-H₂O equilibration was complete, the CO₂ was cryogenically purified and then transferred via an automated sampler to the inlet of the mass spectrometer. A Micromass 903 mass spectrometer was used to analyse the oxygen isotopic composition using dual inlet isotope ratio mass spectrometry. Quality control was guaranteed by repeatedly analysing internal lab standards with each sample set. The internal standards were calibrated periodically using VSMOW, an international standard. The accuracy of the method was determined to be ± 0.2 ‰.

2.5 Statistical Analysis

The differences between volume weighted means for single variables at the two sample locations were tested using the general linear model (GLM), a parametric method. The GLM calculates a two-tailed p-value for each set of variables which are used to determine whether or not the differences between the two locations are significant. Assumptions for this method were checked by examining the residuals. If the assumptions were not met, Welch's approximate t-test, based on heterogeneous errors, was performed.

For this study, p-values less than 0.05 are considered significant at a 95% confidence interval.

A principal component analysis (PCA) was performed on the data to assist in source interpretation for the rain samples. This statistical method uses variables and their relation to one another to create factors which control the variance of the data set. The user must then attempt to interpret the factors, or sources of the variance.

The principal component analysis was performed initially on the data set of 35 samples, using the Minitab 13 statistical program. The technique was not applied to St. John's and McIvers data separately due to the relatively small number of samples available for each site. If values for a particular element were below detection limits, a value of half the detection limit was used, while variables containing a large amount of missing data (such as chloride) were omitted from the analysis. Any outliers discovered within the data set were removed to prevent them from distorting the principal component axes. Once the outliers were removed, a final data set containing 28 samples and 14 variables was used for the analysis.

2.6 Meteorological Analysis

Air mass back trajectories were calculated for each sample by Environment Canada for a 96 hour period before the rain event occurred. Three atmospheric pressure levels, 1000 mb, 925 mb and 850 mb, were calculated for each trajectory. These back trajectories will give insight about where the air masses sampled originated, as well as what they

passed over on their way to the sampling locations. The speed at which the air parcel moves over an area is important. If the air mass moves quickly, there is less opportunity for it to accumulate atmospheric species along its path so it is more likely to transport material from its point of origin.

CHAPTER 3

RESULTS

Thirty-five precipitation samples were collected within the province between January 2002 and February 2003. Twenty-four of the samples were collected from St. John's while the remaining eleven samples were collected from McIvers. All analytical results can be viewed in Appendix II. Duration of collection and approximate sample volumes can be seen in Tables II.1 and II.2. It was impossible to collect every rain event at each site. However an attempt was made to collect events representing a variety of rainfall intensities and durations.

3.1 Chemical Composition

3.1.1 pH and Conductivity

pH and conductivity measurements for each sample can be seen in Tables II.3 and II.4. The St. John's site was more acidic overall, having a pH range of 4.36 - 5.92, while McIvers samples had a smaller range of 4.73 - 5.57. The average pH value for each site was calculated by converting all pH measurements to hydrogen ion concentrations, averaging the values for each site then converting the average value back to pH. This resulted in St. John's having an average pH of 4.88, while McIvers samples have an average value of 5.17.

Variation was also found in conductivities measured at both sites. The mean

values for each site are very similar to one another, with St. John's having a mean of $15 \pm 9.2 \mu\text{S/cm}$ and McIvers a mean of $11.8 \pm 11.9 \mu\text{S/cm}$. The measured ranges are almost identical between the two sites with St. John's having a range of 4 - 44 $\mu\text{S/cm}$ and McIvers with 4 - 43 $\mu\text{S/cm}$. Upon closer inspection only 38% of the St. John's samples have a conductivity below 10 $\mu\text{S/cm}$, with a median value of 12 $\mu\text{S/cm}$ while 73% of the McIvers samples are below that value, and have a median conductivity value of 7 $\mu\text{S/cm}$. Although it is not apparent from the mean and range values, the St. John's samples generally have higher conductivities than the McIvers samples. The difference in conductivity between the two sites is not statistically significant ($p=0.407$).

3.1.2 Major Ions

Values of major anions and cations are shown in Tables II.5 to II.8. All values below detection are assigned a value of 0.025 ppm (~ half the detection limit). Missing data are due to instrument error whereby accurate data could not be acquired for an individual species in a sample during a particular run.

The volume weighted mean (VWM) concentrations can be seen in Figure 3.1. The St. John's samples have higher values for all ions with the exception of Mg^{2+} , which has a slightly higher concentration for McIvers (Table II.9). The differences between Cl^- , NO_3^- , Na^+ , K^+ and Mg^{2+} VWM concentrations for both locations are not significant ($p=0.184$, 0.696, 0.948, 0.171 and 0.697 respectively), while SO_4^{2-} and NH_4^+ concentrations are significantly different ($p=0.019$ and 0.024 respectively) between St. John's and McIvers

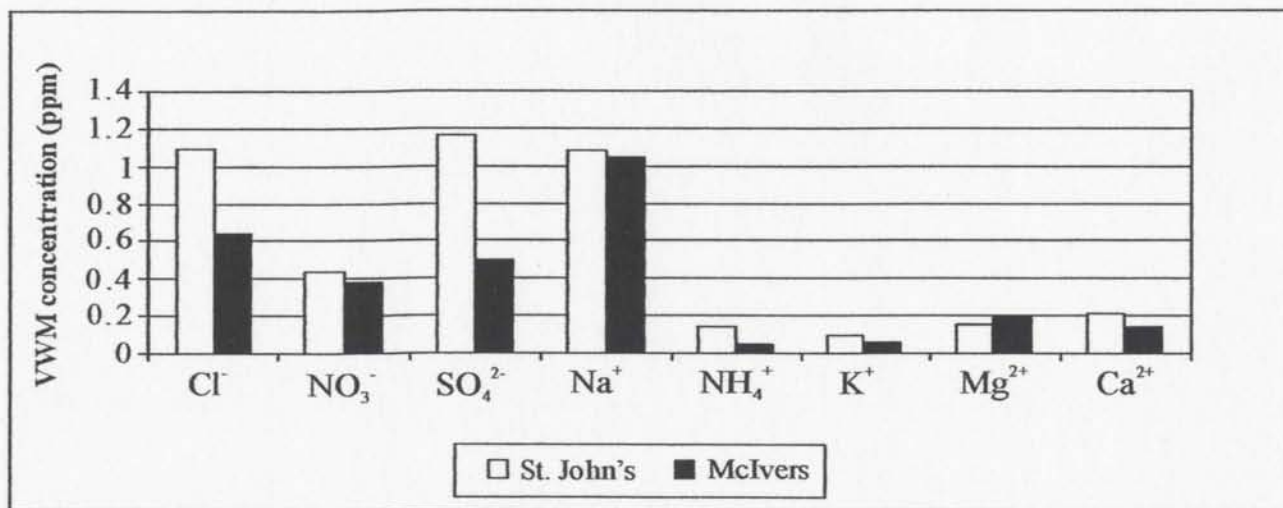


Figure 3.1 VWM ion concentrations for St. John's and McIvers.

(Table II.10). The overall patterns for both sites are very similar to one another with the exception of SO_4^{2-} .

The seasonal VWM concentrations for each locale can be seen in Figures 3.2 and 3.3. Winter months include October to March, while April to September represent summer months. St. John's samples have higher summer VWM concentrations for NO_3^- , SO_4^{2-} , NH_4^+ and Ca^{2+} , while Cl^- , Na^+ and Mg^{2+} exhibit a stronger influence in the winter (Figure 3.2) (Table II.11). K^+ is higher in the winter months, but the concentrations are very similar between the two seasons for this particular cation. The McIvers data show the same pattern with the exception of SO_4^{2-} , which is higher in winter months at that location (Figure 3.3) (Table II.11). Examination of the winter data for both St. John's and McIvers (Figure 3.4) shows a comparable pattern between the sites, with no significant differences in concentration for any species (Table II.10). Looking at the summer values for both locales, a large difference is seen between sulphate values (Figure 3.5). This significant difference in SO_4^{2-} concentration ($p=0.015$) (Table II.10) was not observed in winter data for St. John's and McIvers.

The percent seaspray sulphate (PSS) was also calculated for the data set. The PSS values can be seen in Tables II.12 and II.13. Seaspray is a major source of atmospheric sulphate, so this calculation was performed to determine how much of the sulphate in the samples came from seaspray versus non-seaspray natural or anthropogenic sources. In general, anthropogenic atmospheric sulphate is produced from the combustion of fossil fuels in stationary sources. A small amount of sulphate can be produced naturally through

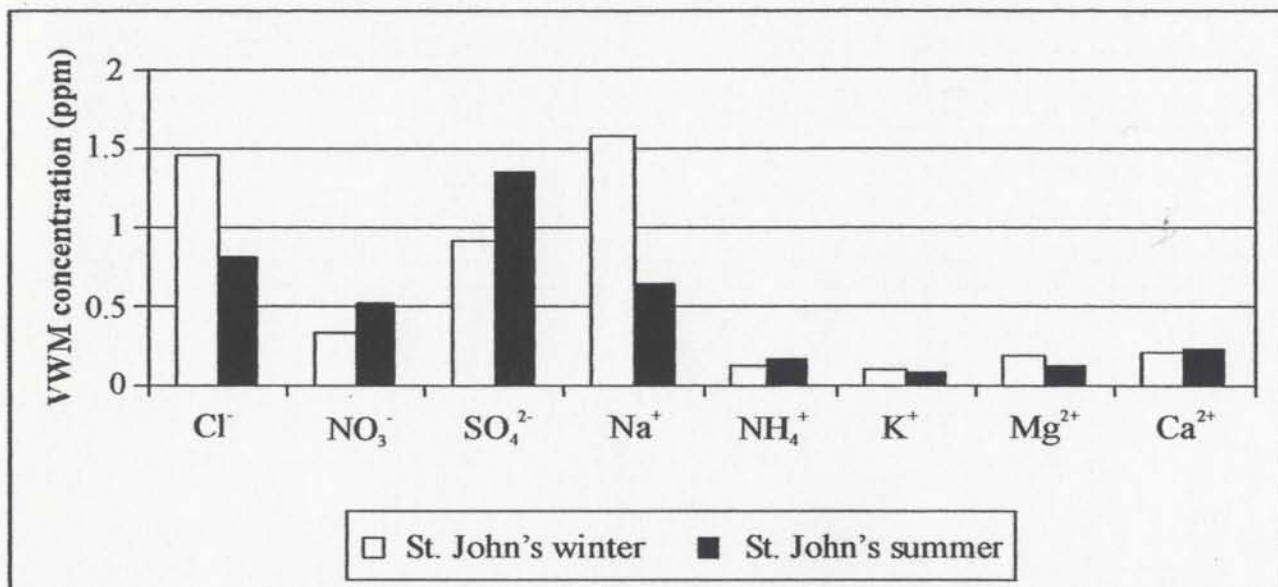


Figure 3.2 Seasonal VWM ion concentrations for St. John's samples.

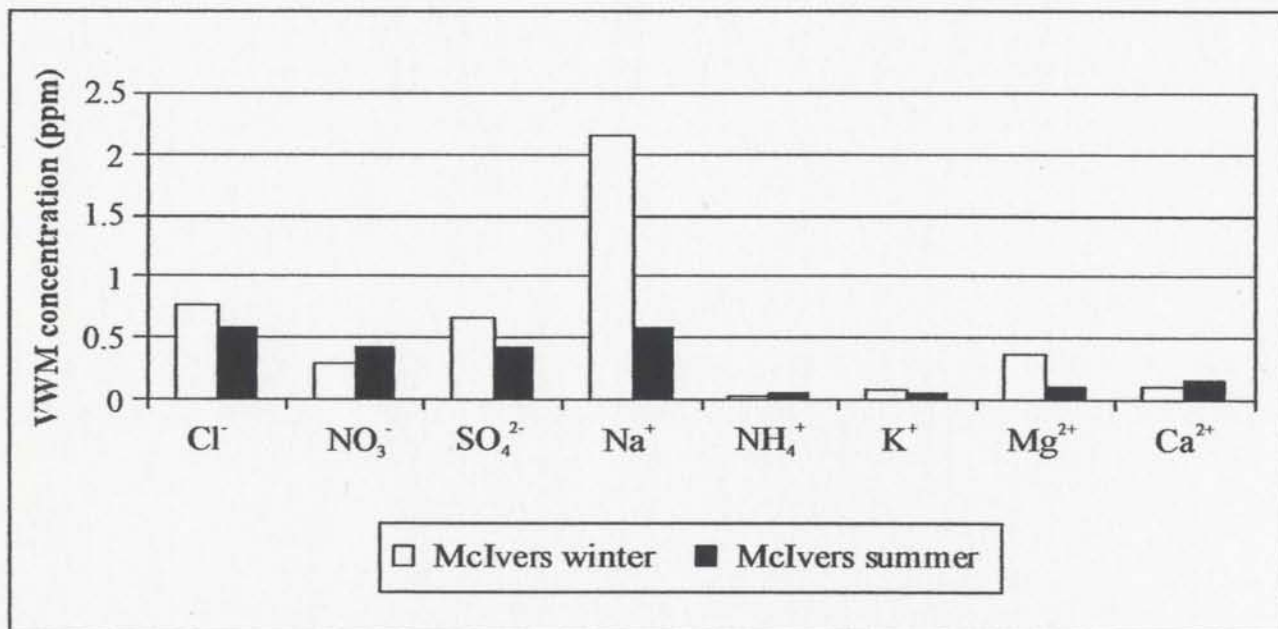


Figure 3.3 Seasonal VWM ion concentrations for McIvers samples.

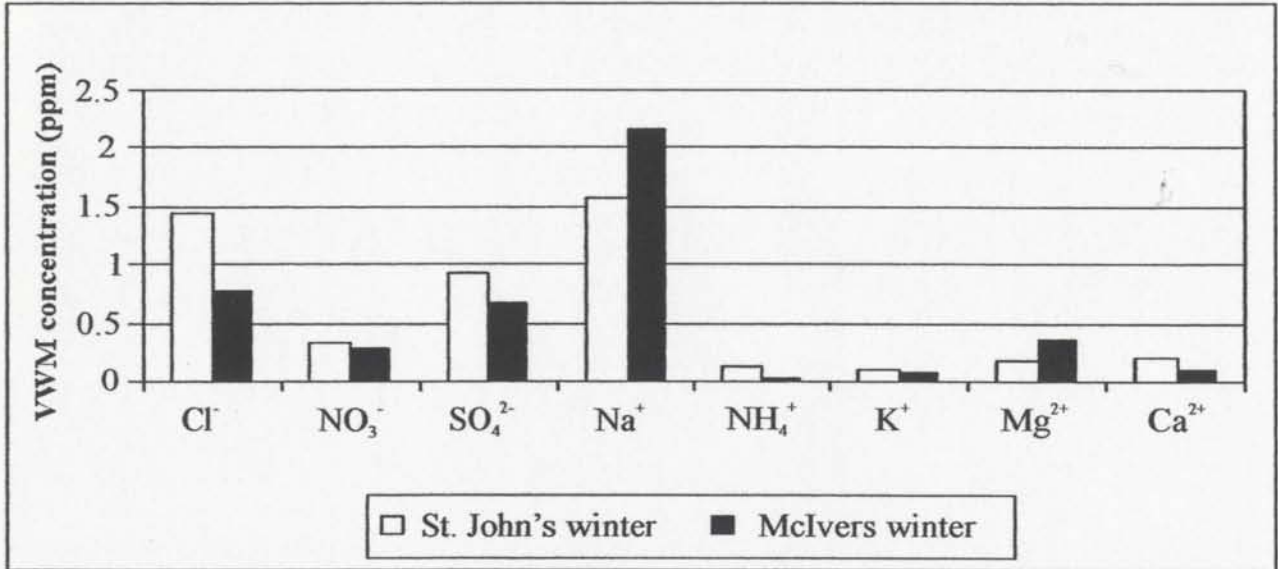


Figure 3.4 Winter VWM ion concentrations for St. John's and McIvers.

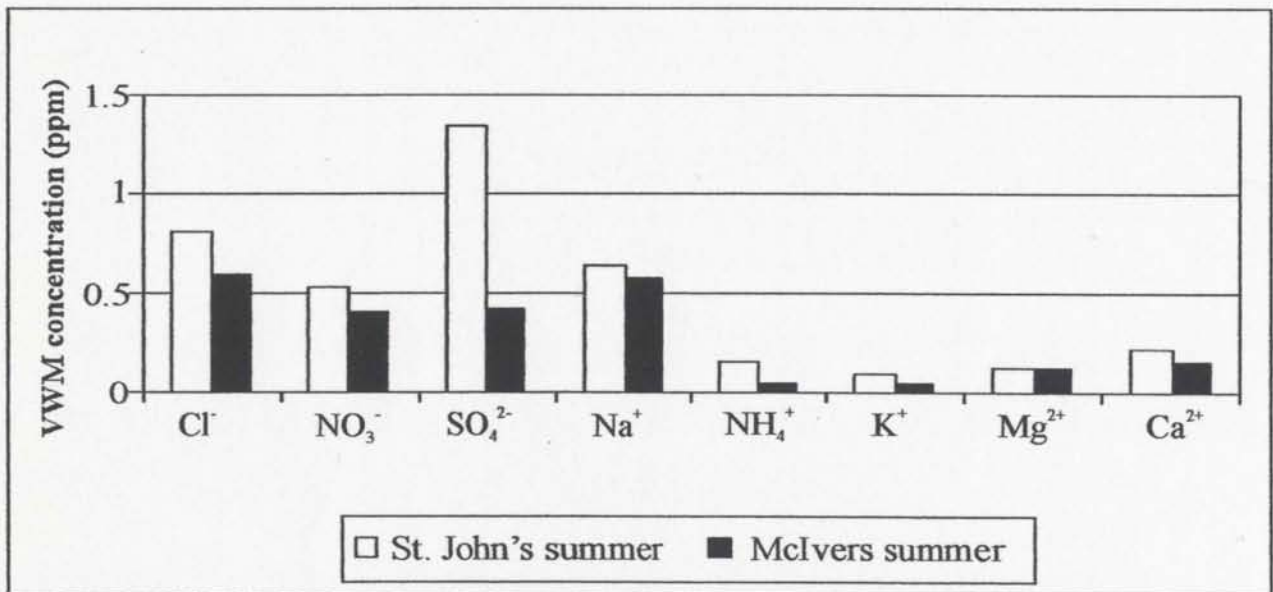


Figure 3.5 Summer VWM ion concentrations for St. John's and McIvers.

biogenic activity in the ocean, but this is very small compared to anthropogenic or seaspray derived sulphate. Overall, the values of PSS for St. John's samples ranged from 1% to 98%. The McIvers samples had a range of 9% to 100%.

3.1.3 Trace Elements

Trace element values are presented in Tables II.14 and II.15. Twenty-five of the thirty-nine elements analysed were below the detection limit of the instrument and have therefore been removed from the data set. Many of the samples had to be rerun several times due to instrument instability and problems with detection limits on particular days. Overall, results were obtained from seven. Each set was evaluated based on detection limits as well as the relative standard deviation (RSD) values calculated for certified standards run on a particular day. If the detection limit for a particular element was low enough to obtain concentration values for that element, and the RSD was less than 10% for a particular run, the data for the element was kept. After the evaluation procedure, if more than one analysis was present for an element, the values were combined and an average value for that particular element was entered into the final data set.

The volume weighted mean concentrations calculated from the final data set for the 14 elements of interest can be seen in Figure 3.6. St. John's samples are higher than McIvers samples for 10 of the elements, while McIvers has higher values for Co, Zn, Sr and Pb (Table II.16). Both locations have zinc concentrations which are much higher than the other elements of interest. It is interesting to note that Mo concentrations for St.

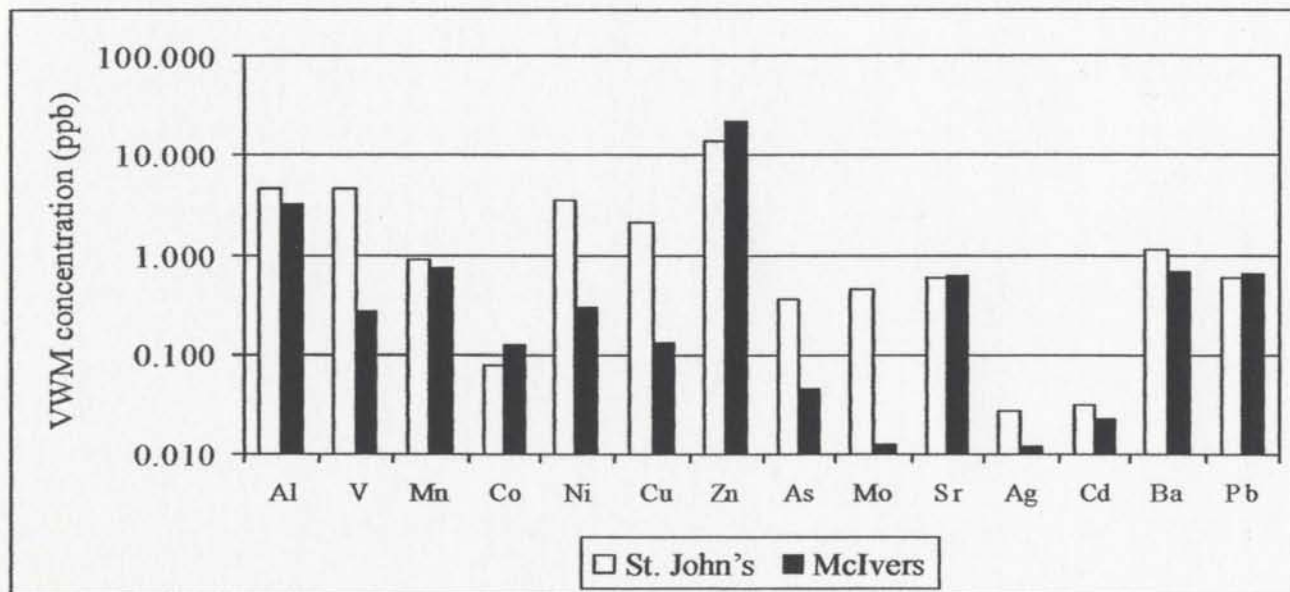


Figure 3.6 Volume weighted mean trace element concentrations for St. John's and McIvers samples. Note the log scale.

John's are 35 times higher than the McIvers VWM for that element. Other elements with much higher concentrations for the St. John's samples are V (16x), Cu (16x) and Ni (11x). Although large differences in concentrations are observed between the two locations, none of the differences between any of the elements measured are statistically significant (Table II.17).

Seasonal VWM concentrations for the St. John's site can be seen in Figure 3.7. St. John's winter samples have higher concentrations of Cu, Zn, As, Sr and Ag than their summer counterparts, which are higher in Al, V, Mn, Co, Ni, Mo, Cd, Ba and Pb. In general, both winter and summer data follow a similar pattern. Winter samples taken at McIvers have higher VWMs of Cu, As, Mo, Sr, Ag and Ba, while the summer samples contain more Al, V, Mn, Co, Ni, Sn, Cd and Pb (Figure 3.8). The McIvers data have a winter VWM of zero for both Ni and Cd, while Cu and Ag have a value of zero in the summer as they were below detection limits for a number of samples. Both winter and summer VWM concentration data follow the same general pattern for the McIvers site. Comparison of the winter data for both St. John's and McIvers reveals a somewhat similar pattern between the two locations, however several of the element concentrations, for example vanadium, differ between the two sites (Figure 3.9). There are no statistically significant differences between any of the winter concentrations between the two locations (Table II.17). The summer trends for both sites (Figure 3.10) also appear to be similar to one another with the exception of Cu and Mo, while Ba is the only element which is significantly different ($p=0.003$) between the locations during that season (Table II.17).

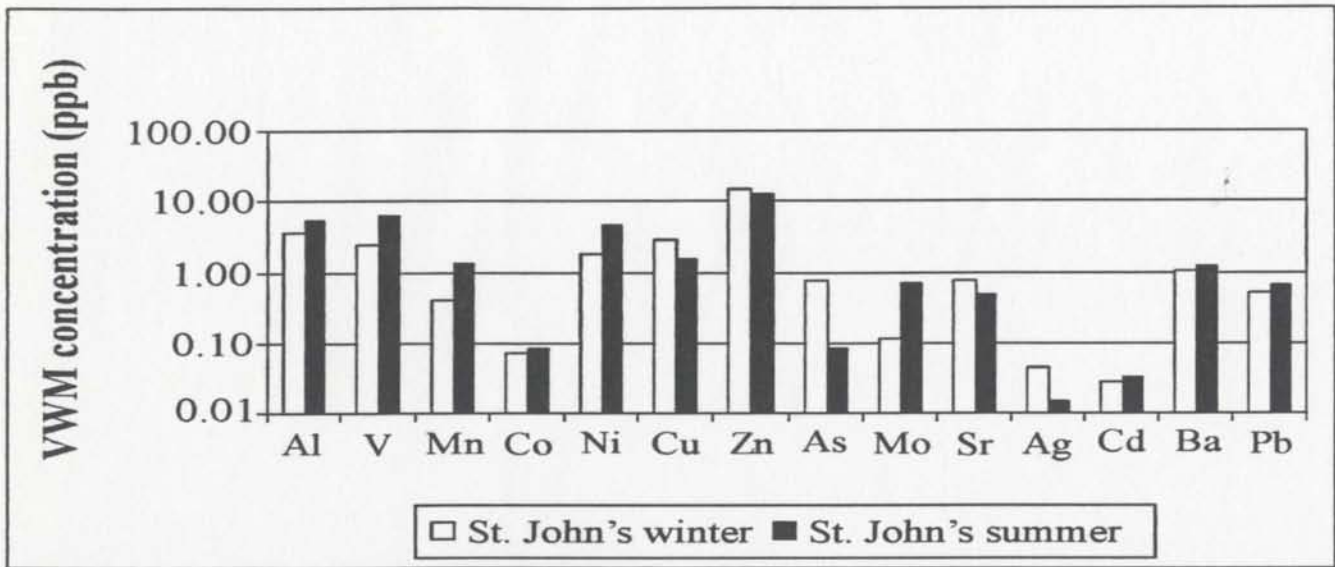


Figure 3.7 Seasonal volume weighted mean trace element concentrations for St. John's samples. Note that suspicious blank values for Cu were high and may cause Cu values to be underestimated. Note the log scale.

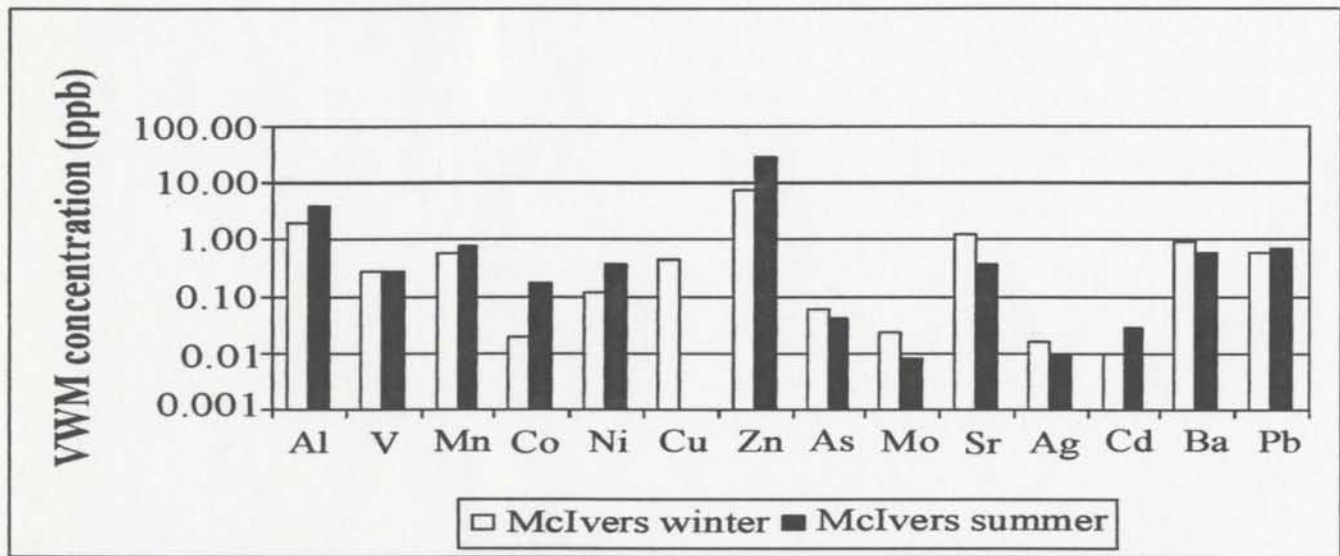


Figure 3.8 Seasonal volume weighted mean trace element concentrations for McIvers samples. Note that suspicious blank values for Cu were high and may cause Cu values to be underestimated. Note the log scale.

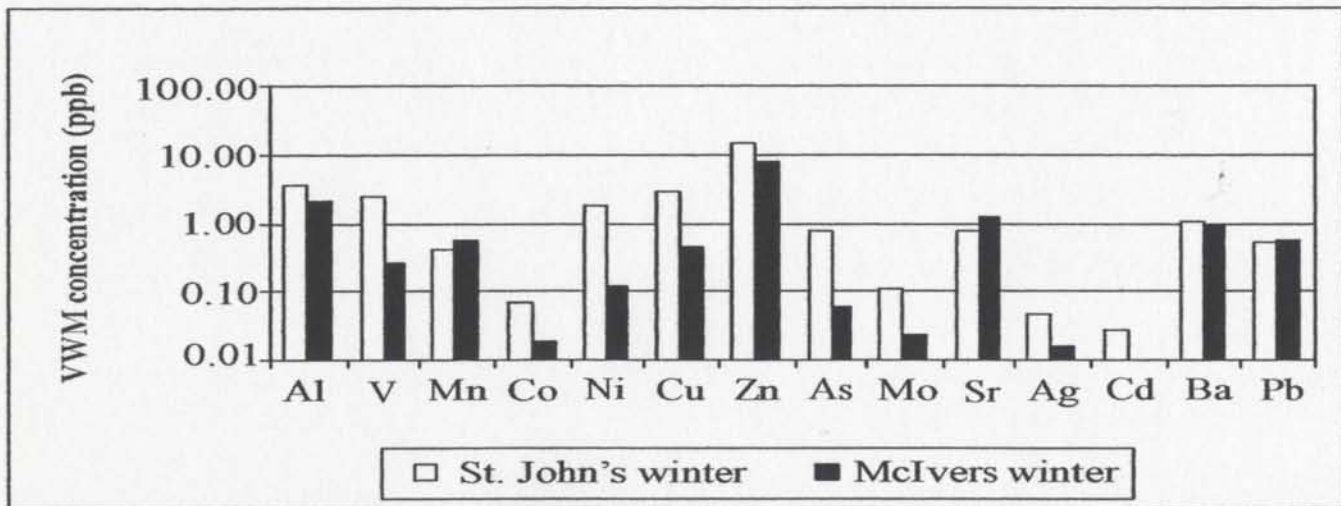


Figure 3.9 Winter volume weighted mean trace element concentrations for St. John's and McIvers samples. Note that suspicious blank values for Cu were high and may cause Cu values to be underestimated. Note the log scale.

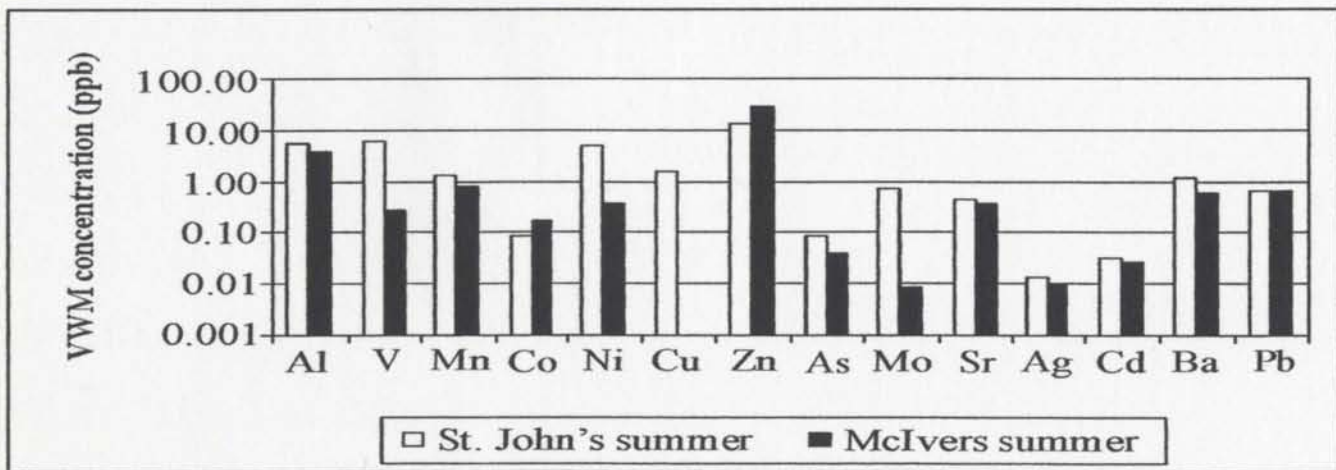


Figure 3.10 Summer volume weighted mean trace element concentrations for St. John's and McIvers samples. Note that suspicious blank values for Cu were high and may cause Cu values to be underestimated. Note the log scale.

Numerical values of the seasonal VWMs calculated for both sites can be seen in Table II.18.

3.2 Isotopic Composition

Isotopic values for nitrogen and oxygen in nitrate and oxygen isotope values of water can be found in Tables II.19 and II.20.

3.2.1 Nitrogen Isotopes

Nitrogen isotopes measured in nitrate varied at both sites. St. John's samples had a range of -9.4 to +2.7 ‰ and a mean value of $-4.1 \pm 2.7\text{‰}$. The volume weighted mean $\delta^{15}\text{N}$ for this site is -3.9‰, with a warm, or summer, season VWM of -3.3‰ and a cool, or winter, season VWM of -4.7‰. McIvers data had a smaller range of -6.0 to +0.5 ‰, with a mean value of $-3.2 \pm 2.4\text{‰}$, which was not significantly different from that of St. John's ($p=0.437$). The overall VWM for this site is -3.0‰. The summer VWM is -2.3‰, while the winter samples have a VWM of -5.3‰. The difference between VWM values for both sites is not significant ($p=0.348$), nor are seasonal differences significant (summer $p=0.903$, winter $p=0.804$). Table 3.1 contains the numerical and volume weighted averages as well as seasonal differences. Overall, the St. John's data had a more depleted ^{15}N signature. The smaller range for the McIvers data may be in part due to the limited number of samples collected at that location. All statistical values for VWM isotopes can be seen in Table II.21.

Table 3.1 Numeric and volume-weighted means and seasonal differences of $\delta^{15}\text{N}$ for both sites (‰).

	St. John's			McIvers		
	Overall Average	Summer	Winter	Overall Average	Summer	Winter
$\delta^{15}\text{N}^{\text{NUM}}$	-4.1	-3.2	-5.3	-3.2	-2.7	-5.2
$\delta^{15}\text{N}^{\text{VWM}^*}$	-3.9	-3.3	-4.7	-3.0	-2.3	-5.3
$\delta^{18}\text{O}_{\text{NO}_3}^{\text{NUM}}$	+40.6	+43.1	+36.6	+40.7	+43.0	+33.7
$\delta^{18}\text{O}_{\text{NO}_3}^{\text{VWM}^*}$	+41.4	+46.0	+34.8	+39.6	+41.6	+34.4
$\delta^{18}\text{O}_{\text{H}_2\text{O}}^{\text{NUM}}$	-7.1	-6.4	-8.1	-10.3	-9.2	-13.5
$\delta^{18}\text{O}_{\text{H}_2\text{O}}^{\text{VWM}^*}$	-7.5	-6.6	-8.6	-10.6	-9.3	-13.6

*VWM = $\frac{\sum \text{volume of sample} \times \text{concentration of species of interest in sample}}{\text{total volume of all samples with species of interest}}$

3.2.2 Oxygen Isotopes (Nitrate)

Nitrate oxygen isotopic signatures ranged from +15.8 to +53.9‰ for St. John's samples, with an average value of $+40.6 \pm 12.0$ ‰. The McIvers samples had a much narrower range of +46.5 to +51.9‰, and an average value of $+40.7 \pm 8.4$ ‰. In both cases, the average values were almost identical, and the maximum values measured at each site only have a difference of two permil. The difference between the sites is not statistically significant ($p=0.501$). The overall VWM concentrations were +41.4‰ and +39.6‰ for St. John's and McIvers samples, respectively, and were not statistically significant ($p=0.348$). Warm season samples collected at St. John's had a VWM of +46.0‰, while winter samples displayed a VWM of +34.8‰. McIvers varied seasonally as well, with a summer VWM of +41.6‰ and a winter value of +34.4‰. The seasonal differences between the two sites were not significantly different for either summer ($p=0.277$) or winter ($p=0.969$). Values can be seen in Table 3.1 and statistical results in Table II.21.

3.2.3 Oxygen Isotopes (Water)

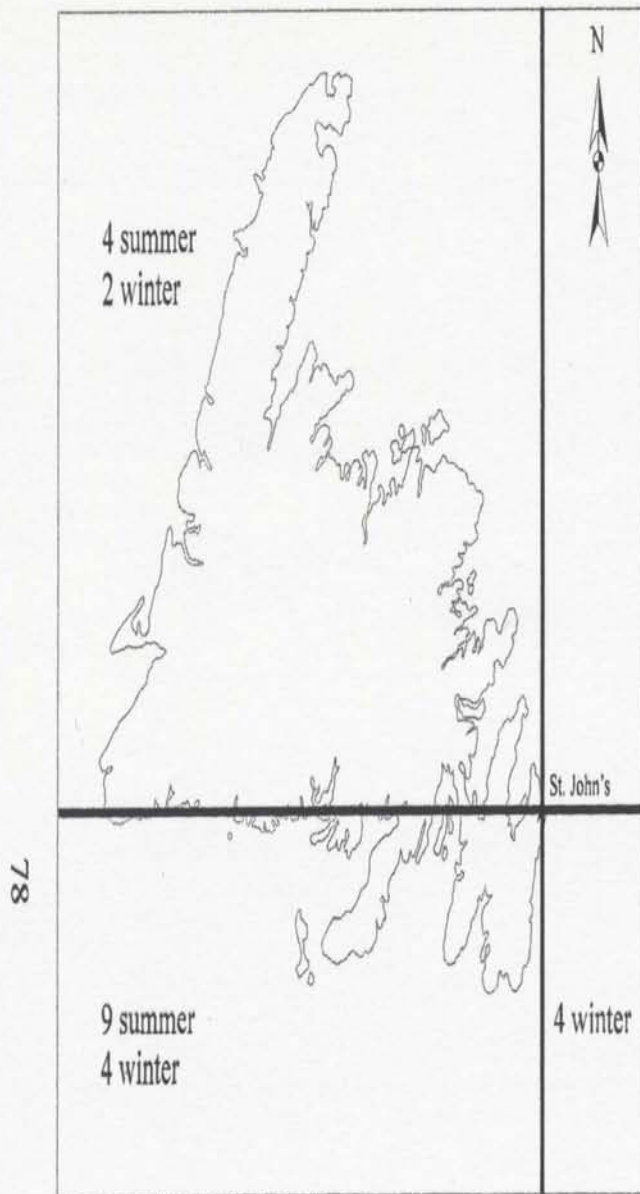
Precipitation collected at St. John's had oxygen isotopic signatures ranging from -3.0 to -16.2‰. McIvers rain water had a range of $\delta^{18}\text{O}$ of -6.4 to -14.3‰. As with the oxygen isotopes of nitrate, the McIvers samples have a narrower range than their St. John's counterparts. The St. John's and McIvers samples have an average isotopic composition of -7.1 ± 3.0 ‰ and -10.3 ± 2.7 ‰, respectively, indicating a more depleted

^{18}O for the McIvers samples, a difference which is statistically significant ($p=0.005$). The VWM isotopic compositions confirm this; St. John's has an overall VWM of -7.5‰ and McIvers -10.6‰ , a statistically significant difference ($p=0.009$). A slight seasonal difference exists at each site. St. John's has a summer VWM of -6.6‰ and a winter VWM of -8.6‰ , while McIvers summer and winter samples have VWM's of -9.3 and -13.6‰ , respectively (Table 3.1). Both summer and winter VWM values are significantly different ($p=0.018$ and 0.038 , respectively; Table II.21).

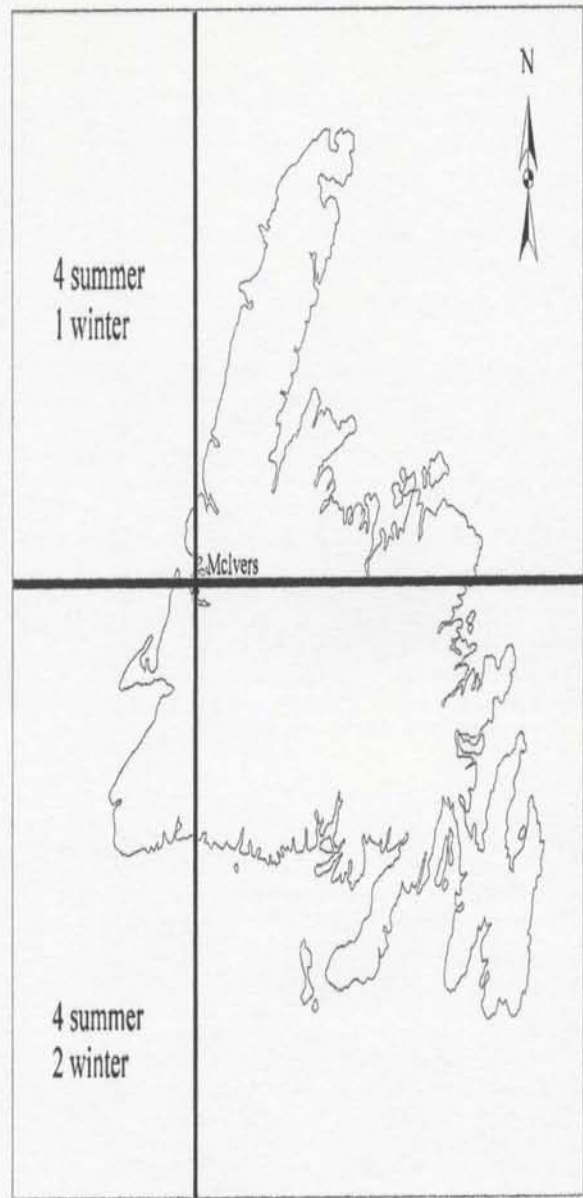
3.3 Air Mass Back Trajectories

Close inspection of the air mass back trajectories calculated for each sample (Appendices III and IV) revealed seven main routes of travel. Two routes were from across Canada; one beginning in the central region and heading east, the other starting in the western provinces and travelling towards Newfoundland. Others came from the north region of the country and the Arctic. A fourth category contained air masses which moved from Canada or the United States across the Great Lakes region or near the Canadian-U.S. border. A fifth direction of travel was through the eastern United States. The final two categories involved ocean travel; one along the eastern seaboard of the US and the maritime provinces of Canada, and the other from an ocean source with no close proximity to land.

Figure 3.11 shows the direction of travel of the back trajectories for each location using a quadrant system. The dominant direction of air mass movement for both St.



(a)



(b)

Figure 3.11 Map of Newfoundland for the (a) St. John's and (b) McIvers locations. Quadrants represent the main direction of travel of an air mass to the sampling site. Values given in a quadrant represent the number of air mass back trajectories traveling to the site within that quadrant as well as the season during which they arrived.

John's and McIvers is from the west, with no seasonal differences observable at either location.

CHAPTER 4

INTERPRETATION

4.1 Basic Inferential Statistics

Volume weighted means for each element at both locations were compared. Two species of interest are significantly different between the two locations: SO_4^{2-} and NH_4^+ (Table 4.1). Both of these ions may be produced naturally or through anthropogenic processes, the latter being a much larger source in the atmosphere. Statistically, the sites are very similar to one another.

Seasonal differences between the volume weighted means (VWMs) of the elements were also calculated. During the winter months, there are no statistically significant differences between any of the species of interest. This may be an indication that both locations are influenced by similar sources of atmospheric constituents during the colder months of the year. During the summer months, however, the VWMs of SO_4^{2-} , NH_4^+ and Ba were significantly different between the St. John's and McIvers sites (Table 4.1). SO_4^{2-} and NH_4^+ are commonly associated with anthropogenic pollution to the atmosphere, while Ba generally indicates an oceanic influence. St. John's summer samples may be influenced more heavily by anthropogenic sources in the summer than McIvers samples, which show stronger oceanic influence, possibly due to the lack of point sources in the area. Statistical results for each species can be seen in Tables II.10 and II.17.

Table 4.1 Statistically significant results of comparison of VWMs of species between locations, with $\alpha=0.05$.

	All	Winter	Summer
Species	p	p	p
SO ₄ ²⁻	0.019	0.336	0.015
NH ₄ ⁺	0.024	0.141	0.049
Ba	0.054	0.887	0.003

4.2 Principal Component Analysis

Principal component analysis (PCA) produced three factors responsible for 64.4% of the total variance; the first factor controlled 27.3%, the second accounted for 22%, and the third factor 15%. The decision to use three factors was based on the fact that the fourth factor accounted for less than 10% of the total variance. The coefficients for each component calculated can be seen in Table 4.2. The larger the coefficient, the more control a particular variable has on that component. The correlation matrix used to calculate the PCA can be seen in Table II.22.

Interpretation of the components is based on those variables that have the highest loading on each component. The first component (Table 4.2) is controlled by NO_3^- , NH_4^+ , SO_4^{2-} , Al and Mn. This likely represents a combination of anthropogenic inputs as well as a crustal influence. Aluminum is used to trace crustal inputs into the atmosphere, which occur as small particles. It has been suggested by Natusch et al (1973) and Wadge et al (1986) that anthropogenic elements may be preferentially deposited onto small particles during combustion processes. This may explain why Al is grouping with other anthropogenic variables such as Mn, used to trace automobile inputs, and NO_3^- , NH_4^+ and SO_4^{2-} , all of which can be produced during various anthropogenic activities such as fossil fuel combustion, biomass burning and petroleum refining (Brasseur et al., 1999).

The second component is controlled by Na^+ , Mg^{2+} and K^+ , elements which indicate a seaspray influence. Co, Cu and Zn also load on this factor, but to a much lesser degree than the seaspray elements. Pacyna et al. (1984) believed that Co was almost exclusively

Table 4.2 Coefficients produced from Principal Component Analysis using data from both locations.

	PC 1	PC 2	PC 3
$\delta^{15}\text{N}$	0.027	0.010	0.444
NO_3^-	-0.463	-0.085	0.001
SO_4^{2-}	-0.402	0.031	-0.261
Na^+	-0.046	0.535	-0.084
NH_4^+	-0.440	-0.158	-0.059
K^+	-0.174	0.421	-0.222
Mg^{2+}	-0.110	0.508	0.021
Al	-0.435	-0.152	0.092
V	0.056	-0.020	-0.377
Mn	-0.407	-0.125	0.168
Co	-0.029	0.264	0.347
Cu	-0.142	0.285	-0.154
Zn	-0.054	0.232	0.490
Mo	0.055	0.035	-0.364
% Variance	27.3	22.0	15.0

emitted to the atmosphere via fossil fuel combustion, while Cu and Zn have several anthropogenic sources such as the combustion of fossil fuel and smelting/refining of ore. Cobalt is also found associated with sulphide ores and may be used in petroleum refining (Schrauzer, 1991). Zinc, and to a lesser degree copper, may also be emitted to the atmosphere via forest fires or other types of wood burning (Pacyna, 1986a). Natural sources, including bubbles bursting in the ocean and vegetation also play a role in the introduction of both Cu and Zn to the atmosphere, although to a much lesser extent than the other sources (Pacyna et al., 1984; Pacyna, 1986b).

V, Mo, Co, Zn and $\delta^{15}\text{N}$ control the third and final component in the analysis. V and Mo are known components of oil which are emitted upon combustion of fossil fuel. Both cobalt and zinc, as stated above, may be emitted to the atmosphere during fossil fuel combustion and possibly ore smelting. These two elements, along with $\delta^{15}\text{N}$ have a positive loading on Factor 3, while V and Mo have negative values. This may indicate that two different processes control this factor, such as oil combustion (V and Mo) and a combination of coal combustion and other anthropogenic activities (Co and Zn). The positive $\delta^{15}\text{N}$ loading on this factor indicates that the nitrogen isotopic composition may be governed by the same processes controlling this factor.

Plots of the coefficients can be seen in Figures 4.1 and 4.2. Variables associated with one another tend to group together. Looking at the plots, three main groups of variables can be seen. These groupings are based on both the coefficients produced from the PCA (Table 4.2) as well as the author's knowledge of common associations of

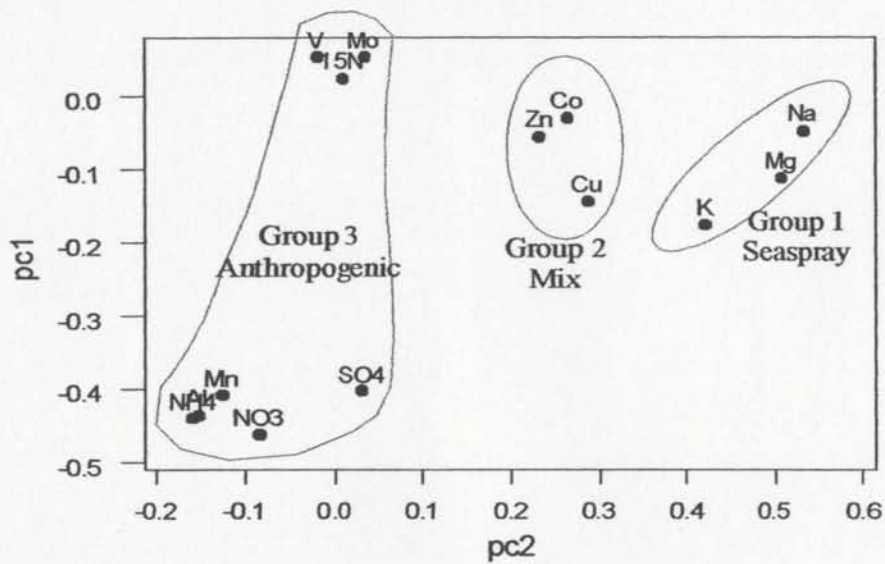


Figure 4.1 PC1 plotted against PC2

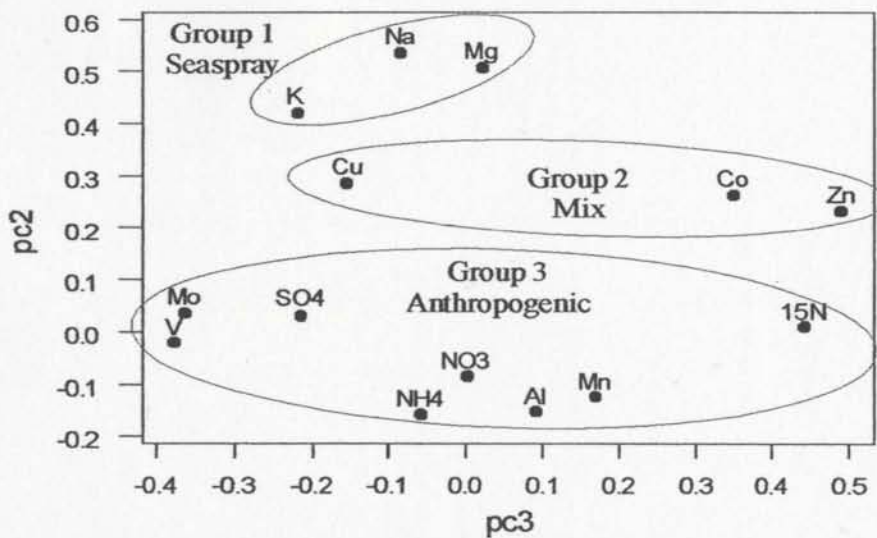


Figure 4.2 PC2 plotted against PC3

elements from different sources (Section 1.3). Group 1 contains the elements Na^+ , Mg^{2+} and K^+ , which are associated with seaspray. These three elements are the main controls of the second component calculated in the analysis (Table 4.2), and tend to group along the PC2 axis in both plots (Figures 4.1 and 4.2). Group 2 also contains three elements: Co, Zn and Cu. Both Co and Zn have positive loadings on Factor 3 (Table 4.2), while copper does not exhibit a strong control on any of the components calculated. This may be an indication that there is more than one source of Cu to the atmosphere. This group may represent a mixture of anthropogenic inputs such as fossil fuel combustion, smelting and wood combustion, but may also have a small seaspray influence (Figures 4.1 and 4.2). The third and largest group contains the following eight variables: V, Mo, $\delta^{15}\text{N}$, NO_3^- , NH_4^+ , SO_4^{2-} , Al and Mn. Group 3 represents a mainly anthropogenic influence from both stationary and mobile fossil fuel combustion (Figures 4.1 and 4.2). The majority of the variables in this group control the first factor calculated in the PCA (Table 4.2), with the exception of V, Mo $\delta^{15}\text{N}$, which are more influential on Factor 3. The Al may represent continental dust picked up by the air masses as they moved across land before reaching the sampling locations. These groupings indicate that the two main controls of variance in the data set are anthropogenic inputs such as fossil fuel combustion, ore smelting and wood burning along with natural inputs from seaspray.

Scores are also calculated during a PCA. A score is computed for each variable of each sample. Plotting the scores may give insight into how the samples group based on the principal components calculated. Figures 4.3 and 4.4 show the scores using user

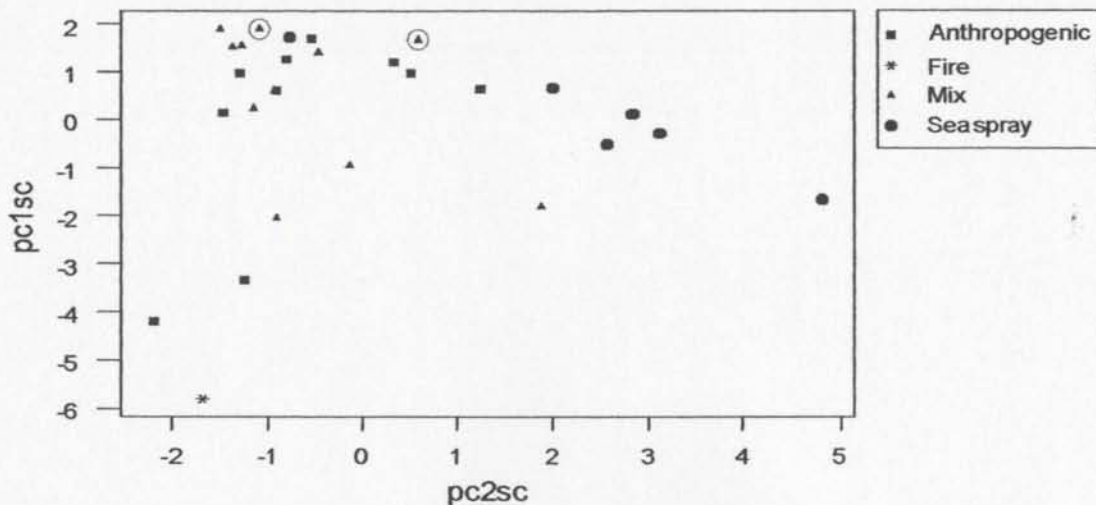


Figure 4.3 Scores of PC1 plotted against scores of PC2 with user defined labels based on chemical composition. Circled Mix samples represent hurricane events.

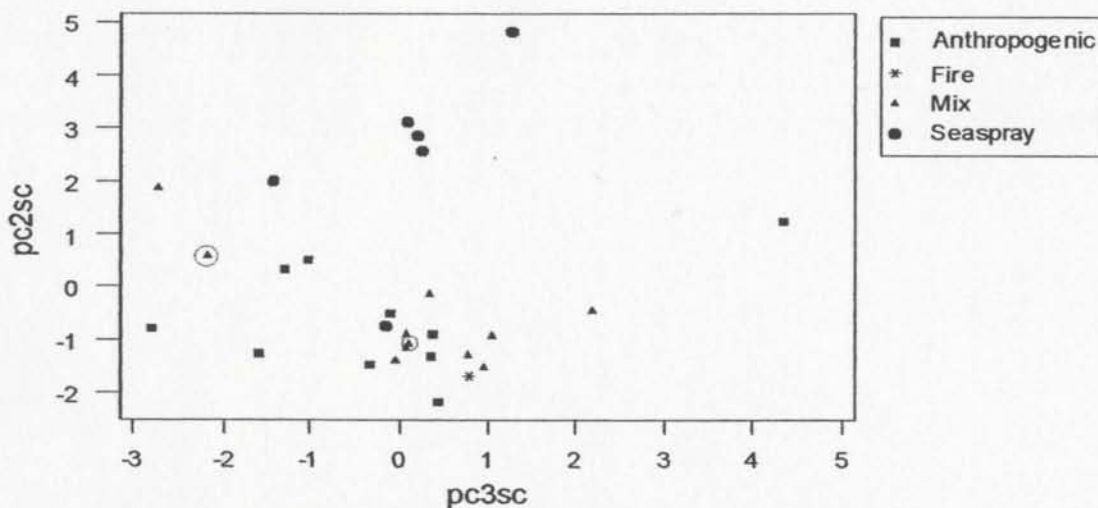


Figure 4.4 Scores of PC2 plotted against scores of PC3 with user defined labels based on chemical composition. Circled Mix samples represent hurricane events.

defined labels created based on chemical and isotope data for each sample. Anthropogenic samples are those which appear to be mainly controlled by anthropogenic sources with little to no seaspray influence, seaspray samples are governed by oceanic inputs, and mix indicates samples which display approximately equal influences of anthropogenic and seaspray inputs. The fire sample was collected in July of 2002 during a period of intense forest fires covering large areas of Quebec (Eric Santerre, pers. comm., 2004) and has a chemical composition reflecting this input. In general, samples controlled by seaspray form a rough group, while all the remaining samples plot together. The score plots can be compared to the previous plots of the components to confirm the idea that the majority of the samples are controlled by anthropogenic inputs involving oil and coal combustion and vehicle emissions. Others have a stronger oceanic influence, while the rest are controlled more by the Cu, Zn and Co group, possibly representing wood burning and ore processing. Figures 4.5 and 4.6 are the same score plots using location as a label. These plots will be discussed in Sections 4.3 and 4.4.

4.3 Air Mass Back Trajectories

All the air mass back trajectories calculated for each sample can be seen in Appendix III and IV. Back trajectories are helpful in delineating potential sources, but several factors which may influence the chemical composition of an air mass must be considered when using back trajectories as an interpretive tool, including the speed of the air parcel. For example, the trajectory calculated for sample SJ02-0531 (Figure III.7)

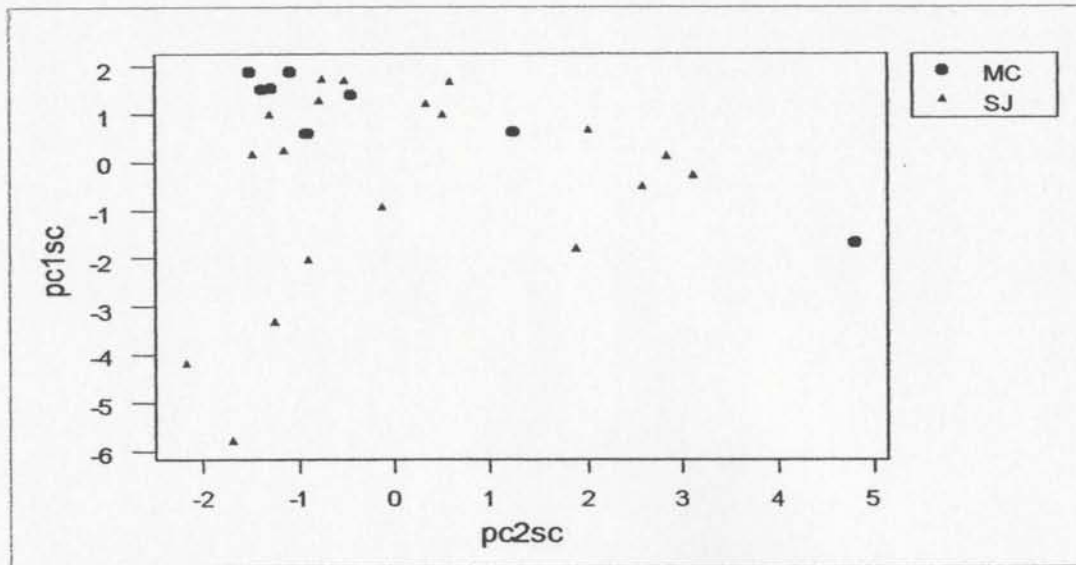


Figure 4.5 Scores of PC1 plotted against scores of PC2 with labels based on location. MC represents McIvers samples, SJ represents samples collected at St. John's.

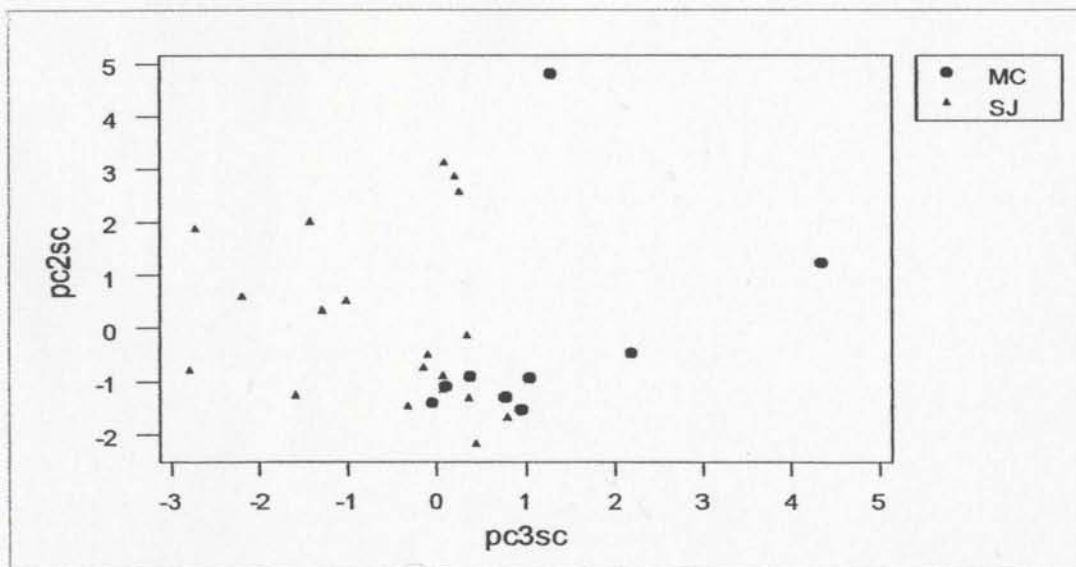


Figure 4.6 Scores of PC2 plotted against scores of PC3 with labels based on location. MC represents McIvers samples, SJ represents samples collected at St. John's.

shows a path which is almost entirely oceanic in nature. One would then expect to see an oceanic, or seaspray signature for this sample. The chemical data, however, show that this sample is more anthropogenic in nature. The air mass was located offshore of the northeastern US for several days, where it may have acquired many of its chemical components. The day before the sample was collected, the air mass moved quickly across the Atlantic provinces on its way to Newfoundland. It is possible that because it moved so quickly, the air mass did not accumulate many oceanic constituents.

These trajectories may be subjective in that they only show the movement of the air mass over the last 96 hours. If the air had travelled over an extremely polluted area before that, it may retain some of the chemistry associated with the area depending on the residence time of the species accumulated. It has been shown in other studies (Wadleigh et al., 1996), however, that the last 24 to 48 hours generally have the most influence on the composition of the air mass.

Another factor to consider when using air mass back trajectories is that the atmosphere is very dynamic. Other air parcels may be moving with or around the calculated trajectory, carrying with them chemical compounds from other areas. As well, there are many pressure levels associated with an air mass. For this study, the 850 and 925 mb levels were observed. It is possible that different chemical constituents may travel in different levels of the air mass, which may complicate the interpretations. The chemistry of the samples along with the potential source areas must make sense together. It must also be considered that rain may have occurred along the trajectory path before the air

mass reached the sampling sites. This could result in a loss of chemical constituents, making the sample more dilute and more reflective of sources closer to the collection site.

4.4 St. John's

St. John's is located along the coast of the island of Newfoundland. Therefore, one would expect a marine influence to be present in precipitation samples collected at this site. In most samples, a marine signature can be seen; however it is often overshadowed by the stronger anthropogenic signals typical of samples collected at this site during this study.

Nitrate concentrations measured for the St. John's samples range from 0.075 to 1.814 ppm. These values are comparable to values measured in other studies in Atlantic Canada and other areas of Newfoundland (Table 4.3). The average pH of the precipitation is 4.88, indicating that St. John's has received acid rain.

Principal Component Analysis of the data reveals that the St. John's samples tend to roughly group together (Figures 4.5 and 4.6). Close comparison of those score plots with the same score plots using labels based on chemical composition shows that the majority of the St. John's samples are anthropogenically influenced, while a few have a stronger seaspray component (Figures 4.3 and 4.4). The samples controlled by anthropogenic sources group together on the location plots (Figures 4.5 and 4.6), while those controlled by seaspray tend to plot away from the larger group. These plots confirm that the two main influences on the chemical and isotopic composition of the samples are

Table 4.3 Precipitation nitrate concentration ranges from this study and other studies in Newfoundland and Atlantic Canada.

Location	NO ₃ ⁻ (ppm)	Type	Comments	Reference
St. John's, Newfoundland	0.05 to 0.88	rain and snow	single events	Jamieson (1995)
Gros Morne National Park, Newfoundland	<0.01 to 1.420	snow		Squires (2002)
Terra Nova National Park, Newfoundland	<0.05 to 0.135	snow		Golletz (2002)
Terra Nova National Park, Newfoundland	<0.02 to 0.220	rain and snow	weekly collection	NEPMoN (2002)
Shelburne, Nova Scotia	0.025 to 6.85	rain	single events (Aug/83 to Jul/85)	Wadleigh et al. (1996)
8 Jackson, Nova Scotia	1.65 ± 2.34	rain and snow	24 h integrated samples. Arithmetic mean ± S.D.	CAPMoN (2003)
Kejimikujik, Nova Scotia	2.40 ± 4.08	rain and snow	24 h integrated samples. Arithmetic mean ± S.D.	CAPMoN (2003)
Harcourt B, New Brunswick	2.24 ± 3.76	rain and snow	24 h integrated samples. Arithmetic mean ± S.D.	CAPMoN (2003)
Goose Bay, Newfoundland	0.68 ± 1.08	rain and snow	24 h integrated samples. Arithmetic mean ± S.D.	CAPMoN (2003)
Bay D'Espoir, Newfoundland	1.14 ± 2.12	rain and snow	24 h integrated samples. Arithmetic mean ± S.D.	CAPMoN (2003)
St. John's, Newfoundland	0.075 to 1.814	rain and snow	single events	This study

anthropogenic and seaspray sources.

The percent seaspray sulphate (PSS) was calculated to aid in source interpretation (Section 1.3). Low PSS values indicate that the majority of the sulphate present in the sample was derived from non-seaspray sources such as stationary fossil fuel combustion sources, while higher values denote a stronger seaspray influence. For this study, PSS values of approximately 50% or more were used as an indication of a higher seaspray influence. Using this cutoff point, seven samples were denoted as having more of a seaspray input (Table II.12). Six of the seven samples (SJS02-0123, SJ02-0314, SJ02-0322, SJ02-0328, SJ03-0201 and SJ03-0202) were collected during the winter months, during which time increased wave activity emits more oceanic components into the atmosphere (Wadleigh et al., 1996). The seventh sample, SJ02-0825 was collected during the summer. Air mass back trajectories calculated for each of these samples (Appendix III) reveal that in general the air masses did spend a large proportion of the four days prior to sampling over the ocean. If the air mass travelled across land, the last 24 to 48 hours were generally spent over the ocean.

Inspection of the chemical data available for these samples (Tables II.5, II.7 and II.14) confirmed that seaspray was an important chemical source. All seven samples are dominated by Na^+ and Cl^- , with smaller amounts of Mg^{2+} , K^+ and Sr , all of which are mainly oceanic in nature.

The remaining 17 samples collected at the St. John's location had stronger anthropogenic signals. The PSS values for many of the samples were less than 10%,

indicating a possible heavy stationary fossil fuel combustion influence. Air mass back trajectories generally show that the air masses moved across an area of heavy pollution, such as the Great Lakes region in southern Ontario and the northern United States, or along the northeastern seaboard of the US. These areas combust oil and coal in power plants and other facilities as a source of energy and heat. Although there are large amounts of vehicle emissions in that region, Shaw (1984) believed that nitrogen oxides emitted from vehicles at ground level would undergo considerable impaction and deposition near the source, and would therefore be less subject to long range transport than industrial emissions which are released from tall stacks up to several hundred metres above ground level. Another possible anthropogenic input may be from the refining and smelting of ores rich in copper, zinc, lead and sulphur. Several areas in Newfoundland have been mined for sulphide ores (Figure 2.1). Although these mines are no longer operating, the tailings, or waste rock, generated from years of processing the ore may still be present. The potential for distribution of the dust by wind exists if these tailings are exposed to the atmosphere. Long range transport of smelting pollutants to Newfoundland is quite possible, as eastern Canada is downwind of large metal smelters in Quebec and central Ontario (Environment Canada, 1998).

Five of the remaining 17 samples (SJ02-0429, SJ02-0531, SJ02-0624, SJ02-0710 and SJ02-1001) have high V and Ni signatures, with minor amounts of Co, Zn, Cu and Pb. Sample SJ03-0131, which was not used in the PCA, follows the same trend. These elements are used to trace oil combustion pollutants in the atmosphere. One sample which

contains little to no V or Ni, but has high concentrations of Cu, Zn and Pb is SJ02-0910. This might represent ore processing or coal combustion.

Another grouping includes those samples that contain a mixture of sources. These samples are not dominated by any one source; they exhibit characteristics of several sources such as seaspray, automobile emissions, fossil fuel combustion, and possibly ore processing or wood combustion. SJ02-0917 and SJ02-1020 represent samples influenced by several sources.

Chemical concentrations appear to be somewhat controlled by the seasons. A stronger anthropogenic influence is seen during the summer months, while the winter samples are dominated by seaspray signatures. St. John's samples have higher Na^+ , Cl^- , and Mg^{2+} concentrations during the winter months, while NO_3^- , SO_4^{2-} and NH_4^+ are dominant during the summer season (Figure 3.2). Trace element data also vary seasonally, with increased oceanic inputs of As and Sr during the colder months and stronger anthropogenically derived elements such as V, Ni, Mn, Mo and Pb during the summer (Figure 3.7). This is contrary to the expected trend of increased fossil fuel combustion during the colder, winter months (Freyer, 1991). This "opposite" trend in anthropogenic and oceanic sources may be influenced by the fact that the rain collector was placed in close proximity to a small oil-fired power station which operates year round. As well, the Come by Chance oil refinery (see Figure 2.2), which also operates year round, may be influencing the chemical composition of the samples collected at St. John's. The stronger oceanic winter influence may also be due to St. John's being a coastal city.

By roughly grouping the samples based on their chemical compositions, an attempt can be made to interpret the isotopic data collected for the samples. Heaton (1990) attributed more depleted ^{15}N signatures to automobile sources while fossil fuel sources displayed more enriched values. As well, Freyer (1991) and Myiake and Wada (1971) stated that soil emissions and oxidation by marine bacteria can produce NO_3^- with a $\delta^{15}\text{N}$ as low as -20‰.

In general, samples which contain components derived from the ocean tend to have a more negative $\delta^{15}\text{N}$ signature (Table 4.4). The nitrogen stable isotope data obtained for these samples ranged from -7.7 to +2.7‰. The positive value came from a snow sample. Unfortunately, this was the only snow sample collected at this location. The more enriched $\delta^{15}\text{N}$ may be related to processes during the formation of snow, but without further samples for comparison this cannot be confirmed. This particular snow sample (SJS02-0123) did have a seaspray signature, but also displayed weak fossil fuel inputs. It is possible that the combustion source NO_3^- may have had a strong impact on the isotopic composition. It should also be pointed out that the other oceanically influenced samples often contain some anthropogenic signals, which may affect the isotopic composition. Using the chemical data available, two samples (SJ02-0314 and SJ03-0202) appear close to being seaspray endmembers. Both are winter samples and have $\delta^{15}\text{N}$ values of -5.7‰ and -7.1‰ respectively, confirming the idea that samples controlled by seaspray tend to have more depleted $\delta^{15}\text{N}$ values.

The group which appears to be controlled by oil combustion tends to have $\delta^{15}\text{N}$

Table 4.4 Isotopic data of seaspray influenced samples for St. John's.

Sample	$\delta^{15}\text{N}$ (‰, N_{AIR})	$\delta^{18}\text{O}_{\text{NO}_3}$ (‰, VSMOW)
SJS02-0123	+2.7	+15.8
SJ02-0314	-5.7	-
SJ02-0322	-7.7	-
SJ02-0328	-3.5	+47.9
SJ02-0825	-3.7	+51.5
SJ03-0201	-2.9	-
SJ03-0202	-7.1	+27.9

values which are more enriched than the seaspray samples (Table 4.5). Freyer (1991) stated that crude oil had $\delta^{15}\text{N}$ values of -2 to +13‰. Because little fractionation of nitrogen isotopes is expected at high temperatures, combustion of this fuel should lead to atmospheric NO_3^- with more enriched signatures than that of natural sources, as found in this study. Sample SJ02-0531 appears to be mainly controlled by oil combustion pollutants, and has a $\delta^{15}\text{N}$ of -2.1‰. However, other samples containing strong oil combustion signatures, such as SJ02-0624, have $\delta^{15}\text{N}$ of -3.6‰, outside the previously reported range for this source. It is possible that the $\delta^{15}\text{N}$ range of NO_x produced during oil combustion is slightly larger than reported as few studies have actually measured these values.

Samples such as SJ02-0624 bring into question the influence of soil and ocean emissions transported over long distances or acquired locally by the air mass. There are no specific chemical signatures associated with soil emissions, making it difficult to evaluate their influence on the overall isotopic composition of a sample. Other samples collected during the colder months (SJ02-1001 and SJ03-0131) appear to be controlled by oil combustion sources, but have $\delta^{15}\text{N}$ values which are much more depleted than expected (-8.63‰ and -8.19‰, respectively). It is unlikely that these samples would be influenced by soil emissions due to the time of year in which they were collected. Another potential contributor to the more depleted ^{15}N signatures is an increase in wave activity which may inject more depleted ^{15}N NO_3^- into the atmosphere from the ocean. It is also possible that automobile emissions could impact their signatures. NO_x emissions

Table 4.5 Isotopic data of samples believed to be influenced by oil combustion for St. John's.

Sample	$\delta^{15}\text{N}$ (‰, N_{AIR})	$\delta^{18}\text{O}_{\text{NO}_3}$ (‰, VSMOW)
SJ02-0429	-3.7	-
SJ02-0531	-2.1	-
SJ02-0624	-3.6	-
SJ02-0710	-1.4	46.1
SJ02-0807	-2.8	52.2
SJ02-1001	-8.6	53.9
SJ02-1114	-2.2	-
SJ03-0131	-8.2	25.8

produced from idling vehicles have reported $\delta^{15}\text{N}$ values as low as -13‰, but the chemical data (Mn) indicates that automobiles are not a major contributor overall to these samples. However, Mn may not be a conclusive indicator of the presence of automobile emissions. This discrepancy between source and expected isotopic composition may be an indication that sources may not be the main control for the $\delta^{15}\text{N}$. There is evidence that atmospheric processes, possibly controlled by climate, may play an important role in nitrogen isotopic compositions in the atmosphere (Hastings et al., 2003) (see below).

One sample, collected in July of 2002, was heavily influenced by massive forest fires burning in Quebec (Eric Santerre, pers. comm., 2004). This sample, SJ02-0709, contained high concentrations of NO_3^- , SO_4^{2-} , Al, Mn, Cu and Zn. As well, it was enriched in K^+ and Ca^{2+} relative to Na^+ , indicating that these two elements were derived from sources other than seaspray, most likely continental sources. Both Cu and Zn are released during the burning of wood, and Russell et al. (1998) stated that biomass burning is an important source of atmospheric NO_3^- . This particular sample had a $\delta^{15}\text{N}$ of -0.5‰, indicating that wood combustion may result in atmospheric nitrate with more ^{15}N enriched nitrogen isotopic compositions.

Several of the remaining St. John's samples are governed by a mixture of sources. They contain characteristic elements for seaspray, oil combustion, automobile emissions, continental sources and coal combustion/ore processing. The $\delta^{15}\text{N}$ values of these mixtures vary, and will be dependent upon the relative importance of each source for the particular sample. Soil denitrification emissions along with nitrate from the ocean have

more depleted nitrogen isotopic values. If these sources are important in a particular sample, they may result in a more negative $\delta^{15}\text{N}$. The St. John's collection site is located near an extensive wetland area surrounding a pond inhabited by ducks, thus it is possible that a depleted signature may be incorporated into the rain in this area. As well, some of the air masses travel over the Atlantic provinces of Canada, which contain large amounts of farmland. It must also be considered that there is a large highway located a few kilometres behind the collection site, and the collection area itself is in close proximity to several main streets near Memorial University and the General Hospital which are used extensively. Automobiles emit nitrate with $\delta^{15}\text{N}$ values of -13 to -2‰ (Heaton, 1990). The burning of bunker C fuel in the power generating station next to the collection site may also have an impact on sample nitrate, as well as long range transport of material from the Come By Chance oil refinery and other distant sources from Canada and the United States. The majority of the samples also contain substantial amounts of Al which is used to trace continental inputs to the atmosphere. The range of $\delta^{15}\text{N}$ values obtained during this study do fall within the range of previously reported values from other studies of atmospheric nitrate (Figure 1.7).

It is generally believed that the $\delta^{15}\text{N}$ signatures of nitrate are dependent upon the sources of the nitrate. Figure 4.7 shows a seasonal trend of $\delta^{15}\text{N}_{\text{NO}_3}$ for this study in which samples are generally more depleted during the winter and more enriched during summer months, as was found in a study by Hastings et al. (2003). They interpreted the negative cold season values as due to anthropogenic sources, while the positive warm

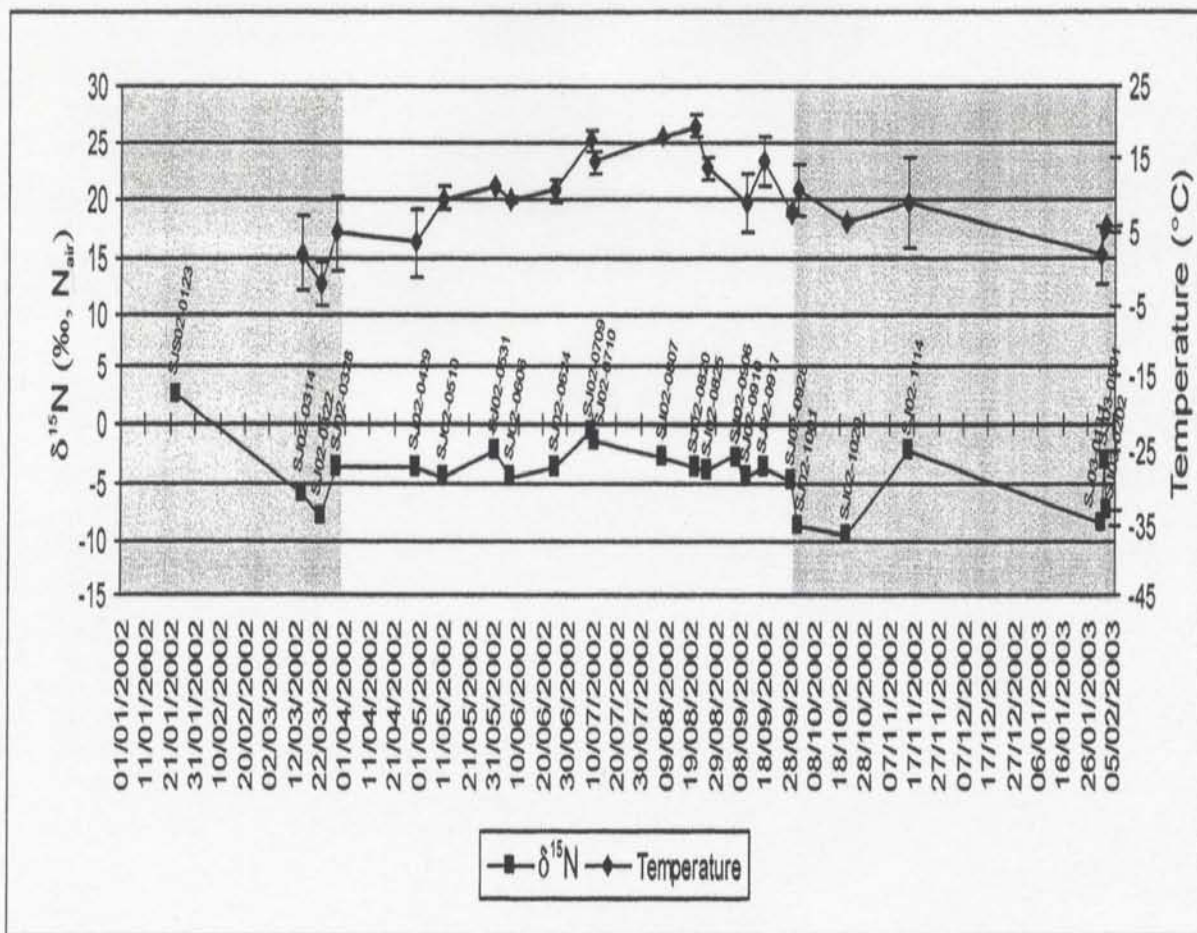


Figure 4.7 $\delta^{15}\text{N}$ variations with temperature for St. John's samples ($r=0.530$, $p=0.008$, $n=23$). Shaded areas represent winter months. Bars represent the temperature range during the sample collection.

season values were attributed to nitrate formed by lightning fixation. The seasonal trend found in this study as well as that by Hastings et al. (2003) is contrary to what has been found by researchers such as Freyer (1978) and Heaton (1986,1987) who attributed lower $\delta^{15}\text{N}$ spring and summer values to soil emissions and higher $\delta^{15}\text{N}$ autumn and winter values to an increase in fossil fuel combustion. Nitrate deposition values may offer some insight into this phenomenon. Because the samples in this study were collected on an event basis, the sample volumes vary. In order to compare the NO_3^- values between samples, the volume component was removed. The amounts deposited ranged from 0.66 to 13 mg NO_3^- . The highest amounts of NO_3^- are deposited during the summer (Figure 4.8). However, the difference between summer and winter values is not very large, indicating that there is a constant amount of background nitrate present in the study area, leading to a decrease in the effect of seasonality at this location. The lack of seasonality in nitrate deposition may be largely due to the fact that the largest single source of NO_x emissions, motor vehicles, are used year round. Vehicle emissions account for about 60% of all emissions in Canada (Environment Canada, 1998).

There are several potential reasons why this particular seasonal trend in $\delta^{15}\text{N}$ exists for this study. It is possible that a stronger oceanic influence during the winter months may lead to a more ^{15}N depleted signature, while the summer months show a fossil fuel influence which may be present year round. As well, a stronger automobile influence during the colder months could potentially decrease $\delta^{15}\text{N}$ compositions of winter samples. These hypotheses will require further work along with a larger number of samples to

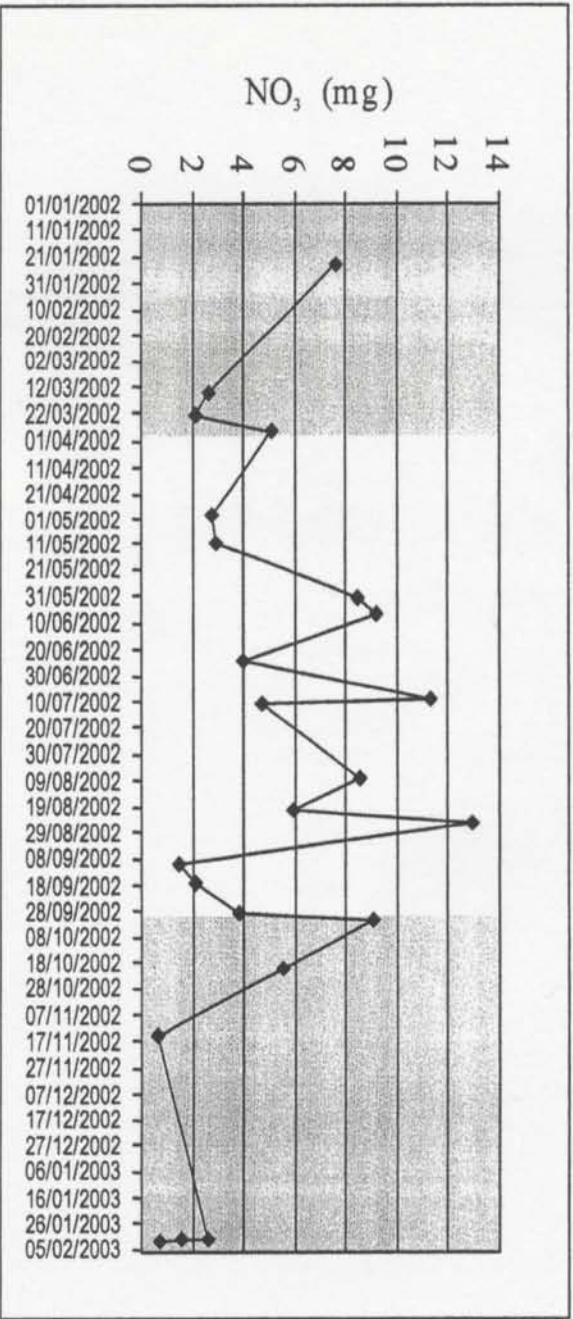


Figure 4.8 NO₃ (mg) variations for St. John's samples. Shaded areas represent winter months.

confirm or disprove them.

Other possibilities to consider when interpreting the isotopic data for the study area is that Newfoundland has a maritime climate with relatively warm winters and cool summers. Because there is such a large range in temperature fluctuations throughout the year, it is difficult to categorize samples based on the four calendar seasons. This is why for this study, only two seasons were used: winter (Oct. - Mar.) and summer (Apr.-Sept.). Due to this climate, the growing season begins later in the spring and early summer and soil activities extend later into fall, which may influence the isotope signatures found at this site. As well, the amount of fossil fuel combustion for heating purposes also varies depending on the temperature. For example, it is common for residents of this province to use oil and wood combustion year round for home heating purposes, even during summer when nighttime temperatures tend to drop.

Seasonality in $\delta^{15}\text{N}$ may also be related to atmospheric formation mechanisms of nitrate, which have a temperature dependence. A Pearson Correlation of the $\delta^{15}\text{N}$ data with temperature produced an r value of 0.530 ($p=0.008$, $n=23$) (Figure 4.7), indicating a slight dependence of isotopic composition on temperature. This variation with temperature has been previously reported by Freyer (1991). He decided that the trend in his study was not due to seasonality in sources since there was a general similarity in $\delta^{15}\text{N}$ data from different environments for nitrate species. Freyer reported more negative signatures during the warmer months while samples collected during autumn and winter displayed more positive values. Freyer et al. (1993) suggested that the large fractionation

($\sim +18\text{‰}$) which occurs during the conversion of NO to NO_2 in the atmosphere may exert more control over the $\delta^{15}\text{N}$ variation than sources. Heaton (1986) also stated that seasonal variations may be controlled by the chemical reactions involved in nitrate formation rather than the dominant source during a particular season. For this study, however, the nitrogen isotopic composition appears to be controlled by the dominant sources of atmospheric nitrate during each season. Stronger anthropogenic influences during the summer result in more positive $\delta^{15}\text{N}$ values, while more dominant oceanic influences in winter result in more negative $\delta^{15}\text{N}$ values.

Three studies have looked at both nitrogen and oxygen isotopes of nitrate in precipitation samples (Kendall et al., 1995b; Durka et al., 1994, Hastings et al., 2003). All three studies found that the $\delta^{18}\text{O}$ of atmospheric nitrate is generally much heavier than that of atmospheric O_2 , which has a $\delta^{18}\text{O}$ value of $+23.5\text{‰}$ (Kendall, 1998) (Figure 1.8). Kendall (1998) hypothesised that the large range of $\delta^{18}\text{O}$ values measured in nitrate precipitation could be due to a number of factors including incomplete fossil fuel combustion in both stationary and mobile sources, fractionations associated with the formation of nitrate in thunderstorms, and photochemical reactions in the atmosphere. She also speculated that different anthropogenic sources of nitrate may have characteristic $\delta^{18}\text{O}$ values analogous with $\delta^{15}\text{N}$ variations found in previously discussed studies. Stationary sources such as power plants produce NO_x which is later oxidised by O_3 ($\delta^{18}\text{O} \sim +90\text{‰}$; Krankowsky et al., 1995) in the atmosphere, resulting in nitrate with high $\delta^{18}\text{O}$ compositions. Automobiles, on the other hand, use atmospheric O_2 as the main source of

nitrate oxygen, giving rise to nitrate with $\delta^{18}\text{O}$ similar to that of O_2 (+23.5‰). The relative contributions of these two main anthropogenic sources may create a seasonal effect in $\delta^{18}\text{O}$ with higher values during the winter when more fossil fuel is combusted for heat, and lower values during the warmer months when the fossil fuel influence is not as strong. Hastings et al. (2003) believed that the $\delta^{18}\text{O}$ of the nitrate is controlled by the interactions of the precursor oxinitrogen species with different oxygen species in the atmosphere, such as OH and O_3 , which have distinct $\delta^{18}\text{O}$ compositions. Their study indicated that seasonal trends in $\delta^{18}\text{O}$ were related to the dominant oxygen species in the atmosphere whereby nitrate collected during the warm season had been oxidised by OH ($\delta^{18}\text{O} \sim -30$ to $+2\%$), while O_3 ($\delta^{18}\text{O} \sim 90$ to 122%) was the dominant oxidant involved in nitrate formation during the colder months.

Sixteen of the twenty-four samples collected were analysed for oxygen isotopes in nitrate. A plot of the isotopic values can be seen in Figure 4.9. A correlation of the $\delta^{18}\text{O}_{\text{NO}_3}$ and temperature resulted in an r value of 0.320 ($p=0.227$, $n=16$). Looking at end-member samples based on chemical data, an attempt was made to characterise sources based on the $\delta^{18}\text{O}_{\text{NO}_3}$. Unfortunately, many of the samples which are considered to be controlled by one main component have no $\delta^{18}\text{O}_{\text{NO}_3}$ information available due to either low nitrate concentrations or instrument error. Only one of the samples analysed had a $\delta^{18}\text{O}_{\text{NO}_3}$ less than the $\delta^{18}\text{O}$ of atmospheric O_2 (+23.5‰). This particular sample (SJS02-0123) had a $\delta^{18}\text{O}_{\text{NO}_3}$ value of +15.8‰, and was a snow sample with a seaspray influence. Because no other snow samples were analysed from this location, it is impossible to tell whether the

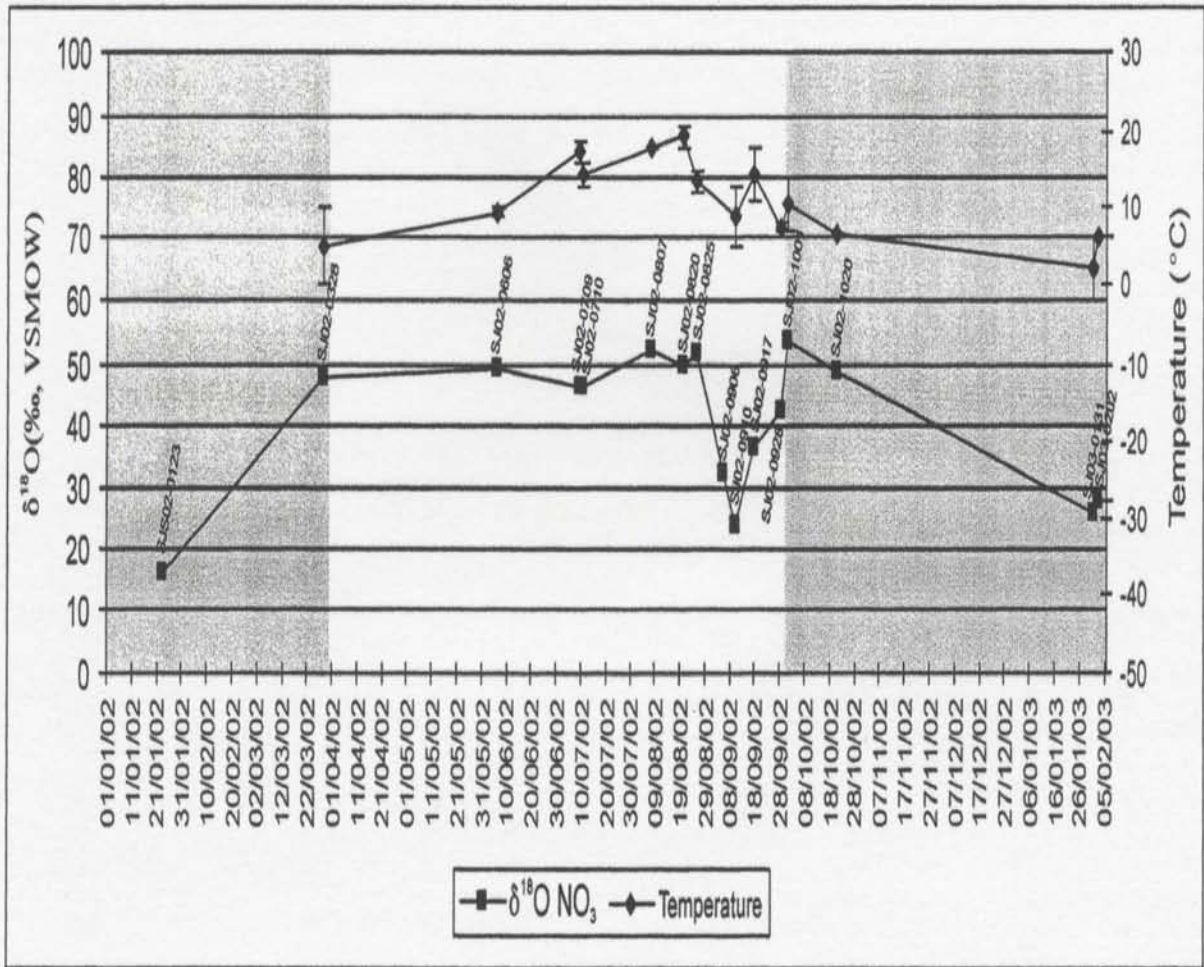


Figure 4.9 $\delta^{18}\text{O}_{\text{NO}_3}$ variations by season and temperature for St. John's samples ($r=0.320$, $p=0.227$, $n=16$). Shaded areas represent winter months. Bars represent the temperature range during the sample collection.

value is related to the fact that the sample was snow, or whether this lower $\delta^{18}\text{O}_{\text{NO}_3}$ is a seaspray signature. Other samples that were influenced by seaspray had varying compositions (Table 4.4).

Only one sample with an oil combustion chemical signature (SJ02-1001) was analysed for $\delta^{18}\text{O}_{\text{NO}_3}$, and had a value of +53.9‰. This is consistent with stationary source NO_x oxidised by O_3 , resulting in higher $\delta^{18}\text{O}$ values. However, because there are no other samples available compare with this, it cannot be proven that the source is controlling the isotopic composition of nitrate.

Looking at all of the $\delta^{18}\text{O}_{\text{NO}_3}$ data available (Figure 4.9), there appears to be a slight seasonal trend whereby samples collected in January and February of each year have lower values than other samples. Unfortunately, missing data points hinder the interpretation. Most of the samples collected from March to November have $\delta^{18}\text{O}_{\text{NO}_3}$ values between +40 and +54‰ with the exception of three samples collected in September of 2002. SJ02-0906, SJ02-0910 and SJ02-0917 have nitrate oxygen isotopic compositions of +32.6‰, +23.7‰ and +36.2‰ respectively. The chemical data for SJ02-0906 does not indicate a particular source for this sample, and it has a calculated percent seaspray value of 7%, indicating the air mass received sulphate from a source other than seaspray. SJ02-0910, which has the second lowest $\delta^{18}\text{O}_{\text{NO}_3}$ recorded for the entire data set, has a mixture of sources indicated by its chemical composition along with a PSS value of 10%, but it has an extremely high Cu concentration of 44 ppb. Cu can come from a variety of sources including ore processing, fossil fuel combustion, wood combustion and bubble bursting in

the ocean. The air mass back trajectory for this sample (Figure III.16) shows that the air mass moved from northern Quebec across Labrador and to the sampling location. It is possible that some of the Cu may have been acquired from ore processing operations in those areas. SJ02-0917 also displays weak characteristics of several sources, with more of a fossil fuel influence than the previous two samples. The reasons why these three samples have lower $\delta^{18}\text{O}_{\text{NO}_3}$ values than other samples collected at this location are unclear. This decrease in isotopic composition was not observed for nitrogen isotopes (Figure 4.7), however NO_3 concentrations (mg) were significantly lower for the above mentioned September samples (Figure 4.8). The lower NO_3 concentrations may be an indication of a depletion event in the atmosphere which might be related to a corresponding $\delta^{18}\text{O}_{\text{NO}_3}$ depletion, however further studies would be required to confirm this theory.

The $\delta^{18}\text{O}_{\text{NO}_3}$ values do not appear to be controlled by source. This observation may be due in part to the lack of endmember samples analysed for oxygen. It is possible, looking at the slight seasonal trends in the data, that atmospheric processes may be the main influence on the oxygen isotopic compositions. Once emitted to the atmosphere, oxinitrogen species may undergo a series of reactions and transformations involving different oxidants which may potentially have very different $\delta^{18}\text{O}$ isotopic signatures. When NO is released to the atmosphere, it may be oxidised by O_3 ($\delta^{18}\text{O} \sim +90$ to $+122\text{‰}$) or HO_2 ($\delta^{18}\text{O} \sim +23.5\text{‰}$) to form NO_2 (Reactions 1.2 and 1.3). The NO_2 produced either by the previous reaction or which is emitted directly into the atmosphere via natural or anthropogenic sources, is oxidised by either a hydroxyl radical (Reaction 1.4) to form

nitric acid, or by ozone to form nitrate (Reaction 1.11).

The reaction involving the hydroxyl radical usually occurs during the day and tends to be more dominant during the summer months when increased solar radiation results in a higher OH concentration in the atmosphere (Freyer et al., 1993). Hydroxyl radicals are formed when ozone molecules are dissociated by solar radiation into atomic oxygen and diatomic oxygen. The atomic oxygen reacts with water in the atmosphere to form two hydroxyl radicals (Schlesinger, 1997). Röckmann et al. (1998) thought that the OH would initially reflect the isotopic composition of ozone, but a fast isotopic exchange between atmospheric water and the hydroxyl molecule can occur, resulting in OH with a possible oxygen isotopic composition of -30 to +2‰.

Freyer et al. (1993) believed that the reaction whereby NO_2 is oxidised by O_3 occurs mainly during the night. The nitrate produced may undergo a reaction with NO_2 to form N_2O_5 (Reaction 1.12) whose atmospheric storage is favoured during cooler temperatures. The authors also believed that this reaction would dominate during the colder winter months. However, Freyer et al. (1993) also stated that maximum ozone concentrations occur during the summer months, leading to a measured increase in the oxidation of NO to NO_2 in the nighttime during their study.

The St. John's study area, being a coastal environment with a maritime climate, typically experiences cool summers and mild winters. During the summer, daytime temperatures are warm while nighttime temperatures are often much cooler. This could explain why samples collected for this study have higher $\delta^{18}\text{O}$ values for the summer

months. It is conceivable that atmospheric reactions involving ozone produce nitrate with a high oxygen isotopic signature, which may not be counteracted as strongly by daytime reactions involving the hydroxyl radicals. As well, this area experiences a large number of days with cloud cover. This may affect the amount of solar radiation, and therefore hydroxyl production, in our atmosphere. An explanation for the lower winter $\delta^{18}\text{O}$ values may be related to the reaction of N_2O_5 with H_2O , which has a much lower $\delta^{18}\text{O}$ value than ozone (Reaction 1.13). If the N_2O_5 molecule is stored during winter months instead of dissociating into NO_2 and NO_3 , it will react with atmospheric water and form nitric acid. Another possibility is that during the mild winters, the hydroxyl radical reaction may be a dominant force, resulting in lower $\delta^{18}\text{O}_{\text{NO}_3}$ values. If there is a limited amount of ozone present in the atmosphere during the winter, NO_x may be oxidised by HO_2 , which receives its oxygen atoms from O_2 . This would result in the nitrate produced having lower $\delta^{18}\text{O}$ values than that produced via oxidation with ozone.

The oxygen isotopic composition of the rainwater collected was also measured. $\delta^{18}\text{O}_{\text{H}_2\text{O}}$ increases with increasing temperature (Dansgaard, 1964). As a result, summer rain is typically enriched in ^{18}O relative to rain in the winter. For this study, $\delta^{18}\text{O}_{\text{H}_2\text{O}}$ values are not strongly correlated with temperature ($r=0.018$, $p=0.934$, $n=23$) (Figure 4.10). The differences between the two seasons is generally not very pronounced, but several samples collected during the winter do have much lower isotopic compositions. Kendall et al. (1995b) proposed that some of the oxygen in atmospheric nitrate was from O_2 , while some was from H_2O . If there is a reaction whereby nitrate acquires some of its oxygen isotopic

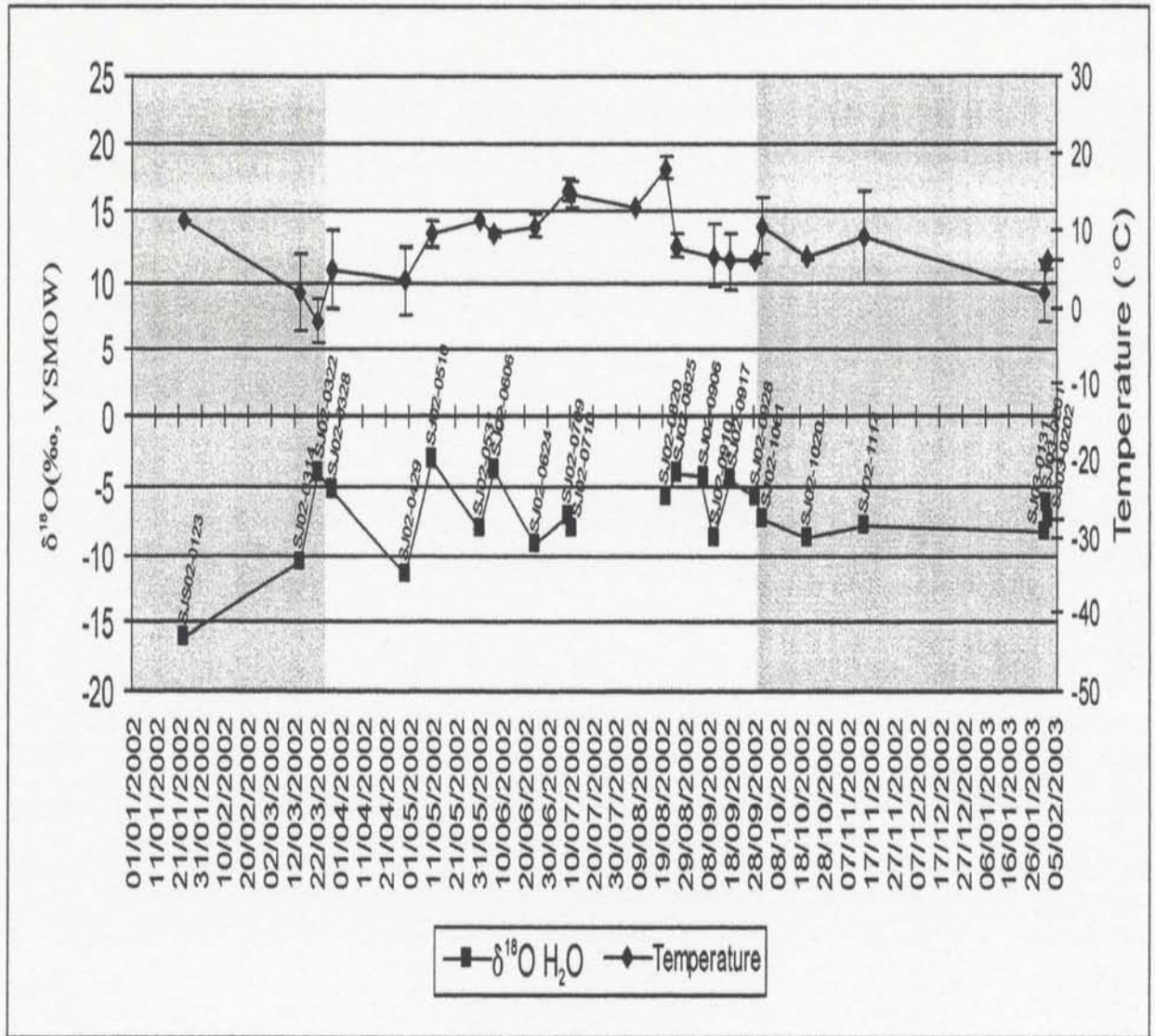


Figure 4.10 $\delta^{18}\text{O}_{\text{H}_2\text{O}}$ variations with temperature for St. John's samples ($r=0.018$, $p=0.934$, $n=23$). Shaded areas represent winter months. Bars represent the temperature range during the sample collection.

signature from atmospheric water, the higher $\delta^{18}\text{O}_{\text{H}_2\text{O}}$ values during the summer may result in higher $\delta^{18}\text{O}_{\text{NO}_3}$ values as well. During the winter when the $\delta^{18}\text{O}_{\text{H}_2\text{O}}$ is more negative, it may deplete the $\delta^{18}\text{O}_{\text{NO}_3}$ signatures. Although H_2O itself is not involved in any of the main oxidation steps of NO_x , it may be indirectly involved through the hydroxyl radical, a molecule which may reflect the oxygen isotopic composition of the water.

Because $\delta^{18}\text{O}_{\text{H}_2\text{O}}$ represents oxygen of the transported air mass, comparing it to the $\delta^{18}\text{O}_{\text{NO}_3}$ may reveal whether this water was involved in oxidation of the nitrate. Figure 4.11, a graph of the water oxygen versus nitrate oxygen, does not reveal a strong association in the data. The coefficient of determination (r^2) calculated for the data is 0.09, confirming that a strong association does not exist between the two oxygen isotopes. One sample with a low $\delta^{18}\text{O}$ value seems isolated from the others. This single low value comes from the snow sample discussed above. No obvious trends between the $\delta^{18}\text{O}$ values for water and nitrate may imply that all of the nitrate was oxidised before being incorporated into the transporting air mass, and therefore the nitrate must have come from distant sources. The associated chemical data may indicate local influences in the sample set. Comparison of oxygen isotopes in water and chemical compounds has worked well in similar studies involving atmospheric sulphates (Jamieson, 1995; Wadleigh et al, 2001), but does not appear to aid in interpretation of the atmospheric nitrates in this study. This may be due to the complex atmospheric transformations that oxinitrogen species undergo before being deposited in wet deposition. Even in studies involving sulphates, a good correlation of oxygen isotopic compositions might not be obtained between the sulphates

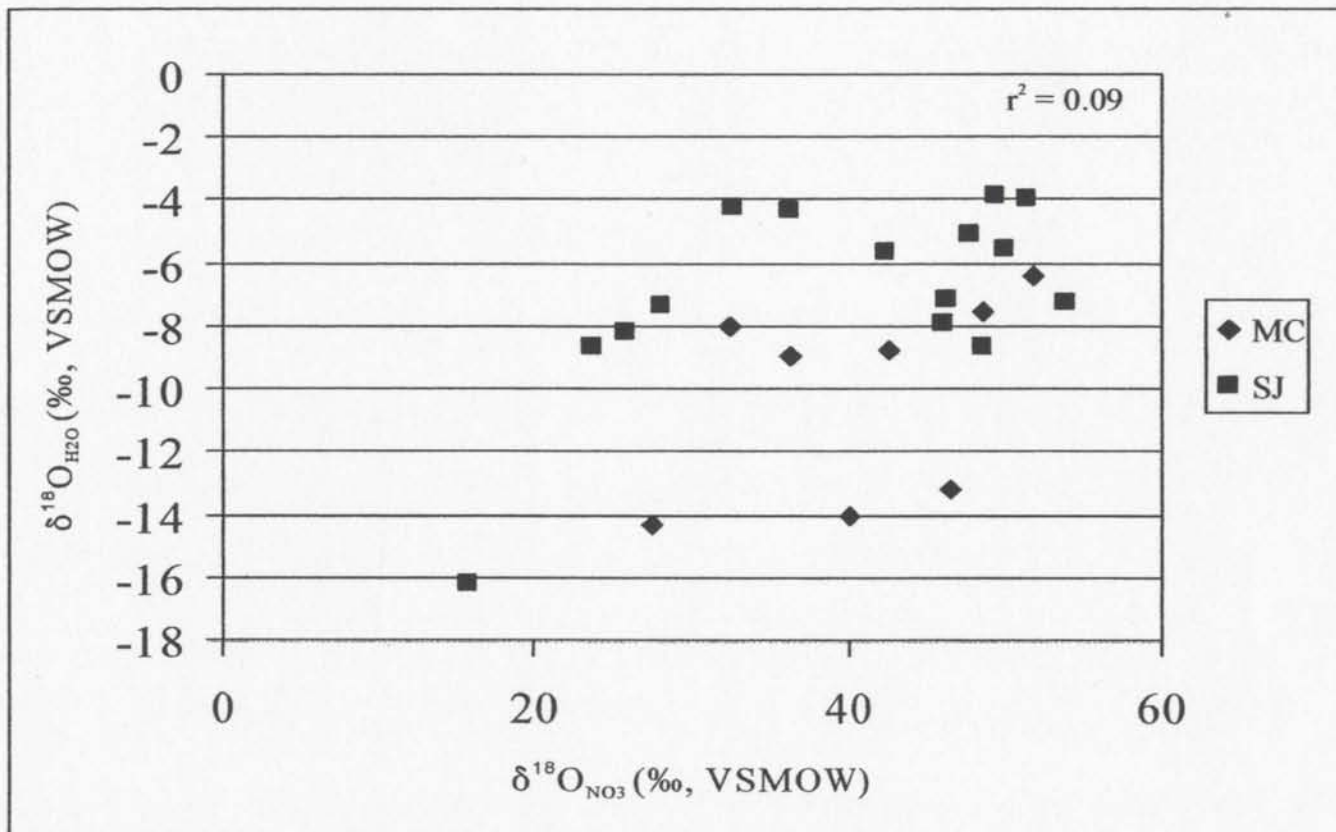


Figure 4.11 $\delta^{18}\text{O}_{\text{NO}_3}$ versus $\delta^{18}\text{O}_{\text{H}_2\text{O}}$ for both locations. MC and SJ represent samples collected at McIvers and St. John's, respectively.

and water except in rare circumstances where the majority of samples are of local origin (Moire Wadleigh, pers. comm. 2004). The most apparent reason for the lack of correlation between $\delta^{18}\text{O}_{\text{H}_2\text{O}}$ and $\delta^{18}\text{O}_{\text{NO}_3}$ is that water is not a main reactant in the formation of atmospheric nitrate.

4.5 McIvers

McIvers is a small town located in the Bay of Islands on the west coast of the island of Newfoundland. There are no major point sources within the coastal community, so a strong marine influence was expected, with the possibility of anthropogenic inputs from long range transport. Most samples display such a mixture with inputs from the ocean, automobile emissions, wood combustion sources and fossil fuel combustion.

Analysis of dissolved nitrate yielded values ranging from 0.057 to 0.686 ppm for this location. These values are comparable to nitrate concentrations found by other precipitation studies in Newfoundland and Atlantic Canada (Table 4.3). Being a more rural environment, McIvers has a smaller range of nitrate concentrations than St. John's, an urban site. Precipitation collected at the McIvers site is slightly acidic, with an average pH of 5.17.

Looking at the score plots from the Principal Component Analysis (Figures 4.5 and 4.6) the McIvers samples tend to group together. Of the nine samples used in the analysis, only one was considered to be mainly of a seaspray origin (Figures 4.3 and 4.4). This particular sample plots to the far right on Figure 4.4, away from the remaining eight

McIvers samples which generally represent a mixture of sources with automobile emissions being the strongest influence. A second sample which tends to plot away from the main group can be seen at about the middle of Figure 4.5. This sample is anthropogenic in nature, but it is controlled by what appears to be a wood combustion signature, which isolates it from the other anthropogenically controlled samples. The McIvers samples appear not to be controlled by the same influences as the samples collected at St. John's.

Eleven samples in total were collected and analysed at this location. Based on PSS values (Table II.13), three of these samples appear to be marine in origin (PSS > ~50%). MCS02-0205, MC02-0413 and MCS03-0126 are dominated by elements derived from the ocean, including Cl^- , Na^+ , Mg^{2+} and Sr (Tables II.6, II.8 and II.15). Air mass back trajectories (Figures IV.1, IV.3 and IV.11) confirm that the air masses did spend at least the last 24 hours prior to collection over the ocean.

Fossil fuel combustion signatures are not as pronounced amongst the McIvers samples, although they do exist. MC02-0624 and MC02-0924 both display chemical characteristics which indicate oil combustion (Table II.15), and had PSS values of 17% and 23% respectively. Other samples in the data set had PSS values lower than 13% indicating a sulphate source other than seaspray, however the chemical data do not support these samples as being influenced as strongly by oil combustion as were the two samples previously discussed. There could be more of an effect from long range transport of coal combustion emissions at this site, which could account for the low PSS values, but

this cannot be verified by the chemical data available. As well, the PSS values may be lower due to possible biogenic sulphate emissions from the ocean. The air mass back trajectory for MC02-0624 (Figure IV.5) shows that the air travelling at the 925mb level originated just to the north of the northeastern United States, where it could have acquired some of its pollutants. The air also travelled across Newfoundland, where it may have been influenced by emissions from the Come by Chance oil refinery. The back trajectory calculated for MC02-0924 (Figure IV.9) indicates that the air mass travelled over the open ocean to the east of the United States, then travelled quickly across the maritime provinces to the sampling location. Emissions from the heavily industrialised eastern seaboard area of the U.S. could easily have influenced the chemical composition of this particular air parcel as it travelled towards Newfoundland.

One sample in particular, MC02-0401, appears to have been dominated by wood combustion emissions. The dominant chemical constituent of this sample is zinc, which is emitted by vegetation and wood combustion to the atmosphere (Pacyna, 1986b). This sample also has a higher concentration of NO_3^- than SO_4^{2-} , which is unusual because the sulphate concentration is greater than nitrate in the majority of the samples collected for both locations. Russell et al. (1998) found that biomass burning, which is similar to wood combustion, was an important source of atmospheric nitrate.

Many of the samples display a mixture of sources based on their chemical compositions. Four of the eleven samples collected (MC02-0401, MC02-0606, MC02-0624 and MC02-0719) have manganese concentrations which are higher than many of the

other components measured (Table II.15). Automobile emissions are likely an important contributor of atmospheric NO_x at this location.

Seasonal trends exist within the chemical data for this site. McIvers data exhibit a stronger oceanic influence during the winter months with an increase in Cl^- , Na^+ , K^+ and Mg^{2+} (Figure 3.3), all of which are found in seaspray. There is also an increase in SO_4^{2-} during the winter months, which may be due to seaspray influence as well. Both NO_3^- and NH_4^+ have higher summer values, indicating an increase in nitrogen sources during this time. In general, the seasonal metal concentrations agree with the major ion data and show a stronger seaspray influence in the winter, including higher concentrations of Sr, Ba, and As (Figure 3.8). Cu has higher values in the winter; there was little or no copper found in summer samples at this site. Many elements associated with pollutant emissions are higher during summer months, such as V, Mn, Co, Ni, Zn and Pb, which agrees with the idea that winter samples are more affected by oceanic inputs, while summer samples contain more anthropogenic pollutants. Overall, the McIvers samples appear to follow a similar seasonal trend to samples collected in St. John's.

Figure 4.12 shows the milligrams of nitrate deposited per sample. The plot indicates that there is more NO_3^- in some of the winter samples, although the VWM concentration indicates that NO_3^- is dominant in the summer months as discussed above. Overall, there is only a small range of NO_3^- from 0.057 to 0.69 mg. This small range in the amount of nitrate present throughout the year indicates that there is always some nitrate present in the atmosphere at this location.

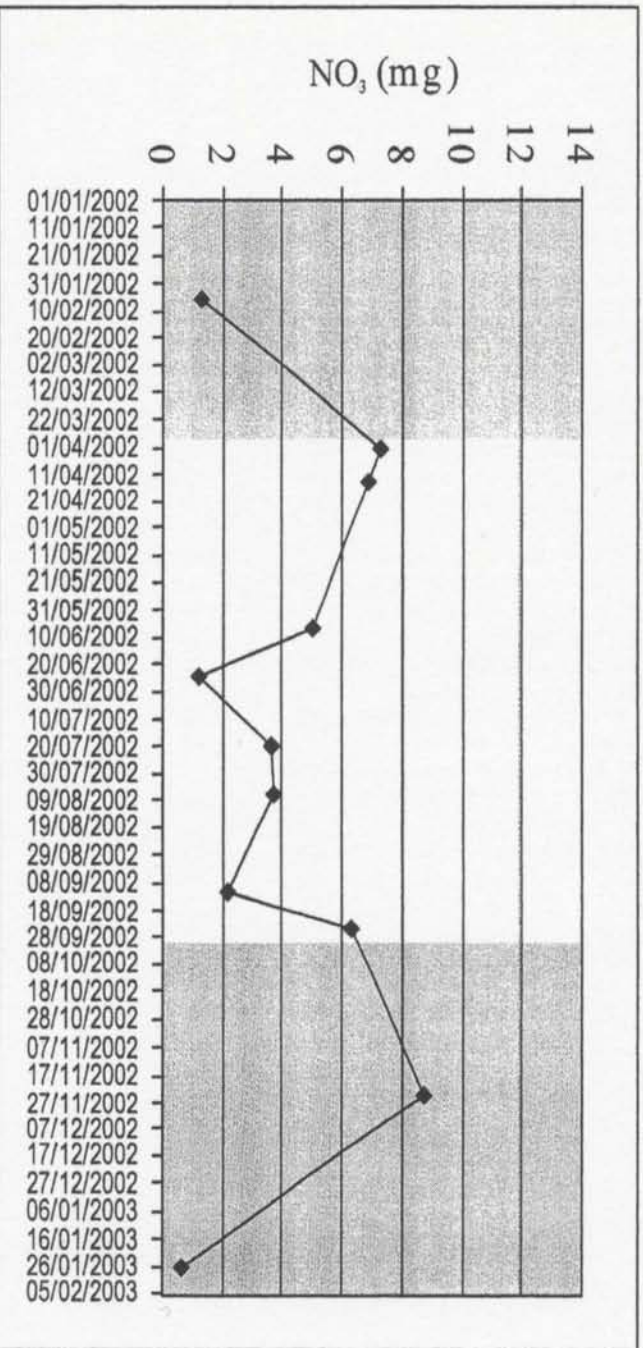


Figure 4.12 NO₃ (mg) variations for McIvers samples. Shaded areas represent winter months.

Looking at the overall chemical constituents of the data set (Tables II.16 and II.18), it is apparent that Zn may be more important at the McIvers site than at the St. John's location. There could be several reasons for this, the first being the close proximity of the closed zinc mine at Daniel's Harbour, located approximately 134 km north of the community. As well, this site does not have a local anthropogenic input which may mask the appearance of weaker signals in the area. The only real possible point source for the McIvers site is the pulp and paper mill in Corner Brook. But this source must not strongly affect this location as there are only weak fossil fuel signatures displayed by the samples, and in general, McIvers is upwind of Corner Brook. The community might experience transport of pollutants from the pulp and paper mill during storm events which often involve changes in the dominant wind direction to an area, however this is not reflected in the chemical data for the samples. As well, being a more rural community, more households burn wood as a main heat source. This occurs year round, accounting for the high Zn concentrations for most of the samples. The other main source of nitrate to the atmosphere at this location would be from automobiles. Obviously there are more cars in use at the St. John's location, but the stronger oil combustion signatures make this influence less apparent at that site compared to McIvers. Inputs from automobiles and wood combustion will play a role in controlling the overall nitrogen isotope signatures found in this area.

Samples collected at this location are influenced by seaspray, wood combustion, automobile inputs and fossil fuel emissions. Samples affected mainly by seaspray (MCS02-

0205 and MC02-0413) have $\delta^{15}\text{N}$ values of -4.7‰ and -3.8‰ (Table II.20).

Unfortunately, the third seaspray sample (MCS03-0126) could not be analysed for nitrogen isotopic composition. MCS02-0205, a winter snow sample, had some automobile influence indicated by the chemical analysis. The second sample (MC02-0413), collected in mid-April, also displayed some influence from car emissions. Their isotopic values (-4.7‰ , -3.8‰) are interpreted to be a combination of seaspray and automobile nitrate.

Samples influenced by fossil fuel combustion, MC02-0624 and MC02-0924, have $\delta^{15}\text{N}$ values of -2.7‰ and -1.2‰ respectively. These values are very similar to the lower end of the range of $\delta^{15}\text{N}$ values of -2 to $+13\text{‰}$ for crude oil given by Freyer (1991). The one sample which displayed a possible wood combustion signature (MC02-0401) has a $\delta^{15}\text{N}$ of $+0.2\text{‰}$, which is consistent with a wood burning source with isotopic composition close to 0‰ .

Due to the small sample set at this location, it is difficult to determine if samples varied seasonally. Figure 4.13 is a plot of the $\delta^{15}\text{N}$ values analysed showing the dates on which the samples were collected. The two winter samples have isotopic compositions which are similar to those of the summer samples. A correlation of $\delta^{15}\text{N}$ and temperature resulted in an r value of 0.351 ($p=0.320$, $n=10$) (Figure 4.13). Although this is not a strong correlation, the $\delta^{15}\text{N}$ values do somewhat vary sympathetically with temperature. As with the St. John's samples, this may indicate that the source of the nitrate may not be the main factor influencing its isotopic composition, and that atmospheric transformations related to temperature could indeed play a role in the overall isotopic signature. Based on

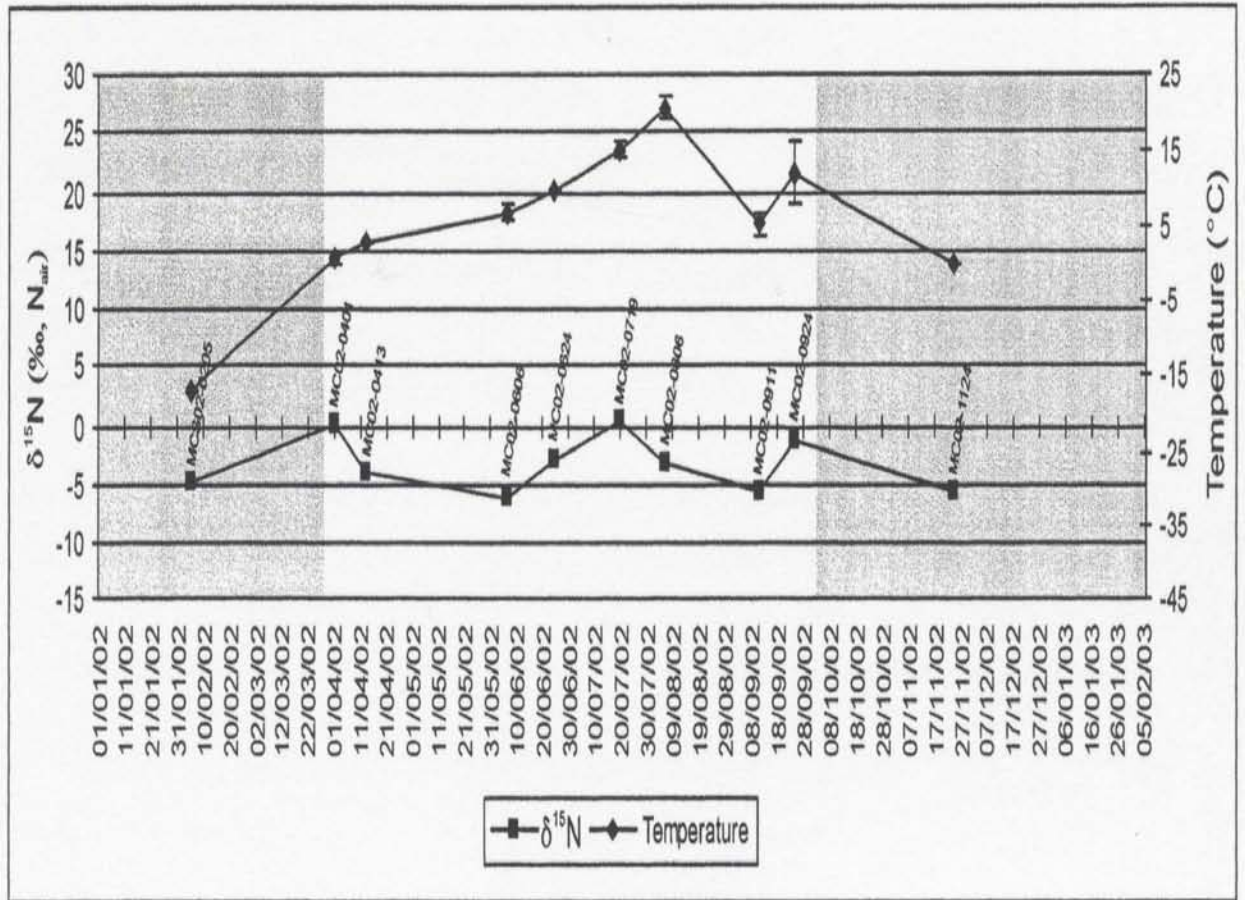


Figure 4.13 $\delta^{15}\text{N}$ variations with temperature for McIvers samples ($r=0.351$, $p=0.320$, $n=10$). Shaded areas represent winter months. Bars represent the temperature range during the sample collection.

isotopic and chemical data, however, the seasonality in nitrate does appear to be controlled by the sources of the atmospheric oxinitrogen species.

McIvers samples are similar to St. John's samples in that most of the samples collected at this site appear to have a continental input indicated by Al concentrations (Table II.15). This may be locally derived continental dust, or it may be a result of material transported from other areas of Canada and the U.S. The Newfoundland Environment Precipitation Monitoring Network (NEPMoN) study indicates that the southwest coast of the province receives the greatest amount of pollutants via long range transport. However, because McIvers is located within the Bay of Islands (Figure 2.1) it may not receive as heavy an influence as the southwest coast.

Three samples have been interpreted to represent a mixture of NO_3^- sources (MC02-0719, MC02-0806 and MC02-0911 (Tables II.6, II.8 and II.15)), and have varying $\delta^{15}\text{N}$ values of +0.5‰, -3.0‰ and -5.4‰, respectively. The isotopic composition of each sample depends on the relative influence of each source; a stronger seaspray influence will result in a more depleted signature, wood combustion may lead to more positive values, while more automobile inputs will likely create a slightly depleted signature. The relative proportion of the sources is very difficult to determine, but may be a key in understanding the processes which control the isotopic signatures of rainfall samples.

Oxygen isotopic compositions of sample nitrate collected at this site can be seen in Figure 4.14. Of the 11 samples collected, 8 were analysed for $\delta^{18}\text{O}_{\text{NO}_3}$, and have a range of +27.4 to +51.9‰, and a Pearson correlation with temperature of 0.277 ($p=0.506$, $n=8$).

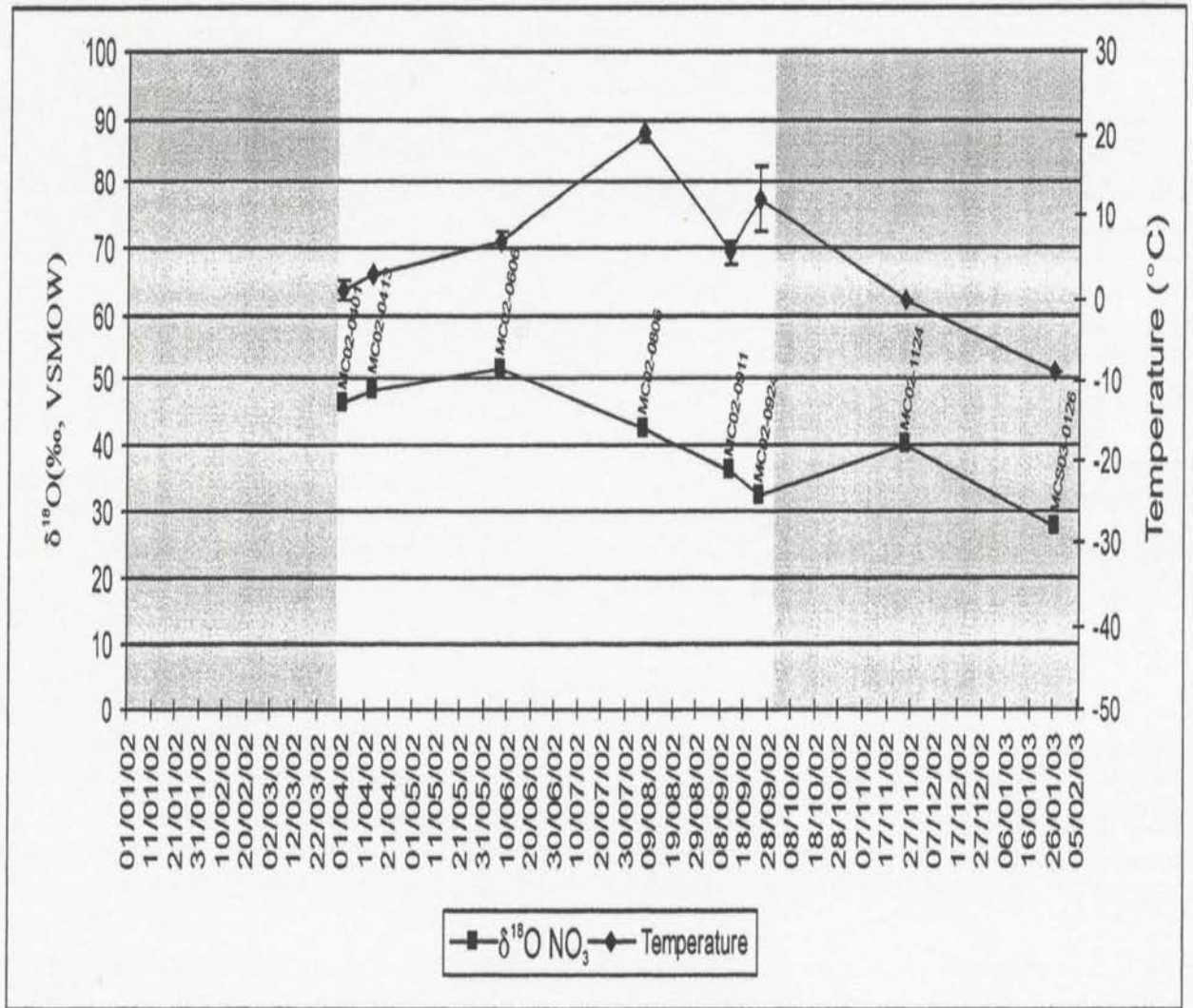


Figure 4.14 $\delta^{18}\text{O}_{\text{NO}_3}$ variations by season and temperature for McIvers samples ($r=0.277$, $p=0.506$, $n=8$). Shaded areas represent winter months. Bars represent the temperature range during the sample collection.

The sample with the lowest isotopic composition was MCS03-0126, a snow sample collected in January of 2003 which has a seaspray influence. There was another snow sample collected at this site, but it was not analysed for nitrate oxygen. Being a snow sample with a value close to that of atmospheric oxygen (+23.5‰), it somewhat agrees with the snow sample collected at the St. John's location (SJS02-0123). However, it cannot be determined from these two samples whether snow has a $\delta^{18}\text{O}_{\text{NO}_3}$ close to that of O_2 , or if these compositions are controlled by source as both samples were dominated by seaspray inputs.

The other sample influenced by seaspray was collected in April of 2002 (MC02-0413) and has a $\delta^{18}\text{O}_{\text{NO}_3}$ of +48.5‰, which is far different from the seaspray sample discussed above. There is no way to determine whether this is a typical $\delta^{18}\text{O}_{\text{NO}_3}$ for oceanic inputs as there are no samples to compare it to at this site. However, samples with a stronger oceanic influence collected at the St. John's site had varying isotopic compositions which indicate seaspray origin is either not a main control on isotopic oxygen values in nitrate, or that the signature varies over a large range.

MC02-0401, which appeared to be most strongly influenced by wood burning emissions, has a $\delta^{18}\text{O}_{\text{NO}_3}$ of +46.5‰. The sample influenced by the combustion of fossil fuel (MC02-0924) had a lower oxygen isotopic signature of +32.4‰. This sample, collected in September, 2002, along with MC02-0911 both have lower $\delta^{18}\text{O}_{\text{NO}_3}$ values than other samples collected at this site with the exception of the snow sample. Low values were also measured in September samples collected in St. John's. The reason for this is

unclear. These two samples also had correspondingly lower NO_3 (mg) values (Figure 4.12). Both locations exhibited lower amounts of NO_3 (mg) and lower temperatures during that particular month compared to August of the same year. This may be coincidental, or it may indicate a mechanistic control on the nitrate oxygen isotopic compositions at both locations. As well, the correspondingly lower temperatures may indicate that temperature plays a role in controlling the oxygen isotopic signatures of atmospheric nitrate. Recall that the oxidation pathways of NO_x are influenced by temperature. Overall, McIvers samples exhibit lower $\delta^{18}\text{O}$ values during winter months, while summer values are typically more enriched in $\delta^{18}\text{O}$. This pattern, as seen with the St. John's samples, appears to be controlled by the oxidation pathways of the nitrogen species as opposed to their sources.

$\delta^{18}\text{O}_{\text{H}_2\text{O}}$ was also analysed for McIvers samples (Figure 4.15). In general, the isotopic composition varies sympathetically with temperature ($r=0.584$, $p=0.059$, $n=11$), which is expected. Overall, rain collected during the summer season is more enriched in ^{18}O than that collected during the winter months. Looking at the plot of $\delta^{18}\text{O}_{\text{H}_2\text{O}}$ versus $\delta^{18}\text{O}_{\text{NO}_3}$ (Figure 4.11) it appears that a group of 3 samples follow a different trend than the remaining McIvers data. However, this is due only to differences in the $\delta^{18}\text{O}_{\text{H}_2\text{O}}$ data as the $\delta^{18}\text{O}_{\text{NO}_3}$ values for those three samples are comparable to the others.

4.6 Events Captured at Both Sites

In general, NO_3^- in the St. John's samples appears to have been derived from

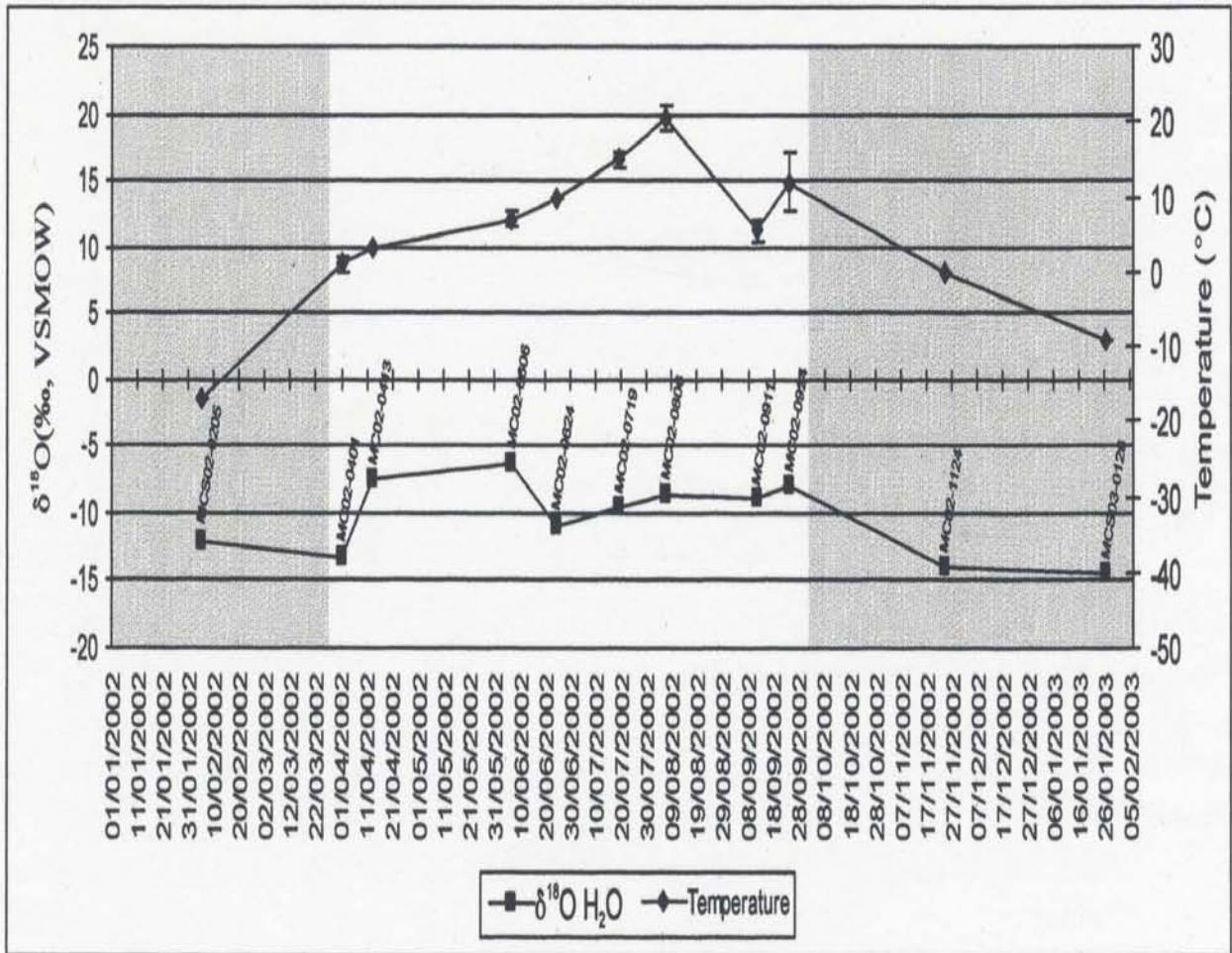


Figure 4.15 $\delta^{18}\text{O}_{\text{H}_2\text{O}}$ variations with temperature for McIvers samples ($r=0.584$, $p=0.059$, $n=11$). Shaded areas represent winter months. Bars represent the temperature range during the sample collection.

stationary fossil fuel combustion while McIvers samples contain NO_x emitted from cars and wood combustion from home heating. There are two samples within each data set that were collected on the same day at both locations: SJ02-0606 and MC02-0606, and SJ02-0624 and MC02-0624. These sample sets may give insight into possible sources of the nitrate found at each location.

The first set of samples, SJ02-0606 and MC02-0606, have identical volumes and exhibit similar chemical compositions (Tables II.1 to II.15) with the St. John's sample having higher concentrations than its McIvers counterpart. Although the signals are not as strong at McIvers, the relative proportion of the elements are the same as in the other sample, suggesting that both samples had a common source. Both samples are dominated by Mn with lesser amounts of V, indicating that automobile inputs and fossil fuel combustion emissions are important. Back trajectories calculated for both samples (Figure III.8 and Figure IV.4) show that the air mass travelled from Quebec, across the Atlantic provinces to Newfoundland. Because the St. John's sample displays higher concentrations, it is possible that this sample may have picked up emissions from the Come by Chance oil refinery, or that locally emitted pollutants were incorporated into the air mass prior to the rain event. Nitrogen isotopic compositions for SJ02-0606 and MC02-0606 are -4.3‰ and -6.0‰ respectively. These values are similar, with the St. John's sample possibly being more enriched due to additional fossil fuel inputs. The $\delta^{18}\text{O}_{\text{NO}_3}$ values for the samples are $+49.4\text{‰}$ for St. John's and $+51.9\text{‰}$ for McIvers.

The second dual location sample set is SJ02-0624 and MC02-0624. In this case,

sample volumes are very different from one another, with the St. John's sample more than double the McIvers volume. As well, it appears that the rain event reached McIvers in the morning, but did not begin at the St. John's site until the early evening. The chemical compositions of these two samples are also quite different from one another. SJ02-0624 has an extremely high concentration of V and Ni compared to all other samples collected during this study, while the McIvers sample contains no V and a small amount of Ni compared to its east coast counterpart. MC02-0624 does contain a significantly higher concentration of Zn, indicating a possible wood combustion source. Smelting emissions are ruled out in this case as there is no Cu and little Pb present in the sample. Both samples contain Mn. The St. John's sample may have an increased Mn concentration due to the extremely heavy fossil fuel influence, and may also contain automobile emissions. Back trajectories reveal that for both locations the air masses travelled from northeastern Canada through Quebec and over Newfoundland before reaching the collection sites (Figure III.9 and Figure IV.5). It is possible that the air mass acquired emissions from the Come by Chance oil refinery, however one would think that if this were the case both samples would contain approximately the same amount of V and Ni, which they do not. Because of this, it appears that the St. John's sample was heavily influenced by the local point source in the area. $\delta^{15}\text{N}$ signatures were similar, -3.6‰ for the St. John's sample, and -2.7‰ for the McIvers rain. A possible explanation for the more enriched isotopic composition in the McIvers data is that this sample was more influenced by wood combustion, which tends to have a $\delta^{15}\text{N}$ of $\sim 0\text{‰}$ as seen in the previous two sections.

Natural soil and ocean emissions along with car emissions may play a role in creating a more depleted $\delta^{15}\text{N}$ than expected for the St. John's sample which had such a strong fossil fuel input. Unfortunately, no $\delta^{18}\text{O}_{\text{NO}_3}$ measurements were available for these samples.

CHAPTER 5

CONCLUSIONS

5.1 Overview

The purpose of this study was to attempt to characterize sources of nitrate in single event precipitation samples using stable nitrogen and oxygen isotopes. Chemical data and meteorological information were used to aid in source interpretation. To the author's knowledge, the method used for isolating and processing dissolved nitrate in precipitation for stable isotopic analysis in this study had not been previously applied to single rain events, making this study unique.

Samples collected at both the St. John's and McIvers sites indicated that both sites receive a marine influence from the surrounding ocean, but also indicated anthropogenic pollution sources. Chemical data at both sites show a stronger marine influence in the colder months, while stronger anthropogenic signatures were measured in summer samples. This is contrary to other studies that indicate anthropogenic influences such as fossil fuel combustion increase during colder periods. It is possible that an increase in wave activity during the winter months causes more oceanic components to be emitted into the atmosphere near the two sites, which become the dominant chemical signals in the precipitation collected.

Nitrogen isotopes measured from dissolved nitrate at both sites show seasonal variation. Winter samples were more depleted in $\delta^{15}\text{N}$ compared to their summer

counterparts. This trend can be explained based on the dominant sources of nitrate present in the atmosphere during each season. Nitrogen compounds emitted from the ocean can have $\delta^{15}\text{N}$ values as low as -20‰ , therefore an increase in oceanic inputs during the winter may lead to lower $\delta^{15}\text{N}$ signatures. During the summer, a stronger anthropogenic influence is seen. Wood combustion and fossil fuel combustion from stationary sources such as power plants tend to have $\delta^{15}\text{N}$ of around 0‰ . Local and distant sources of stationary fossil fuel emissions appear to have stronger influences during the warmer months, leading to summer nitrate with more positive nitrogen isotopic signatures. Based on the chemical data available, automobile emissions, which can have $\delta^{15}\text{N}$ values ranging from -2 to -13‰ , appear to be present in the atmosphere at both locations year round, which may influence the isotopic composition. However, the $\delta^{15}\text{N}$ at both sites appear to be controlled by the sources dominant at the time of collection.

Nitrate $\delta^{18}\text{O}$ values also seem to follow a seasonal trend. The limited work done on atmospheric nitrate oxygen isotopes in the past indicates that there is a possibility that the $\delta^{18}\text{O}$ values may be controlled by the source of the atmospheric nitrate, the source of the oxygen, or the atmospheric processes which produce the nitrate from both natural and anthropogenic emissions. In this study, it appears that the $\delta^{18}\text{O}$ signatures are controlled by transformations of oxinitrogen species in the atmosphere, which are related to temperature. During the summer, ozone ($\delta^{18}\text{O} \sim +90$ to $+122\text{‰}$) is the dominant oxidiser in the atmosphere, resulting in more positive $\delta^{18}\text{O}$ nitrate values during the warmer months. Winter months tend to have lower $\delta^{18}\text{O}$, which may possibly be explained by

lower ozone concentrations during that season, or greater oxidation by either HO_2 or OH in the atmosphere, both of which have lower $\delta^{18}\text{O}$ values than O_3 . Atmospheric water may also play a role in the generation of nitric acid from N_2O_5 , a reaction which is dominant in the cooler months. The interpretation of the seasonality in $\delta^{18}\text{O}$ compositions may be hindered in this study due to the small number of samples measured for nitrate oxygen isotopic composition.

By comparing the isotopic composition of nitrate oxygen to that of the atmospheric water, it was hoped that some insight would be gained into whether the pollution sources affecting the samples were local or distant. This comparison has worked well for studies using sulphates in the past. However, it could not be determined from the data in this study whether the nitrate collected had been formed locally or distantly. This is due largely to the fact that the formation of nitrate in the atmosphere occurs when oxinitrogen species are oxidised by either HO_2 , OH or O_3 ; water is not the major oxidiser therefore the nitrate formed would not carry the $\delta^{18}\text{O}$ composition of the atmospheric water. The one reaction involving water (with N_2O_5) may occur prior to the nitrate's incorporation into the sampled air mass. Although the process of comparing the oxygen isotopes did not work well for atmospheric nitrates, it may have useful implications in groundwater studies.

A final observation is that the St. John's samples appeared to be affected by the power plant near which the collector was placed. This local point source operates year round, emitting metals and NO_x emissions into the atmosphere. The samples collected at this site generally had much stronger V and Ni influences than their McIvers counterparts,

which displayed only weak fossil fuel signatures. The strongest indication of this is in the comparison of a rain event collected at both locations on the same day (Section 4.7). Both samples (SJ02-0624 and MC02-0624) were expected to display similar chemical and isotopic compositions as it was the same air mass bringing the precipitation to both locations. However, the St. John's site had a much stronger influence from fossil fuel combustion indicated by the chemical data. The isotopic signatures were similar, indicating that the McIvers sample may also have been affected by fossil fuel combustion emissions which were most likely transported over some distance. Although the McIvers data generally had weak fossil fuel combustion signatures, the percent seaspray was often lower than expected. A possible explanation for this is that the McIvers site may be receiving biogenic sulphate from the ocean.

The isotopic results of this study contradict those found by past researchers in different areas of the world. There are several main anthropogenic sources of NO_x emissions in Newfoundland, but these appear to be small compared to industrial emissions in the collection areas of well known studies from both Germany and South Africa. Because there are relatively small anthropogenic inputs, the influence of the ocean in this study area may play a much larger role than in other studies of this nature. As well, the Newfoundland climate may play a key role in controlling the atmospheric transformations of the nitrogen species in this location.

5.2 Further work

There has been an increase in studies of stable isotopes of nitrate in recent years. More researchers are attempting to understand atmospheric nitrate and processes associated with this major pollutant and acidifying component of rain. This study has provided valuable isotopic measurements of atmospheric nitrate, but much more work is needed in this area. More single event precipitation studies in different locations with higher sampling rates are needed to explore this atmospheric constituent in more detail. As well, collection of samples from specific point sources such as smoke stacks and ore processing facilities would give further insight into the isotopic signatures associated with these potential sources. We have shown that snow may be affected by different processes than rain, therefore the collection of rain versus snow would clarify whether these two types of precipitation have distinct isotopic compositions. Single event samples collected at both locations in this study proved useful, thus a network of collection sites operating at the same time could be very beneficial in further understanding how nitrogen species are transformed in the atmosphere. Further work in Newfoundland is needed to confirm or disprove the theories presented in this work. The limited number of samples available for this study may have hindered interpretations, therefore a longer study period may bring insight into the main sources of the atmospheric nitrate found over Newfoundland, as well as the factors which control the stable isotopic signatures associated with them. It would be beneficial to sample precipitation in specific geographical locations within the province, such as the southwest coast, the northern peninsula, areas near abandoned ore mines, as

well as other areas within St. John's to maximize the influence of different sources and processes which introduce nitrate into the atmosphere.

REFERENCES

REFERENCES

- Aherne, J and Farrell, E.P., 2002. Deposition of sulphur, nitrogen and acidity in precipitation over Ireland: chemistry, spatial distribution and long-term trends. *Atmospheric Environment*, vol. 36, pp. 1379-1389.
- Ångström, A. and Högberg, L., 1952. On the content of nitrogen in atmospheric precipitation in Sweden, II. *Tellus*, vol. 4 no. 4, pp. 271-279.
- Balasubramanian, R., Victor, T., and Chun, N., 2001. Chemical and statistical analysis of precipitation in Singapore. *Water, Air and Soil Pollution*, vol. 130, pp.451-456.
- Berg, T., Royset, O., Steinnes, E., and Vadset, M., 1995. Atmospheric trace element deposition: Principal component analysis of ICP-MS data from moss samples. *Environmental Pollution*, vol. 88, pp. 67-77.
- Berner, E.K., and Berner, R.A., 1996. *Global Environment: Water, air and geochemical cycles*. Prentice-Hall, Inc., Upper Saddle River, New Jersey.
- Brasseur, G., Atlas, E., Erickson, D., Fried, A., Greenberg, J., Guenther, A., Harley, P., Holland, E., Klinger, L., Ridley, B., and Tyndall, G., 1999. Trace gas exchanges and biogeochemical cycles. *In Atmospheric Chemistry and Global Change. Edited by G.P. Brasseur, J.J. Orlando and G.S. Tyndall*. Oxford University Press, New York, New York, pp.159-205.
- Brasseur, G. and Schimel, D., 1999. Atmospheric chemistry and the earth system. *In Atmospheric Chemistry and Global Change. Edited by G.P. Brasseur, J.J. Orlando and G.S. Tyndall*. Oxford University Press, New York, New York, pp.1-18.
- Chang, C.C.Y, Langston, J., Riggs, M., Campbell, D.H., Silva, S.R. and Kendall, C., 1999. A method for nitrate collection for ^{15}N and ^{18}O analysis from waters with low nitrate concentrations. *Canadian Journal of Fisheries and Aquatic Sciences*, vol. 56, p. 1856-1864.
- Chang, C.C.Y., Kendall, C., Silva, S.R., Battaglin, W.A., and Campbell, D.H., 2002. Nitrate stable isotopes: tools for determining nitrate sources among different land uses in the Mississippi River Basin. *Canadian Journal of Fisheries and Aquatic Science*, vol. 59, pp.1874-1885.

- Coplen, T.B., Hopple, J.A., Böhlke, J.K., Peiser, H.S., Rieder, S.E., Krouse, H.R., Rosman, K.J.R., Ding, T., Vocke, R.D.Jr., Révész, K.M., Lamberty, A., Taylor, P., and De Bièvre, P., 2002. Compilation of Minimum and Maximum Isotope Ratios of Selected Elements in Naturally Occurring Terrestrial Materials and Reagents. Water-Resources Investigations Report 01-4222 by US Department of the Interior/US Geological Survey.: 98 pp.
- Dansgaard, W., 1964. Stable Isotopes in Precipitation. *Tellus*, vol. 16, pp. 436-438.
- DX-100 Ion Chromatograph Operator's Manual, 1991. Document no. 031132, Release 1.
- Environment Canada, 1998. 1997 Canadian Acid Rain Assessment; Volume 1: Summary of Results. Minister of Environment. Ottawa: Environment Canada, Atmospheric Environment Service.
- Eriksson, E., 1952a. Composition of Atmospheric Precipitation: I. Nitrogen Compounds. *Tellus*, vol. 4, no.3, pp. 215-232.
- Eriksson, E., 1952b. Composition of Atmospheric Precipitation: II. Sulfur, chloride, iodine compounds. *Tellus*, vol. 4, no.4, pp. 281-303.
- Faure, G., 1998. Principles and applications of geochemistry, 2nd ed. Prentice-Hall Inc., New Jersey.
- Freyer, H.D., 1978. Seasonal trends of NH_4^+ and NO_3^- nitrogen isotope composition in rain collected at Julich, Germany. *Tellus*, vol. 30, pp. 83-92.
- Freyer, H.D., 1991. Seasonal variation of $^{15}\text{N}/^{14}\text{N}$ ratios in atmospheric nitrate species. *Tellus*, vol. 43B, pp. 30-44.
- Freyer, H.D., Kley, D., Volz-Thomas, A. and Kobel, K., 1993. On the interaction of isotopic exchange processes with photochemical reactions in atmospheric oxides of nitrogen. *Journal of Geophysical Research*, vol. 98, no. D8, pp. 14791-14796.
- Galloway, J.N., Likens, G.E., and Edgerton, E.S., 1976. Acid precipitation in the northeastern United States: pH and acidity. *Science*, vol. 194, pp.722-724.
- Galloway, J.N., and Likens, G.E., 1981. Acid precipitation: The importance of nitric acid. *Atmospheric Environment*, vol. 15, no.6, pp.1081-1085.

- Galloway, J.N., Thornton, J.D., Norton, S.A., Volchok, H.L., and McLean, R.A.N., 1982. Trace metals in atmospheric deposition: a review and assessment. *Atmospheric Environment*, vol. 16, pp. 1677-1700.
- Ganor, E., Altshuler, S., Foner, H.A., Brenner, S. and Gabbay, J., 1988. Vanadium and nickel in dustfall as indicators of power plant pollution. *Water, Air and Soil Pollution*, vol. 42, pp. 241-252.
- Garty, J., Weissman, L., Cohen, Y., Karnieli, A., and Orlovsky, L., 2001. Transplanted lichens in and around the Mount Carmel National Park and the Haifa Bay industrial region in Israel: Physiological and chemical responses. *Environmental Research Section A*, vol. 85, pp. 159-176.
- Golletz, T., 2002. Modelling the nitrogen budget in a boreal maritime watershed, Terra Nova National Park, Newfoundland. MSc Thesis. Memorial University of Newfoundland, St. John's, Newfoundland, 56p.
- Harrison, R.M., Grenfell, J.L., Peak, J.D., Clemitshaw, K.C., Penkett, S.A., Cape, J.N. and McFadyen, G.G., 2000. Influence of airmass back trajectory upon nitrogen compound composition. *Atmospheric Environment*, vol. 34, pp. 1519-1527.
- Hastings, M.G., Sigman, D.M., and Lipschultz, F., 2003. Isotopic evidence for sources of nitrate in rain at Bermuda. *Journal of Geophysical Research*, vol. 108, no. D24, 4790, doi:10.1029/2003JD003789.
- Heaton, T.H.E., 1986. Isotopic studies of nitrogen pollution in the hydrosphere and atmosphere: a review. *Chemical Geology (Isotope Geoscience Section)*, vol. 59, pp.87-102.
- Heaton, T.H.E., 1987. $^{15}\text{N}/^{14}\text{N}$ ratios of nitrate and ammonium in rain at Pretoria, South Africa. *Atmospheric Environment*, vol. 21 no.4, pp. 843-852.
- Heaton, T.H.E., 1990. $^{15}\text{N}/^{14}\text{N}$ ratios of NO_x from vehicle engines and coal-fired power stations. *Tellus*, vol.42B, pp. 304-307.
- Hoefs, J., 1987. *Stable Isotope Geochemistry*, 3rd ed. Springer-Verlag, New York.
- Hoefs, J., 1997. *Stable Isotope Geochemistry*, 4th ed. Springer-Verlag, New York.
- Hoering, T., 1957. The isotopic composition of ammonia and the nitrate ion in rain. *Geochimica et Cosmochimica Acta*, vol. 12, pp. 97-102.

- Huhn, G., Schulz, H., Stärk, H., Tölle, R., and Schüürmann, G., 1995. Evaluation of regional heavy metal deposition by multivariate analysis of element contents in pine tree barks. *Water, Air and Soil Pollution*, vol. 84, pp. 367-383.
- Irwin., J.G., Campbell, G., and Vincent, K., 2002. Trends in sulphate and nitrate wet deposition over the United Kingdom: 1986-1999. *Atmospheric Environment*, vol. 36, pp.2867-2879.
- Jamieson, R.E., 1995. A stable isotopic study of natural and anthropogenic sulphur in precipitation in eastern Canada. MSc Thesis. Memorial University of Newfoundland, St. John's, Newfoundland, 183p.
- Jamieson, R.E. and Wadleigh, M.A., 1999. A study of the oxygen isotopic composition of precipitation sulphate in eastern Newfoundland. *Water, Air and Soil Pollution*, vol.110, pp.405-420.
- Johnston, J.C., and Thiemens, M.H., 1997. The isotopic composition of tropospheric ozone in three environments. *Journal of Geophysical Research*, vol.102, pp. 25395-25404.
- Jylhä, K., 2000. Removal by snowfall of emissions from a coal-fired power station: observations and modelling. *Water, Air and Soil Pollution*, vol.120, pp.397-420.
- Kendall, C., Sklash, M.G. and Bullen, T.D., 1995a. Isotope Tracers of water and solute sources in catchments. *In Solute Modelling in Catchment Systems. Edited by S.T. Trudgill.* John Wiley and Sons Ltd., New York, pp.261-303.
- Kendall, C, Campbell, D.H., Burns, D.A., Shanley, J.B., Silva, S.R., and Chang, C.C.Y., 1995b. Tracing sources of nitrate in snowmelt runoff using the oxygen and nitrogen isotopic compositions of nitrate. *Biogeochemistry of Seasonally Snow-Covered Catchments (Proceedings of a Boulder Symposium), IAHS Publ no.228,* pp.339-347.
- Kendall, C., 1998. Tracing nitrogen sources and cycling in catchments. *In Isotope tracers in catchment hydrology. Edited by C. Kendall and J.J. McDonnell.* Elsevier, Amsterdam, pp.519-576.
- Kendall, C., and Caldwell, E.A., 1998. Fundamentals of Isotope Geochemistry. *In Isotope tracers in catchment hydrology. Edited by C. Kendall and J.J. McDonnell.* Elsevier, Amsterdam, pp.51-86.

- Kim, K.-R. and Craig, H., 1993. Nitrogen-15 and oxygen-18 characteristics of nitrous oxide: a global perspective. *Science*, vol. 262, pp. 1855-1857.
- Krankowsky, D., Bartecki, F., Klees, G.G., Mauersberger, K. and Schellenbach, K., 1995. Measurement of heavy isotope enrichment in tropospheric ozone. *Geophysical Research Letters*, vol. 22, no. 13, pp. 1713-1716.
- Krupa, S.V., 2002. Sampling and physico-chemical analysis of precipitation: a review. *Environmental Pollution*, vol. 120, pp.565-594.
- Létolle, R., 1980. Nitrogen-15 in the natural environment. *In Handbook of Environmental Isotope Geochemistry*, vol.1: The Terrestrial Environment, A. Edited by P. Fritz and J.Ch. Fontes. Elsevier Scientific Publishing Co., Amsterdam, the Netherlands, pp.407-433.
- Lim, B., Jickells, T.D., and Davies, T.D., 1991. Sequential sampling of particles, major ions and total trace metals in wet deposition. *Atmospheric Environment*, vol. 25a, no.3/4, pp.745-762.
- Loranger, S., and Zayed, J., 1994. Manganese and lead concentrations in ambient air and emission rates from unleaded and leaded gasoline between 1981 and 1992 in Canada: A comparative study. *Atmospheric Environment*, vol. 28, no. 9, pp. 1645-1651.
- Mackenzie, F.T. and Mackenzie, J.A., 1995. *Our Changing Planet: An introduction to earth system science and global environmental change*. Prentice-Hall Inc, Englewood Cliffs, New Jersey. 387p.
- Michalski, G., Savarino, J., Böhlke, J.K., and Thiemens, M., 2002. Determination of the total oxygen isotopic composition of nitrate and the calibration of a $\Delta^{17}\text{O}$ nitrate reference material. *Analytical Chemistry*, vol. 74, no. 19, pp. 4989-4993.
- Mignon, C., and Caccia, J., 1990. Separation of anthropogenic and natural emission so particulate heavy metals in the western Mediterranean atmosphere. *Atmospheric Environment*, vo. 24A, no. 2, pp. 399-405.
- Model 122 and 123 Conductivity/Temperature Meter Hand-held Set Instruction Manual, Orion. No date specified.

- Moore, H., 1974. Isotopic measurement of atmospheric nitrogen compounds. *Tellus*, vol. 26, no.1-2, pp. 169-174.
- Moore, H., 1977. The isotopic composition of ammonia, nitrogen dioxide and nitrate in the atmosphere. *Atmospheric Environment*, vol. 11, pp. 1239-1243.
- Myiake, Y., and Wada, E., 1971. The isotope effect on the nitrogen in biochemical oxidation-reductions. *Records of Oceanographic Works in Japan*, vol. 11, pp. 1-6.
- Natusch, D.F.S., Wallace, J.R and Evans, C.A., 1973. Toxic trace elements: preferential concentration in respirable particles. *Science*, vol. 183, pp. 202-204.
- NEPMoN (Newfoundland Environment Precipitation Monitoring Network), 2002. Annual report for the years 1999-2000. Pollution Prevention Division, Department of Environment, Government of Newfoundland and Labrador. St. John's.
- NIST (National Institute of Standards and Technology) Report of Investigation Reference Materials 8547-8552, 1993.
- Norcliffe, G., and Bates, J., 1997. Implementing lean production in an old industrial space: restructuring at Corner Brook, Newfoundland, 1984-1994. *The Canadian Geographer*, vol. 41, no.1, pp.41-60.
- Nygård, S., and Harju, L., 1983. A study of the short range pollution around a power plant using heavy fuel oil by analysing vanadium in lichens. *The Lichenologist*, vol. 15, no. 1, pp.89-93.
- Pacyna, J.M., Semb, A. and Hanssen, J.E., 1984. Emission and long-range transport of trace elements in Europe. *Tellus*, vol.36B, pp.163-178.
- Pacyna, J.M., 1986a. Emission factors of atmospheric elements. *In Toxic Metals in the Atmosphere. Edited by J.O. Nriagu and C.I. Davidson.* Wiley and Sons, New York, New York, pp.1-32.
- Pacyna, J.M., 1986b. Atmospheric trace elements from natural and anthropogenic sources. *In Toxic Metals in the Atmosphere. Edited by J.O. Nriagu and C.I. Davidson.* Wiley and Sons, New York, New York, pp.33-52.
- Que Hee, S.S., 1994. Availability of elements in leaded/unleaded automobile exhausts, a leaded paint, a soil, and some mixtures. *Archives of Environmental Contamination and Toxicology*, vol. 27, pp. 145-153.

- Ridley, B. and Atlas, E., 1999. Nitrogen Compounds. *In Atmospheric Chemistry and Global Change. Edited by G.P. Brasseur, J.J. Orlando and G.S. Tyndall.* Oxford University Press, New York, New York, pp.235-287
- Ro., C.U., Tang, A.J.S., Chan, W.H., Kirk, R.W., Reid, N.W., and Lusi, M.A., 1988. Wet and dry deposition of sulfur and nitrogen compounds in Ontario. *Atmospheric Environment*, vol.22, no.12, pp.2763-2772.
- Robinson, E. and Robbins, R.C., 1970. Gaseous nitrogen compound pollutants from urban and natural sources. *Journal of the Air pollution Control Association*, vol. 20, no.5, pp.303-306.
- Röckmann, T., Brenninkmeijer, C.A.M., Saueressig, G., Bergamaschi, P., Crowley, J.N., Fischer, H., and Crutzen, P.J., 1998. Mass-independent oxygen isotope fractionation in atmospheric CO as a result of the reaction CO + OH. *Science*, vol. 281, pp. 544-546.
- Russell, K.M., Galloway, J.N., Macko, S.A., Moody, J.L. and Scudlark, J.R., 1998. Sources of nitrogen in wet deposition to the Chesapeake Bay region. *Atmospheric Environment*, vol. 32, no. 14-15, pp. 2453-2465.
- Savarino, J. and Thiemens, M.H., 1999. Mass-independent oxygen isotope (^{16}O , ^{17}O , ^{18}O) fractionation found in H_xO_x reactions. *Journal of Physical Chemistry A*, vol. 103, pp. 9221-9229.
- Savoie, D.L. and Prospero, J.M., 1989. Comparison of oceanic and continental sources of non-sea-salt sulphate over the Pacific ocean. *Nature*, vol. 339, pp. 685-687.
- Schlesinger, W.H., 1997. *Biogeochemistry: an analysis of global change*, 2nd Ed. Academic Press, San Diego, California.
- Schrauzer, G.N., 1991. Cobalt. *In Metals and their compounds in the environment: Occurrence, analysis, and biological relevance. Edited by E. Merian.* VCH, New York, NY, pp. 879-908.
- Shaw, R.W., 1984. The atmospheric pathway for oxides of nitrogen. *Environmental Protection Service Report EPS 2/TS/2.* Environment Canada, 10p.
- Silva, S.R., Kendall, C., Wilkison, D.H., Ziegler, A.C., Chang, C.C.Y. and Avanzino, R.J., 2000. A new method for collection of nitrate from water and the analysis of nitrogen and oxygen isotope ratios. *Journal of Hydrology*, vol. 228, pp. 22-36.

- Sloof, J.E., 1995. Pattern recognition in lichens for source apportionment. *Atmospheric Environment*, vol. 29, no. 3, pp. 333-343.
- Sperber, K.R., 1987. The concentration and deposition of nitrate, sulfate and ammonium as a function of wind direction from precipitation samples. *Atmospheric Environment*, vol. 21, no.12, pp.2629-2641.
- Squires, D., 2002. The chemical composition (major ions) of alpine snow cover - Gros Morne National Park, Newfoundland. MSc Thesis. Memorial University of Newfoundland, St. John's, Newfoundland, 51p.
- Stickrod II, R.D. and Marshall, J.D., 2000. On-line nitrate- $\delta^{15}\text{N}$ extracted from groundwater determined by continuous-flow elemental analyzer/isotope ratio mass spectrometry. *Rapid Communications in Mass Spectrometry*, vol. 14, pp.1266-1268.
- Takahashi, A. and Fukita, S., 2000. Long-term trends in nitrate to non-seasalt sulfate ratio in precipitation collected in western Japan. *Atmospheric Environment*, vol. 34, pp. 4551-4555.
- Tørseth, K., Semb, A., Schaug, J., Hanssen, J.E. and Aamlid, D., 2000. Processes affecting deposition of oxidised nitrogen and associated species in the coastal areas of Norway. *Atmospheric Environment*, vol. 34, pp. 207-217.
- Tyndall, G. and Orlando, J., 1999. Chemical and photochemical processes. *In Atmospheric Chemistry and Global Change. Edited by G.P. Brasseur, J.J. Orlando and G.S. Tyndall.* Oxford University Press, New York, New York, pp.85-114.
- Vestreng, V., 2003. Emission Data reported to CLRTAP. EMEP/MS-CW Technical Report, review and revision. MSC-W Status report 2003, EMEP/MS-CW Note 1/2003.
- Vitousek, P.M., Aber, J.D., Howarth, R.W., Likens, G.E., Matson, P.A., Schindler, D.W., Schlesinger, W.H. and Tilman, D.G., 1997. Human alteration of the global nitrogen cycle: sources and consequences. *Ecological Applications*, vol. 7, no. 3, pp. 737-750.
- Wadge, A., Hutton, M. and Peterson, P.J., 1986. The concentrations and particle size relationships of selected trace elements in fly ashes from U.K. coal-fired power plants and a refuse incinerator. *Science of the Total Environment*, vol. 54, pp.13-27.

- Wadleigh, M.A., Schwarcz, H.P., and Kramer, J.R., 1996. Isotopic evidence for the origin of sulphate in coastal rain. *Tellus*, vol. 48B, pp. 44-59.
- Wadleigh, M.A., Schwarcz, H.P., and Kramer, J.R., 2001. Areal distribution of sulphur and oxygen isotopes in sulphate of rain over eastern North America. *Journal of Geophysical Research*, vol. 106, no. D12, pp. 20883-20895.
- Xu, Q., Zhang, W., Xu, C. and Jin, L., 2000. Continuous and simultaneous determination of anions and cations in rainwater by ion chromatography. *Analyst*, vol. 125, pp. 1065-1069.
- Yeatman, S.G., Spokes, L.J., Dennis, P.F. and Jickells, T.D., 2001. Comparisons of aerosol nitrogen isotopic composition at two polluted coastal sites. *Atmospheric Environment*, vol. 35, pp. 1307-1320.
- Yun, M., Longerich, H.P., and Wadleigh, M.A., 2003. The determination of 18 trace elements in lichens for atmospheric monitoring using inductively coupled plasma-mass spectrometry. *Canadian Journal of Analytical Sciences and Spectroscopy*, vol. 48, pp. 171-180.

APPENDIX I

Nitrate Extraction

Prior to isotopic analysis, precipitation nitrate had to be preconcentrated then converted to silver nitrate. The following is a detailed description of the procedure used in this study.

Preconcentration of nitrate was accomplished by gravity dripping each sample through a Gelman capsule, a 5 ml column containing Bio-Rad AG 50W-X8 cation resin (hydrogen form) and a 5 ml column containing Bio-Rad AG2-X8 anion resin (chloride form). To prepare the resins for use, each was rinsed with deionised water and a 5 ml aliquot was placed in a 20 ml column.

The sample was allowed to flow through this system at a rate of approximately 1 L per hour. When samples have low concentrations, faster flow rates may result in lower yields. When almost all of the sample had dripped through the columns, some of the eluent was collected and analysed via ion chromatography to ensure that no nitrate had bled through the column. If it was determined that the nitrate did bleed through the sample was discarded.

Once the entire sample was passed through the columns, the anion column was removed for further processing. The resin now contained all of the anions that were present in the sample. Once all the excess water had been allowed to drip out of the anion exchange resin, it was stripped using 30 ml of 3 N HCl. The acid was added in ten 3 ml aliquots. The stopcock on the bottom of the column was closed and 3 ml of HCl was added. After 30 seconds had passed, the stopcock was opened and the eluent dripped into

a clean 50 ml polyethylene beaker. The next 3 ml aliquot was added, and the procedure was repeated until 30 ml of 3 N HCl had passed through the column, after which the column was blown dry with a vacuum pressure bulb.

The beaker containing the sample was then placed in a slush made from isopropanol alcohol and liquid nitrogen, where 16 g of pure silver oxide was added in four 4 g additions to neutralize the sample. Prior to its use, the silver oxide had been cleaned by numerous rinsings with deionised and distilled water, then tested for background nitrate. The sample was stirred with a flat-bottomed glass stirring stick between each addition of silver nitrate to break up any clumps of unreacted Ag_2O and to allow the heat of the reaction to dissipate. After the final addition of Ag_2O , mixing of the sample continued to ensure that all of the nitrate present had reacted with the silver oxide powder. After several additions of Ag_2O the solution became cloudy. The pH was measured using pH paper, and should be between 5 and 6. If the pH was too acidic, small additions of Ag_2O were added until neutralization of the sample occurred. If the sample was clear, it was filtered through a rinsed Whatman no.1 filter paper into a 50 ml polyethylene test tube to remove all AgCl precipitated from the reaction. In most cases, the solution of silver nitrate remained cloudy and was vacuum filtered through a 0.45 μm nylon membrane into a vacuum flask and transferred to a 50 ml test tube.

Sulphates were then removed from the sample through the addition of 4.5 ml of 1 M BaCl_2 . The solution was shaken and placed in a refrigerator overnight allowing BaSO_4 to precipitate from the solution (as well as BaPO_4 if there are any phosphates present).

The solution was filtered through a rinsed Whatman no.1 or vacuum filtered through a 0.45 μm nylon filter into a glass beaker. The sample was allowed to gravity drain through a 9 ml Bio-Rad AG 50W-X8 cation exchange resin column to remove any excess Ba^{2+} ions from the sample. The eluent was collected in a clean plastic beaker to which 1 to 2 g of pure Ag_2O was added to remove any excess Cl^- ions, which precipitate as AgCl . The pH was checked using pH paper, and if it was found to be 5 to 6, the sample was vacuum filtered through a 0.45 μm nylon filter into a pre-weighed 50 ml polyethylene centrifuge tube and placed in the refrigerator for storage. If the pH was too acidic, small additions of Ag_2O were added until the sample was neutralized. At this point, the sample should consist entirely of silver nitrate in solution.

Prior to submitting samples for $\delta^{15}\text{N}$ analyses, the AgNO_3 solution had to be prepared in a solid form, accomplished via freeze drying. An aliquot of AgNO_3 from the sample was freeze dried in a clean centrifuge tube then redissolved by adding 2 ml of deionised water. The solution was once again freeze dried, and the small amount of solid material remaining was redissolved with 200 μL of deionised water for every silver capsule to be used. 200 μL aliquots of the solution were pipetted into 10 x 10 mm silver capsules held in an aluminum block. Each capsule was lightly pinched shut and the block was placed in a freeze drier. Once the sample was completely freeze dried, the capsules were un-pinched and between 2 and 5 mg of sucrose was added to each capsule. The capsules are then crimped shut using a crimping tool and submitted for mass spectrometry.

APPENDIX II

Table II.1 Descriptions of St. John's samples.

Sample	Date Opened	Time	Date Closed	Time	Volume (L)
SJS02-0123*	Jan.23/02	4:00 pm	-	-	14
SJ02-0314	Mar.13/02	2:30 pm	Mar.14/02	8:00 pm	23
SJ02-0322	Mar.21/02	8:00 pm	Mar.22/02	11:00 pm	4.5
SJ02-0328	Mar.26/02	6:00 pm	Mar.28/02	2:00 am	20
SJ02-0429	Apr.29/02	8:30 am	Apr.30/02	11:30 am	8.5
SJ02-0510	May 10/02	11:30 am	May 11/02	7:30 am	5
SJ02-0531	May 30/02	9:30 pm	Jun.1/02	2:30 pm	19
SJ02-0606	Jun.5/02	10:30 pm	Jun.6/02	10:00 pm	8
SJ02-0624	Jun.24/02	4:30 pm	Jun.25/02	10:00 am	17
SJ02-0709	Jul.9/02	6:40 pm	Jul.10/02	9:00 am	6.25
SJ02-0710	Jul.10/02	10:30 am	Jul.11/02	9:00 am	8.5
SJ02-0807	Aug.7/02	5:00 pm	Aug.9/02	12:30 pm	23.25
SJ02-0820	Aug.20/02	9:00 am	Aug.21/02	9:00 am	4.5
SJ02-0825	Aug.24/02	10:30 pm	Aug.26/02	8:00 am	18
SJ02-0906	Sep.5/02	7:00 pm	Sep.6/02	5:30 pm	3.5
SJ02-0910	Sep.10/02	12:00 am	Sep.10/02	11:00 pm	4
SJ02-0917	Sep.16/02	6:30 pm	Sep.17/02	4:30 pm	9
SJ02-0928	Sep.27/02	11:15 pm	Sep.29/02	12:00 pm	20
SJ02-1001	Oct.1/02	11:15 am	Oct.2/02	11:00 am	8
SJ02-1020	Oct.20/02	11:30 am	Oct.21/02	8:30 am	4
SJ02-1114	Nov.14/02	10:00 am	Nov.15/02	11:00 pm	4
SJ03-0131	Jan.31/03	5:00 pm	Feb.1/03	1:00 pm	11
SJ03-0201	Feb.1/03	1:30 pm	Feb.2/03	12:00 pm	10
SJ03-0202	Feb.2/03	1:00 pm	Feb.3/03	11:30 am	15

* denotes snow samples

Table II.2 Descriptions of McIvers samples.

Sample	Date Opened	Time	Date Closed	Time	Volume (L)
MCS02-0205*	Feb.5/02	-	-	-	10
MC02-0401	Apr.1/02	3:30 pm	Apr.2/02	6:00 am	15
MC02-0413	Apr.13/02	10:30 am	Apr.13/02	3:30 pm	10
MC02-0606	Jun.5/02	9:30 pm	Jun.6/02	6:00 am	8
MC02-0624	Jun.24/02	9:30 am	Jun.24/02	5:00 pm	8
MC02-0719	Jul.19/02	9:30 am	Jun.19/02	9:00 pm	9
MC02-0806	Aug.6/02	11:00 am	Aug.6/02	4:00 pm	8
MC02-0911	Sep.11/02	8:00 pm	Sep.12/02	8:00 am	11
MC02-0924	Sep.24/02	6:00 pm	Sep.25/02	8:00 am	19
MC02-1124	Nov.23/02	11:00 am	Nov.24/02	8:00 am	15
MCS03-0126*	Jan.26/03	-	-	-	12

* denotes snow samples

Table II.3 pH and conductivity for St. John's samples.

Sample	pH	Conductivity ($\mu\text{S}/\text{cm}$)
SJS02-0123*	4.96	20
SJ02-0314	5.44	7
SJ02-0322	5.42	44
SJ02-0328	5.92	16
SJ02-0429	4.59	23
SJ02-0510	5.19	9
SJ02-0531	5.42	4
SJ02-0606	4.79	12
SJ02-0624	4.36	28
SJ02-0709	4.59	19
SJ02-0710	4.76	13
SJ02-0807	4.91	9
SJ02-0820	4.63	18
SJ02-0825	4.88	8
SJ02-0906	5.07	10
SJ02-0910	5.73	8
SJ02-0917	5.23	9
SJ02-0928	5.42	7
SJ02-1001	4.40	26
SJ02-1020	4.62	28
SJ02-1114	5.80	10
SJ03-0131	4.73	12
SJ03-0201	5.53	7
SJ03-0202	5.56	13

* denotes a snow sample

Table II.4 pH and conductivity for McIvers samples.

Sample	pH	Conductivity ($\mu\text{S}/\text{cm}$)
MCS02-0205*	5.09	43
MC02-0401	5.20	6
MC02-0413	4.84	29
MC02-0606	4.73	8
MC02-0624	5.47	4
MC02-0719	5.28	7
MC02-0806	5.44	7
MC02-0911	5.46	4
MC02-0924	5.33	4
MC02-1124	5.42	8
MCS03-0126*	5.57	10

* denotes a snow sample

Table II.5 Anion concentrations for St. John's samples.

Sample	Cl (ppm)	NO ₃ ⁻ (ppm)	SO ₄ ²⁻ (ppm)
SJS02-0123*	1.1	0.54	0.76
SJ02-0314	0.71	0.11	0.36
SJ02-0322	0.025	0.47	3.2
SJ02-0328	2.8	0.25	0.73
SJ02-0429	2.2	0.33	2.4
SJ02-0510	0.98	0.58	1.0
SJ02-0531	0.04	0.45	0.74
SJ02-0606	0.16	1.2	1.4
SJ02-0624	0.36	0.23	3.8
SJ02-0709	-	1.8	1.3
SJ02-0710	-	0.56	1.3
SJ02-0807	0.27	0.37	0.94
SJ02-0820	-	1.3	1.9
SJ02-0825	2.8	0.72	1.3
SJ02-0906	0.33	0.73	0.90
SJ02-0910	0.45	0.37	0.82
SJ02-0917	0.80	0.24	0.68
SJ02-0928	0.55	0.19	0.40
SJ02-1001	0.14	1.1	3.1
SJ02-1020	5.6	1.4	1.7
SJ02-1114	1.3	0.17	0.72
SJ03-0131	0.24	0.24	1.1
SJ03-0201	0.81	0.08	0.36
SJ03-0202	2.0	0.10	0.47

* denotes a snow sample

Table II.6 Anion concentrations for McIvers samples.

Sample	Cl ⁻ (ppm)	NO ₃ ⁻ (ppm)	SO ₄ ²⁻ (ppm)
MCS02-0205*	-	0.13	1.5
MC02-0401	0.30	0.49	0.35
MC02-0413	3.3	0.69	1.6
MC02-0606	0.07	0.63	0.53
MC02-0624	-	0.16	0.24
MC02-0719	0.36	0.40	0.35
MC02-0806	-	0.47	0.20
MC02-0911	0.05	0.20	0.26
MC02-0924	0.06	0.33	0.09
MC02-1124	0.11	0.58	0.32
MCS03-0126*	1.6	0.06	0.39

* denotes a snow sample

Table II.7 Cation concentrations for St. John's samples.

Sample	Na ⁺ (ppm)	NH ₄ ⁺ (ppm)	K ⁺ (ppm)	Mg ²⁺ (ppm)	Ca ²⁺ (ppm)
SJS02-0123*	2.3	0.025	0.11	0.38	0.12
SJ02-0314	0.74	0.06	0.04	0.05	0.06
SJ02-0322	6.1	0.47	0.26	0.96	0.45
SJ02-0328	2.5	0.12	0.14	0.24	0.22
SJ02-0429	1.5	0.24	0.09	0.32	0.17
SJ02-0510	0.30	0.23	0.07	0.19	0.25
SJ02-0531	0.06	0.08	0.02	0.07	0.11
SJ02-0606	0.15	0.33	0.07	0.21	0.28
SJ02-0624	0.38	0.14	0.03	0.08	0.11
SJ02-0709	0.07	0.68	0.13	0.04	0.25
SJ02-0710	0.04	0.23	0.04	0.02	0.07
SJ02-0807	-	-	-	-	-
SJ02-0820	0.04	0.28	0.07	0.025	0.32
SJ02-0825	2.4	0.025	0.16	0.34	0.32
SJ02-0906	0.24	0.22	0.05	0.04	-
SJ02-0910	0.32	0.41	0.14	0.05	0.38
SJ02-0917	0.62	0.025	0.14	0.10	0.29
SJ02-0928	0.46	0.025	0.16	0.07	0.28
SJ02-1001	0.07	0.44	0.06	0.025	0.34
SJ02-1020	2.4	0.19	0.13	0.33	0.41
SJ02-1114	1.1	0.13	0.09	0.13	0.41
SJ03-0131	0.30	0.06	0.05	0.025	0.12
SJ03-0201	0.81	0.08	0.05	0.07	0.29
SJ03-0202	1.8	0.09	0.17	0.21	0.26

* denotes a snow sample

Table II.8 Cation concentrations for McIvers samples.

Sample	Na ⁺ (ppm)	NH ₄ ⁺ (ppm)	K ⁺ (ppm)	Mg ²⁺ (ppm)	Ca ²⁺ (ppm)
MCS02-0205*	6.2	0.025	0.25	1.2	0.27
MC02-0401	0.42	0.025	0.05	0.11	0.21
MC02-0413	3.4	0.14	0.17	0.70	0.33
MC02-0606	0.18	0.03	0.05	0.04	0.12
MC02-0624	0.16	0.02	0.02	0.04	0.19
MC02-0719	0.26	0.19	0.07	0.03	0.15
MC02-0806	0.30	0.025	0.025	0.01	0.13
MC02-0911	0.11	0.02	0.04	0.025	0.09
MC02-0924	0.08	0.025	0.025	0.025	0.06
MC02-1124	0.16	0.025	0.02	0.02	0.02
MCS03-0126*	1.3	0.025	0.04	0.14	0.07

* denotes a snow sample

Table II.9 Volume weighted mean concentrations of major ions for both locations (in ppm).

Ion	St. John's VWM*	n	std error	McIvers VWM*	n	std error
Cl ⁻	1.09	20	0.24	0.64	8	0.39
NO ₃ ⁻	0.44	24	0.07	0.38	11	0.10
SO ₄ ²⁻	1.17	24	0.17	0.49	11	0.25
Na ⁺	1.08	23	0.30	1.05	11	0.42
NH ₄ ⁺	0.14	23	0.03	0.04	11	0.04
K ⁺	0.09	23	0.01	0.06	11	0.02
Mg ²⁺	0.16	23	0.05	0.19	11	0.07
Ca ²⁺	0.21	23	0.02	0.14	11	0.03

*VWM = $\frac{\sum \text{volume of sample} \times \text{concentration of species of interest in sample}}{\text{total volume of all samples with species of interest}}$

Table II.10 Statistical results of comparison of VWMs of ions for both locations using parametric (t) or non-parametric (t_{welch}) methods, with $\alpha=0.05$. D.F indicates degrees of freedom.

Ion	All samples			Winter samples			Summer samples		
	t*	d.f.	p	t*	d.f.	p	t*	d.f.	p
Cl ⁻	0.93 _w	13	0.184	0.72 _w	2	0.433	0.41	15	0.684
NO ₃ ⁻	0.52 _w	20	0.696	0.19 _w	3	0.433	0.74 _w	15	0.235
SO ₄ ²⁻	2.2 _w	20	0.019	0.47 _w	3	0.336	2.4 _w	15	0.015
Na ⁺	0.00	33	0.948	0.50	11	0.624	0.14	19	0.885
NH ₄ ⁺	2.1 _w	20	0.024	1.3 _w	3	0.141	1.8 _w	15	0.049
K ⁺	1.4	32	0.171	0.22	11	0.830	1.6	19	0.117
Mg ²⁺	0.39	32	0.697	0.69	11	0.424	0.19 _w	15	0.425
Ca ²⁺	1.98	31	0.057	1.3	11	0.215	1.6	19	0.123

*values with X_w indicate a non-parametric test was used

Table II.11 Seasonal volume weighted mean concentrations of major ions for both locations (in ppm).

Ion	St. John's VWM*						McIvers VWM*					
	Winter	n	std error	Summer	n	std error	Winter	n	std error	Summer	n	std error
Cl ⁻	1.45	9	0.42	0.81	11	0.31	0.77	2	0.85	0.59	6	0.43
NO ₃ ⁻	0.33	10	0.11	0.52	14	0.09	0.29	3	0.19	0.41	8	0.12
SO ₄ ²⁻	0.92	10	0.26	1.35	14	0.23	0.67	3	0.46	0.42	8	0.31
Na ⁺	1.58	10	0.58	0.64	13	0.26	2.17	3	1.01	0.58	8	0.32
NH ₄ ⁺	0.12	10	0.04	0.16	13	0.04	0.03	3	0.06	0.05	8	0.05
K ⁺	0.10	10	0.02	0.09	13	0.02	0.09	3	0.04	0.05	8	0.02
Mg ²⁺	0.19	10	0.10	0.13	13	0.05	0.36	3	0.18	0.12	8	0.06
Ca ²⁺	0.21	10	0.04	0.22	13	0.03	0.10	3	0.07	0.15	8	0.03

*VWM = $\frac{\sum \text{volume of sample} \times \text{concentration of species of interest in sample}}{\text{total volume of all samples with species of interest}}$

Table II.12 Percent Seaspray Sulphate
for St. John's samples.

Sample	PSS (%)
SJS02-0123*	76
SJ02-0314	52
SJ02-0322	51
SJ02-0328	86
SJ02-0429	15
SJ02-0510	7
SJ02-0531	2
SJ02-0606	3
SJ02-0624	3
SJ02-0709	1
SJ02-0710	1
SJ02-0820	1
SJ02-0825	48
SJ02-0906	7
SJ02-0910	10
SJ02-0917	23
SJ02-0928	29
SJ02-1001	1
SJ02-1020	37
SJ02-1114	37
SJ03-0131	7
SJ03-0201	57
SJ03-0202	98

Table II.13 Percent Seaspray Sulphate
for McIvers samples.

Sample	PSS (%)
MCS02-0205*	100
MC02-0401	31
MC02-0413	53
MC02-0606	9
MC02-0624	17
MC02-0719	19
MC02-0806	38
MC02-0911	11
MC02-0924	23
MC02-1124	13
MCS03-0126*	83

* denotes a snow sample

Table II.14 ICP-MS data for St. John's samples (ppb)

Sample	Al				V				Mn				Co			
	value	n	s.d	no. of runs	value	n	s.d	no. of runs	value	n	s.d	no. of runs	value	n	s.d	no. of runs
SJS02-0123*	2.02	3	0.43	2	1.04	9	0.29	5	0.50	5	0.04	3	<DL	-	-	-
SJ02-0314	2.08	6	0.61	3	0.11	3	0.20	2	0.00	4	0.12	2	0.000	3	0.004	1
SJ02-0322	9.14	3	1.15	3	1.45	4	0.40	4	1.97	3	0.29	3	0.268	3	0.04	1
SJ02-0328	4.90	3	0.62	3	0.20	2	0.09	2	0.65	2	0.19	2	0.207	3	0.12	1
SJ02-0429	8.35	4	2.03	3	23.88	5	1.88	4	1.04	4	0.18	3	0.246	4	0.03	3
SJ02-0510	8.51	4	0.90	3	0.65	5	0.22	4	1.68	4	0.14	3	0.019	3	0.002	2
SJ02-0531	4.34	3	2.50	3	0.84	4	0.18	4	0.36	3	0.04	3	0.000	2	0.01	2
SJ02-0606	10.09	5	1.60	3	1.05	9	0.36	5	2.07	5	0.12	3	0.003	2	0.001	2
SJ02-0624	3.69	3	0.57	3	36.52	4	2.42	4	3.04	3	0.25	3	0.526	3	0.03	3
SJ02-0709	14.62	3	2.09	3	0.10	3	0.25	3	8.36	3	0.82	3	0.009	2	0.002	2
SJ02-0710	4.31	3	0.22	3	2.64	4	0.17	4	0.11	3	0.01	3	0.000	1	-	1
SJ02-0807	4.42	6	1.80	3	1.86	6	0.44	3	0.48	4	0.01	2	0.000	2	0.01	2
SJ02-0820	26.42	5	2.00	4	1.03	5	0.14	3	4.69	3	0.24	2	0.047	3	0.001	2
SJ02-0825	4.92	6	0.90	3	0.09	5	0.20	4	0.68	2	0.10	2	0.005	2	0.004	2
SJ02-0906	3.30	3	0.44	3	0.04	2	0.37	2	0.02	2	0.03	2	<DL	-	-	-
SJ02-0910	1.01	2	0.34	2	0.13	3	0.15	3	0.00	2	0.06	2	0.000	1	-	1
SJ02-0917	1.88	3	0.58	3	3.28	3	0.62	3	0.71	2	0.02	2	0.013	2	0.01	2
SJ02-0928	1.43	3	0.67	3	0.42	3	0.16	3	0.00	2	0.02	2	0.073	2	0.01	2
SJ02-1001	12.52	3	1.06	3	1.78	3	0.33	3	0.80	2	0.19	2	0.118	3	0.02	3
SJ02-1020	5.84	3	0.25	3	4.57	3	0.54	3	0.25	2	0.02	2	0.055	2	0.002	2
SJ02-1114	1.30	2	0.10	2	10.29	2	3.62	2	0.41	2	0.44	2	0.063	2	0.04	2
SJ03-0131	1.62	4	0.23	2	13.84	5	0.86	2	0.71	4	0.25	2	0.086	5	0.01	2
SJ03-0201	1.92	2	1.75	2	1.81	2	0.04	2	0.00	2	0.03	2	0.000	1	-	1
SJ03-0202	1.97	2	1.26	2	0.02	2	0.02	2	0.00	2	0.02	2	0.000	1	-	1

Table II.14 ICP-MS data for St. John's samples (ppb) continued

Sample	Ni				Cu				Zn				As			
	value	n	s.d	no. of runs	value	n	s.d	no. of runs	value	n	s.d	no. of runs	value	n	s.d	no. of runs
SJS02-0123*	0.48	2	0.20	1	6.16	7	0.84	4	12.80	2	0.15	1	0.05	3	0.003	2
SJ02-0314	0.14	1	-	1	0.00	5	0.22	3	8.18	2	0.34	1	0.18	5	0.01	3
SJ02-0322	7.86	1	-	1	7.36	3	1.24	3	80.04	1	-	1	1.13	4	0.30	4
SJ02-0328	0.65	1	-	1	5.88	3	1.19	3	25.82	1	-	1	3.52	4	0.30	4
SJ02-0429	13.12	2	0.42	1	0.00	4	0.12	3	15.92	2	2.72	1	0.16	4	0.02	3
SJ02-0510	0.27	1	-	1	1.82	4	0.32	3	29.69	1	-	1	0.15	4	0.02	3
SJ02-0531	1.13	1	-	1	0.00	2	0.32	2	10.88	1	-	1	0.08	2	0.004	2
SJ02-0606	0.37	1	-	1	0.00	6	0.30	4	19.98	1	-	1	0.09	2	0.007	2
SJ02-0624	32.07	1	-	1	0.00	3	0.37	3	5.77	1	-	1	0.05	2	0.003	2
SJ02-0709	0.15	1	-	1	2.69	4	0.70	4	17.02	1	-	1	0.12	3	0.02	3
SJ02-0710	0.33	1	-	1	0.50	3	0.46	3	2.32	1	-	1	0.04	2	0.004	2
SJ02-0807	0.97	2	0.40	1	0.00	6	0.44	3	3.64	1	1.50	1	0.01	3	0.005	2
SJ02-0820	1.29	1	-	1	0.00	5	0.38	3	19.09	1	-	1	0.05	3	0.005	2
SJ02-0825	0.27	1	-	1	0.80	9	1.16	5	43.63	1	-	1	0.23	5	0.02	4
SJ02-0906	1.01	1	-	1	0.07	3	0.58	3	8.73	1	-	1	0.02	2	0.006	1
SJ02-0910	0.00	1	-	1	44.03	3	7.84	3	2.91	1	-	1	0.02	2	0.006	1
SJ02-0917	1.35	1	-	1	2.04	3	0.25	3	5.71	1	-	1	0.05	2	0.03	1
SJ02-0928	0.03	1	-	1	0.11	4	1.16	4	6.66	1	-	1	0.05	3	0.008	3
SJ02-1001	0.45	1	-	1	2.35	3	0.63	3	6.63	1	-	1	0.11	3	0.02	3
SJ02-1020	4.48	1	-	1	2.52	3	0.54	3	4.49	1	-	1	0.06	2	0.0004	2
SJ02-1114	6.44	1	-	1	0.00	2	0.18	2	18.63	1	-	1	0.03	2	0.02	2
SJ03-0131	8.09	2	1.87	1	0.70	5	1.83	2	8.98	3	3.83	1	0.03	5	0.004	2
SJ03-0201	1.22	1	-	1	0.09	2	0.91	2	7.84	1	-	1	0.14	2	0.02	2
SJ03-0202	0.08	1	-	1	3.53	2	0.13	2	7.38	1	-	1	0.07	2	0.01	2

Table II.14 ICP-MS data for St. John's samples (ppb) continued

Sample	Mo				Sr				Ag				Cd			
	value	n	s.d	no. of	value	n	s.d	no. of	value	n	s.d	no. of	value	n	s.d	no. of
				runs				runs				runs				runs
SJS02-0123*	0.03	3	0.06	2	1.26	9	0.15	5	0.30	8	0.04	4	0.02	1	-	1
SJ02-0314	0.01	4	0.005	2	0.16	5	0.05	4	<DL	4	0.004	2	0.03	2	0.01	2
SJ02-0322	0.46	4	0.04	4	3.07	4	0.35	4	<DL	2	0.002	2	0.08	3	0.01	3
SJ02-0328	0.09	1	-	1	0.91	4	0.09	4	<DL	3	0.02	3	0.04	2	0.004	2
SJ02-0429	1.38	5	0.17	4	1.05	5	0.05	4	<DL	3	0.006	2	0.05	4	0.005	3
SJ02-0510	0.06	4	0.004	3	0.54	5	0.05	4	<DL	4	0.01	3	0.03	3	0.006	2
SJ02-0531	0.09	4	0.04	4	0.16	4	0.02	4	<DL	2	0.007	2	<DL	-	-	-
SJ02-0606	0.06	4	0.02	3	0.51	9	0.07	5	<DL	6	0.03	4	0.03	2	0.003	2
SJ02-0624	3.93	4	0.25	4	0.30	4	0.03	4	<DL	1	-	1	0.11	4	0.006	4
SJ02-0709	0.06	2	0.07	2	0.50	4	0.05	4	0.02	4	0.03	4	0.08	5	0.02	5
SJ02-0710	0.06	4	0.01	4	0.08	4	0.02	4	<DL	3	0.02	3	0.05	2	0.009	2
SJ02-0807	0.14	6	0.06	3	0.20	6	0.02	3	0.02	4	0.01	2	0.017	1	-	1
SJ02-0820	0.18	5	0.03	3	0.68	5	0.06	3	0.03	5	0.02	3	0.03	4	0.01	3
SJ02-0825	0.06	6	0.02	4	1.31	9	0.12	5	<DL	3	0.005	3	0.03	4	0.02	3
SJ02-0906	0.09	3	0.02	3	0.30	3	0.03	3	<DL	3	0.01	3	<DL	-	-	-
SJ02-0910	0.03	3	0.02	3	0.26	3	0.07	3	0.11	3	0.06	3	<DL	-	-	-
SJ02-0917	0.12	3	0.01	3	0.47	3	0.03	3	<DL	2	0.01	2	<DL	-	-	-
SJ02-0928	1.08	3	1.80	3	0.34	4	0.04	4	<DL	4	0.02	4	<DL	-	-	-
SJ02-1001	0.04	3	0.01	3	0.48	3	0.07	3	<DL	3	0.009	3	0.03	1	-	1
SJ02-1020	0.24	3	0.02	3	1.34	3	0.12	3	<DL	3	0.02	3	0.02	2	0.006	2
SJ02-1114	0.37	2	0.12	2	0.65	2	0.20	2	<DL	2	0.004	2	<DL	-	-	-
SJ03-0131	0.37	5	0.15	2	0.22	4	0.07	2	<DL	4	0.005	2	0.02	1	-	1
SJ03-0201	0.07	2	0.05	2	0.38	2	0.01	2	<DL	2	0.01	2	<DL	-	-	-
SJ03-0202	0.02	2	0.01	2	0.84	2	0.01	2	<DL	2	0.001	2	<DL	-	-	-

Table II.14 ICP-MS data for St. John's samples (ppb) continued

Sample	Ba				Pb			
	value	n	s.d	no. of	value	n	s.d	no. of
				runs				runs
SJS02-0123*	0.62	6	0.15	3	0.33	7	0.05	4
SJ02-0314	0.55	4	0.22	4	0.10	6	0.07	4
SJ02-0322	1.26	4	0.32	4	2.13	4	0.13	4
SJ02-0328	0.74	4	0.14	4	0.02	4	0.03	4
SJ02-0429	1.05	5	0.43	4	0.58	5	0.04	4
SJ02-0510	1.57	5	0.29	4	4.11	5	0.20	4
SJ02-0531	1.34	3	0.79	3	0.02	4	0.03	4
SJ02-0606	1.50	7	0.24	4	1.44	9	0.14	5
SJ02-0624	0.48	4	0.12	4	0.37	4	0.04	4
SJ02-0709	2.29	4	0.12	4	0.62	4	0.03	4
SJ02-0710	0.95	4	0.29	4	1.11	4	0.11	4
SJ02-0807	1.27	6	0.22	3	0.32	6	0.05	3
SJ02-0820	3.13	5	0.35	3	0.91	5	0.11	3
SJ02-0825	1.03	9	0.43	5	0.59	9	0.05	5
SJ02-0906	1.52	3	0.07	3	0.49	3	0.06	3
SJ02-0910	0.82	3	0.25	3	4.02	3	0.67	3
SJ02-0917	0.99	3	0.38	3	0.29	3	0.08	3
SJ02-0926	1.14	4	0.51	4	0.05	4	0.09	4
SJ02-1001	3.10	3	1.93	3	1.73	3	0.14	3
SJ02-1020	1.21	3	0.14	3	2.98	3	0.18	3
SJ02-1114	1.44	2	0.05	2	0.02	2	0.01	2
SJ03-0131	1.91	4	0.76	2	0.63	4	0.14	2
SJ03-0201	1.15	2	1.07	2	0.02	2	0.21	2
SJ03-0202	0.44	2	0.22	2	0.40	2	0.15	2

Table II.15 ICP-MS data for McIvers samples (ppb)

Sample	Al				V				Mn				Co			
	value	n	s.d	no. of	value	n	s.d	no. of	value	n	s.d	no. of	value	n	s.d	no. of
				runs				runs				runs				runs
MCS02-0205*	2.61	4	1.19	3	0.31	1	-	1	1.87	4	0.12	3	0.016	2	0.002	1
MC02-0401	5.13	3	0.32	3	0.43	1	-	1	1.20	3	0.11	3	0.531	3	0.06	1
MC02-0413	5.72	4	0.81	3	<DL	-	-	-	1.40	5	0.16	3	0.359	10	0.06	5
MC02-0606	4.50	4	0.32	3	0.19	4	0.24	3	1.18	4	0.07	3	0.055	3	0.004	2
MC02-0624	3.24	3	1.94	3	0.000	1	-	1	1.21	3	0.19	3	0.078	2	0.01	2
MC02-0719	4.35	7	0.63	3	0.254	4	0.06	2	1.02	7	0.14	3	0.055	5	0.01	2
MC02-0806	3.79	4	1.00	3	0.305	1	-	1	0.24	2	0.02	2	0.055	2	0.003	2
MC02-0911	0.87	2	0.64	2	<DL	-	-	-	0.27	2	0.23	2	0.042	2	0.02	2
MC02-0924	2.97	3	1.71	3	0.344	1	-	1	0.28	2	0.08	2	0.031	1	-	1
MC02-1124	2.46	2	0.92	2	<DL	-	-	-	0.00	2	0.03	2	0.020	1	-	1
MCS03-0126*	0.98	4	0.01	3	<DL	-	-	-	0.23	3	0.01	2	<DL	-	-	-

Sample	Ni				Cu				Zn				As			
	value	n	s.d	no. of	value	n	s.d	no. of	value	n	s.d	no. of	value	n	s.d	no. of
				runs				runs				runs				runs
MCS02-0205*	<DL	-	-	-	0.98	4	0.15	3	10.67	1	-	1	0.134	4	0.003	3
MC02-0401	0.00	1	-	1	0.00	2	0.03	2	71.85	1	-	1	0.064	2	0.01	2
MC02-0413	<DL	-	-	-	0.00	7	0.92	3	43.69	1	-	1	0.067	7	0.01	4
MC02-0606	0.27	2	0.16	1	0.00	5	0.58	3	19.28	2	12.53	1	0.042	3	0.008	2
MC02-0624	2.31	1	-	1	0.00	2	0.68	2	55.00	1	-	1	0.022	1	-	1
MC02-0719	<DL	1	-	1	0.00	6	0.55	3	10.53	2	6.48	1	0.042	4	0.01	2
MC02-0806	0.74	1	-	1	0.00	5	0.38	4	10.47	1	-	1	0.022	1	-	1
MC02-0911	<DL	-	-	-	0.00	3	0.50	3	8.64	1	-	1	<DL	-	-	-
MC02-0924	0.17	1	-	1	0.00	3	0.06	3	7.06	1	-	1	<DL	-	-	-
MC02-1124	<DL	-	-	-	0.00	3	0.19	3	3.31	1	-	1	<DL	-	-	-
MCS03-0126*	<DL	-	-	-	0.55	3	0.15	2	10.81	2	1.48	1	0.029	2	0.007	2

Table II.15 ICP-MS data for McIvers samples (ppb) continued

Sample	Mo				Sr				Ag				Cd			
	value	n	s.d	no. of	value	n	s.d	no. of	value	n	s.d	no. of	value	n	s.d	no. of
				runs				runs				runs				runs
MCS02-0205*	0.061	2	0.01	1	3.587	5	0.31	4	0.015	1	-	1	<DL	-	-	-
MC02-0401	0.01	2	0.002	2	0.352	4	0.04	4	<DL	-	-	-	0.039	2	0.002	2
MC02-0413	<DL	-	-	-	2.077	14	0.24	6	<DL	1	-	1	0.063	11	0.02	6
MC02-0606	0.01	3	0.04	2	0.188	6	0.02	4	<DL	2	0.000	2	0.027	1	-	1
MC02-0624	0.03	2	0.07	2	0.120	4	0.04	4	<DL	2	0.003	2	0.069	1	-	1
MC02-0719	0.00	4	0.01	2	0.137	8	0.03	4	<DL	2	0.02	1	<DL	-	-	-
MC02-0806	0.00	4	0.03	3	0.033	9	0.05	5	<DL	5	0.02	3	0.011	1	-	1
MC02-0911	0.00	1	-	1	0.070	3	0.08	3	<DL	2	0.02	2	<DL	-	-	-
MC02-0924	0.00	2	0.002	2	0.034	4	0.03	4	<DL	3	0.006	3	<DL	-	-	-
MC02-1124	0.00	1	-	1	0.103	3	0.02	3	<DL	3	0.009	3	<DL	-	-	-
MCS03-0126*	0.022	1	-	1	0.678	3	0.005	2	0.026	2	0.02	2	<DL	-	-	-

171

Sample	Ba				Pb			
	value	n	s.d	no. of	value	n	s.d	no. of
				runs				runs
MCS02-0205*	2.43	4	0.54	4	1.03	5	0.22	4
MC02-0401	0.57	3	0.28	3	0.04	4	0.07	4
MC02-0413	0.62	9	0.22	4	0.15	12	0.10	6
MC02-0606	0.56	6	0.19	4	0.78	6	0.07	4
MC02-0624	1.25	3	0.40	3	0.04	3	0.16	3
MC02-0719	0.35	3	0.04	2	0.52	8	0.11	4
MC02-0806	0.50	7	0.16	5	0.13	10	0.08	5
MC02-0911	0.63	2	0.57	2	0.00	3	0.05	3
MC02-0924	0.43	3	0.22	3	2.39	4	0.31	4
MC02-1124	0.37	1	-	1	0.05	3	0.05	3
MCS03-0126*	0.43	2	0.11	2	0.87	3	0.14	2

Table II.16 Volume weighted mean concentrations of trace elements for both locations (in ppb).

Element	St. John's VWM	n	std error	no. of runs	McIvers VWM	n	std error	no. of runs
Al	4.7	85	0.75	4	3.3	51	1.1	4
V	4.6	96	1.7	6	0.27	12	2.5	3
Mn	0.90	70	0.27	3	0.74	37	0.39	3
Co	0.08	52	0.03	4	0.12	30	0.05	3
Ni	3.5	29	1.4	1	0.30	7	2.0	1
Cu	2.1	93	0.97	5	0.13	41	1.4	5
Zn	14	28	3.6	1	22	13	5.3	1
As	0.36	66	0.16	4	0.05	23	0.23	4
Mo	0.46	85	0.16	5	0.01	22	0.25	3
Sr	0.58	106	0.15	6	0.62	63	0.22	7
Ag	0.03	79	0.01	7	0.01	25	0.02	4
Cd	0.03	42	0.005	6	0.02	16	0.007	7
Ba	1.1	99	0.12	6	0.69	44	0.18	6
Pb	0.59	105	0.18	6	0.65	61	0.26	7

*VWM = $\frac{\sum \text{volume of sample} \times \text{concentration of species of interest in sample}}{\text{total volume of all samples with species of interest}}$

Table II.17 Statistical results of comparison of VWMs of trace elements for both locations using parametric (t) or non-parametric (t_{welch}) methods, with $\alpha=0.05$. D.F indicates degrees of freedom.

Ion	All samples			Winter samples			Summer samples		
	t*	d.f.	p	t*	d.f.	p	t*	d.f.	p
Al	1.1 _w	20	0.151	0.86 _w	3	0.228	0.92 _w	15	0.185
V	1.5 _w	20	0.080	0.83 _w	3	0.235	1.3 _w	15	0.099
Mn	0.35 _w	20	0.364	0.46	11	0.655	0.68 _w	15	0.255
Co	0.76	33	0.454	0.98 _w	3	0.199	0.98	20	0.339
Ni	1.3 _w	20	0.103	1.0 _w	3	0.195	1.2 _w	15	0.129
Cu	1.2 _w	20	0.132	1.5 _w	3	0.113	-	-	-
Zn	1.3	33	0.198	0.77 _w	3	0.249	1.8	20	0.085
As	1.1 _w	20	0.137	0.87 _w	3	0.225	1.6 _w	15	0.068
Mo	1.5 _w	20	0.076	1.0 _w	3	0.192	1.6 _w	15	0.068
Sr	0.78	33	0.442	0.78	11	0.451	0.49 _w	15	0.317
Ag	0.78 _w	20	0.223	0.50 _w	3	0.325	0.73 _w	15	
Cd	0.93	33	0.362	1.8 _w	3		0.44	20	0.667
Ba	2.0	33	0.054	0.14	11	0.887	3.2 _w	15	0.003
Pb	-0.19 _w	20	0.573	-0.15 _w	3	0.553	-0.07 _w	15	0.527

*values with X_w indicate a non-parametric test was used

Table II.18 Seasonal volume weighted mean concentrations of trace elements for St. John's and McIvers (in ppb).

Element	St. John's VWM*						McIvers VWM*					
	Winter	n	std error	Summer	n	std error	Winter	n	std error	Summer	n	std error
Al	3.6	10	0.93	5.4	14	1.1	2.0	3	1.6	3.8	8	1.4
V	2.4		1.3	6.2		2.7	0.27		2.2	0.28		3.5
Mn	0.40		0.19	1.3		0.42	0.58		0.34	0.80		0.55
Co	0.071		0.026	0.086		0.049	0.019		0.046	0.17		0.065
Ni	1.8		0.85	4.8		2.2	0.12		1.5	0.38		3.0
Cu	2.9		0.80	1.6		1.6	0.44		1.4	-		-
Zn	15		4.5	13		5.1	7.7		8.0	29		6.7
As	0.74		0.39	0.081		0.015	0.058		0.69	0.041		0.020
Mo	0.11		0.042	0.71		0.27	0.024		0.073	0.008		0.36
Sr	0.74		0.31	0.47		0.13	1.2		0.55	0.36		0.18
Ag	0.045		0.028	0.014		0.003	0.017		0.050	0.010		0.005
Cd	0.027		0.005	0.033		0.008	0.010		0.009	0.028		0.010
Ba	1.02		0.27	1.2		0.12	0.95		0.47	0.59		0.15
Pb	0.51		0.24	0.65		0.26	0.58		0.41	0.68		0.34

*VWM = $\frac{\sum \text{volume of sample} \times \text{concentration of species of interest in sample}}{\text{total volume of all samples with species of interest}}$

Table II.19 Isotope data for St. John's samples.

Sample	$\delta^{15}\text{N}_{\text{NO}_3}$ (‰)	$\delta^{18}\text{O}_{\text{NO}_3}$ (‰)	$\delta^{18}\text{O}_{\text{H}_2\text{O}}$ (‰)
SJS02-0123*	2.7	15.8	-16.2
SJ02-0314	-5.7	-	-10.6
SJ02-0322	-7.7	-	-3.9
SJ02-0328	-3.5	47.8	-5.1
SJ02-0429	-3.7	-	-11.5
SJ02-0510	-4.3	-	-3.0
SJ02-0531	-2.1	-	-8.0
SJ02-0606	-4.3	49.4	-3.8
SJ02-0624	-3.6	-	-9.2
SJ02-0709	-0.5	46.4	-7.1
SJ02-0710	-1.4	46.1	-7.9
SJ02-0807	-2.8	52.2	-
SJ02-0820	-3.6	50.0	-5.6
SJ02-0825	-3.7	51.5	-4.0
SJ02-0906	-2.6	32.6	-4.2
SJ02-0910	-4.3	23.7	-8.6
SJ02-0917	-3.5	36.2	-4.3
SJ02-0928	-4.7	42.4	-5.6
SJ02-1001	-8.6	53.9	-7.2
SJ02-1020	-9.4	48.6	-8.7
SJ02-1114	-2.2	-	-7.6
SJ03-0131	-8.2	25.8	-8.2
SJ03-0201	-2.9	-	-6.2
SJ03-0202	-7.1	27.9	-7.3

* denotes a snow sample

Table II.20 Isotope data for McIvers samples.

Sample	$\delta^{15}\text{N}_{\text{NO}_3}$ (‰)	$\delta^{18}\text{O}_{\text{NO}_3}$ (‰)	$\delta^{18}\text{O}_{\text{H}_2\text{O}}$ (‰)
MCS02-0205*	-4.7	-	-12
MC02-0401	0.2	46.5	-13.2
MC02-0413	-3.8	48.5	-7.5
MC02-0606	-6.0	51.9	-6.4
MC02-0624	-2.7	-	-11.0
MC02-0719	0.5	-	-9.5
MC02-0806	-3.0	42.6	-8.7
MC02-0911	-5.4	36.0	-9.0
MC02-0924	-1.2	32.4	-8.0
MC02-1124	-5.6	39.9	-14.1
MCS03-0126*	-	27.4	-14.3

* denotes a snow sample

Table II.21 Statistical results of comparison of VWMs of stable isotopes for both locations using parametric (t) or non-parametric (t_{welch}) methods, with $\alpha=0.05$. D.F indicates degrees of freedom.

Ion	All samples			Winter samples			Summer samples		
	t*	d.f.	p	t*	d.f.	p	t*	d.f.	p
$\delta^{15}\text{N}$	0.396 _w	12	0.349	0.26	9	0.804	0.12	18	0.903
$\delta^{18}\text{O}_{\text{NO}_3}$	0.397 _w	15	0.348	0.04	6	0.969	1.13	14	0.277
$\delta^{18}\text{O}_{\text{H}_2\text{O}}$	2.78	32	0.009	2.36	11	0.038	2.60	19	0.018

*values with X_w indicate a non-parametric test was used

Table II.22 Correlation matrix of the 14 elements used to produced the PCA

	^{15}N	NO_3^-	SO_4^{2-}	Na^+	NH_4^+	K^+	Mg^{2+}	Al	V	Mn	Co	Cu	Zn
NO_3^-	-0.075												
SO_4^{2-}	-0.354	0.695											
Na^+	-0.064	-0.050	0.131										
NH_4^+	-0.028	0.777	0.669	-0.196									
K^+	-0.114	0.171	0.278	0.689	0.156								
Mg^{2+}	0.025	0.105	0.232	0.895	-0.068	0.654							
Al	-0.023	0.770	0.654	-0.192	0.683	0.058	-0.066						
V	-0.273	-0.107	0.176	-0.014	-0.013	0.004	-0.086	-0.149					
Mn	0.213	0.713	0.340	-0.189	0.736	0.172	-0.057	0.745	-0.105				
Co	0.119	-0.002	0.067	0.274	-0.104	0.127	0.341	0.041	-0.029	0.023			
Cu	0.051	0.132	0.201	0.498	0.165	0.516	0.356	0.031	-0.033	0.101	-0.008		
Zn	0.266	0.034	-0.028	0.223	-0.106	0.111	0.360	0.129	-0.180	0.203	0.707	-0.074	
Mo	-0.192	-0.101	0.017	-0.024	-0.083	0.357	-0.064	-0.081	0.356	-0.080	-0.028	-0.081	-0.175

APPENDIX III

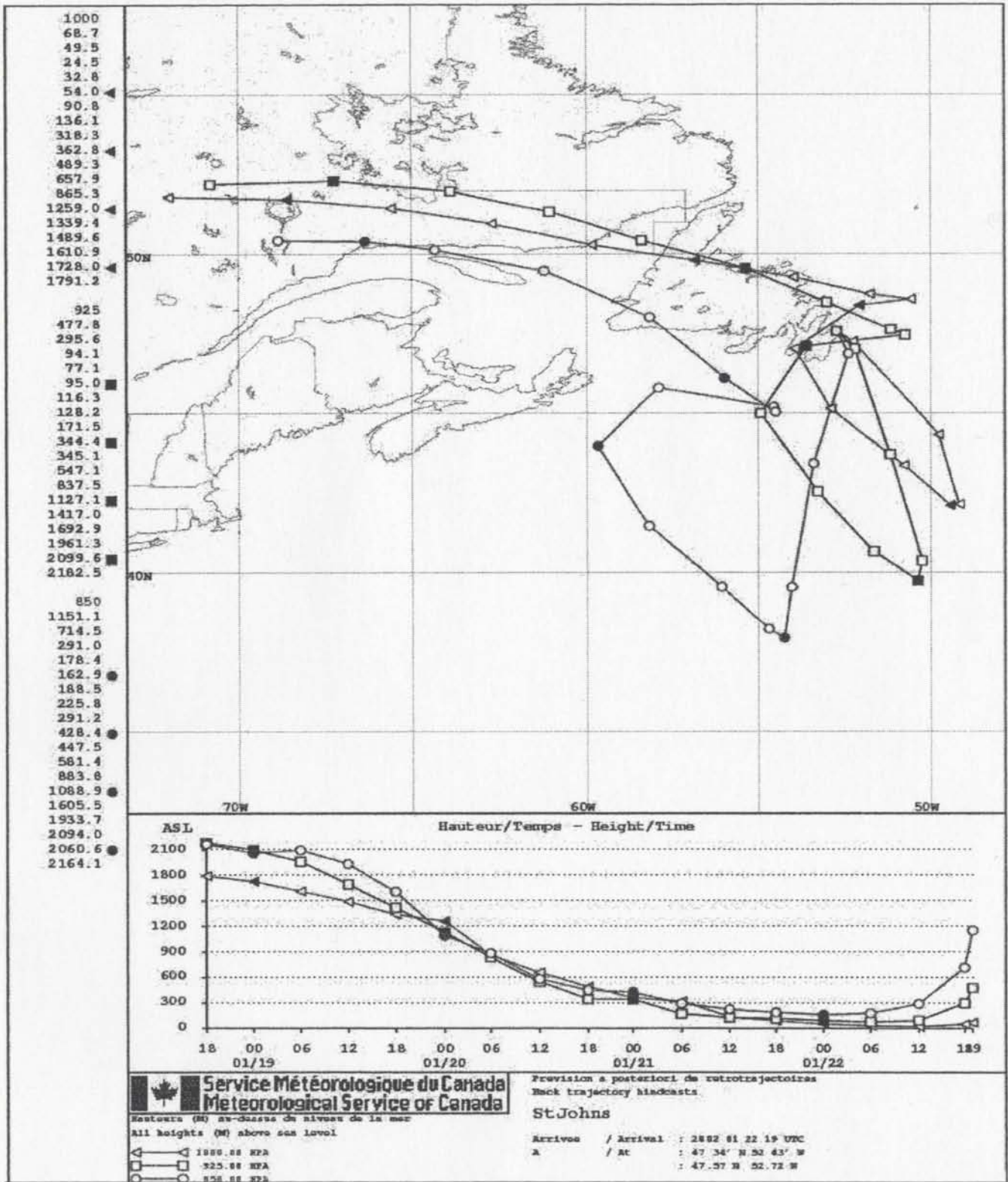


Figure III.1 Air mass back trajectory calculated for sample SJS02-0123

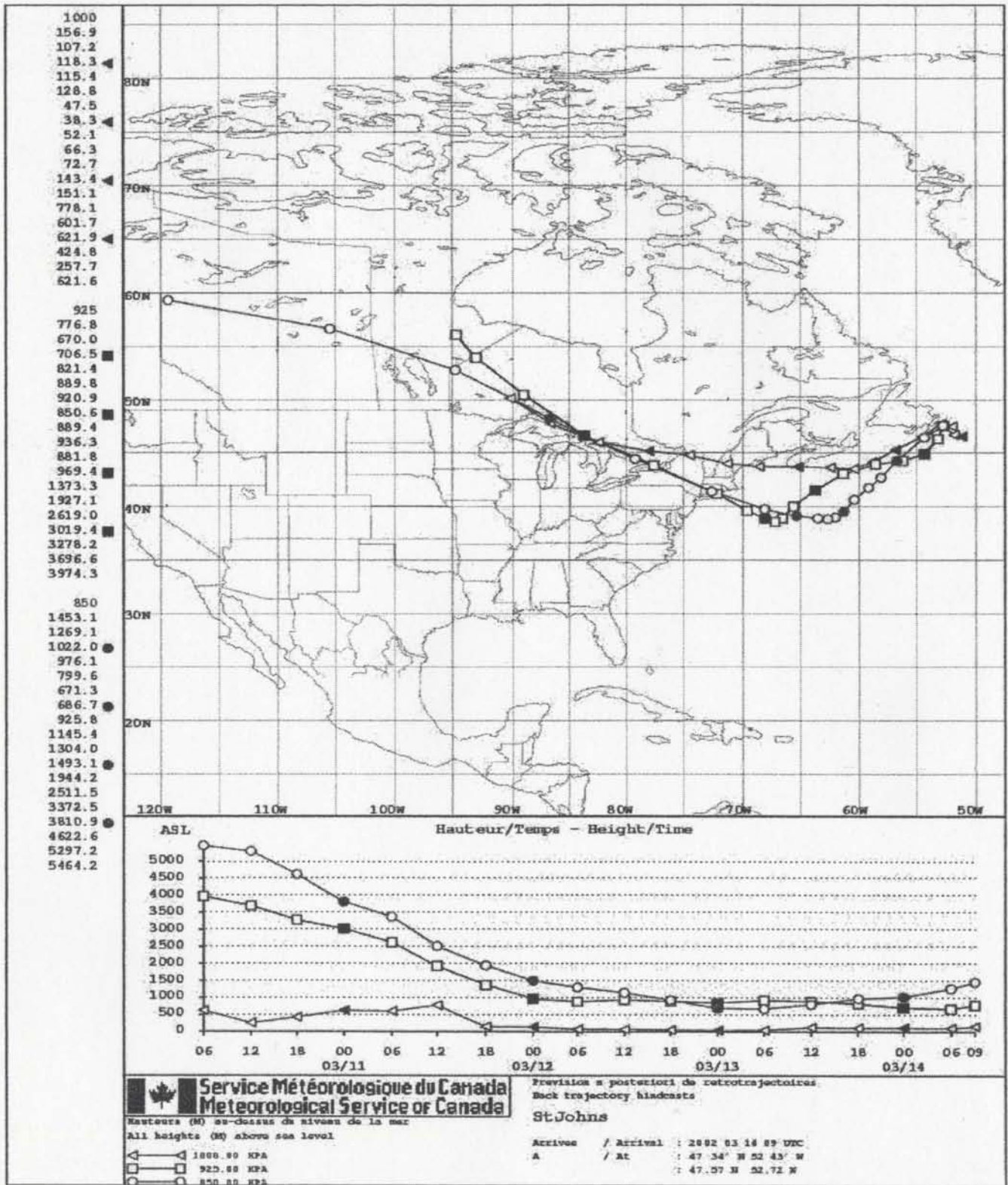


Figure III.2 Air mass back trajectory calculated for sample SJ02-0314

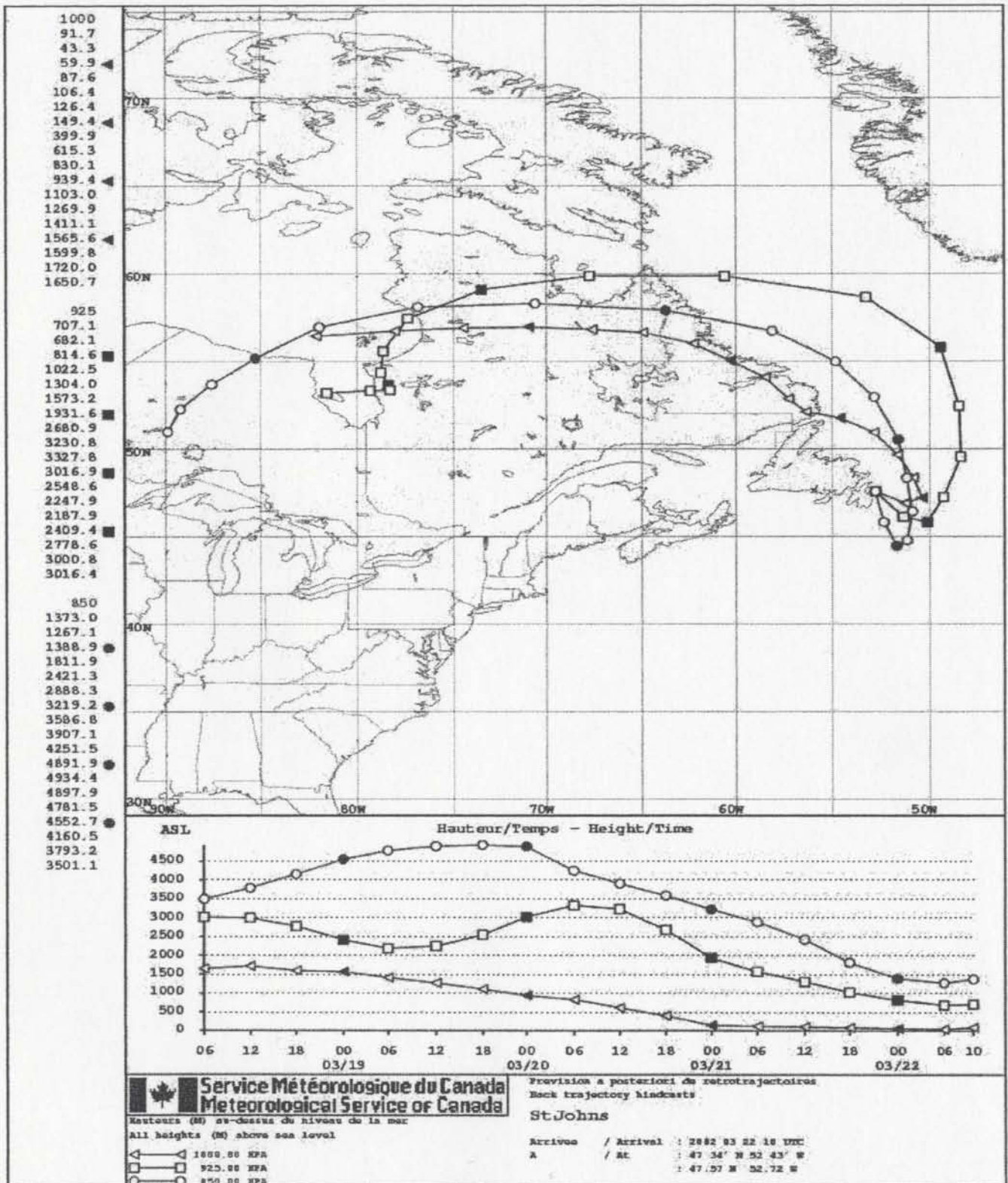


Figure III.3 Air mass back trajectory calculated for sample SJ02-0322

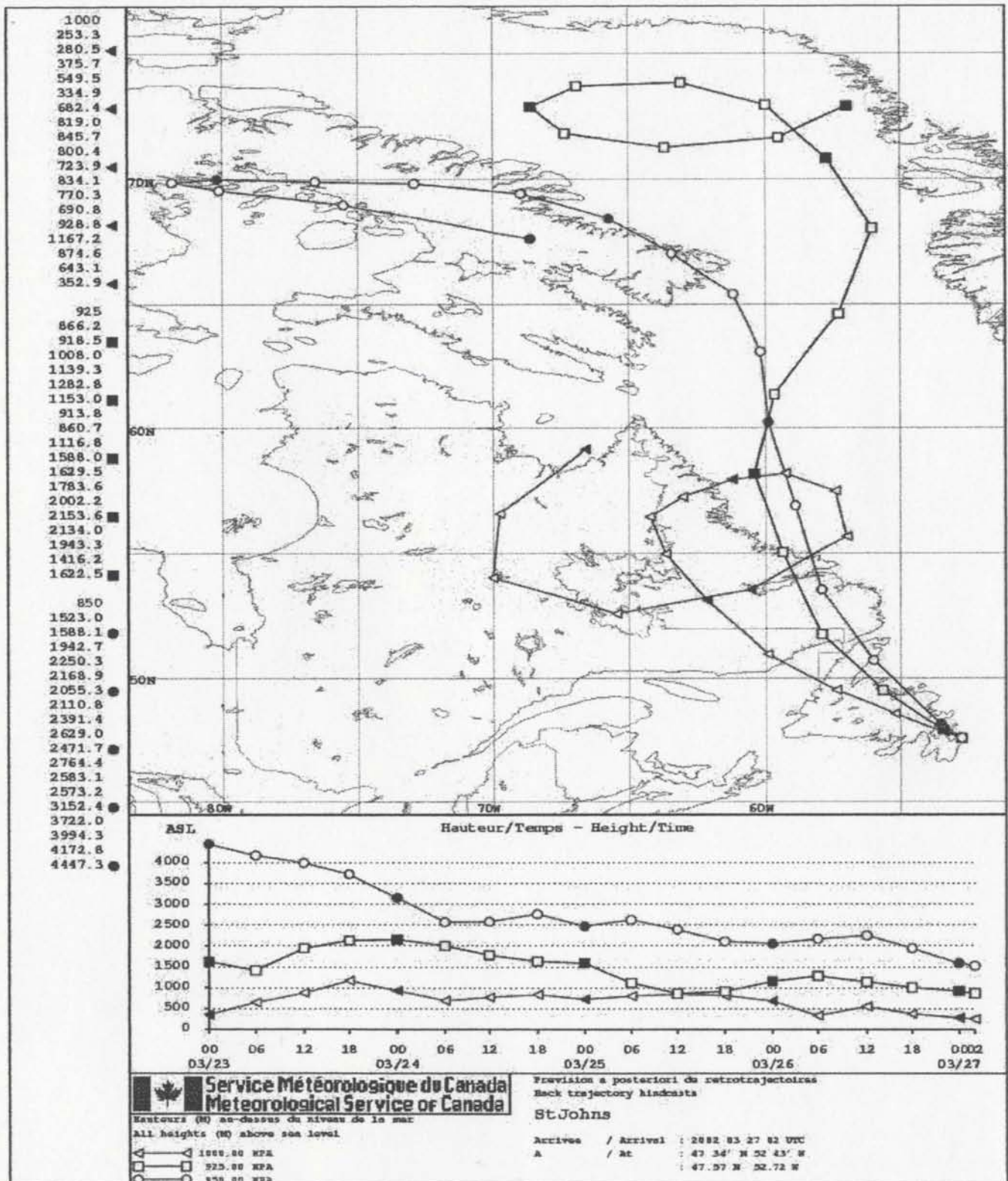


Figure III.4 Air mass back trajectory calculated for sample SJ02-0328

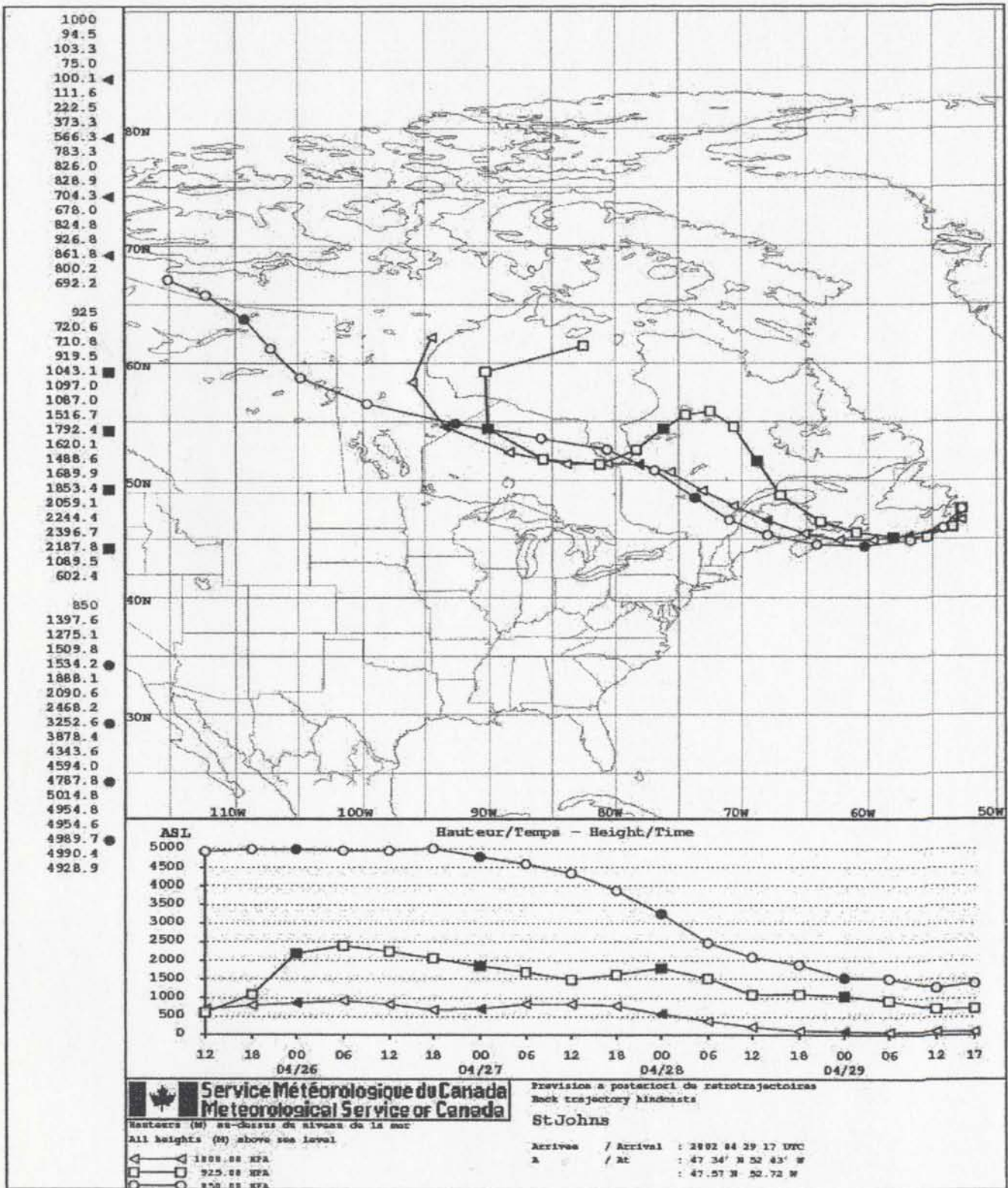


Figure III.5 Air mass back trajectory calculated for sample SJ02-0429

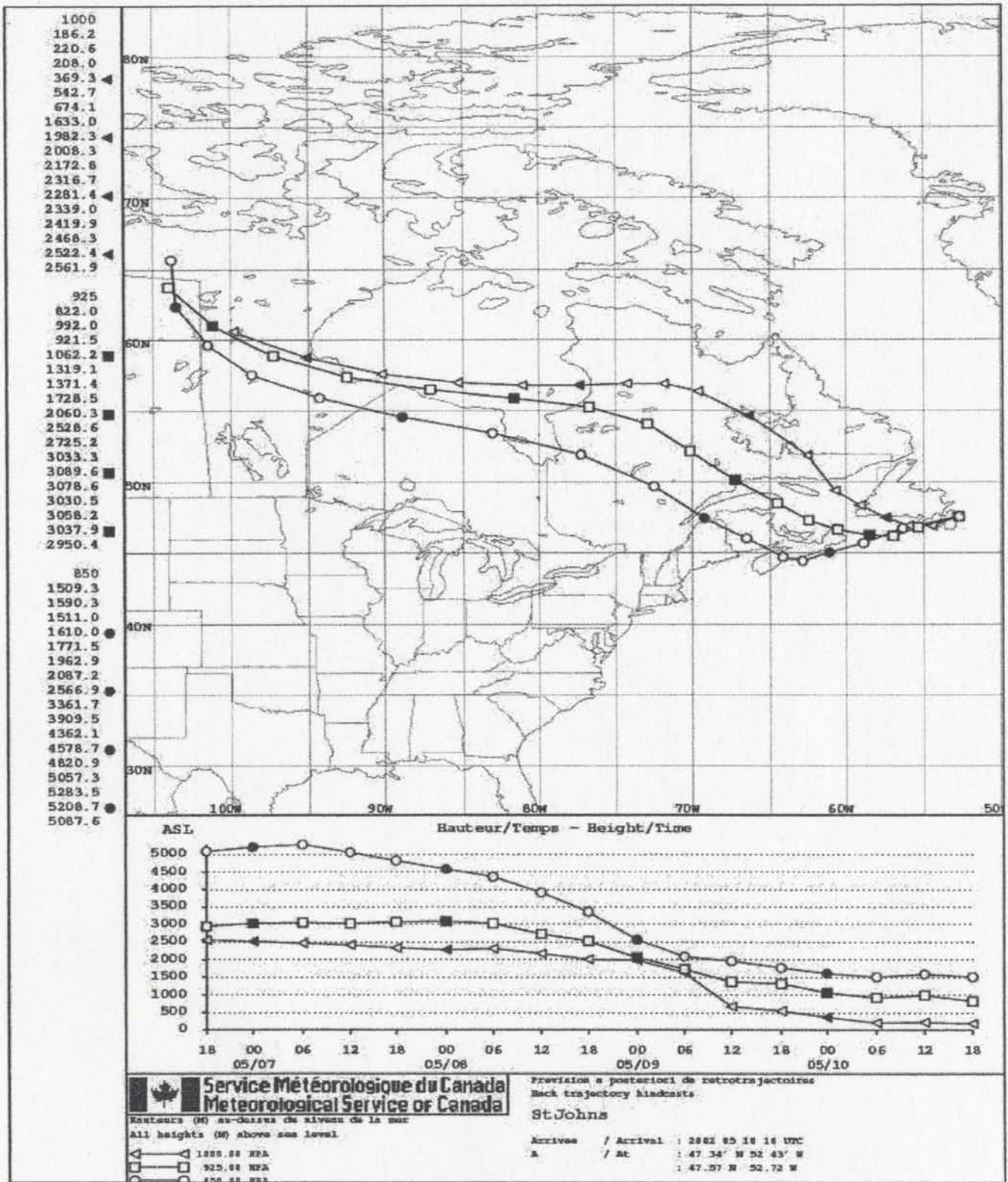


Figure III.6 Air mass back trajectory calculated for sample SJ02-0510

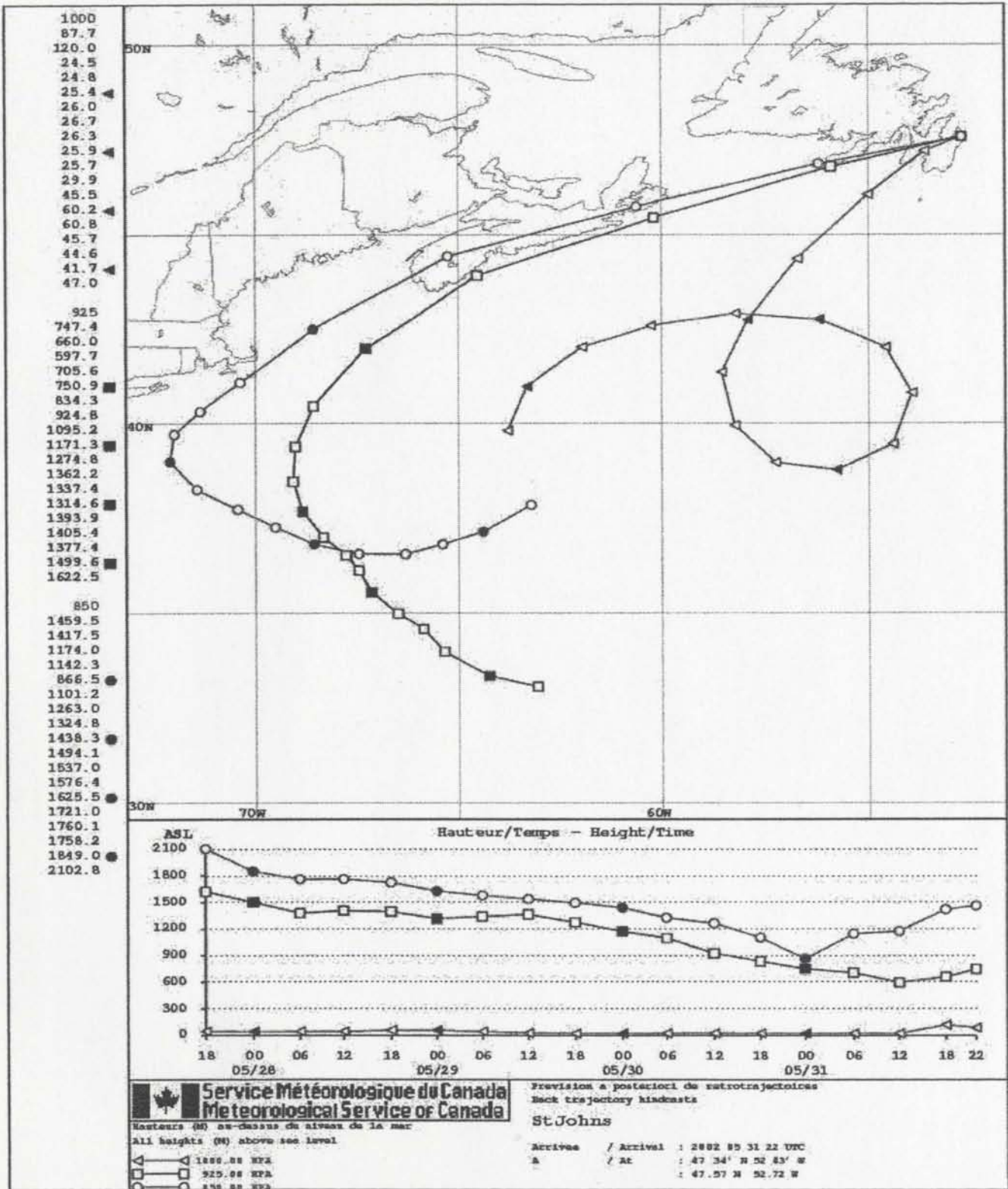


Figure III.7 Air mass back trajectory calculated for sample SJ02-0531

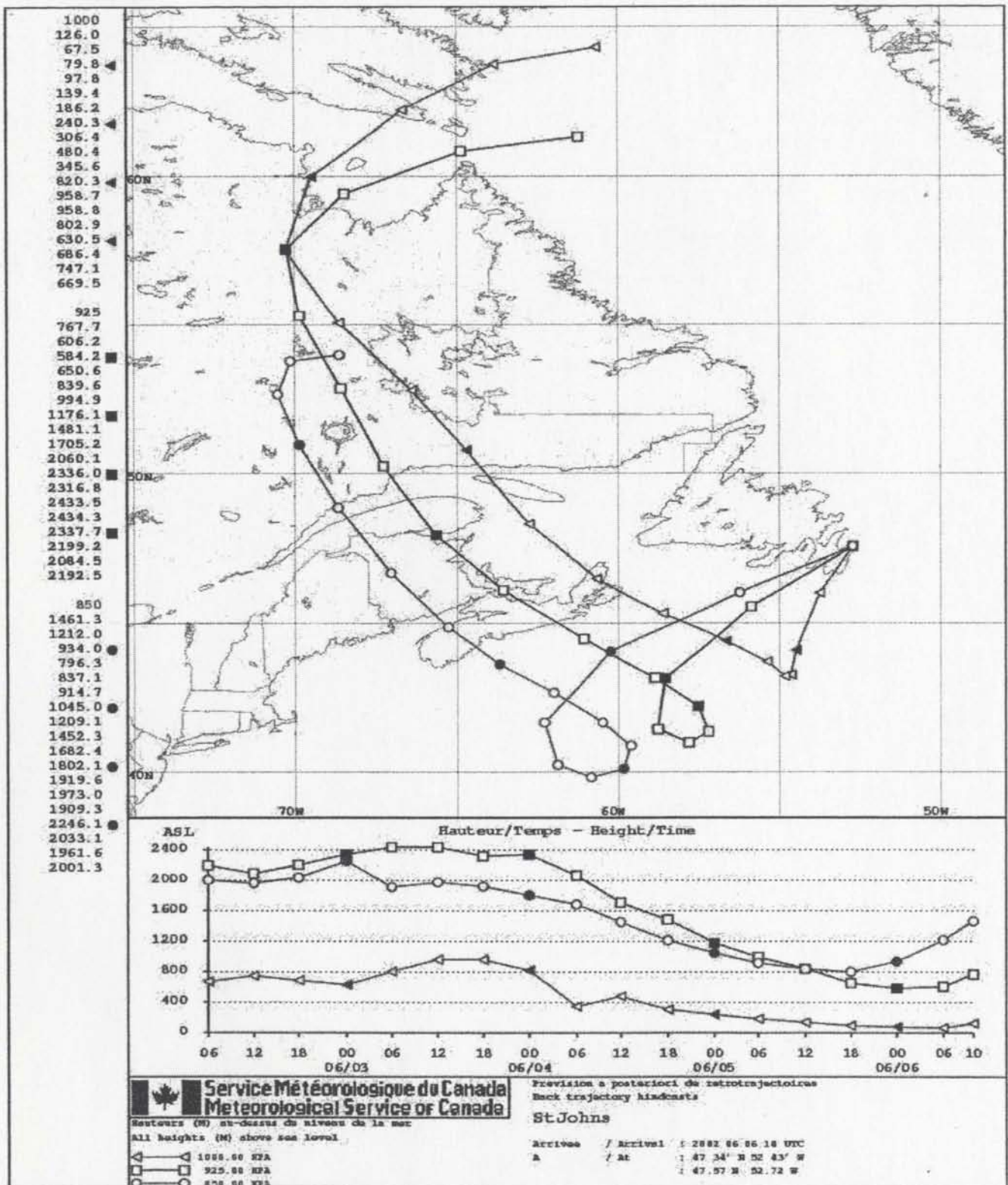


Figure III.8 Air mass back trajectory calculated for sample SJ02-0606

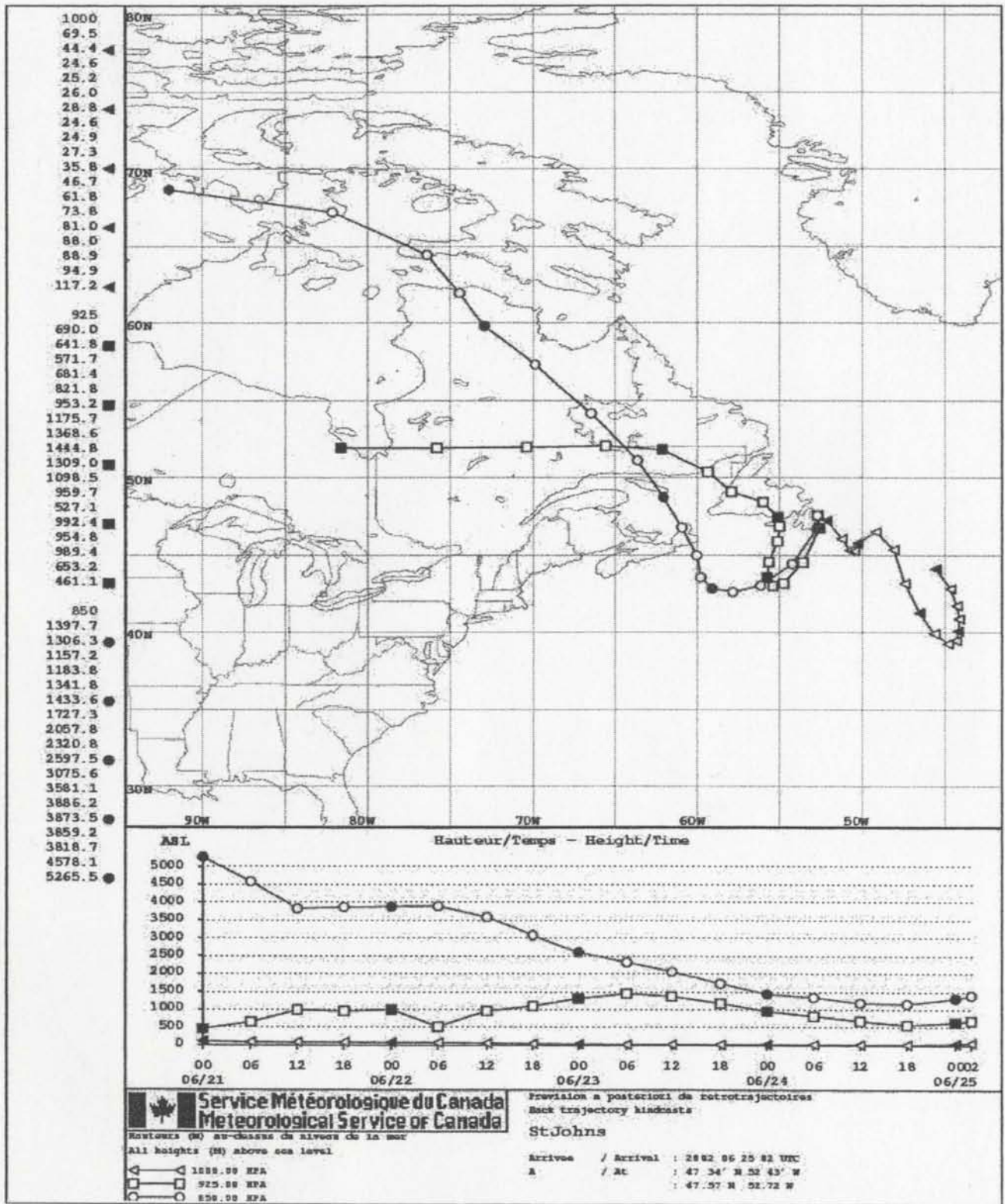


Figure III.9 Air mass back trajectory calculated for sample SJ02-0624.

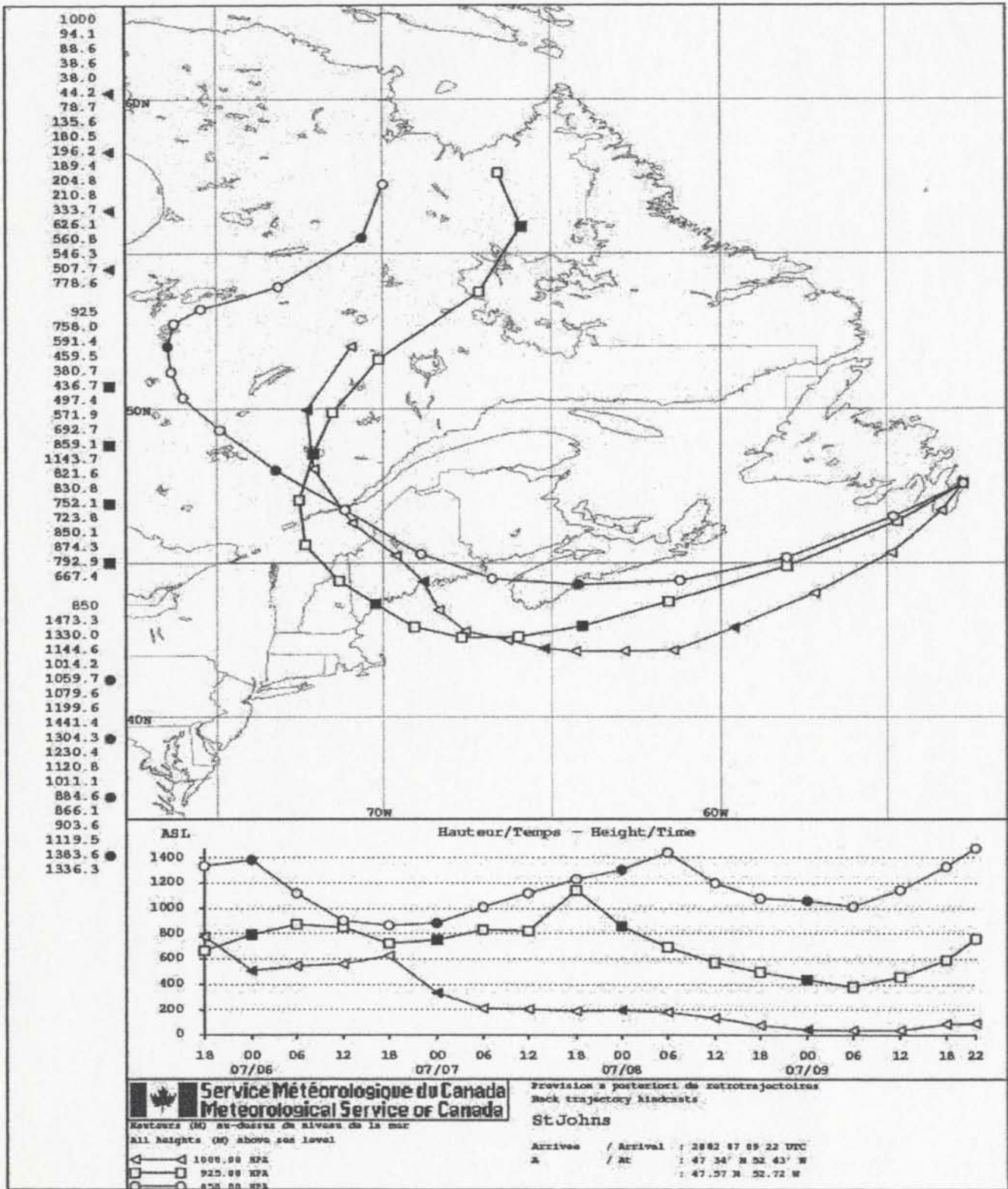


Figure III.10 Air mass back trajectory calculated for sample SJ02-0709

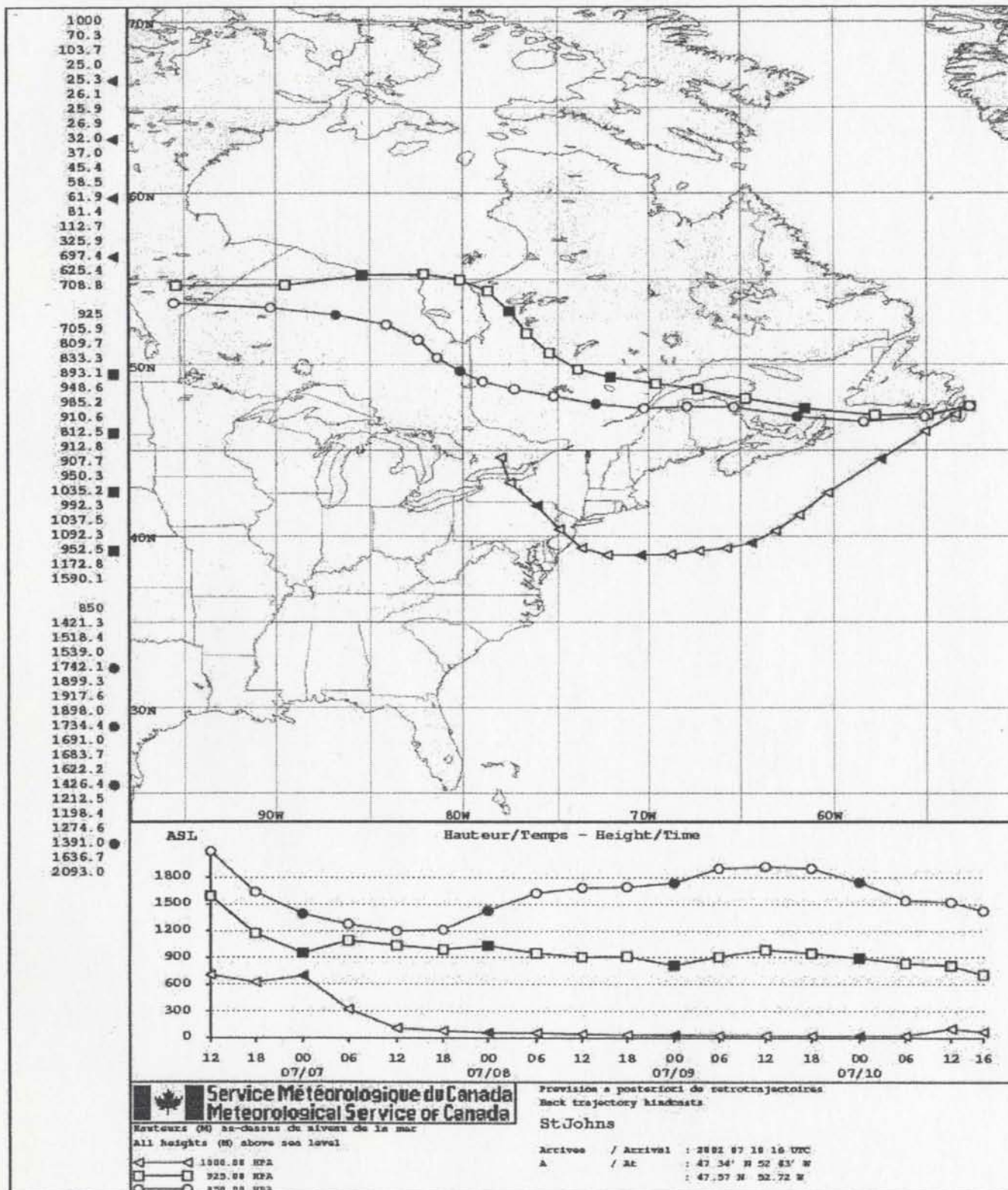


Figure III.11 Air mass back trajectory calculated for sample SJ02-0710

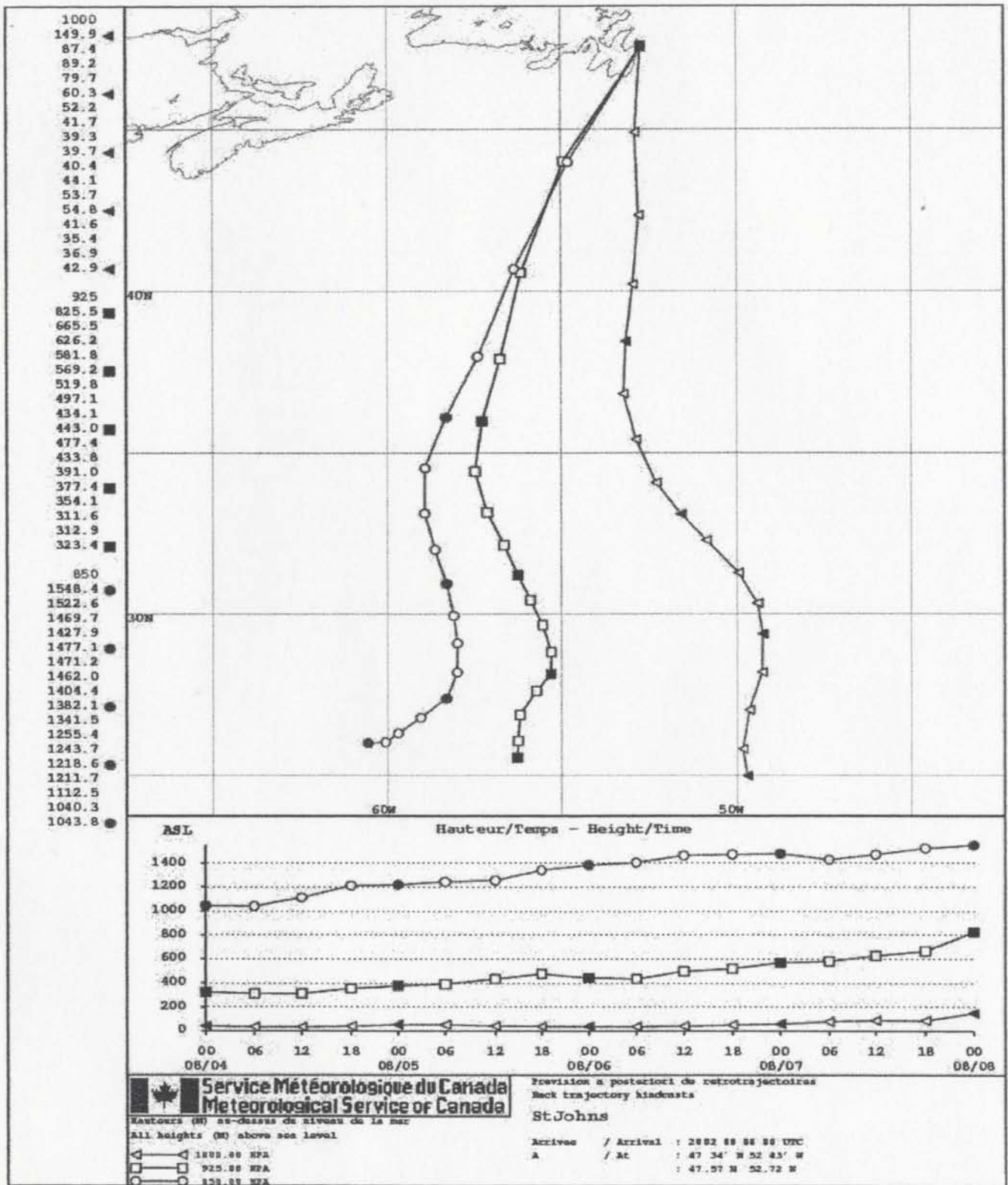


Figure III.12 Air mass back trajectory calculated for sample SJ02-0807

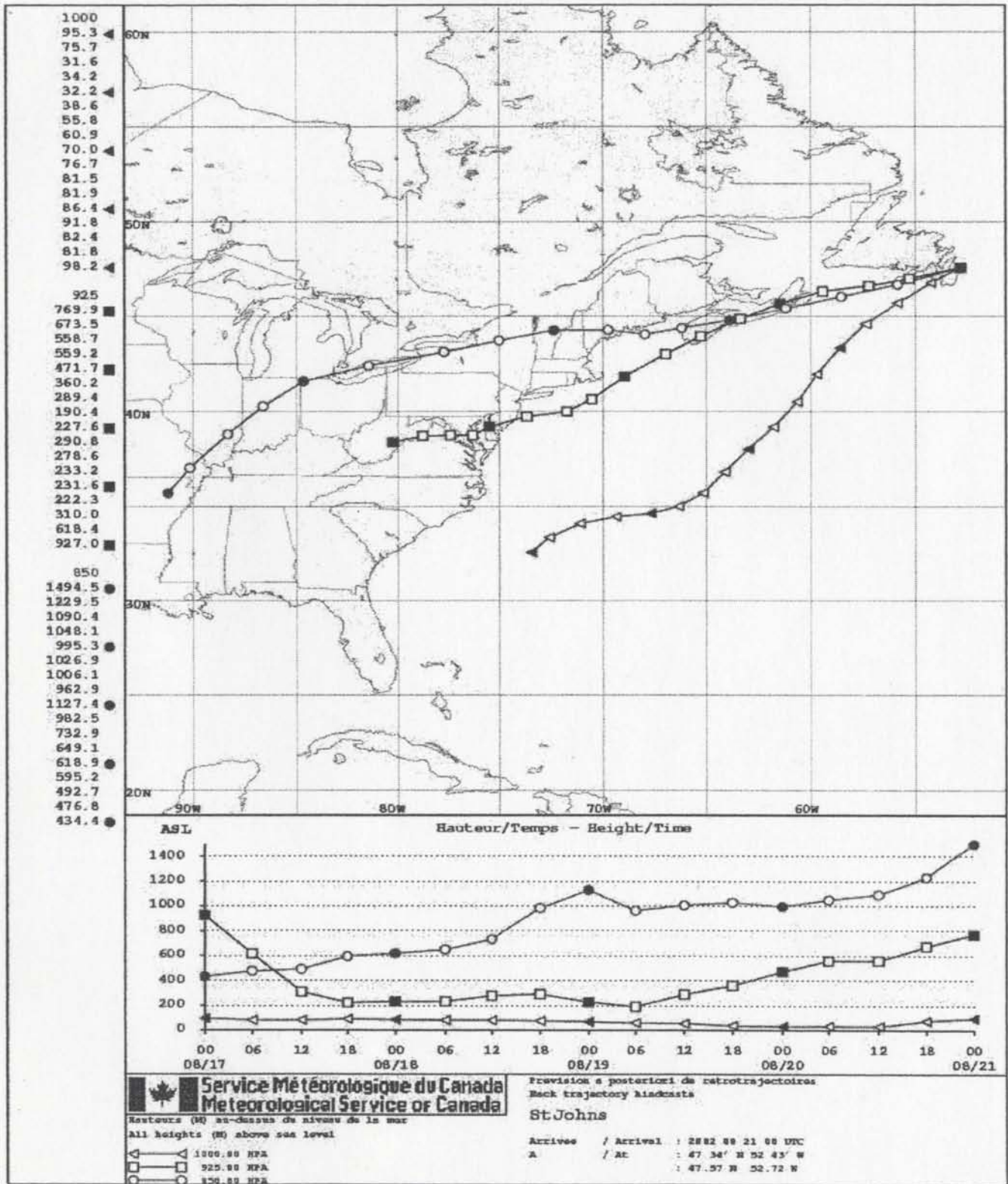


Figure III.13 Air mass back trajectory calculated for sample SJ02-0820

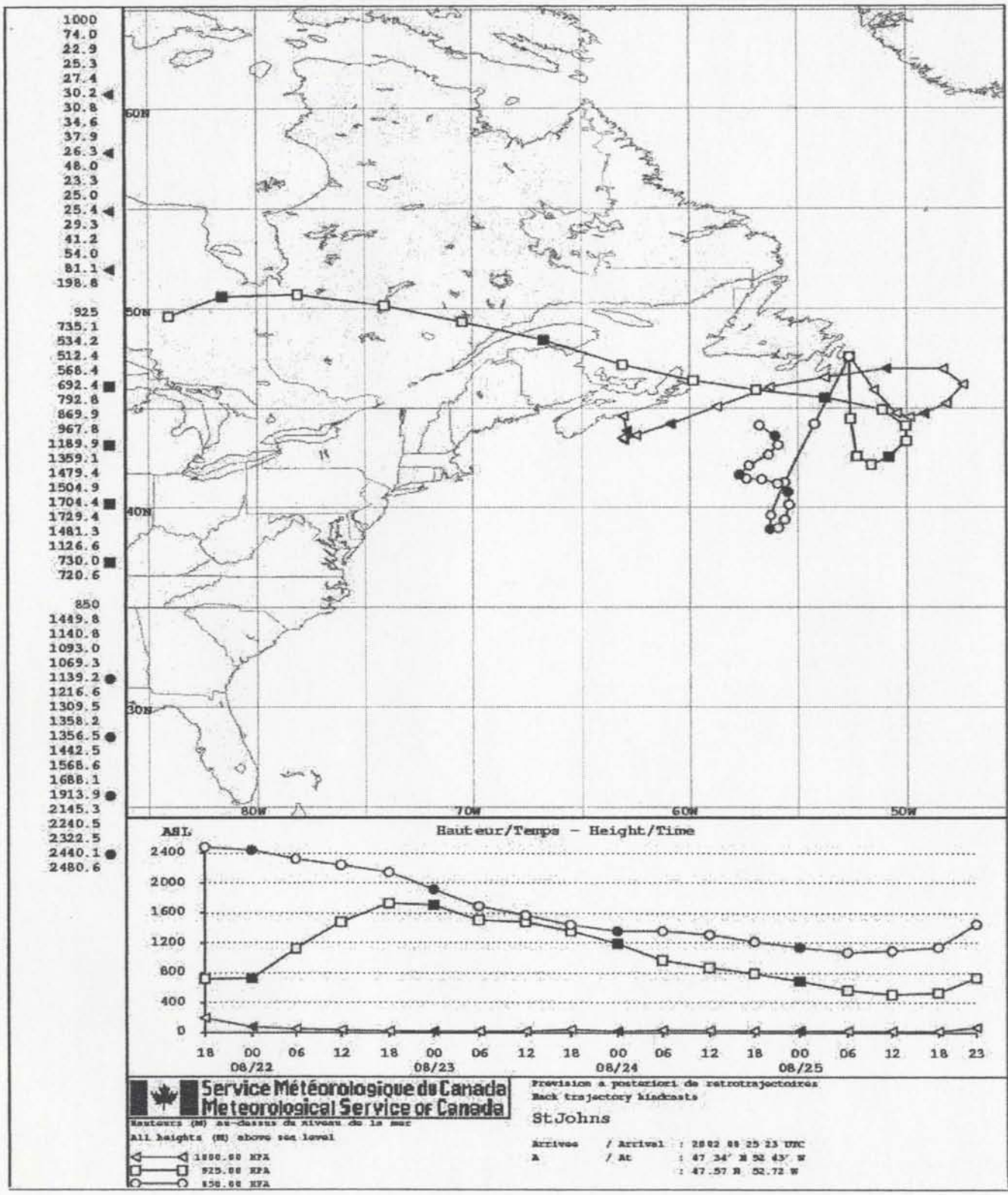


Figure III.14 Air mass back trajectory calculated for sample SJ02-0825

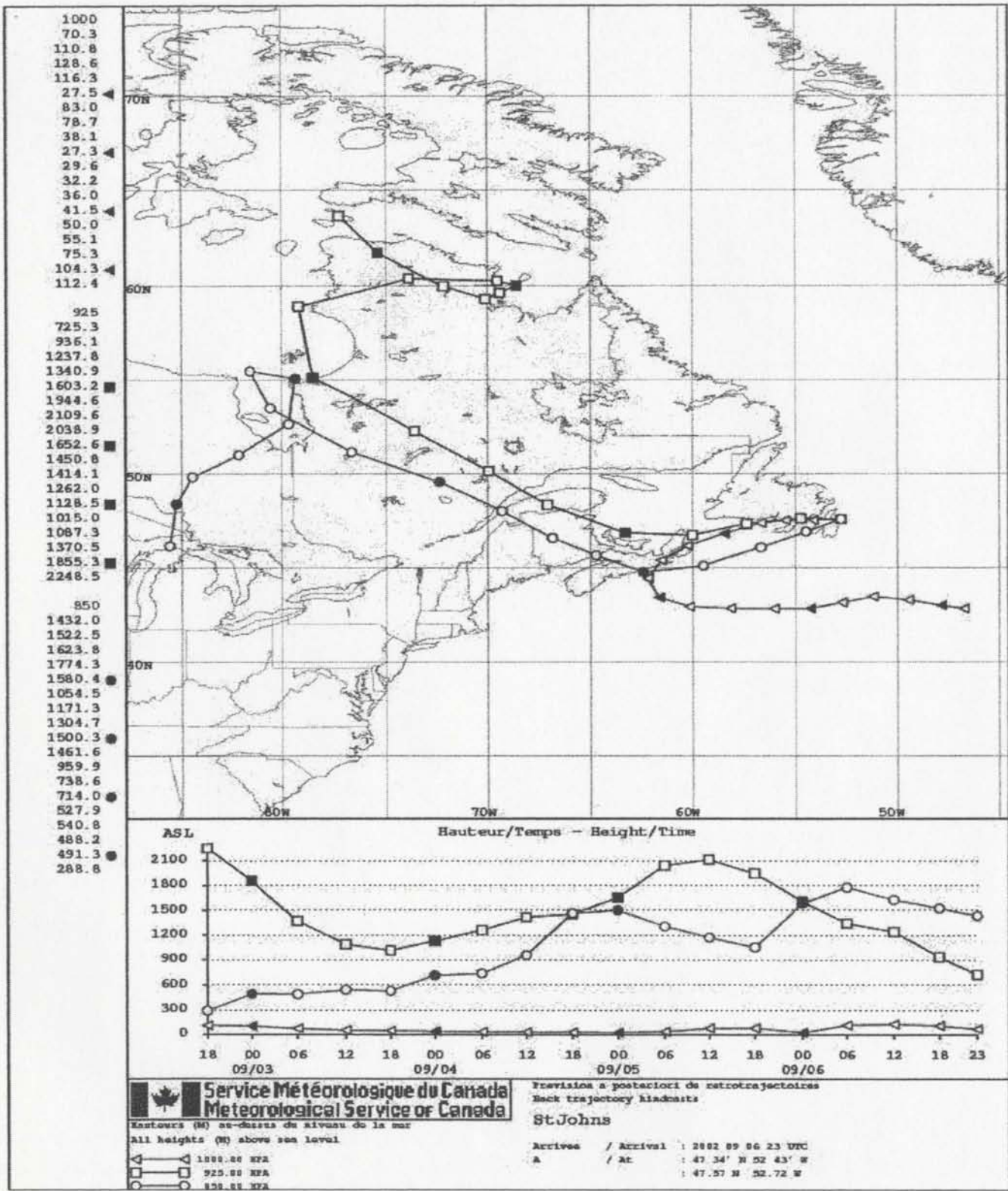


Figure III.15 Air mass back trajectory calculated for sample SJ02-0906

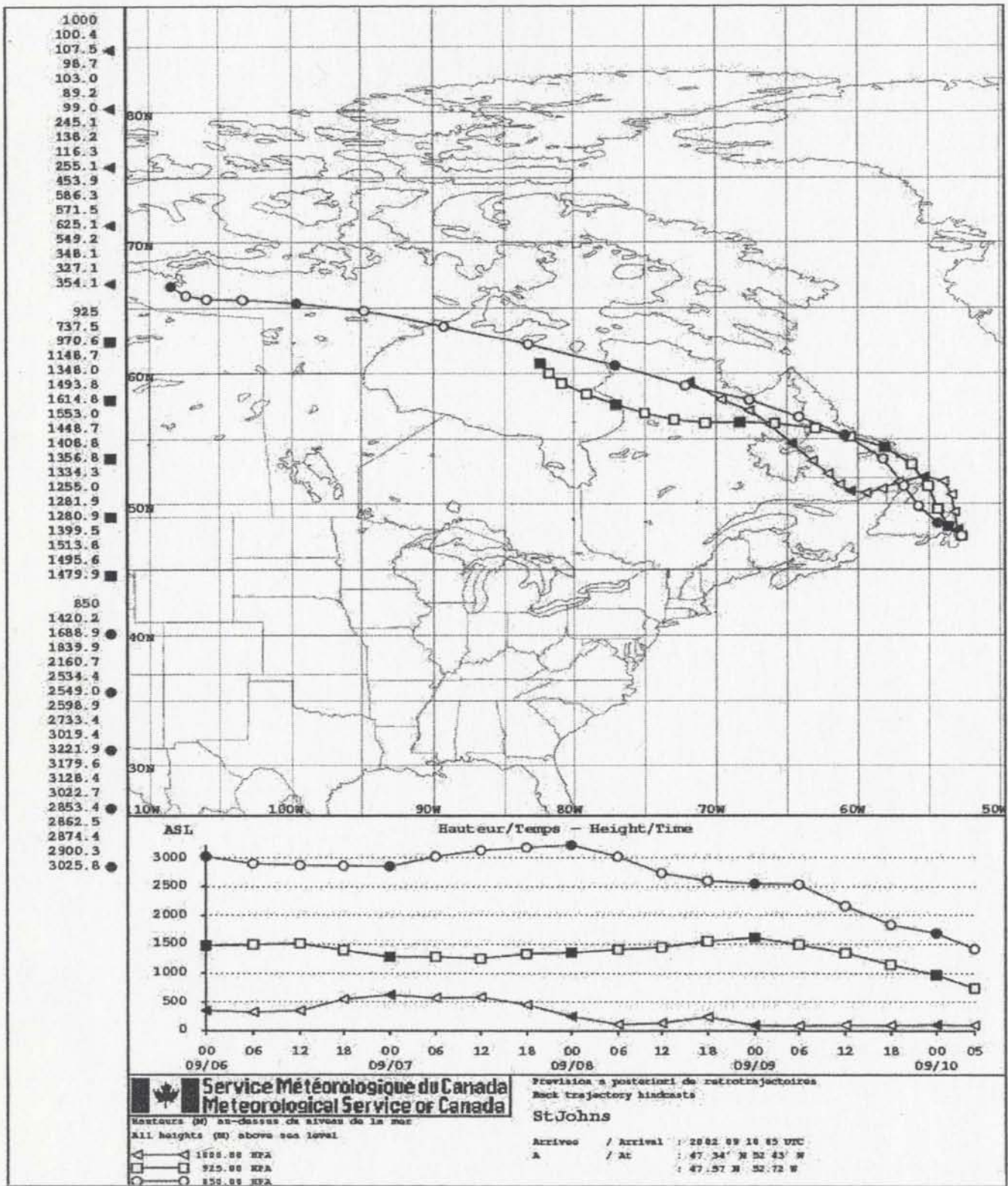


Figure III.16 Air mass back trajectory calculated for sample SJ02-0910

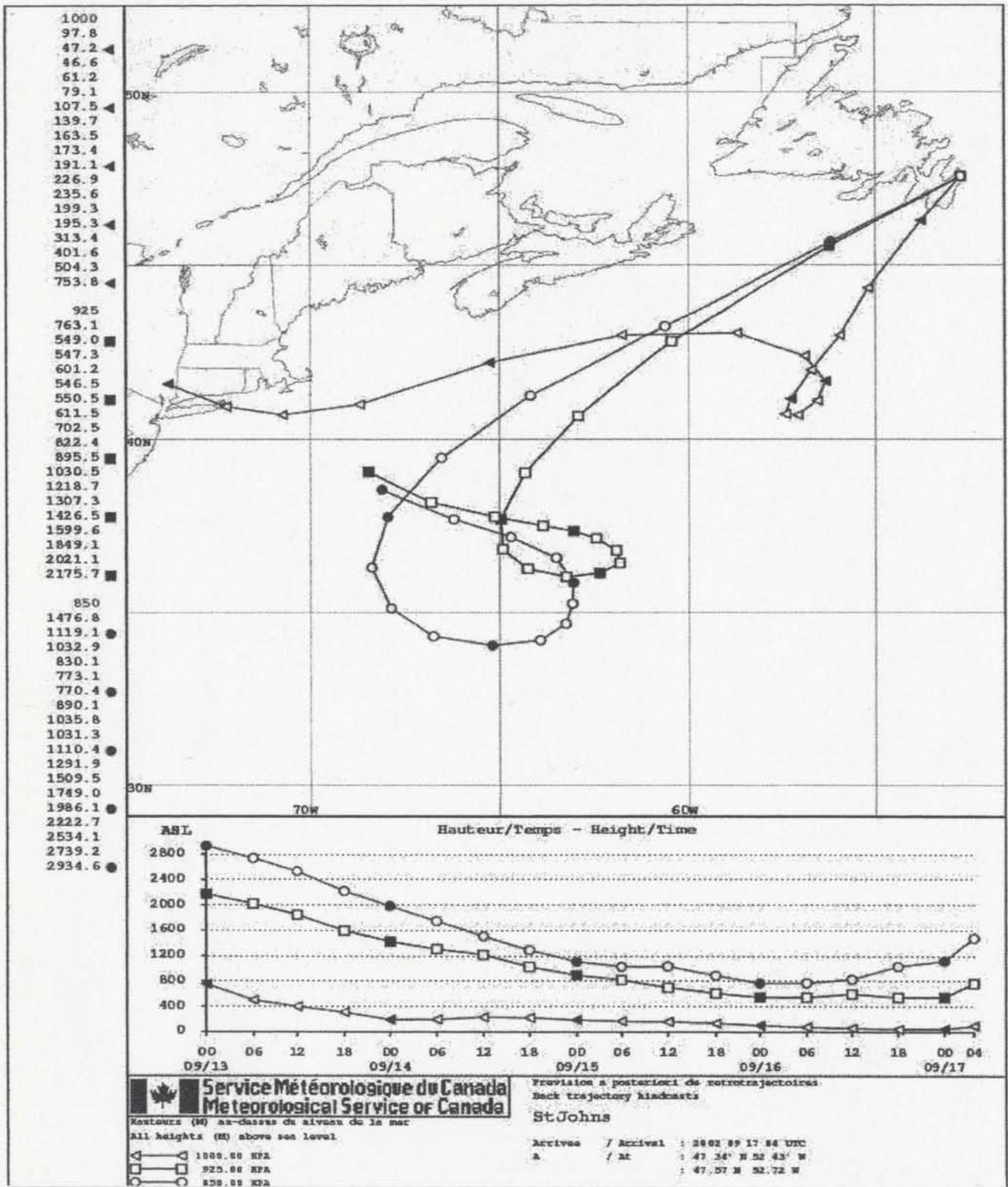


Figure III.17 Air mass back trajectory calculated for sample SJ02-0917

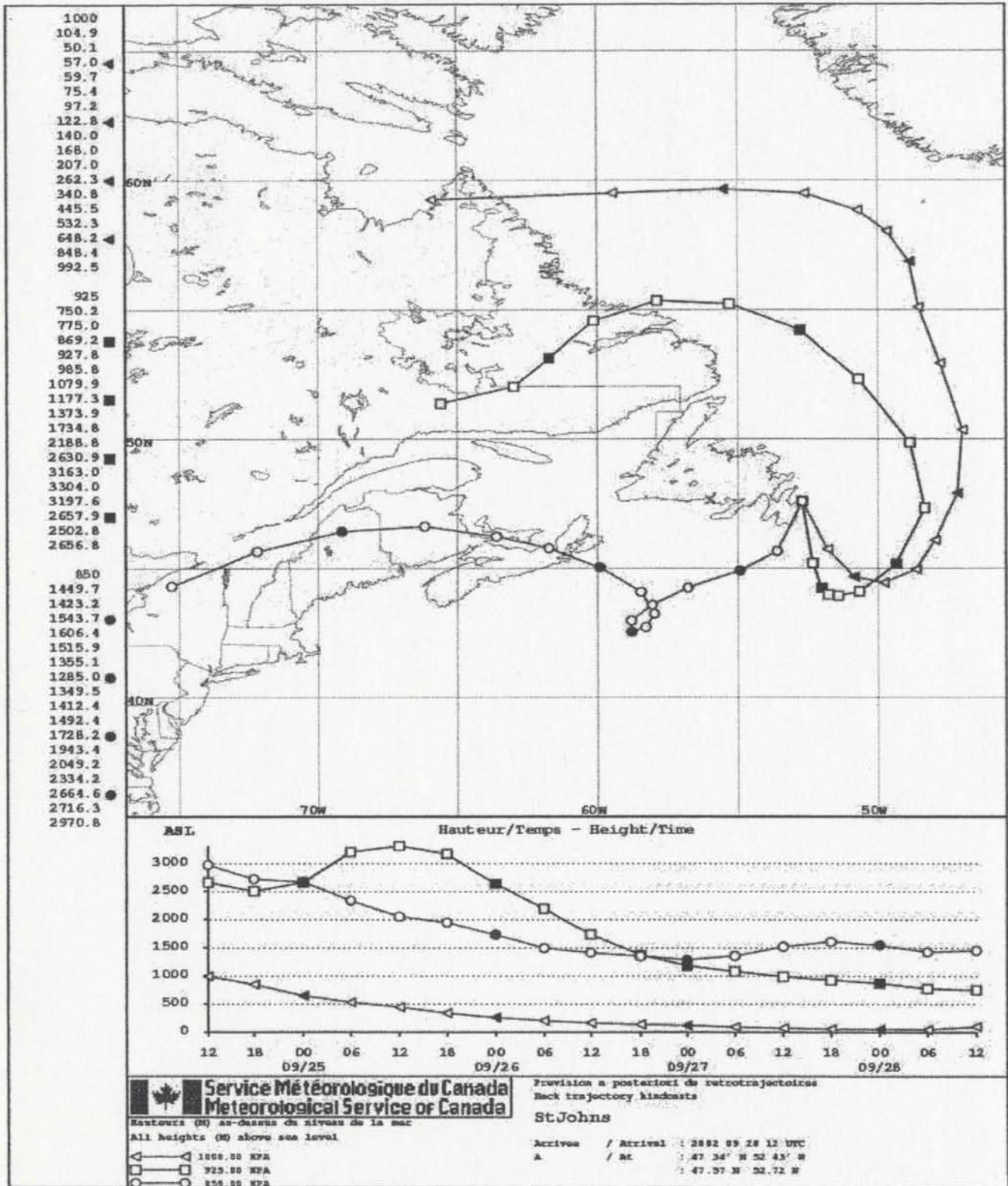


Figure III.18 Air mass back trajectory calculated for sample SJ02-0928

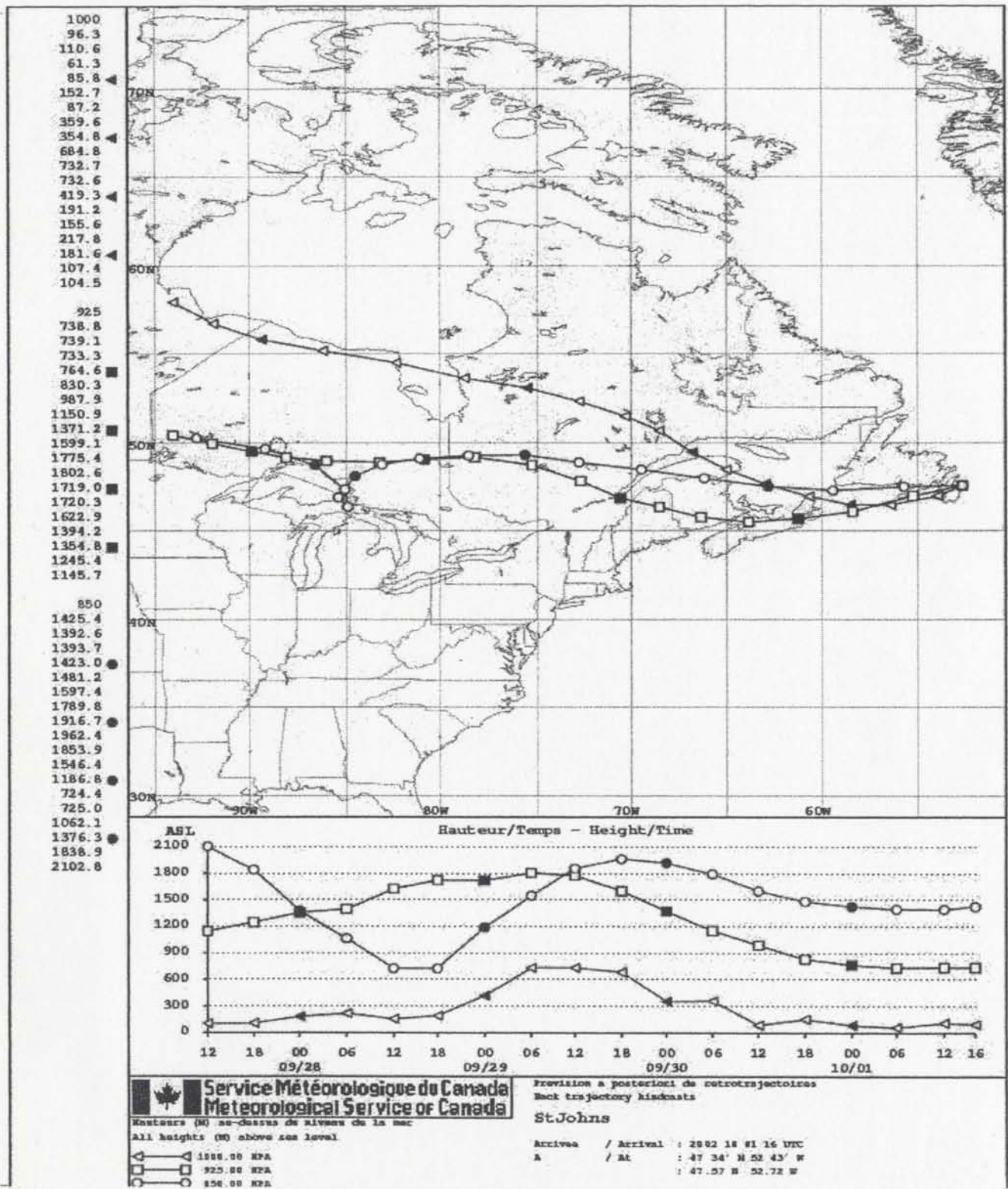


Figure III.19 Air mass back trajectory calculated for sample SJ02-1001

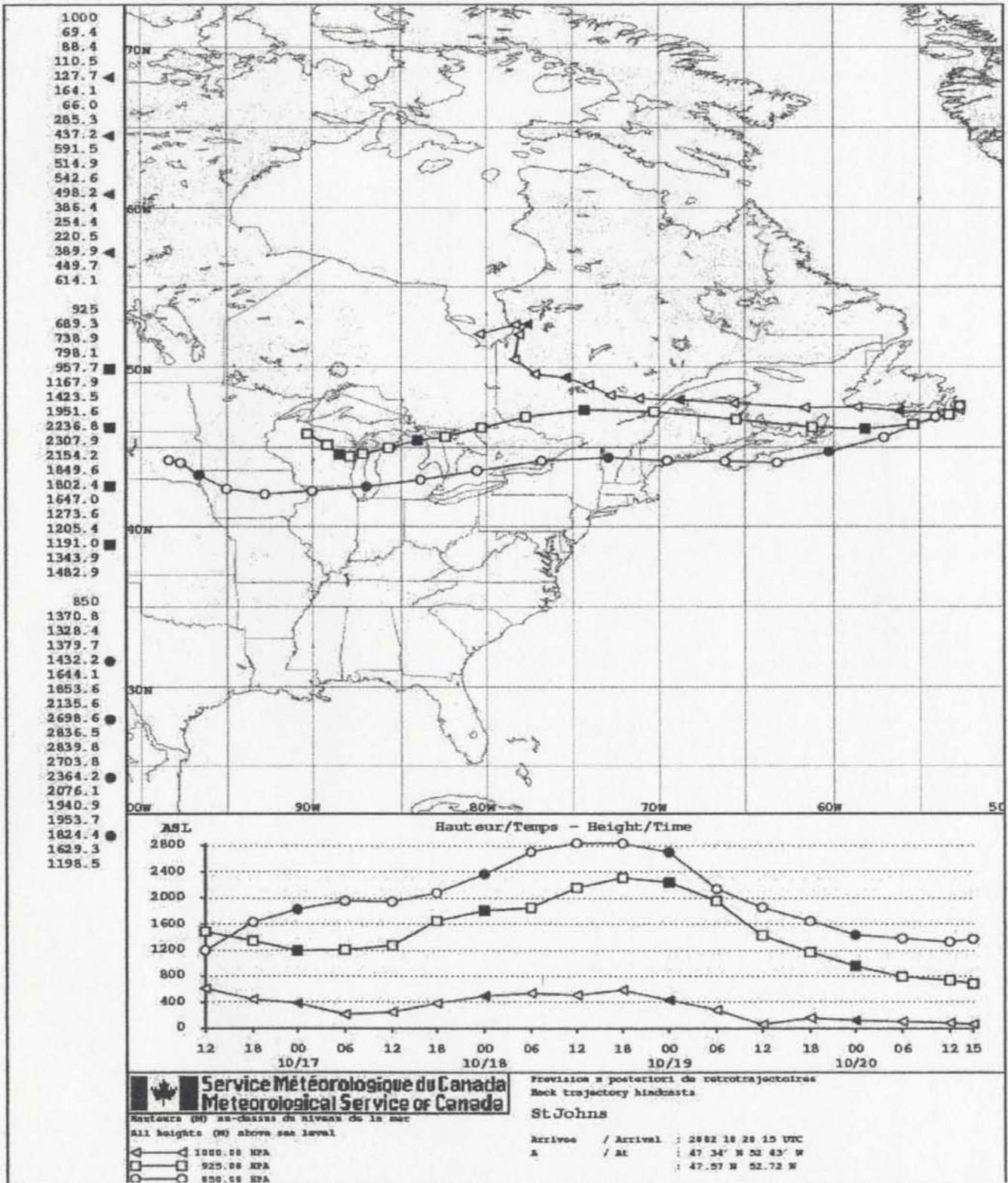


Figure III.20 Air mass back trajectory calculated for sample SJ02-1020

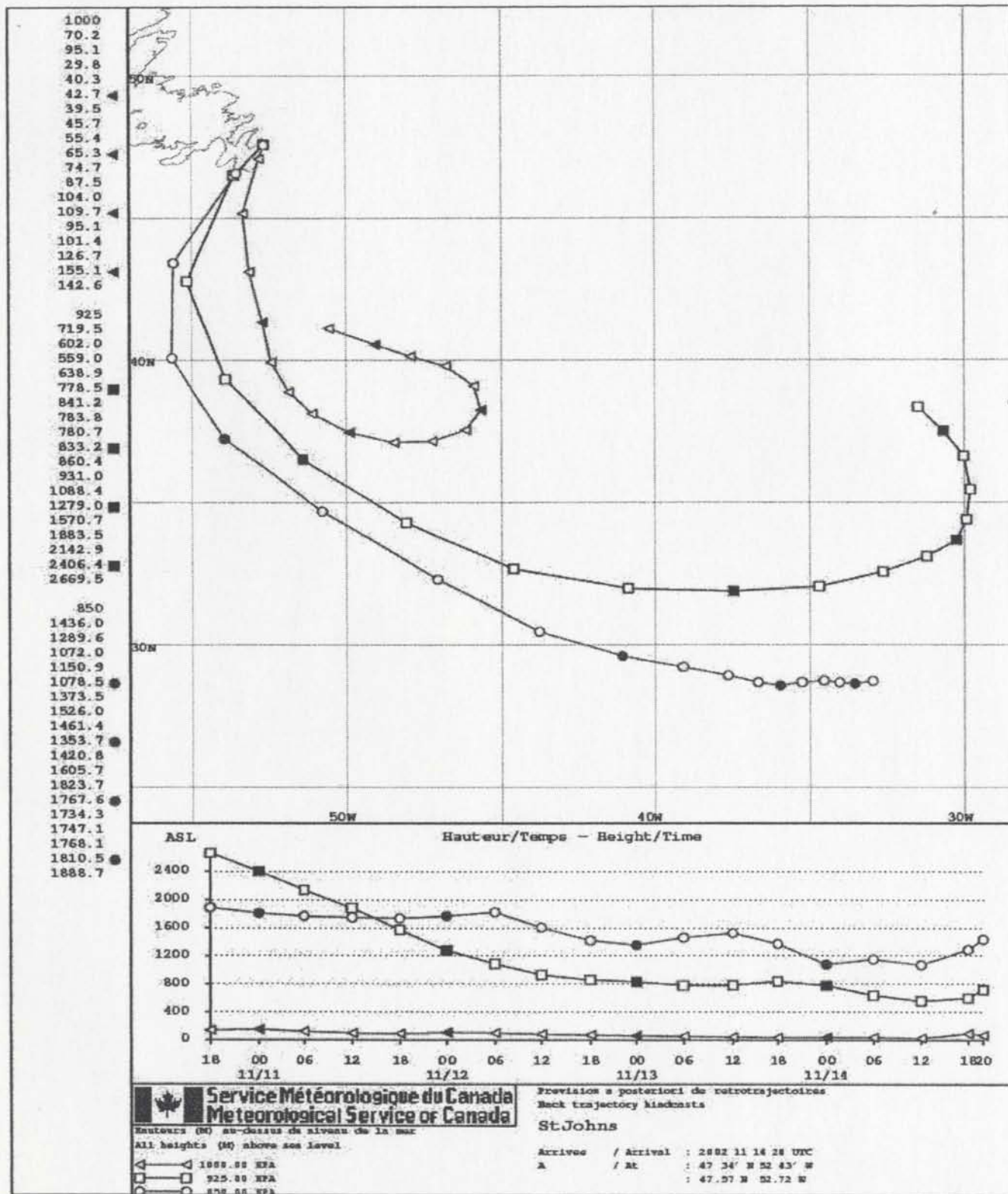


Figure III.21 Air mass back trajectory calculated for sample SJ02-1114

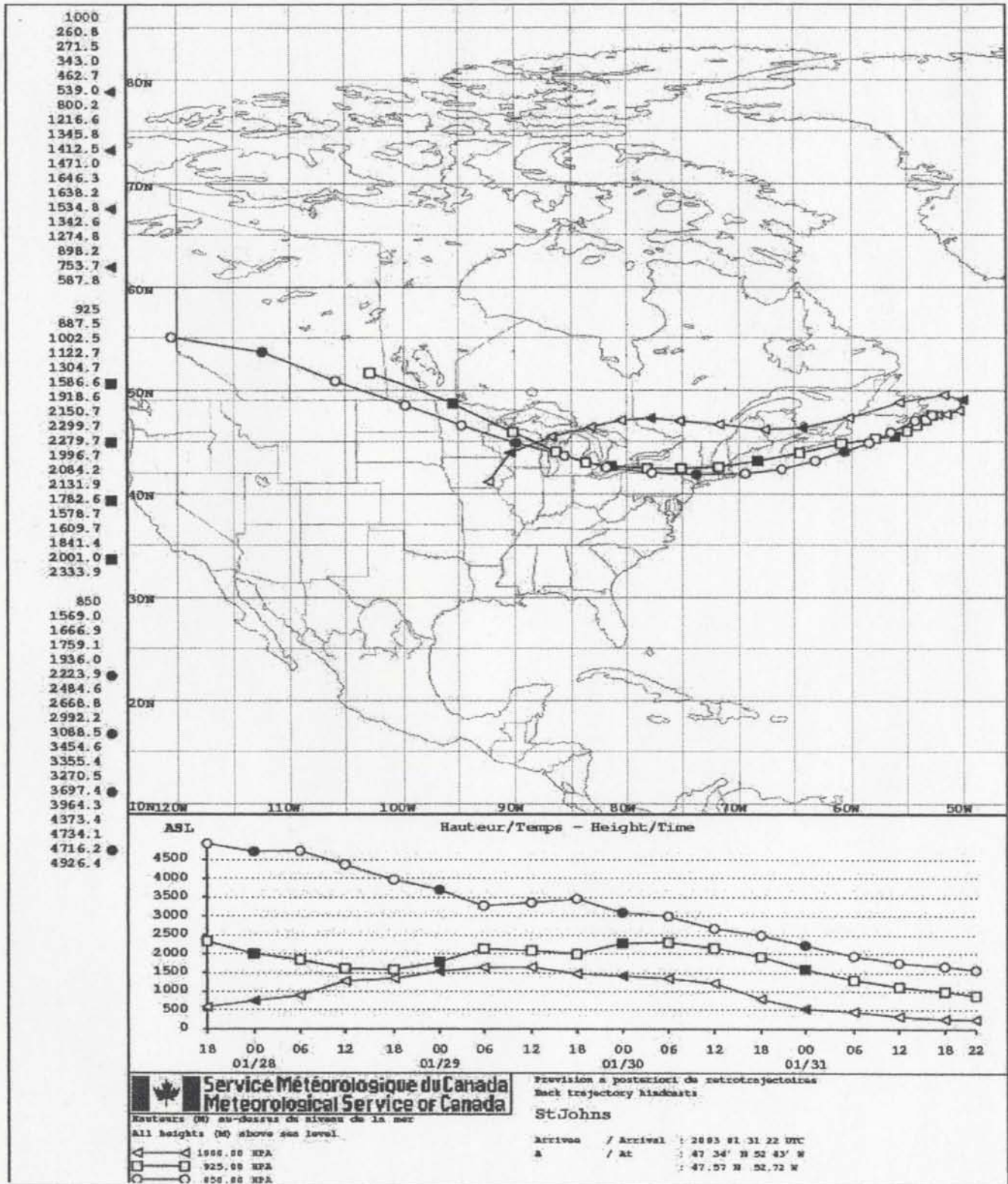


Figure III.22 Air mass back trajectory calculated for sample SJ03-0131

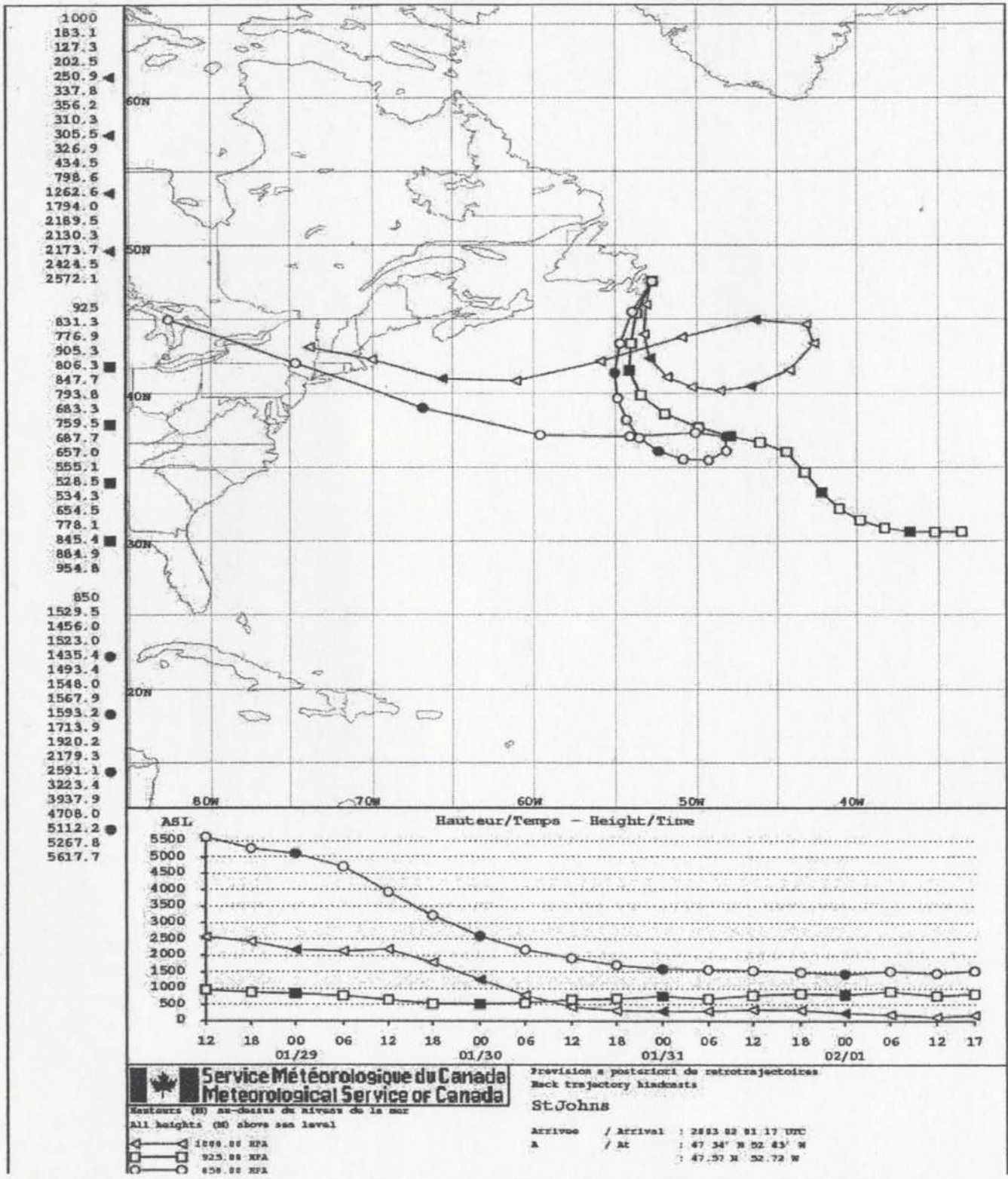


Figure III.23 Air mass back trajectory calculated for sample SJ03-0201

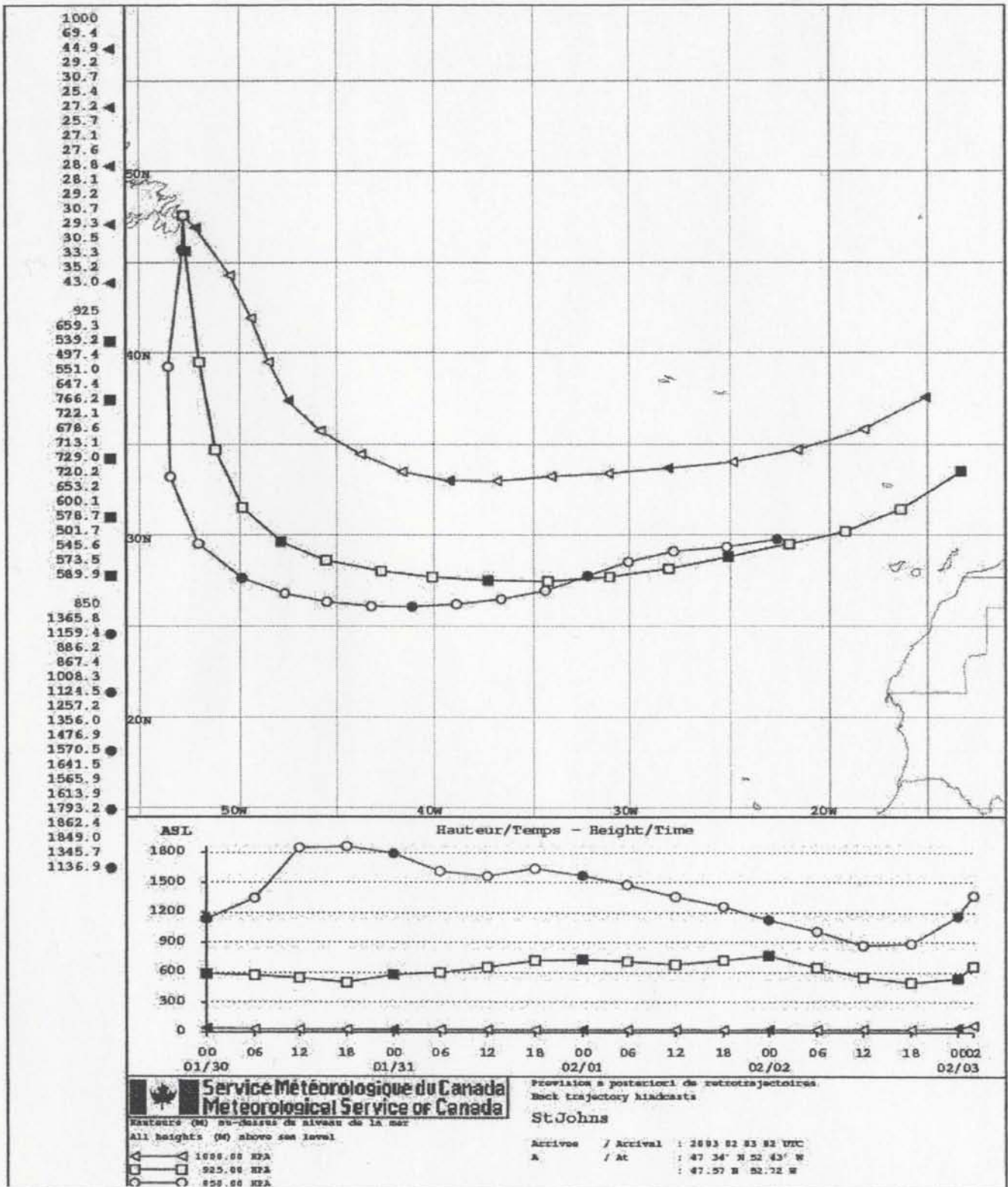


Figure III.24 Air mass back trajectory calculated for sample SJ03-0202

APPENDIX IV

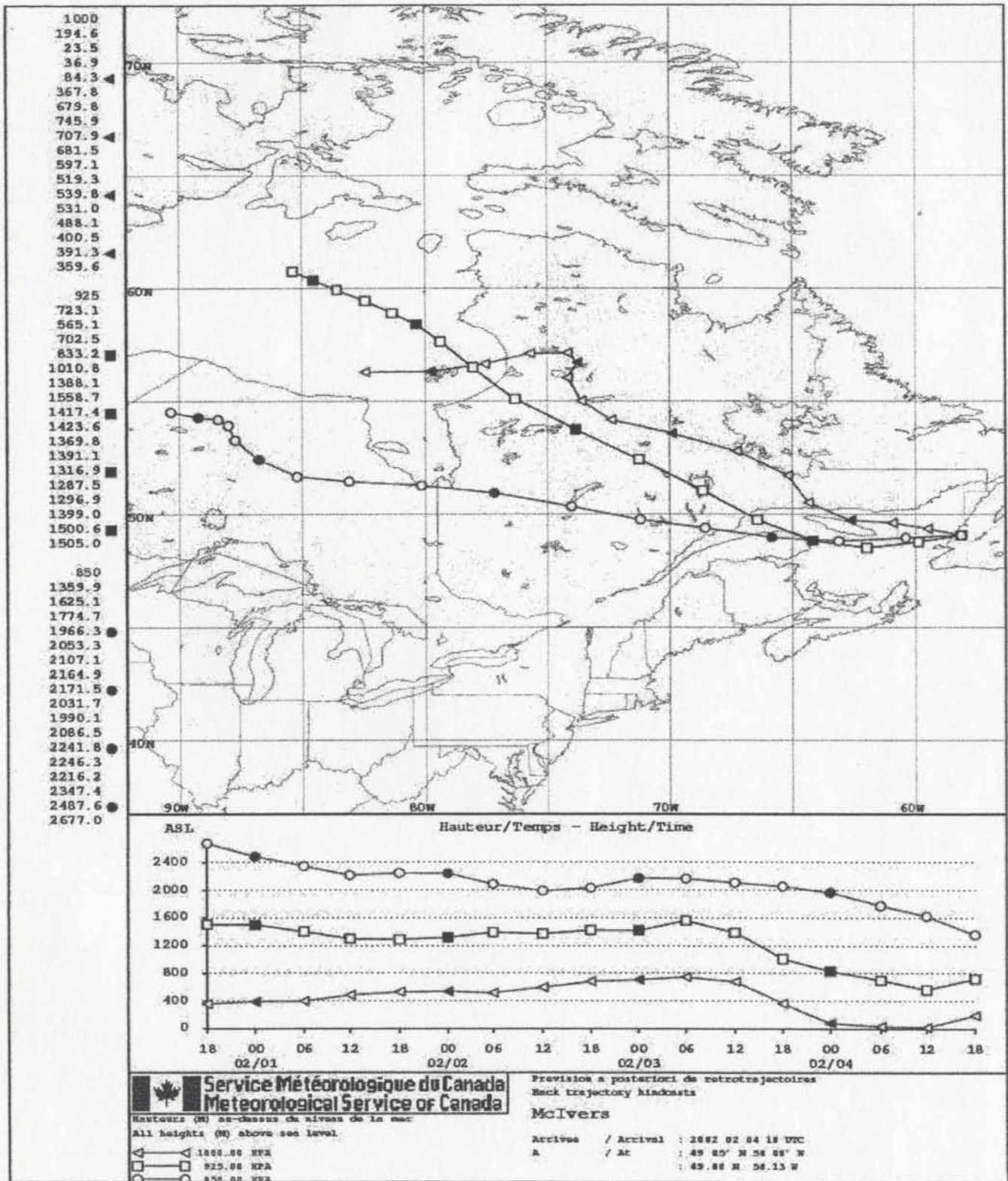


Figure IV.1 Air mass back trajectory calculated for sample MCS02-0205

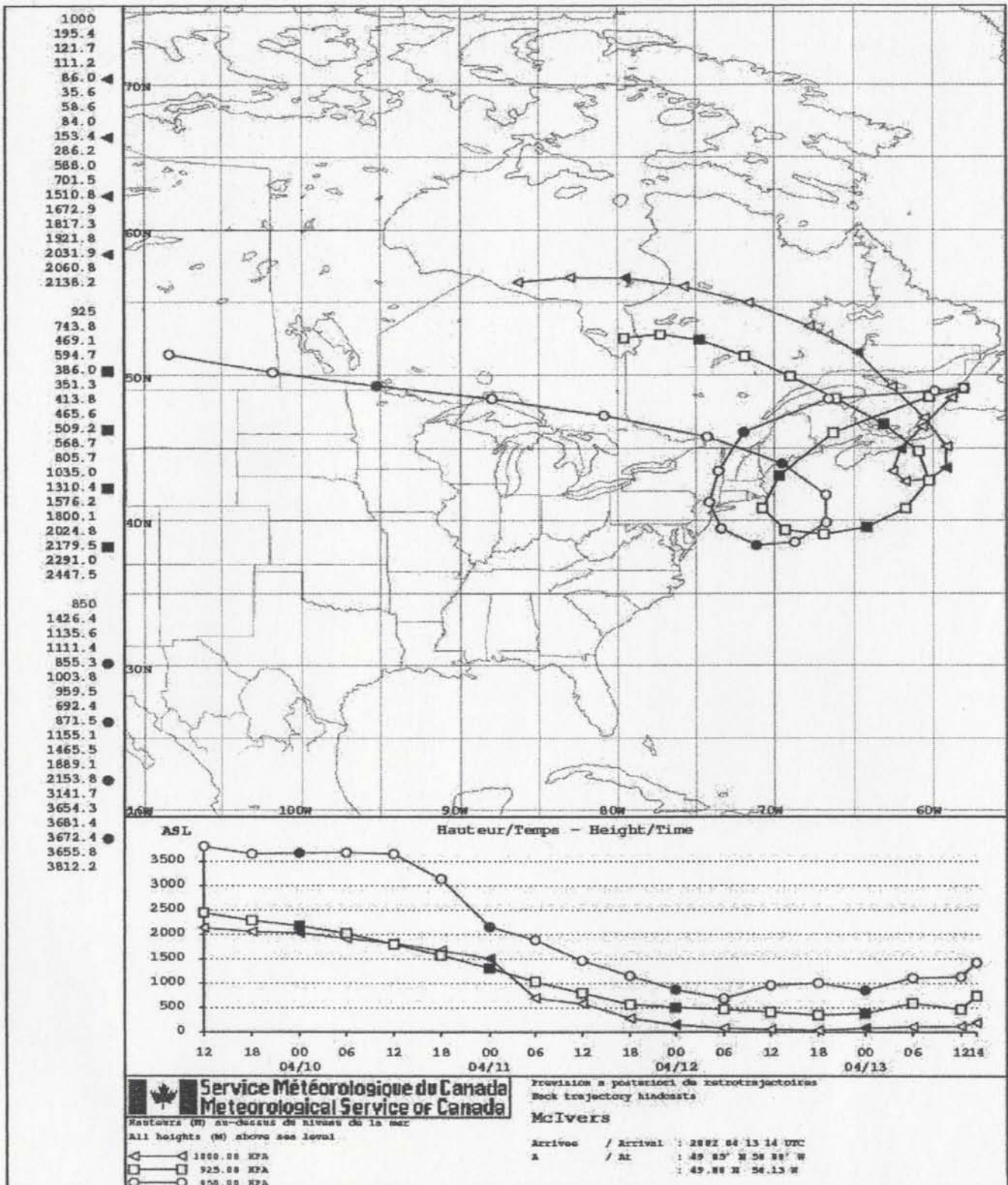


Figure IV.3 Air mass back trajectory calculated for sample MC02-0413

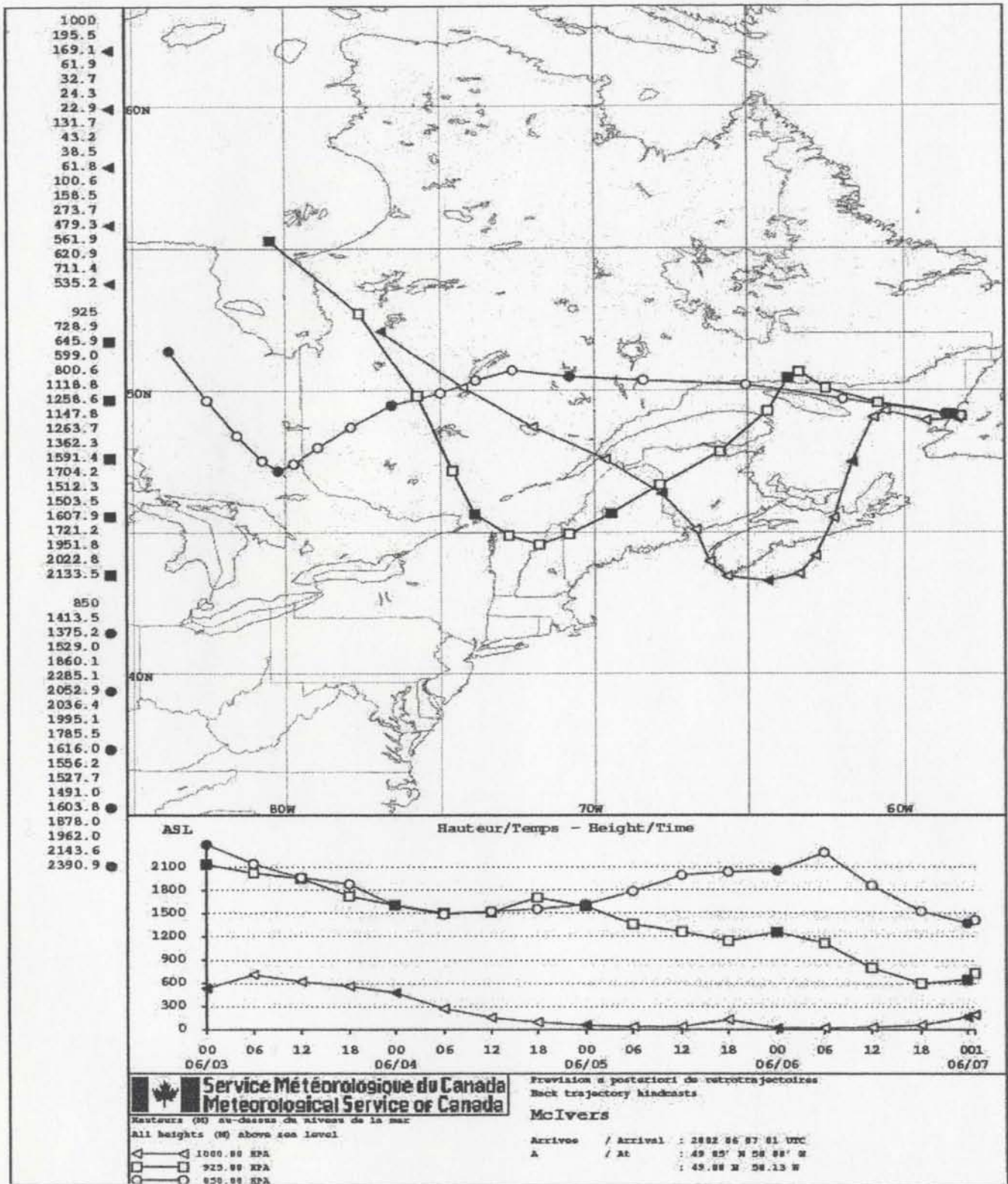


Figure IV.4 Air mass back trajectory calculated for sample MC02-0606

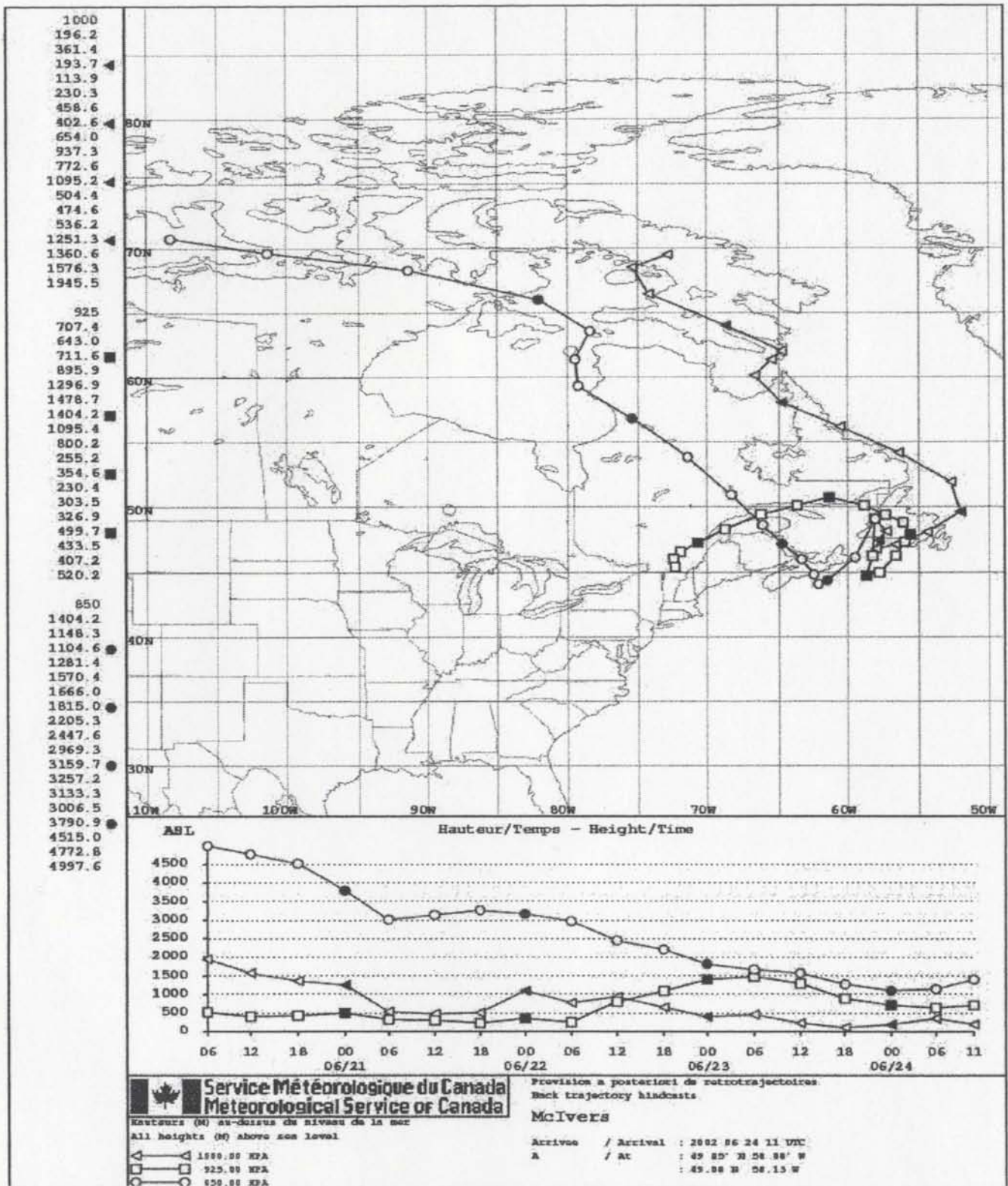


Figure IV.5 Air mass back trajectory calculated for sample MC02-0624

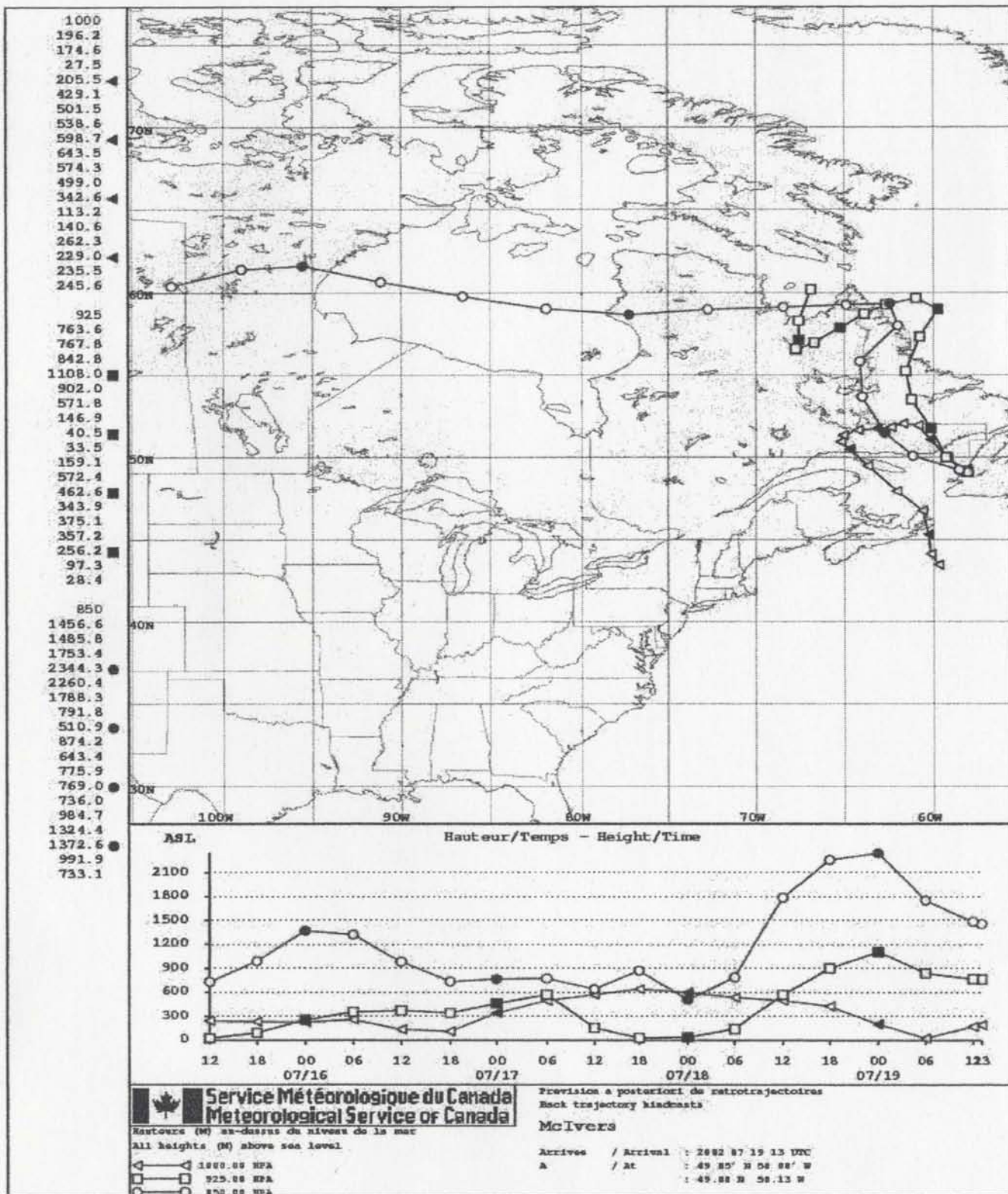


Figure IV.6 Air mass back trajectory calculated for sample MC02-0719

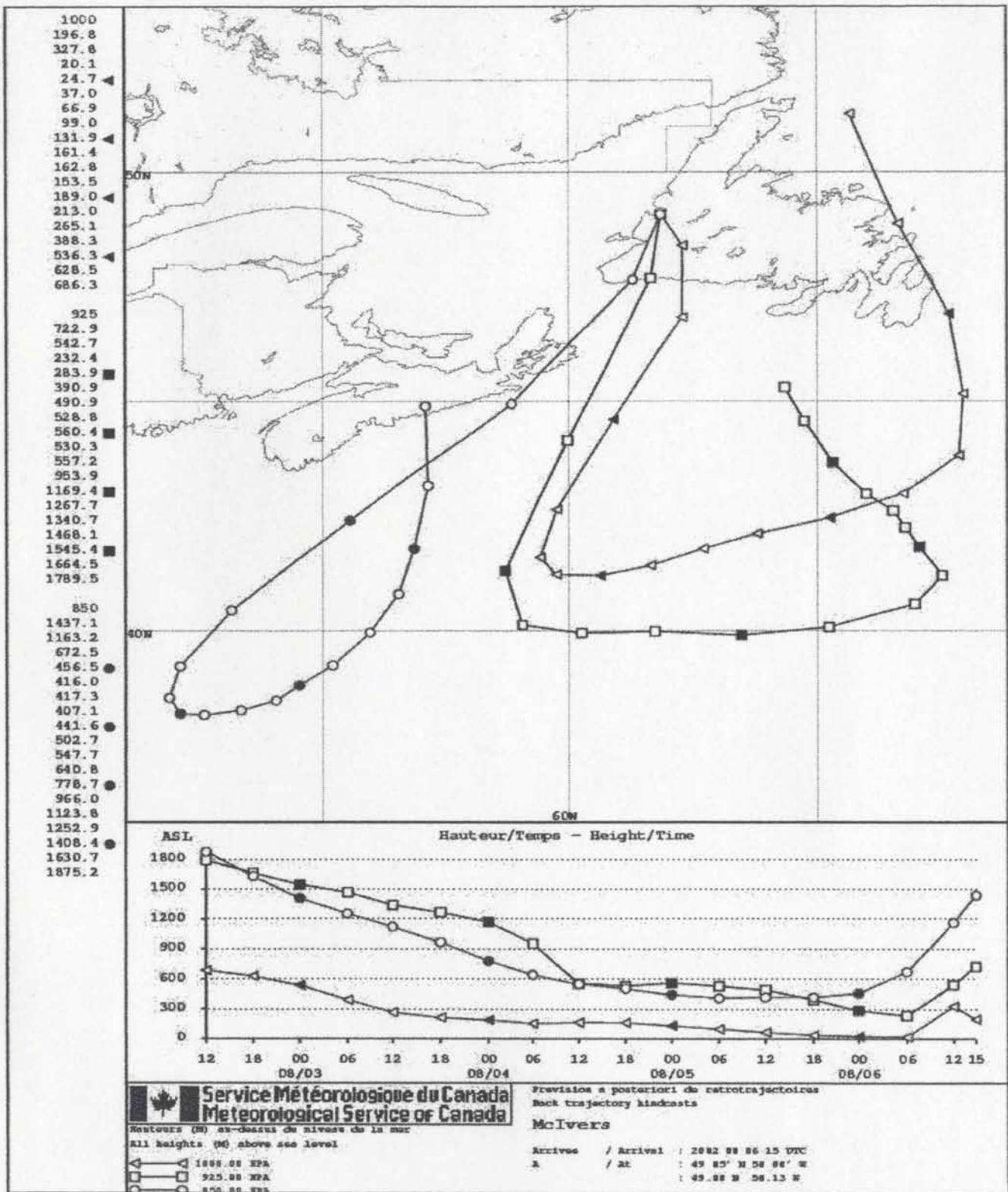


Figure IV.7 Air mass back trajectory calculated for sample MC02-0806

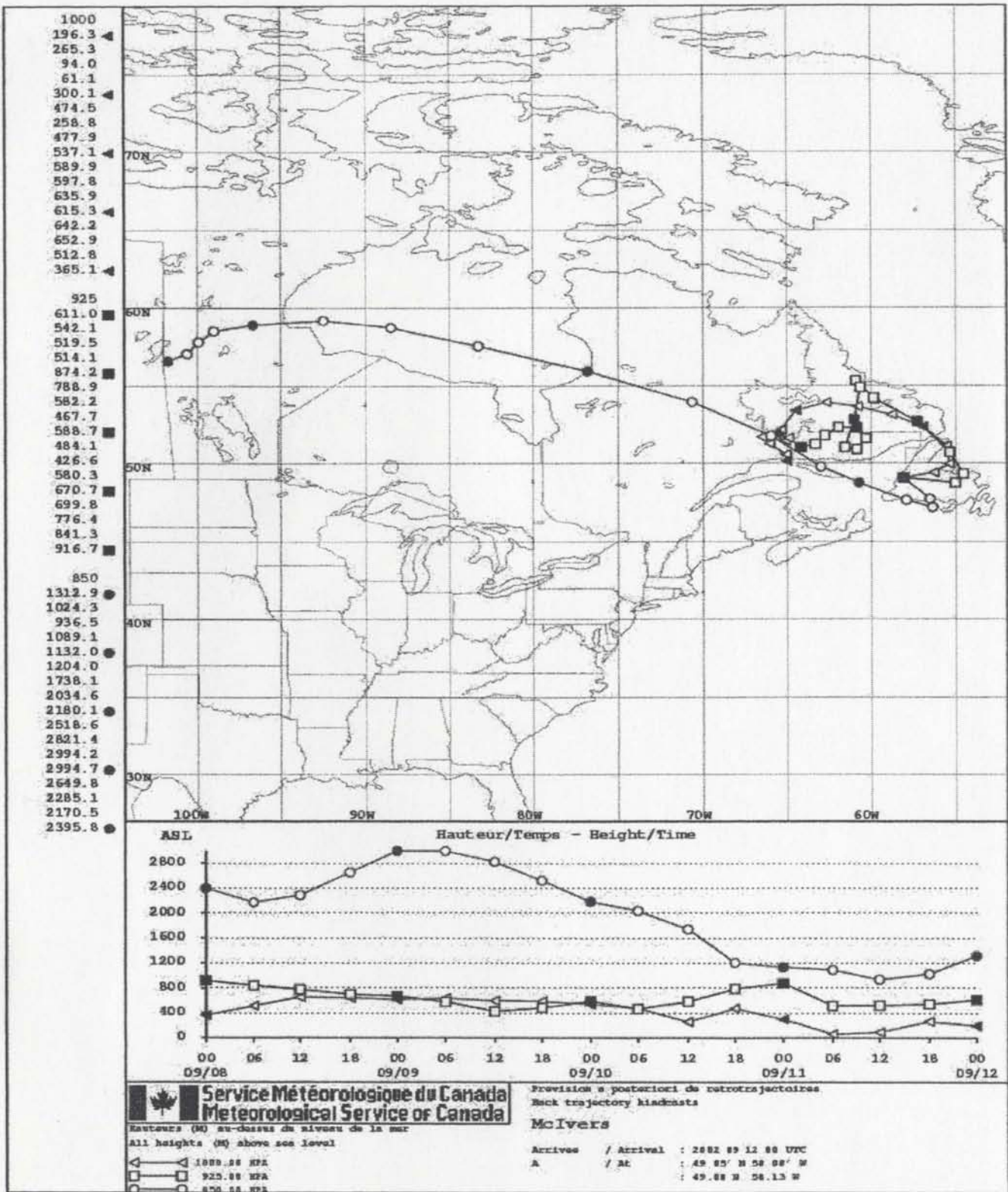


Figure IV.8 Air mass back trajectory calculated for sample MC02-0911

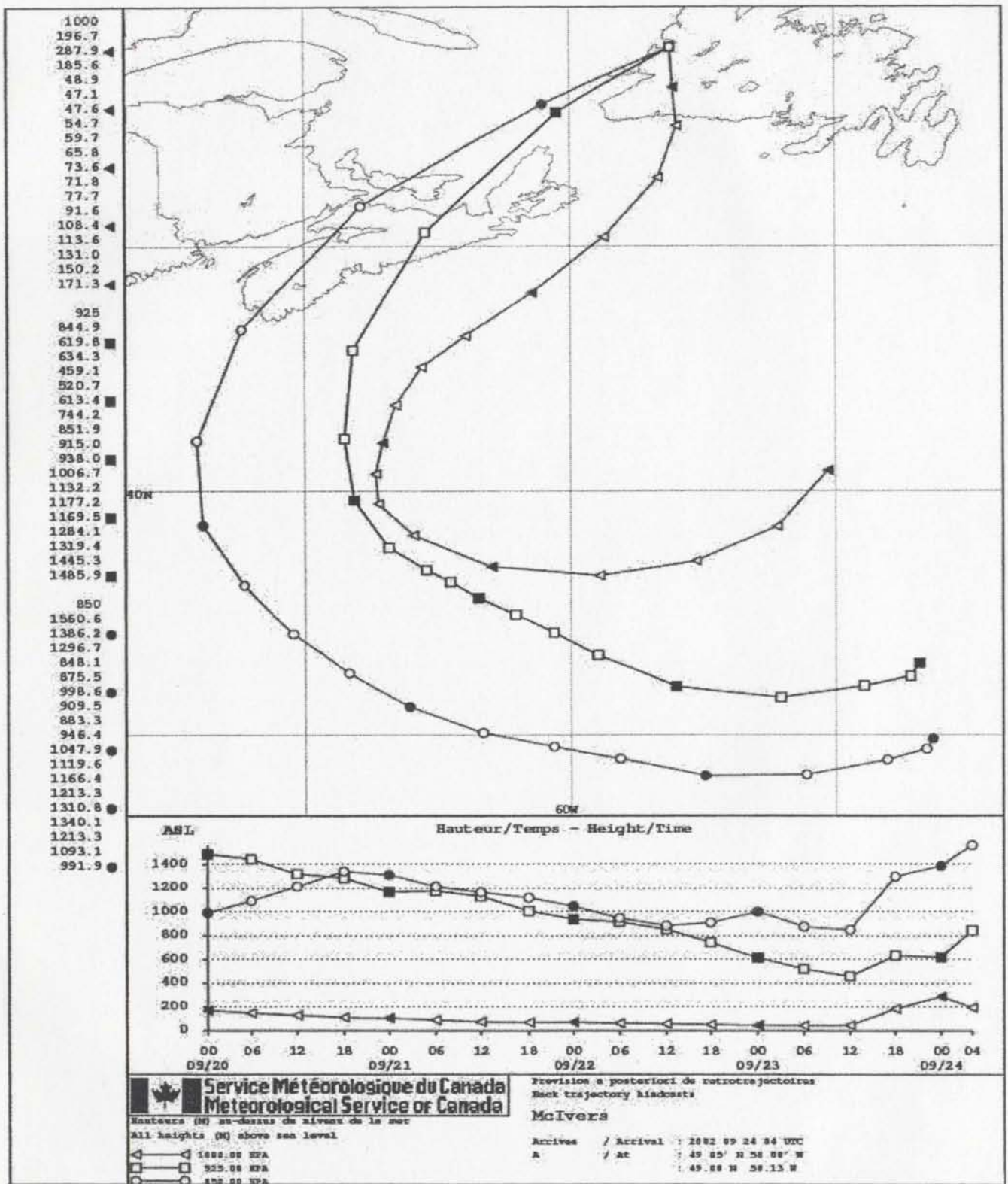


Figure IV.9 Air mass back trajectory calculated for sample MC02-0924

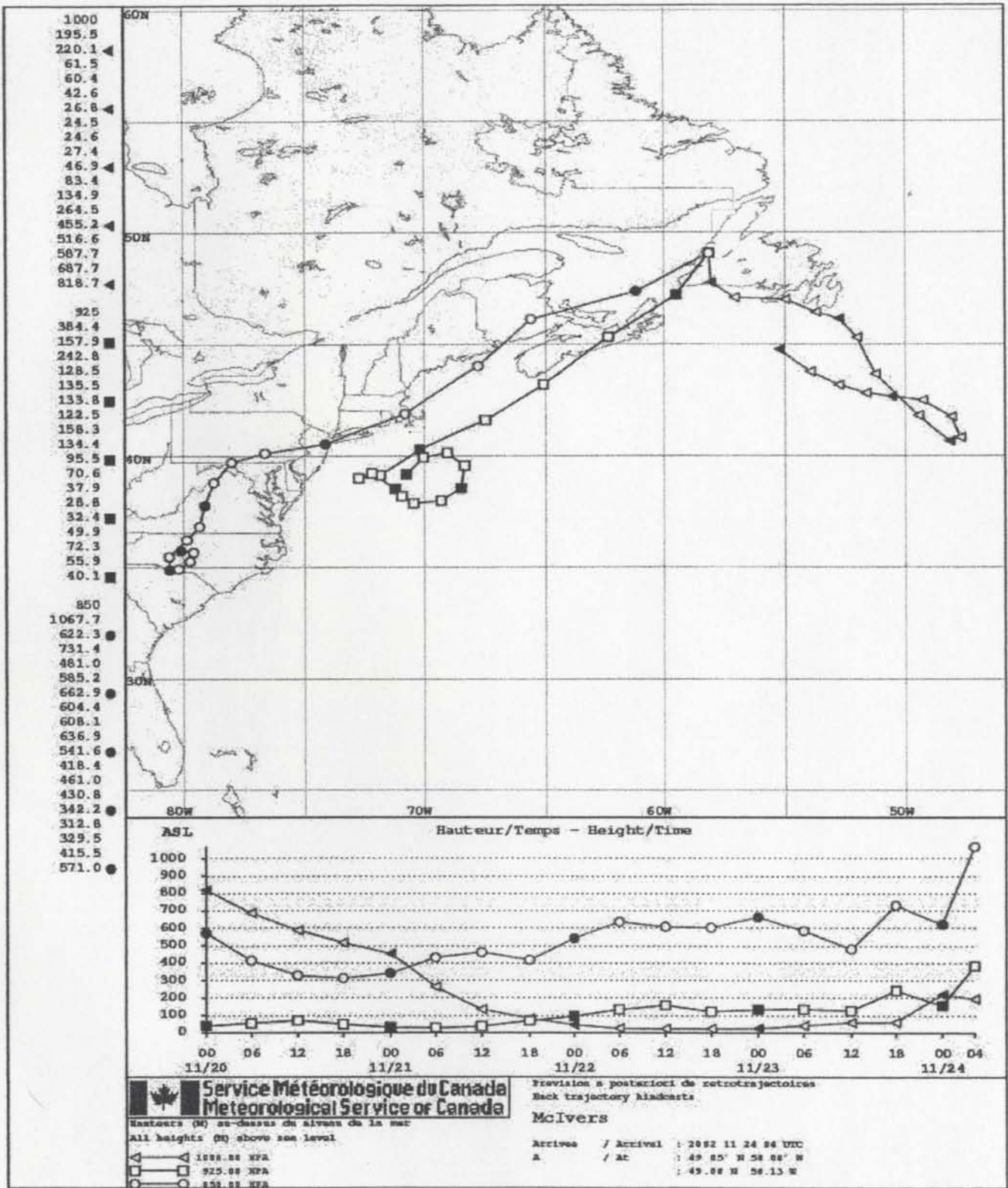


Figure IV.10 Air mass back trajectory calculated for sample MC02-1124
214

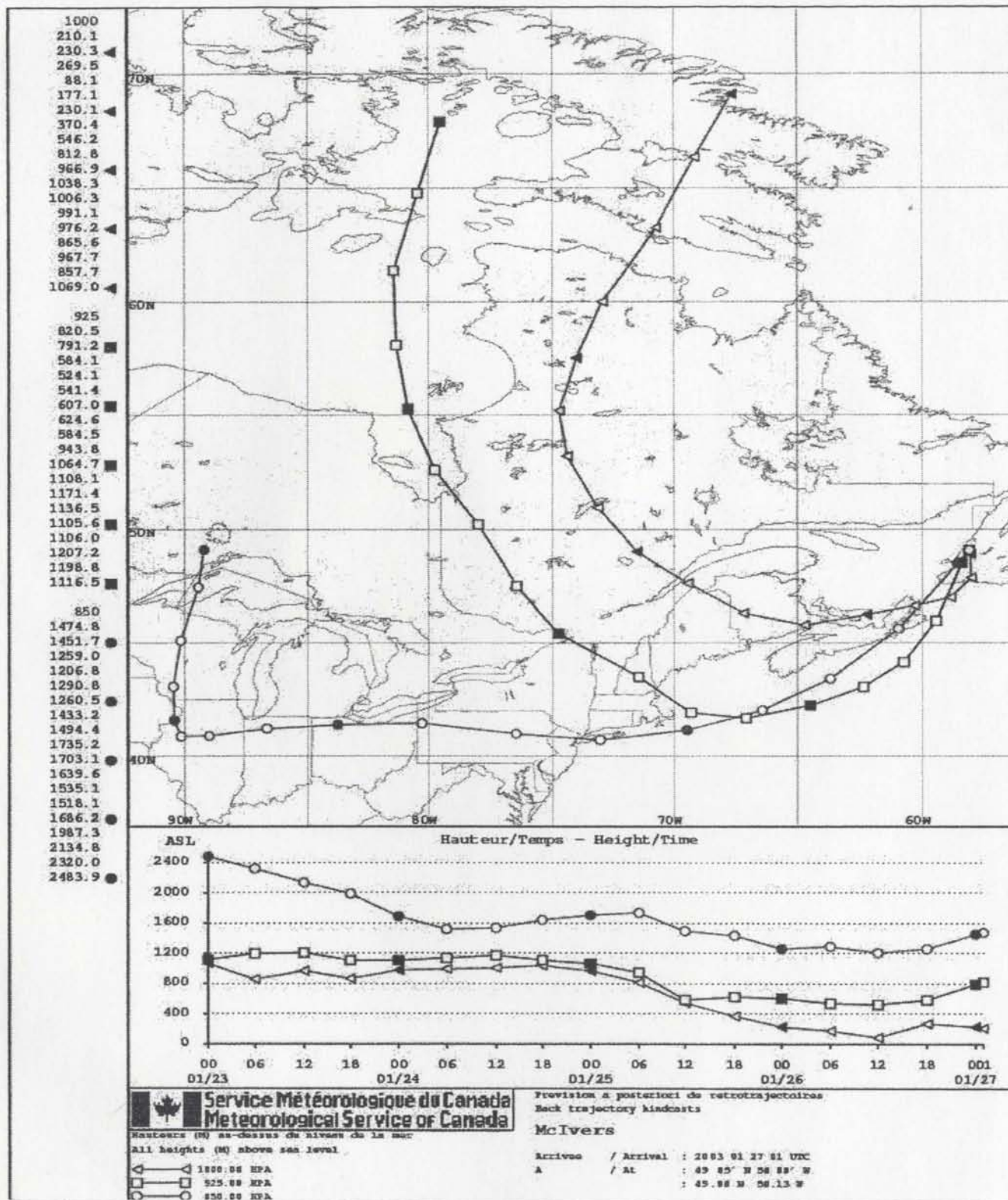


Figure IV.11 Air mass back trajectory calculated for sample MCS03-0126

4728 SA

